

***In vitro* studies on the effects of bioactives from quinoa and amaranth seeds against breast cancer and inflammation**

by

TANIYA. M. S
10BB17J39009

A thesis submitted to the
Academy of Scientific & Innovative Research
for the award of the degree of
DOCTOR OF PHILOSOPHY
in
SCIENCE

Under the supervision of
Dr. Priya S.
Principal scientist



CSIR-National Institute for Interdisciplinary
Science and Technology (CSIR-NIIST), Thiruvananthapuram,
Kerala-695019, India



Academy of Scientific and Innovative Research
AcSIR Headquarters, CSIR-HRDC campus
Sector 19, Kamla Nehru Nagar,
Ghaziabad, U.P. – 201 002, India

July 2023



राष्ट्रीय अंतर्विषयी विज्ञान तथा प्रौद्योगिकी संस्थान NATIONAL INSTITUTE FOR INTERDISCIPLINARY SCIENCE AND TECHNOLOGY

वैज्ञानिक तथा औद्योगिक अनुसंधान परिषद्
इन्डस्ट्रियल एस्टेट पी.ओ., पाप्पनकोड, तिरुवनंतपुरम, भारत - 695 019

Council of Scientific & Industrial Research
Industrial Estate P.O., Pappanamcode, Thiruvananthapuram, India - 695 019

CERTIFICATE

This is to certify that the work incorporated in this Ph.D. thesis entitled, "***In vitro* studies on the effects of bioactives from quinoa and amaranth seeds against breast cancer and inflammation**" submitted by **Taniya. M. S** to the Academy of Scientific and Innovative Research (AcSIR) in fulfillment of the requirements for the award of the Degree of **Doctor of Philosophy in science**, embodies original research work carried-out by the student. We, further certify that this work has not been submitted to any other University or Institution in part or full for the award of any degree or diploma. Research material(s) obtained from other source(s) and used in this research work has/have been duly acknowledged in the thesis. Image(s), illustration(s), figure(s), table(s) etc., used in the thesis from other source(s), have also been duly cited and acknowledged.

Taniya. M.S

Date: 17/7/2023

Dr. Priya.S

Date: 17/7/2023



डॉ. प्रिया. एस / Dr. PRIYA. S
प्रधान वैज्ञानिक/Principal Scientist
कृषी संसाधन एवं प्राकृतिक उत्पाद प्रभाग
Agro Processing and Technology Division
सी एस आई आर - राष्ट्रीय अंतर्विषयी विज्ञान तथा प्रौद्योगिकी संस्थान
CSIR-National Institute for Interdisciplinary
Science and Technology (NIIST), Govt. of India
तिरुवनन्तपुरम/Thiruvananthapuram-695019

STATEMENTS OF ACADEMIC INTEGRITY

I Taniya. M. S., a Ph.D. student of the Academy of Scientific and Innovative Research (AcSIR) with Registration No. 10BB17J39009 hereby undertake that, the thesis entitled "*In vitro* studies on the effects of bioactives from quinoa and amaranth seeds against breast cancer and inflammation" has been prepared by me and that the document reports original work carried out by me and is free of any plagiarism in compliance with the UGC Regulations on "*Promotion of Academic Integrity and Prevention of Plagiarism in Higher Educational Institutions (2018)*" and the CSIR Guidelines for "*Ethics in Research and in Governance (2020)*".



Date : 17/07/2023

Place : Thiruvananthapuram

It is hereby certified that the work done by the student, under my/our supervision, is plagiarism-free in accordance with the UGC Regulations on "*Promotion of Academic Integrity and Prevention of Plagiarism in Higher Educational Institutions (2018)*" and the CSIR Guidelines for "*Ethics in Research and in Governance (2020)*".



Name : Dr. Priya S

Date : 17/7/2023

Place : Thiruvananthapuram



डॉ. प्रिया. एस / Dr. PRIYA. S
प्रधान वैज्ञानिक/Principal Scientist
कृषी संसाधन एवं प्राकृतिक उत्पाद प्रभाग
Agro Processing and Technology Division
सी एस आई आर - राष्ट्रीय अंतरविषयी विज्ञान तथा प्रायोगिकी संस्थान
CSIR-National Institute for Interdisciplinary
Science and Technology (NIIST), Govt. of India
Thiruvananthapuram-695019

DECLARATION

I, Taniya M. S, bearing AcSIR Registration No. 10BB17J39009 declare:

- (a) that the plagiarism detection software is currently not available at my work-place institute.
- (b) that my thesis entitled, “**In vitro studies on the effects of bioactives from quinoa and amaranth seeds against breast cancer and inflammation**” is plagiarism free in accordance with the UGC Regulations on “*Promotion of Academic Integrity and Prevention of Plagiarism in Higher Educational Institutions (2018)*” and the CSIR Guidelines for “*Ethics in Research and in Governance (2020)*”.
- (c) that I would be solely held responsible if any plagiarised content in my thesis is detected, which is violative of the UGC regulations 2018.



Date : 17/07/2022

Place : Thiruvananthapuram

Acknowledgement

This thesis is the outcome of a joint endeavor by every person who helped me throughout my education and made me capable of achieving my dreams. At this time, I would like to thank everyone who helped and supported me along the way.

Without a doubt, the first person to be acknowledged and given credit for this work is my research supervisor, Dr. Priya S, Principal Scientist, CSIR-NIIST for giving me excellent guidance and unwavering attention till the end of my PhD journey. She was very approachable and generous with her time in troubleshooting every single issue in the experiments. She has also provided the resources required for the advancement of my research work.

I'm grateful to Dr. C. Anandharamakrishnan and Dr. A. Ajayaghosh, the current and former directors of CSIR-NIIST, for considering me worthy of working at this reputed CSIR laboratory and for a serene environment that allowed me to complete my research work. I am deeply indebted to the present and former heads of the Agro-processing and Technology division Er. Venugopal VV, Dr Raghu KG and Dr. Dileep Kumar BS for their immense support and encouragement. I would especially like to express my gratitude to Dr. Raghu KG for all of his amazing support and friendly guidance along the way.

I am extremely grateful to my doctoral advisory committee members Dr. Dileep Kumar BS, Dr. Raghu K G and Dr. Kaustabh Kumar Maiti for their timely suggestions, good advice, support and constructive criticism which greatly helped to improve my research project. My sincere thanks to the AcSIR coordinators Dr. Karunakaran V, Dr. Suresh CH, and Dr. Luxmi Varma for helping me out with the AcSIR formalities.

I am very thankful to Dr. Tripti Mishra, APTD for helping with LCMS data analysis. My sincere thanks to Mr. Dhanesh M (NEXLIFE) to carry out the NGS analysis. I am also grateful to Dr. Sandya S (IISc Bangalore) for ESI-QTOF-MS and LCMS analysis. I would like to extend my sincere thanks to Dr. Binod P, MPTD and his team member Dr. Anju Thomas for performing the HPLC analysis. I would like to thank all other scientists and technical assistants of the Agro-processing and technology division for their support and help.

I also express my gratitude to all the staff members of CSIR-NIIST (administrative, academic program committee, IT lab, library, etc..) who helped me in one or the other way to have a comfortable campus life during my tenure. My sincere thanks to Mr. Pratheesh and Mr. Sreejith for their helping hands and technical assistance.

My heartfelt thanks to my research group Dr. Shilpa G, Dr. Lakshmi S, Mr. Ashin M Ms. Asheela and Mrs. Anusree for their support, encouragement, and friendship. I would be amiss if I didn't mention my junior Anusha for her immense support and friendship during this journey. Many thanks to all my friends and seniors especially

Dr. Anupama, Dr. Sindhu G., Dr. Vandana, Mrs. Liza, Mrs. Evelin, Dr. Sruthi, Ms. Gopika, Mrs. Roopasree, Mrs. Sannya, Mrs. Nidhina, Ms. Raveena, Dr. Lakshmi Krishnan, Dr. Vishnu Priya, Dr. Jesmina, Dr. Lekshmi Sunder, Dr. Surya Lakshmi, Dr. Poornima, Mr. Billu Abraham, Dr. Salin Raj, Dr. Preetha Rani, Dr. Sreelakshmi Mohan, Mr. Shyam, Dr. Shyni G.L., Dr. Genu George, Dr. Nayana and all my lab mates.

I am extremely thankful to the Academy of Scientific and Innovative Research (ACSIR) for enrolling me in their PhD program. I am very much indebted to the Council of Scientific and Industrial Research (CSIR) for providing research fellowships (JRF & SRF). I duly acknowledge the financial assistance provided by the Kerala State Council for Science, Technology, and Environment (KSCSTE, Govt. of Kerala) and the Science and Engineering Research Board (SERB) for carrying out my research studies.

At this point of accomplishment, words cannot express my gratitude towards my mother Dency Anto and my grandmother Late Lilly C.G. for their strong aspiration and immense support throughout my life. Their academic carrier and guidance helped me to dream big. Also, I want to express my gratitude to my family in-law's pappa and mummy especially the little smiling face of my nephews, for their presence and prayers, which helped me relax and focused throughout my hectic writing period.!

I am most grateful to my better half Job Joseph without his support, love and care, I can't imagine accomplishing such a feat. I am also grateful to my baby Kaitlyn, for cooperating and understanding my busy schedule. Above all, I would thank the lord almighty for giving me strength and power throughout all the challenging moments of completing this thesis.

Certainly, several people have helped to complete this work. I thank the ones whose contributions I may not have mentioned here.

Taniya. M. S

Dedicated to my mother Dency Anto K

TABLE OF CONTENTS

List of tables	xv
List of Figures	xvii
Abbreviations	xxi
INTRODUCTION	1
CHAPTER 1: Review of Literature	7
1.1. Diet in human health	7
1.2. Pseudocereals; thinking out of cereal box	7
1.2.1. Exploring the healthful amaranth grain	8
1.2.1.1. Morphological characteristics of amaranth seed	8
1.2.1.2. Major bioactive components in amaranth seeds	9
1.2.1.2.1. Protein	9
1.2.1.2.1.2. Lipids	9
1.2.1.2.1.3. Minerals and vitamins	9
1.2.1.2.1.4. Carbohydrates	10
1.2.1.2.1.5. Antinutritional elements	10
1.2.1.3. Health Benefits of amaranth grain	10
1.2.2. Exploring the healthful quinoa grain	13
1.2.2.1. Morphological characteristics of Quinoa seed	13
1.2.2.2. Major bioactive components in quinoa seed	14
1.2.2.2.1. protein	14
1.2.2.2.2. Carbohydrates	14
1.2.2.2.3. Lipids	14
1.2.2.2.4. Minerals and vitamins	15
1.2.2.2.5. Antinutritional elements	15
1.2.2.3. Health Benefits of quinoa grain	16
1.3. Breast cancer	17
1.3.1. Lifestyle and risk factors of breast cancer	18
1.3.2. Pathogenicity	18

1.3.3. The most aggressive Triple-negative breast cancer	19
1.3.4. Emergence of bioactive peptides against cancer	20
1.4. Inflammation	22
1.4.1. Acute inflammation	22
1.4.2. Chronic inflammation	22
1.4.3. Inflammation mediators	23
1.4.3.1. Vasoactive amines	23
1.4.3.2. Vasoactive peptides	23
1.4.3.3. Cytokines	23
1.4.3.4. Chemokines	23
1.4.3.5. Fragments of complement components	24
1.4.3.6. Lipid mediators and proteolytic enzymes	24
1.4.4. Major receptors in inflammation	24
1.4.5. Major activated pathways during inflammation- TLR and NF- κ B signalling pathways	25
1.4.6. Aetiology	25
1.4.7. Chronic inflammation diseases	26
1.4.7.1. Neurological diseases	26
1.4.7.2. Obesity	26
1.4.7.3. Fibrosis	26
1.4.7.4. Post-Covid illnesses	27
1.4.7.5. Asthma	27
1.4.7.6. Inflammatory bowel disease (IBD)	27
1.4.7.7. Cancer	28
1.4.8. Anti-inflammatory medications	28
1.4.9. Secondary metabolites- anti-inflammatory agents	29
1.5. Objective of the present study	31
1.6. Cell lines used for the present study	31
1.7. Standard drugs used for the present study	32
1.8. References	32

CHAPTER 2: Materials and Methods	41
2.1. MATERIALS	41
2.1.1. Cell lines and cell culture essentials	41
2.1.2. Chemicals and Biochemicals	41
2.1.3. Antibodies	41
2.1.4. Assay Kits	42
2.2. METHODOLOGY	42
2.2.1. Isolation of proteins by ammonium sulphate precipitation	42
2.2.2. Estimation of proteins by Lowry method	43
2.2.3. Simulated gastrointestinal digestion of proteins	43
2.2.4. Essential amino acid analysis	44
2.2.5. Mass spectrometry and functional analysis of peptides	44
2.2.6. Isolation of secondary metabolites from amaranth and quinoa seeds	45
A. Sequential extraction (Soxhlet method)	45
B. Direct extraction (Soxhlet method)	46
2.2.7. Assay of Total Antioxidant Capacity by Phosphomolybdenum method	46
2.2.8. Free radical scavenging activity Assay by DPPH method	46
2.2.9. Analysis of total phenolic content	46
2.2.10. Anticancer studies: Cell culture and maintenance	47
2.2.11. Cytotoxicity analysis by MTT assay	47
2.2.12. Cellular morphology analysis using phase contrast microscopy	48
2.2.13. Nuclear fragmentation analysis using DAPI staining	48
2.2.14. Analysis of plasma membrane damage using Acridine orange/ethidium bromide (AO/EtBr) dual staining	49
2.2.15. Phosphatidylserine translocation assay by Annexin V staining	49
2.2.16. Caspase 3 assay	50
2.2.17. Scratch wound assay	50
2.2.18. Human apoptosis antibody array analysis	50
2.2.19. Anti-inflammatory studies: Cell culture maintenance and treatment	52
2.2.20. Nitric Oxide analysis	52
2.2.21. RNA sequencing (RNA-Seq) and Analysis	53

A. RNA Isolation	53
B. RNA Integrity Check	54
C. RNA Quantification	54
D. Enrichment of mRNA and development of libraries	54
E. Quantification of Libraries	55
F. Validation of Libraries	55
G. Next-generation sequencing analysis	55
H. Alignment and Expression analysis	56
I. Differential expression analysis	56
J. Heatmap generation	56
K. Volcano plot generation	56
L. Protein-protein interaction (PPI) networks visualisation and cluster detection	56
M. Discovery of hub genes	57
N. Gene Enrichment analysis	57
O. Gene ontology	57
P. Pathway analysis	57
2.2.22. Enzyme-linked immunosorbent assay	57
2.2.23. ROS analysis	58
2.2.24. Cell lysate preparation	59
2.2.25. Immunoprecipitation	59
2.2.26. Western blot analysis	59
2.2.27. Immunofluorescence analysis	60
2.2.28. Cytokine array analysis	61
2.2.29. Statistical Analysis	62
2.2.30. References	63
CHAPTER 3: isolation of bioactive peptides and secondary metabolites from amaranth and quinoa seeds and their screening for antioxidant, in vitro anti-breast cancer and in vitro anti-inflammatory properties	65
3.1. Introduction	65

3.2. Methodology	66
3.3. Results	67
3.3.1. Protein isolation by Ammonium sulphate precipitation	67
3.3.2. In vitro gastrointestinal digestion of isolating peptides from amaranth and quinoa seeds	67
3.3.3. Isolation of bioactive molecules rich extract from amaranth and quinoa seeds by sequential extraction and direct soxhlet extraction	68
3.3.4. Antioxidant analysis of protein isolates and solvent extracts of amaranth and quinoa seeds	69
3.3.4.1. DPPH free radical scavenging analysis of protein isolates of amaranth and quinoa seeds	69
3.3.4.2. Total antioxidant activity of protein isolates of amaranth and quinoa seeds	69
3.3.4.3. DPPH free radical scavenging analysis of solvent extracts of amaranth and quinoa seeds	69
3.3.4.4. Total antioxidant activity of solvent extracts of amaranth and quinoa seeds	70
3.3.4.5. Phenolic contents in solvent extracts of amaranth and quinoa seeds	70
3.3.5. Anti-breast cancer analysis of protein isolates and solvent extracts of amaranth and quinoa seeds	71
3.3.5.1. Cytotoxicity analysis of protein isolates of amaranth and quinoa seeds	71
3.3.5.2. Cytotoxicity analysis of solvent extracts of amaranth and quinoa seeds	72
3.3.5.3. Morphology analysis of protein hydrolysates and solvent extracts of amaranth and quinoa seeds	72
3.3.6. Anti-inflammatory activity of protein isolates and solvent extracts of amaranth and quinoa seeds	73
3.3.6.1. The effects of protein hydrolysates of amaranth and quinoa seeds on anti-inflammatory activity	73
3.3.6.2. The effects of solvent extracts of amaranth and quinoa seeds on anti-inflammatory activity	74
3.4. Discussion	76
3.5. Conclusion	78
3.6. References	79

CHAPTER 4: In vitro evaluation of the anti-breast cancer potential of Amaranth bioactive peptides against MDA-MB-231 cells	83
4.1. Introduction	83
4.2. Methodology	84
4.3. Results	85
4.3.1. Effects of ASP-HD on the cell viability of MDA-MB-231	85
4.3.2. Effect of ASP-HD on cellular morphology of MDA-MB-231	85
4.3.3. Effects of ASP-HD on nuclear fragmentation	86
4.3.4. Effects of ASP-HD on the loss of membrane integrity	87
4.3.5. Effects of ASP-HD on phosphatidylserine translocation	87
4.3.6. Effects of ASP-HD on caspase-3 activation	88
4.3.7. Effects of ASP-HD on the expression of apoptotic proteins	89
4.3.8. Effects of ASP-HD on cellular migration	89
4.3.9. Comparison of the essential amino acid contents in ASP, ASP-D and ASP-HD	90
4.3.10. Peptide sequencing of ASP-HD and functional analysis by Gene Ontology	90
4.4. Discussion	92
4.5. Conclusion	94
4.6. References	94
CHAPTER 5: Next generation sequencing and analysis of genes and pathways responsible for the anti-inflammatory activity of methanolic extract of quinoa seeds in RAW cells	
5.1. Introduction	97
5.2. Methodology	99
5.3. Results	100
5.3.1. Total RNA and quality checking	100
5.3.2. mRNA Enrichment and Library Preparation and quality checking	100
5.3.3. NGS data quality checking	101
5.3.5. Functional annotation of differentially expressed genes	102
5.3.5.1. Screening of differentially expressed genes	102
5.3.5.2. Protein-protein interaction network and topological analysis	104

5.3.5.3. Hub Gene Evaluation	105
5.3.5.4. Analysis of GO Function and KEGG Enrichment of Related Targets	106
5.4. Discussion	111
5.5. Conclusion	114
5.6. Reference	114

CHAPTER 6: In vitro validation studies of specific cytokines and regulatory molecules responsible for the anti-inflammatory activity of quinoa extract 119

6.1. Introduction	119
6.2. Methodology	120
6.3. Results	121
6.3.1. Effects of Q-80M on the release of pro and anti-inflammatory cytokines in LPS stimulated RAW264.7 cells	121
6.3.2. Effects of Q-80M on LPS-induced iNOS and COX-2 overexpression in RAW 264.7 cells	121
6.3.3. Effects of Q-80M on LPS-induced ROS generation in RAW cells	122
6.3.4. Effects of Q-80M on the expression of Toll-like receptors	123
6.3.5. Effects of Q-80M on LPS-induced NF- κ B nuclear translocation	124
6.3.6. Effects of Q-80M on the degradation of I κ B- α	125
6.3.7. Effects of Q-80M on anti-inflammatory and proinflammatory cytokines	126
6.3.8. Identification of bioactive compounds from Q-80M extract by LC-MS analysis	126
6.4 Discussion	129
6.5 Conclusion	132
6.6 References	133

CHAPTER 7: SUMMARY AND CONCLUSION 139

LIST OF TABLES

Table No.	Title	Page No.
Chapter 1- Review of literature		
Table 1.1	Health benefits of Amaranth seeds evaluated by in vitro and in vivo methods	11
Table 1.2	Health benefits of Quinoa evaluated by in vitro and in vivo methods	16
Table 1.3	List of anticancer bio-peptides	20
Table 1.4	Anti-inflammatory compounds from natural sources	29
Chapter 3- Isolation of bioactive peptides and secondary metabolites from Amaranth and Quinoa seeds and their screening for in vitro antioxidant, anti-breast cancer and anti-inflammatory effects		
Table 3.1	Cytotoxicity of amaranth and quinoa seed protein isolates and solvent extracts in MDA-MB-231 cells.	72
Table 3.2	Cytotoxicity of amaranth and quinoa seed protein isolates against RAW 264.7 cell.	73
Chapter 5- Identification of genes and pathways responsible for the anti-inflammatory activity of Quinoa extract (Q-80M) through NGS analysis		
Table 5.1	Complete quality checking status of total RNA	100
Table 5.2	The complete library validation report of samples	101
Table 5.3	Raw sequence data and its quality	101
Table 5.4	Read alignment statistics	102
Table 5.5	Number of Differentially expressed genes	103

LIST OF FIGURES

Figure No.	Title	Page No.
Chapter 1: Review of Literature		
Figure 1.1	Amaranth and quinoa seeds	7
Figure 1.2	Seeds structure of amaranth and quinoa	8
Figure 1.3	Breast cancer incidence in the world population	17
Figure 1.4	Stages of breast cancer	19
Figure 1.5	TLR and NFκB Pathways during Inflammation	25
Figure 1.6	Mechanisms of action of functional foods on cancer and inflammation	30
Chapter 3: Isolation of bioactive peptides and secondary metabolites from Amaranth and Quinoa seeds and their screening for in vitro antioxidant, anti-breast cancer and anti-inflammatory effects		
Figure 3.1	Protein isolation and in vitro simulated gastrointestinal of amaranth and quinoa seeds	67
Figure 3.2	Direct and sequential extraction of amaranth and quinoa seeds	68
Figure 3.3	DPPH radicals scavenging activity of amaranth and quinoa seeds protein hydrolysates	69
Figure 3.4	Total antioxidant activity of amaranth and quinoa seeds protein hydrolysates	70
Figure 3.5	DPPH radicals were the scavenging activity of amaranth and quinoa seeds solvent extracts	70
Figure 3.6	Total antioxidant activity of amaranth and quinoa seeds solvent extracts	71
Figure 3.7	Total polyphenol content in amaranth and quinoa seeds solvent extracts	71
Figure 3.8	Morphological alterations in breast cancer cells by amaranth and quinoa seed solvent extracts	73
Figure 3.9	NO reduction capacity of amaranth and quinoa seed protein hydrolysates in LPS-induced RAW 264.7 cells	74
Figure 3.10	Cytotoxicity of amaranth and quinoa solvent extracts in RAW cells	74
Figure 3.11	NO reduction capacity of amaranth and quinoa seed solvent extracts in LPS-induced RAW 264.7 cells	75
Figure 3.12	Cytotoxicity of AM and Q-80M in RAW 264.7 cells	75

Figure 3.13	Effect of AM and Q-80M extracts on NO production in LPS-induced RAW 264.7 cells.	76
Chapter 4: <i>In vitro</i> evaluation of the anti-breast cancer potential of Amaranth bioactive peptides (ASP-HD) against MDA-MB-231 cells		
Figure 4.1	Effect of amaranth seed protein hydrolysates in MDA-MB-231 cells	85
Figure 4.2	Morphological alterations in breast cancer cells by ASP-HD	86
Figure 4.3	<i>Effects of ASP-HD on nuclear fragmentation</i>	86
Figure 4.4	Effects of ASP-HD on the loss of membrane integrity	87
Figure 4.5	Effects of ASP-HD on phosphatidylserine translocation	88
Figure 4.6	Effects of ASP-HD on caspase3 activation	88
Figure 4.7	Effects of ASP-HD on the expression of apoptotic proteins	89
Figure 4.8	Effects of ASP-HD on cellular migration	90
Figure 4.9	Comparison of the essential amino acid contents in ASP, ASP-D and ASP-HD	91
Figure. 4.10	Functional annotation analysis of ASP-HD	91
Chapter 5: Identification of genes and pathways responsible for the anti-inflammatory activity of Quinoa extract (Q-80M) through NGS analysis		
Figure 5.1	Workflow of mRNA-seq data analysis and functional annotation	100
Figure 5.2	Heat map and volcano plot of control versus Inflammation	103
Figure 5.3	Heat map and volcano plot of Inflammation versus Q80-M treatment	104
Figure 5.4	Protein-protein interaction networks and cluster genes of the control versus inflammation	105
Figure 5.5	Protein-protein interaction networks and cluster genes of the inflammation versus Q80-M pretreatment	105
Figure 5.6	Top ten hub genes of Inflammation control versus inflammation	106
Figure 5.7	Top ten hub gene of Inflammation versus Q80-M pretreatment	106

Figure 5.8	Bubble plot of GO analysis- Control versus Inflammation	107
Figure 5.9	Bubble plot of GO analysis Inflammation versus Q-80M pretreatment	108
Figure 5.10	The comparison of control versus inflammation and inflammation versus Q-80M pretreatment in Cytokine-cytokine receptor interaction pathway	108
Figure 5.11	The comparison of control versus inflammation and inflammation versus Q-80M pretreatment in the TNF signalling pathway	109
Figure 5.12	The comparison of control versus inflammation and inflammation versus Q-80M pretreatment in the Chemokine signalling pathway	109
Figure 5.13	The comparison of control versus inflammation and inflammation versus Q-80M pretreatment in NOD-like receptor signalling pathway	110
Figure 5.14	The comparison of control versus inflammation and inflammation versus Q-80M pretreatment in NF- κ B signalling pathway	110
Figure 5.15	Significantly downregulated genes in Inflammation versus Q-80M pretreatment	111
Chapter 6: <i>In vitro</i> validation studies of specific cytokines and regulatory molecules responsible for the anti-inflammatory activity of Q-80M extract		
Figure 6.1	The effect of Q-80M on cytokines	122
Figure 6.2	Effects of Q80-M on the overexpression of COX-2 and iNOS in LPS-simulated RAW cells.	123
Figure 6.3	Effects of Q80-M on LPS-stimulated ROS production in RAW 264.7 cells.	124
Figure 6.4	The effect of Q80-M on TLR4 activation in LPS-induced RAW 264.7 cells.	125
Figure 6.5	The effect of Q-80M on nuclear translocation of NF- κ B	126
Figure 6.6	Effect of Q-80M on I κ B α degradation	127
Figure 6.7	Effect of Q-80M on LPS-induced cytokine in RAW264.7 cell line by cytokine array experiment.	128
Figure 6.8	Bioactive compounds identified in Q-80M extract by LC/ESI-MS analysis.	128
Figure 6.9	Summary of the effects of Q-80M on LPS-induced RAW264.7 cells	132

Chapter 7: Summary and Conclusion		
Figure 7.1	Summary of the preliminary screening of protein hydrolysates and solvent extracts	140
Figure 7.2	Summary of anti-breast cancer activity of ASP-HD with the EAA content and the functional annotation	141
Figure 7.3	Summary of the anti-inflammatory activity of Q-80M by whole genome transcriptomic analysis	142
Figure 7.4	Summary of the anti-inflammatory activity of Q-80M by experimental validation	143

LIST OF ABBREVIATIONS

A-80M	Amaranth seed 80% methanol extract (direct extraction)
ABTS	2,2'-azino-bis (3-ethylbenzothiazoline-6-sulfonic acid)
AEA	Amaranth seed ethyl acetate extract (sequential)
AH	Amaranth seed hexane extract (sequential)
AM	Amaranth seed methanol extract (sequential)
AO	Acridine orange
ASP	Amaranth seed crude protein
ASP-D	Amaranth seed protein digested
ASP-HD	Amaranth seed protein digested after heat denaturation
BBB	Blood-brain barrier
BC	Breast cancer
Bcl-2	B-cell leukaemia/lymphoma-2
BRCA2	Breast cancer type 2 susceptibility protein
BRCA1	Breast cancer type 1 susceptibility protein
CD	Crohn's disease
Cdk1	Cyclin-dependent kinase 1
cDNA	Complementary DNA
CNS	Central nervous system
COX	Cyclooxygenase
CRP	C-reactive protein
DAPI	4',6-diamidino-2-phenylindole
DCFDA	2',7'-dichlorofluorescein diacetate
DEG	Differentially expressed genes
DMEM	Dulbecco's Modified Eagle Medium
DMSO	Dimethyl sulfoxide
DPPH	2,2-diphenyl-1-picrylhydrazyl
EAA	Essential amino acids
EC ₅₀	Effective concentration
EDTA	Ethylene diamine tetra acetic acid

EGFR	Epidermal growth factor receptor
ELISA	Enzyme-linked immunosorbent assay
ELISA	Enzyme-linked immunosorbent assay
ER	Estrogen receptors
EtBr	Ethidium bromide
FAO	Food and Agriculture Organization
FBS	Fetal bovine serum
FGFR1	Fibroblast growth factor receptor 1
FRAP	Ferric reducing antioxidant power
GAE	Gallic Acid Equivalent
GM-CSFR	Granulocyte-macrophage colony-stimulating factor receptor
GO	Gene Ontology
GPCRs	G protein-coupled receptors
HDAC1	Histone deacetylases
HER2	Human epidermal growth factor receptor 2
HPLC	High-performance liquid chromatography
HRP	Horseradish peroxidase
IBD	Inflammatory bowel disease
IF	Immunofluorescence
IKK	I kappa B kinase
IL	Interleukin
iNOS	Inducible nitric oxide synthase
JAK	Janus kinases
KDa	Kilodaltons
KEGG	Kyoto Encyclopedia of Genes and Genomes
LDL-c	Low-Density Lipoprotein Cholesterol
miRNA	Micro-Ribonucleic Acid
mTOR	mammalian target of rapamycin
MTT	3-(4,5-Dimethylthiazol-2-yl)-2,5-diphenyl tetrazolium bromide
NGS	Next-generation sequencing

NO	Nitric oxide
NOX4	NADPH oxidase 4
NSAIDs	Nonsteroidal anti-inflammatory medicines
ORAC	Oxygen Radical Absorbance Capacity
PAMP	Pathogen-associated molecular patterns
PARP	Poly (ADP-ribose) polymerase
PMSF	Phenylmethanesulfonyl fluoride
PPI	Protein-protein interaction
PR	Progesterone receptors
PS	Phosphatidylserine
PSCg	Pseudocereal grains
PTEN	Phosphatase and tensin homolog
PVP	Polyvinylpyrrolidone
Q-80M	Quinoa seed 80% methanol extract (direct extraction)
QC	Quality checking
QEA	Quinoa seed ethyl acetate extract (sequential)
QH	Quinoa seed hexane extract (sequential)
QM	Quinoa seed methanol extract (sequential)
QSP	Quinoa seed crude protein
QSP-D	Quinoa seed protein digested
QSP-HD	Quinoa seed protein digested after heat denaturation
RB	Retinoblastoma protein
ROS	Reactive oxygen species
RT	Room temperature
siRNA	Small interfering RNA
STAT	Signal transducer and activator of transcription
TGF- β 1	Transforming Growth Factor-Beta
Th	Helper T cells
TLR4	Toll-like receptor 4
TNBC	Triple-negative breast cancer

TNF- α	Tumour necrosis factor-alpha
TP53	Tumor protein p53
UC	Ulcerative colitis
WHO	World Health Organization

INTRODUCTION

Food is one of the most essential factors in life. It is the ideal vehicle for delivering all the required nutrients to the human body. Our diets must be nutritionally well-balanced and sufficient to supply enough energy, protein, fat, carbs, vitamins, minerals, dietary fibre and water (Cena & Calder, 2020). Although conventional cereals don't offer a balanced diet, they necessitate additional sources of these nutrients (Rodríguez et al., 2020). Moreover, the human population's food requirement graph is rising daily. By 2030, food demand will increase between 35-65%. Many research projects are underway to find an alternative food supply for this global issue (van Dijk et al., 2021). Pseudocereals have met the requirements for being an alternate food source as per the studies. They possess intriguing nutritional qualities and they are resilient crops that quickly adapt to a new environment with high grain yield with less production time (Jan et al., 2023). The nutritional composition of pseudocereal seeds includes carbohydrates (66-68%), fibre (11-12%), protein (15-17%), and fat (6-10%). Compared to conventional cereals, they offer a higher nutritional profile (Pseudogetreide & Schoenlechner, 2016). In many Western nations, rice has been replaced by amaranth and quinoa seed (Martínez-Villaluenga et al., 2020). The cultivation of pseudocereals began 5000 years ago, and ancient civilisations (Inca, Maya, and Aztecs) used it as a sacred staple meal (Orona-Tamayo et al., 2019). Now, the cultivation of pseudocereals has spread globally from the United States to other continents including Europe and Asia (such as China and India). The total production of pseudocereals has increased by almost thrice between 2000 and 2016, from 52.6 thousand tonnes to 148.7 thousand tons (Gil-ramirez et al., 2018). Food products like bread, Chinese steamed bread, pasta, nibbles, biscuits, edible films, drinks, and food-grade packaging materials are made from amaranth and quinoa seeds. Due to its gluten-free status, it has become a more appealing substitute for regular cereals (Tang & Tsao, 2017).

Pseudocereals are a reliable source of plant-based protein, especially for vegan diets. Among pseudocereals, the most commonly used seeds are amaranth and quinoa. Amaranth and quinoa seeds contain all nine essential amino acids. Compared to other plant proteins, pseudo-cereal proteins have superior bioavailability and are similar to animal proteins (Alvarez-Jubete et al., 2009). Amaranth and quinoa seed are rich in protein. Proteins have a great role in growth and development. Protein-derived biopeptides have opened up new therapeutic avenues, due to their small size and specific interaction with cell organelles without causing any adverse consequences (Saadi et al., 2015). Like proteins, amaranth and quinoa seeds are good sources of phytochemicals. These seeds contain high levels of phenols, flavonoids, terpenes, and nitrogen-containing chemicals. Phytochemical research is being extensively conducted to treat detrimental diseases such as cancer, chronic inflammation, diabetes, and others (López et al., 2019).

Cancer is one of the deadliest diseases. About 10 million people die every year due to cancer. By 2040, that number is anticipated to increase by 50%. Breast cancer was the most prevalent type of cancer in 2020, with 2.3 million women diagnosed and 68500 deaths reported. The most aggressive and highly metastatic breast cancer subtype is triple-negative breast cancer (TNBC)(Harbeck et al., 2019). TNBC lacks oestrogen, progesterone, and ERBB2 receptor expression, which makes it exceptionally invasive and less responsive to therapy. TNBC has no specific therapeutic methods other than chemotherapy. Many kinds of research are conducted to treat TNBC with fewer side effects (Medina et al., 2020).

Chronic inflammation is another disease with detrimental effects. Acute inflammation is beneficial to health. It protects the human body against infection and injuries. Long-term inflammation causes the loss of immunological tolerance and leads to tissue damage by inflammatory mediators and cytokine production (L. Kiss, 2022). Eventually, this will lead to chronic inflammation. Chronic inflammation accounts for more than half of all deaths worldwide. It has been identified as the underlying cause of a wide range of diseases, including cardiovascular, neurological, and gastrointestinal disorders, diabetes, arthritis, fibrosis, and cancer (Wang et al., 2021). The scientific community has focused on finding selective inhibitors to prevent inflammation. The safety of utilising the available non-steroid anti-inflammatory drugs has come under question because of the considerable risk of stroke, cardiac issues, renal failure, and arterial hypertension (Bindu et al., 2020).

In this background, we undertake our research using nutrient-rich amaranth and quinoa seeds because they are rich sources of phytochemicals and bioactive peptides, have few adverse effects, and may have the ability to target specific treatments. The current work investigates the *in vitro* anticancer and anti-inflammatory activities of amaranth and quinoa seeds. The isolated biopeptides and bioactive-rich solvent extracts were isolated from amaranth and quinoa seeds. These extracts were evaluated for their antioxidant, anticancer, and anti-inflammatory activities. Based on our research, we discovered a biopeptide extract that effectively kills triple-negative breast cancer MDA-MB-231 cells. Additionally, we discovered an extract with potent anti-inflammatory activity against LPS-induced NO generation. We investigated the anti-breast cancer effectiveness of biopeptides in terms of their apoptotic characteristics and cell migration. In parallel, we investigated the genomic expression regulation of extracts with anti-inflammatory activity. We also confirm the extract's anti-inflammatory effects on cytokine and inflammation-regulating molecules.

Chapter 1: Review of Literature

This chapter gives a general overview of the importance of diet and explores the healthfulness of pseudocereals, especially on the amaranth and quinoa seeds. A brief look at two serious diseases such as breast cancer and chronic inflammation with their epidemiology, aetiology, and medications. This chapter provides a list of natural biopeptides and plant extracts that fight against cancer and inflammation.

Chapter 2: Materials and Methods

This chapter describes the overview of materials, detailed experimental protocols, and statistical data analysis.

Chapter 3: Isolation of bioactive peptides and secondary metabolites from Amaranth and Quinoa seeds and their screening for *in vitro* antioxidant, anti-breast cancer and anti-inflammatory effects

This chapter deals with the isolation of proteins and their bioactive peptides generated by *in vitro* simulated gastrointestinal digestion. It also describes the isolation of bioactive extracts from amaranth and quinoa seeds using direct and sequential soxhlet extraction. All the biopeptide isolates and solvent extracts were screened for their *in vitro* antioxidant, anti-inflammatory and anti-breast cancer effects.

Chapter 4: *In vitro* evaluation of the anti-breast cancer potential of Amaranth bioactive peptides (ASP-HD) against MDA-MB-231 cells

This chapter deals with a detailed analysis of the anti-breast cancer effects of amaranth seed protein hydrolysates. From the preliminary screening, ASP-HD showed significant cytotoxicity in MDAMB-231 cells. The apoptotic and anticancer activity of ASP-HD were examined through DNA fragmentation, phosphatidylserine translocation, membrane integrity loss, caspase-3 activity, Apoptosis array and cell migration analysis. We have also done the amino acid analysis to find out the list of essential amino acids in amaranth protein hydrolysates. Also, this chapter contains the results of the mass spectrometry and gene ontology analysis of ASP-HD peptides.

Chapter 5: Next-generation sequencing and analysis of genes and pathways responsible for the anti-inflammatory activity of methanolic extract of quinoa seeds in RAW cells

This chapter provides a detailed transcriptomic study of Q-80M effects on LPS-stimulated RAW cells effects. The preliminary screening assay found that Q-80M (quinoa seed 80% methanol extract, direct extraction) showed significant anti-inflammatory activity in LPS-stimulated RAW 264.7 cells. We performed transcriptome analysis to understand the genes and pathways responsible for the anti-inflammatory effects of Q-80M. Also, this chapter discusses the identification of upregulated and downregulated PPI networks on LPS stimulation and Q80-M pretreatment. Functional annotation analyses revealed the effect of Q-80M on LPS-stimulated inflammation. Also, this chapter discusses the role of Q-80M on major inflammatory pathways and their impact on downregulating inflammation.

Chapter 6: *In vitro* validation studies of specific cytokines and regulatory molecules responsible for the anti-inflammatory activity of Q-80M extract

This chapter confirmed the anti-inflammatory activity of Q-80M extracts on LPS-induced RAW cells. The impact of Q-80M on proinflammatory and anti-inflammatory cytokines, inflammatory enzymes and regulators was examined. Also, this chapter

provides the details of the bioactive molecules present in the anti-inflammatory Q-80M extract.

Chapter 7: Summary and Conclusion

This chapter summarizes the whole findings of the thesis. Also, discuss the future direction of the study.

References

1. Alvarez-Jubete, L., Arendt, E. K., & Gallagher, E. Nutritive value and chemical composition of pseudocereals as gluten-free ingredients. *International Journal of Food Sciences and Nutrition*. 2009; 60(SUPPL.4), 240–257. <https://doi.org/10.1080/09637480902950597>
2. Bindu, S., Mazumder, S., & Bandyopadhyay, U. Non-steroidal anti-inflammatory drugs (NSAIDs) and organ damage: A current perspective. *Biochemical pharmacology*. 2020; 180, 114147. <https://doi.org/10.1016/j.bcp.2020.114147>
3. Cena, H., & Calder, P. C. Defining a healthy diet: Evidence for the role of contemporary dietary patterns in health and disease. *Nutrients*. 2020; 12(2), 1–15. <https://doi.org/10.3390/nu12020334>
4. Gil-ramirez, A., Salas-veizaga, D. M., Grey, C., Nordberg, E., Rodriguez-meizoso, I., & Linares-pastén, J. A. Industrial Crops & Products Integrated process for sequential extraction of saponins, xylan and cellulose from quinoa stalks (*Chenopodium quinoa Willd .*). *Industrial Crops & Products*. 2018; 121(April), 54–65. <https://doi.org/10.1016/j.indcrop.2018.04.074>
5. Harbeck, N., Penault-Llorca, F., Cortes, J., Gnant, M., Houssami, N., Poortmans, P., Ruddy, K., Tsang, J., & Cardoso, F. Breast cancer. In *Nature Reviews Disease Primers* 2019; 5(1). <https://doi.org/10.1038/s41572-019-0111-2>
6. Jan, N., Hussain, S. Z., Naseer, B., & Bhat, T. A. (). Amaranth and quinoa as potential nutraceuticals: A review of anti-nutritional factors, health benefits and their applications in food, medicinal and cosmetic sectors. *Food Chemistry*. 2023; 18 100687. <https://doi.org/10.1016/j.fochx.2023.100687>
7. L. Kiss, A. Inflammation in Focus: The Beginning and the End. *Pathology and Oncology Research*. 2022; 27(January), 1–7. <https://doi.org/10.3389/pore.2021.1610136>
8. López, D. N., Galante, M., Raimundo, G., Spelzini, D., & Boeris, V. Functional properties of amaranth, quinoa and chia proteins and the biological activities

- of their hydrolyzates. *Food Research International*. 2019; 116, 419–429. <https://doi.org/10.1016/j.foodres.2018.08.056>
9. Martínez-Villaluenga, C., Peñas, E., & Hernández-Ledesma, B. Pseudocereal grains: Nutritional value, health benefits and current applications for the development of gluten-free foods. *Food and Chemical Toxicology*. 2020; 111178. <https://doi.org/10.1016/j.fct.2020.111178>
 10. Medina, M. A., Oza, G., Sharma, A., Arriaga, L. G., Hernández, J. M. H., Rotello, V. M., & Ramirez, J. T. Triple-negative breast cancer: A review of conventional and advanced therapeutic strategies. *International Journal of Environmental Research and Public Health*. 2020; 17(6), 1–32. <https://doi.org/10.3390/ijerph17062078>
 11. Orona-Tamayo, D., Valverde, M. E., & Paredes-López, O. Bioactive peptides from selected latin american food crops—A nutraceutical and molecular approach. *Critical Reviews in Food Science and Nutrition*. 2019; 59(12), 1949–1975. <https://doi.org/10.1080/10408398.2018.1434480>
 12. Pseudogetreide, V. Von, & Schoenlechner, R. Properties of pseudocereals, selected speciality cereals and legumes for food processing with special attention to gluten-free products. 2016; 67(4), 239–248. <https://doi.org/10.1515/boku-2016-0019>
 13. Rodríguez, J. P., Rahman, H., Thushar, S., & Singh, R. K. (). Healthy and Resilient Cereals and Pseudo-Cereals for Marginal Agriculture: Molecular Advances for Improving Nutrient Bioavailability. *Frontiers in Genetics*. 2020; 1–29. <https://doi.org/10.3389/fgene.2020.00049>
 14. Saadi, S., Saari, N., Anwar, F., Abdul Hamid, A., & Ghazali, H. M. Recent advances in food biopeptides: Production, biological functionalities and therapeutic applications. *Biotechnology Advances*. 2015; 33(1), 80–116. <https://doi.org/10.1016/j.biotechadv.2014.12.003>
 15. Tang, Y., & Tsao, R. Phytochemicals in quinoa and amaranth grains and their antioxidant, anti-inflammatory, and potential health beneficial effects: a review. *Molecular Nutrition and Food Research*. 2017; 61(7), 1–16. <https://doi.org/10.1002/mnfr.201600767>
 16. van Dijk, M., Morley, T., Rau, M. L., & Saghai, Y. A meta-analysis of projected global food demand and population at risk of hunger for the period 2010–2050. *Nature Food*. 2021; 2(7), 494–501. <https://doi.org/10.1038/s43016-021-00322-9>
 17. Wang, R. X., Zhou, M., Ma, H. L., Qiao, Y. B., & Li, Q. S. The Role of Chronic Inflammation in Various Diseases and Anti-inflammatory Therapies Containing Natural Products. *ChemMedChem*. 2021; 16(10), 1576–1592. <https://doi.org/10.1002/cmdc.202000996>

CHAPTER 1

REVIEW OF LITERATURE

1.1. Diet in human health

Food is the best vehicle to import all the essential nutrients to the human body. So, our diet should be nutritionally well-balanced with protein, fats, carbohydrates, vitamins, minerals, dietary fibre and water. Unbalanced diet consumption leads to malnutrition or overnutrition and manifests in chronic diseases.

The food consumption trend in India has varied over the years; the calorie intake and dependency on plant, dairy and animal-based diets have increased (Vepa 2004). In 2030 global food demand will increase by 35%. The primary agenda of 2030 is the global food security of all the people in the world. International assessments have mainly used four broad indicators to measure the various dimensions of food security: food demand, the people at risk of hunger, food prices and childhood undernutrition (van Dijk et al. 2021). Just three grains - rice, maize and wheat - supply two-thirds of calories and are staple foods for over four billion people. One of the best solutions to this problem is an alternative food source. An alternative food source should satisfy specific criteria like hunger, climate resilience, high production and less water use. Pseudocereals are a readily available food source that fits all the requirements for an alternative food source and can be used as a source of nutrients to fight hunger, increase food production, and boost the nation's economy (Mariutti et al. 2021).

1.2. Pseudocereals; thinking out of cereal box

Around the world, phytonutrient-rich pseudocereal grains (PSCg) are now in trend. They are stapled crops in many civilizations having considerable potential for creating novel food items. In the past few years, gluten-free PSCg production has increased with demand and consumption, especially for celiac patients (Comino et al. 2013). First and foremost, it is important to emphasise their superior nutritional profile when compared to the aforementioned main cereals. It has recently been recognized that PSCg can improve many health benefits. PSCg differ in nutritional constituents like dietary fibre, polyphenols, minerals, vitamins, protein, and amino acid content. They have a lot of bioactive compounds with valuable functional properties (Bene and Constantino. 2022). The story behind the naming of pseudocereal is that they are false



Figure 1.1: Amaranth and quinoa seeds

cereals resembling monocot seeds, but PSCg is a dicotyledon. Amaranth (*Amaranthus spp.*, Amaranthaceae) and quinoa (*Chenopodium quinoa* Wild, Chenopodiaceae) are two of the finest pseudocereals, and their images are given in Figure 1.1 (Ninfali et al. 2020).

1.2.1. Exploring the healthful amaranth grain

Amaranth is an ancient plant from the Amaranthaceae family, believed to have originated from Central and South America. There are roughly 400 distinct types, and 70 different amaranthus species found worldwide, with just a handful being cultivated in various nations. Common species, including *Amaranthus cruentus*, *Amaranthus caudatus*, and *Amaranthus hypochondriacus*, are widely domesticated for grain production and are called "pseudocereals" in the trade. Amaranth is a resilient crop; it grows in different climatic conditions, tolerant to drought, poor soils and pest attacks. It can quickly adapt to a new environment with high grain yield and less production time (Nanak and Resources 2014; N. Kumar et al. 2013).

1.2.1.1. Morphological characteristics of amaranth seed

Amaranth grains are lenticular in shape, small in size (approximately 1mm in diameter), and weight ranges from 0.6–1.2 mg. Its colour varies from light yellow to golden. The seed has four main parts: the seed coat, endosperm, embryo, and perisperm. The embryo of an amaranth seed is campylotropous, i.e., the ends of the embryo are seen closer. The perisperm comprises starch polygonal cells with thin membranes, and the embryo contains globoids (protein-filled storage vacuoles) rich cotyledons and radicle cells (Figure 1.2). Vascular bundles in the radicle are calcium-concentrated salts, likely oxalate. Amaranth seeds germinate faster than cereals because of their extensive vascular system arranged as a hexagonal network surrounding each cell to drain water and nutrients to the root (Ninfali et al., 2020; Aderibibe et al., 2022).

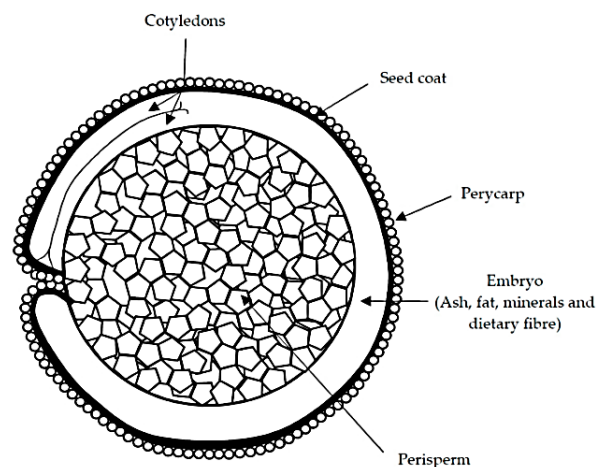


Figure 1.2: Seeds structure of amaranth and quinoa, Data source: Alonso-Miravalles and O'Mahony 2018

1.2.1.2. Major bioactive components in amaranth seeds

1.2.1.2.1. Protein

Amaranth seed has great protein contents, ranging from 11.9% to 19.01% (Akin Idowu et al., 2013). Amaranth seed contains around 65% albumin, 17% globulin, 11% prolamin, and 7% glutelin. Depending on the extraction technique, the number of fractions in the separated protein and its nutritional and functional qualities may vary. Amaranth protein is highly digestible (90%) and has greater bioavailability, which are significant factors to consider in their protein quality. Sulphur-containing amino acids valine and lysine are abundant in albumins. Globulin is abundant with valine, leucine, prolamin, threonine, phenylalanine, glutelin, and histidine. In addition to having a solid amino acid profile, amaranth protein is gluten-free, making it a viable option for people with celiac disease because the gliadin level is less than 0.01% (Coelho and Silva 2018). Additionally, amaranth grains contain 0.54 g of the amino acid leucine per 100 g, which is more than in rice and corn. Amaranth seeds contain most antihypertensive peptides, particularly globulin 11S, which can lower the angiotensin-converting enzyme (Kamal et al., 2021).

1.2.1.2.1.2. Lipids

Amaranth grain contains a good amount of oil (5–10%) compared to other cereals. Amaranth seed contains the predominant amount of unsaturated fatty acids (67–80%), with the most being linoleic acid (25–62%), oleic acid (19–35%), palmitic acid (12–25%), stearic acid (2.0–8.6%), and linolenic acid (0.3–2.2%). The ratio between saturated and unsaturated fatty acids in amaranth grain oil ranged from 0.26 to 0.31. Amaranth lipid is unique because it is composed of a significant number of active substances, such as tocopherols (2%), squalene (27%), phospholipids (10%–20%), and phytosterols (2%–2%). According to reports, amaranth seeds contain all four tocopherols and homologs of tocotrienols, such as α -tocopherol (1.40–31.4 mg/kg), γ -tocopherol (0.01–48.79 mg/kg), δ -tocotrienol (0.06–8.69 mg/kg), and β -tocotrienol (0.51–43.83 mg/kg) (Rastogi and Shukla 2013; Ogrodowska et al., 2014). Tocopherols significantly function in metabolic control having anti-inflammatory and anticancer effects. Tocotrienols have anticancer, neuroprotective, and hypocholesterolemic effects (Alvarez-Jubete et al., 2009). Squalene is an unsaturated hydrocarbon that is a necessary precursor to sterols and is also linked to antibacterial, anti-oxidative, anti-tumour, and very active anticancer characteristics (Khan and Technology 2019).

1.2.1.2.1.3. Minerals and vitamins

Amaranth grain comprises abundant minerals. Iron (72–174 mg/kg), phosphorus (455 mg/kg), copper (81 mg/kg), zinc (36.2–40.0 mg/kg), and sodium (160–480 mg/kg) are present in significant amounts; the levels of calcium (1,300–2,850 mg/kg), potassium (4333 mg/kg), and magnesium (2,300–3,360 mg/kg) are relatively high. Other minerals in amaranth include chromium, manganese, nickel, lead, cadmium and

cobalt. Major vitamins in the amaranth seeds are riboflavin, ascorbic acid, folate, niacin and thiamin. Among the gluten-free seeds amaranth contains a high amount of calcium which is beneficial for celiac patients due to osteopenia and osteoporosis. Amaranth is an excellent source for preventing vitamin deficiencies since it contains all the essential vitamins for everyday life to a large degree (Rodríguez et al. 2020).

1.2.1.2.1.4. Carbohydrates

Amaranth grain is softer and thinner; its carbohydrate content ranges from 60 to 65%. Amaranth is a top-notch dietary fibre source with total fibre content that ranges from 2.7 to 17.3%, comparable to typical cereal grains. Amaranth seeds with a light colour, have 8% dietary fibre, whereas dark colour grains have 16%. Amaranth seeds contain insoluble and soluble polysaccharides. The major insoluble polysaccharides are lignin, cellulose, and hemicelluloses. The soluble polysaccharides of amaranth seed have pectic polysaccharides called xyloglucans. In amaranth, starch is the predominant carbohydrate, ranging between 45 and 65%. Amaranth grain starch has a high viscosity and a high gelatinization temperature, so it is referred to as "waxy starch" and is composed chiefly of amylopectins (89.0–99.9%). The starch granules of amaranth are small (0.825 mm), which gives them a high water-binding capacity, higher swelling power, lower gelatinization at high temperatures and strong resistance to amylases. It makes amaranth a preferred source of starch in the food sector and other industries (N. Kumar et al. 2013; Rodríguez et al. 2020).

1.2.1.2.1.5. Antinutritional elements

Amaranth grain has nutritional advantages, but it also has some antinutritional elements. Small amounts of polyphenols, saponins, hemagglutinins, phytin, nitrates (V), and oxalates are present in amaranth seed. As a food, the presence of oxalates and phytates is more concerning. In plants, phytate stores phosphorous, but humans cannot digest phytate, which impedes nutritional absorption by binding with proteins. Phytate and oxalate have also been observed to impair the digestion of starch. Since phytic acid is consistently distributed throughout the grain, boiling could lower the phytate content. Oxalate binds calcium and reduces calcium absorption. Small quantities of saponin in amaranth grains bind with the mineral components, reducing the mineral availability. High tannins are found in the grain hull; they can be discarded by peeling off the hull. Boiling significantly impacted the lowering of tannin, phytate, and oxalate concentrations (Aderibigbe et al., 2022).

1.2.1.3. Health Benefits of amaranth grain

Amaranth has been found to have rich bioactive substances with health-promoting properties (Table 1.1). Amaranth grains are becoming essential food ingredients for preventing and managing chronic diseases. Amaranth has multifunctional properties, like antioxidant, antihypertensive, anti-inflammatory, anti-diabetic, and anticancer

activities. The exploration of amaranth species can create a great impact on industrial and health applications. (Al-Mamun et al. 2016; Aderibigbe et al. 2022).

Health benefits	Cell model	Research findings	References
Antioxidant activity	Caco-2 TC7 cells	Amaranth peptides decrease ROS and reduced glutathione levels.	(García Fillería & Tironi, 2021)
Anticancer, Antioxidant activity	MCF-7, A549 and HEK 293 cells.	Protein hydrolysates have a greater antioxidant effect in FRAP, DPPH, and ABTS assays. Flow cytometry analysis showed an increased number of early apoptotic and late necrotic cells and caspase 3/7 activity.	(Ramkisson et al., 2020)
Anti-tumour	UMR106 cell line.	Protein isolate from the seeds of <i>Amaranthus mantegazzianus</i> inhibits cell adhesion and induced apoptosis and necrosis.	(Barrio & Añón, 2010)
Chemo protectant	NIH-3T3 cells	Amaranth lunasin-like peptide, internalize into the nucleus and inhibits histone acetylation and prevents the transformation to cancerous foci.	(Maldonado-Cervantes et al., 2010)
Anti-inflammatory response	Raw 264.7 cells	Germinated amaranth seed digested peptides have high total antioxidant activity and anti-inflammatory effect by reducing NO.	(Eslim sugey et al. 2021)
Reverses endothelial dysfunction in	Dyslipidemic rabbits	Amaranth reverts endothelial dysfunction by increasing faecal cholesterol excretion and reducing blood and tissue cholesterol oxidation.	(Caselato-Sousa et al., 2014)

Affect glucose and lipid metabolism	Male mice	Sprout consumption could be beneficial for decreased body weight, total cholesterol, low-density lipoprotein, atherogenic index, triglyceride and glucose levels.	(Corzo-Ríos et al., 2021)
Antioxidant activity	-	The <i>A. hybridus</i> extract showed antioxidant activity in DPPH and FRAP assay and xanthine oxidase inhibition.	(Nana et al., 2012)
Anti-inflammatory effect	THP-1 and Raw 264.7 cell lines	Amaranth hydrolysates inhibited LPS-induced inflammation by inhibiting the NF-κB signalling pathway.	(Montoya-Rodríguez et al., 2014)
Anti-diabetic and anti-cholesterolemic activity	Male diabetic Wistar rats	Amaranth grain improved calcium signalling and showed anti-diabetic and anti-cholesterolemic activity,	(Kasozi et al., 2018)
Antitumour	HT-29 cells	Amaranth-digested peptides would exert a potential antiproliferative activity, loss of membrane integrity and significant increase in early and late apoptotic/necrotic also of caspase-3 activity	(Sabbione et al., 2019)
Antithrombotic effect	Male Wistar rats	The anticoagulant result was noticed by the clotting time values and had inhibitory effects on the coagulation phase of haemostasis.	(Soriano-Santos & Escalona-Buendía, 2015)
Reducing lipid peroxidation	Zebrafish	Inhibition of lipid peroxidation and ROS production	(Vilcacundo et al., 2018)
Control postprandial glycemia	Mice	Amaranth Glutelin hydrolysates	(Jorge et al., 2015)

Table 1.1: Health benefits of Amaranth evaluated by in vitro and in vivo methods

1.2.2. Exploring the healthful quinoa grain

Quinoa is one of the oldest crops; quinoa has been domesticated by indigenous peoples in the Andean area of Bolivia and Peru for more than 7000 years. The Inca's believed quinoa was a sacred plant, a gift from the sun god; they called it "chisiya mama" or "the mother grain". They thought it was an incredible source of nutrients. Quinoa seeds were transported to other South American nations, where they now serve as many peoples' most important staple foods. Quinoa seeds were used to make local fermented drinks (chichi) and folk medicine. They served as a whole and quick meal for the Incan army during marches and conquests. Quinoa fields were destroyed during the Spanish conquest of Southern America because the conquerors believed this magical sacred plant might empower the Incan people and endanger imperial conquest and control. The Andean people kept quinoa in communal areas after the Spanish conquest for many years, permitting in situ conservation of its genetic material (Kuktaite et al. 2021). The Food and Agriculture Organization (FAO) designated quinoa as an Andean staple and strategic food crop in 1986 and has expanded worldwide. This crop's nutritional value has been re-discovering within the previous 50 years, which has increased output. From 8 nations in 1980 to 40 in 2010 and more than 100 in 2021, the number of countries cultivating quinoa has expanded significantly. Bolivia, Ecuador, and Peru, three countries in South America, are the main producers of quinoa seeds. Quinoa is regarded as a novel nutritious food with unique health benefits and is occasionally referred to as a "superfood" because of its nutritional qualities. The UN General Assembly proclaimed 2013 as the "International Year of Quinoa" (M. Lin et al. 2019).

1.2.2.1. Morphological characteristics of Quinoa seed

The cylindrical and flattened quinoa seeds range from 1.5 to 4 mm in diameter and weigh roughly 350 seeds per gram. Variables in seed characteristics include size and colour. Seed colours range from white to black, with the possibility of yellow, rose, red, purple, and violet tones. The colour of the plant and its fruits were initially used to distinguish quinoa. Later, it was based on the plant's morphological types. Despite the enormous variety, quinoa is considered a single species (Vega-g et al. 2010). The pericarp is externally represented by the testa, hilum, and raphe; internally by the embryonic axis (cotyledons, radicle, and hypocotyl-radicle), perisperm, and endosperm. The embryo and seed coat comprises the bran portion rich in protein and fat, surrounded by the starch-rich perisperm. The increased quantities of protein and fat in quinoa are due to the presence of a higher percentage of bran fraction (seed coat and embryo) than in conventional cereals (Figure 1.2). Epigeal, phanerocotylar type germination is observed, with radicle protrusion occurring three hours after seeding and fully formed seedlings appearing 24 hours later. Plants appear nine days after sowing and are fully formed twelve days later (Rodrigues et al., 2020).

1.2.2.2. Major bioactive components in quinoa seed

1.2.2.2.1. protein

Quinoa has a higher protein content than most cereal species. On a dry basis, quinoa seeds contain an average protein composition ranging from 8 to 22%. The most abundant protein fractions are 11S-type globulins and 2S albumins, which together make up 27.9–60.2% and 13.2–42.3% respectively of the total protein in quinoa. Chenopodin (globulin 11S) contains significant glutamine-glutamic acid, asparagine-aspartic acid, arginine, serine, leucine, and glycine (Filho et al. 2017). Glutamine (18.1–31.6) and prolamins comprise a lesser protein percentage (0.5-19.3%) of the total protein in seeds, indicating it is not allergenic. More relevant is the fact that the protein quality of quinoa is considerably high. Quinoa seed contains all the essential amino acids. Protein quality can be measured by examining protein digestibility, accessible lysine, net protein utilisation, or protein efficiency ratio (Berghofer and Schoenlechner 2007). In this regard, the quinoa protein contents are unquestionably higher when compared to cereals and are equivalent to casein values. Quinoa has elevated levels of lysine, the limiting amino acid in grains. Quinoa is an intriguing food for children's nutrition since it contains high levels of arginine and histidine, which are crucial for babies and young children (Martínez-Villaluenga, Peñas, and Hernández-Ledesma 2020).

1.2.2.2.2. Carbohydrates

Carbohydrates are found in the perisperm of the seed and make up around 64.2% of the dry weight of quinoa. Most of the carbohydrates in quinoa consist of starch; it may vary in composition, structure, granular size, and physiochemical properties. The majority of the starch is made up of D-xylose (120 mg/100 g) and maltose (101 mg/100 g), with just trace amounts of glucose (19 mg/100 g) and fructose (19.6 mg/100 g) (Mohamed Ahmed, Al Juhaimi, and Özcan 2021). In quinoa starch, the amylopectin (7.7 to 25.7%.) is made up primarily of short chains and a small number of long chains, giving it distinctive structural and functional properties (Kuktaite et al. 2021). Quinoa starch is ideally suited as a thickener and textural stabiliser for dressings, sauces, and other creamy food items. Its excellent functional properties include small granular size, low pasting temperature, high water absorption capacity, swelling power, low gelatinisation temperature, freeze-thaw stability, and storage stability. Quinoa's carbohydrate content is vital for the fermentation of malted beverages. Quinoa seeds are an excellent source of dietary fibre, making up between 2.6 and 10% of the total weight of dietary fibre (Pereira et al. 2019).

1.2.2.2.3. Lipids

Quinoa is considered an alternative to other oil seeds because of its high quality and plentiful lipids. The oil content of quinoa varies from 2.0% to 9.5% dryly. Quinoa contains high levels of fatty acids such as linoleic acid (50.2–56.1%), oleic acid (22.0–

24.5%), palmitic acid (9.9–11.0%), and linolenic acid (5.4–7.0%). Triglycerides, the primary building block of fats, comprise most neutral lipids. All of the quinoa's fatty acids are shielded by vitamin E, a natural antioxidant. Squalene concentrations varied from 33.9 to 58.4 mg/100 g. The quinoa seed oil contains many phytosterols. *B-sitosterol* (63.7 mg/100 g), *campesterol* (15.6 mg/100 g), and *stigmasterol* (3.2 mg/100 g) are the three highest concentrations of phytosterols in quinoa oil (Shen et al. 2022). These phytosterols play a crucial role in keeping a healthy heart. It has a similar structure to cholesterol and competes with it for absorption in the gut, thereby reducing the cholesterol level in the bloodstream and maintaining cardiovascular health (Mohamed Ahmed, Al Juhaimi, and Özcan 2021).

1.2.2.2.4. Minerals and vitamins

Quinoa has a wide range of mineral compositions; it varies with soil type and fertiliser. Minerals like Phosphorous, Potassium, and Magnesium were found in the embryo, whereas calcium and phosphorous were found in the pericarp. Sulphur is equally distributed in the embryo. According to reports, iron is highly soluble, making it potentially accessible to anaemic populations. The quinoa seed has the highest calcium, phosphorous, iron, potassium, magnesium, and zinc levels (Martínez-Villaluenga, Peñas, and Hernández-Ledesma 2020). Many of these minerals are present in more significant amounts than in cereals. Its phosphorous level is nearly five times greater than that of rice and more than that of cow's milk. Quinoa seed can be a suggested food for humans since it is a good source of vitamins. For every 100 g of edible quinoa, there are 0.4 mg of thiamine, 78.1 mg of folic acid, 16.4 mg of ascorbic acid, 0.20 mg of pyridoxine, and 0.61 mg of pantothenic acid. The amounts of riboflavin, tocopherol and carotene in quinoa are significantly higher than in cereals (Berghofer and Schoenlechner 2007).

1.2.2.2.5. Antinutritional elements

The antinutritional elements found in quinoa seeds include saponins, phytic acid, tannins, nitrates, oxalates, and trypsin inhibitors. The outer layers of the grain have higher quantities of these chemicals. The outer layers of the quinoa grain naturally contain a bitter coating called saponin. Saponins can get rid of by the dry method of abrasive peeling. The loss of nutrients like protein, vitamins, and minerals, along with the bran, is a drawback of this procedure (Ruales and Nair 1993). For this reason, it is advised to employ the wet process in combination with polishing, which ensures that derivatives of quinoa will have their saponin concentrations significantly decreased, hence limiting nutrient loss. Although quinoa contains more phytic acid than other grains, the incorporation of calcium into the bones or the absorption of iron was negatively impacted. The level of phytic acid was significantly decreased by about 30% due to the brushing and rinsing procedure. Other processes, including steeping, germination, and fermentation, can drastically lower the amount of phytic acid. When quinoa grain is adequately washed and prepared (cooked), tannins may be eliminated to minimise their adverse effects and increase digestibility. Trypsin inhibitor levels in

quinoa are pretty low compared to those in regularly ingested cereals; hence they do not pose a significant health risk. Since quinoa wholemeal's nitrate levels are twice as low as those found in vegetables like spinach, lettuce, radishes, and beets, quinoa has no adverse effects on diet or health (Filho et al. 2017).

1.2.2.3. Health Benefits of quinoa grain

Considering the content and qualities of quinoa, there is only a small amount of human trials and in vivo studies (Table 1.2). Quinoa consumption or its bioactive components have advantages against obesity, high cholesterol, cancer, inflammation, and complications of diabetes.

Health benefits	Research findings	Reference
Antioxidant activity	Both ABTS and DPPH experiments showed strong antioxidant capacity.	(Paško et al., 2009)
Antioxidant and cytoprotective Effects	The antioxidant activity in DPPH, ABTS, assays and cytoprotective impact.	(Ong et al., 2020)
Liver protection and anti-fibrosis effect	Quinoa powder offers excellent defence against oxidative stress, pro-inflammatory factor expression, Transforming Growth Factor-Beta (TGF-β1) and tumour necrosis factor-alpha (TNF-α)/interleukin 6 (IL-6) in the liver, and anti-fibrosis	(Lin et al., 2019)
Liver cholesterol and lessens obesity-associated inflammation,	Consuming quinoa significantly decreased IL-6, protein carbonyls, and plasma total-cholesterol, LDL-c, elevated plasma insulin levels	(Noratto et al., 2019)
Antioxidant activity	Quinoa extracts showed outstanding antioxidant capacity in DPPH and FRAP assays.	(Park et al., 2017)
Antioxidant and immunoregulatory activity	Quinoa polysaccharides showed antioxidant activity in DPPH and ORAC assays and considerably boost the release of NO, TNF-α and IL-6 from macrophages.	(Yao et al., 2014)

Antioxidant and anti-proliferation	In HCT 116 cells, black quinoa seed oil induced apoptosis, the best antioxidant and anti-proliferation effect.	(Shen et al., 2022)
Antioxidant activity	Supercritical CO ₂ extraction of quinoa protein hydrolysate showed outstanding antioxidant activity in the ABTS assay	(Olivera-Montenegro et al., 2021)

Table 1. 2: Health benefits of Quinoa evaluated by in vitro and in vivo methods

A growing number of research investigations are conducted on pseudocereals for their health benefits and the production of nutrient-dense gluten-free products like bread, pasta, pastries, and pancakes. Protein concentrations and phytonutrient contents in amaranth and quinoa seeds indicate their potential to prevent many chronic diseases. Further research on amaranth and quinoa is required to explore their health benefits. World’s most death-causing diseases are cancer and chronic inflammation. Many drugs and therapies are developed to treat this disease, but still, research is going on to find the drug with fewer side effects. Our study focuses on the bioactivity of amaranth and quinoa on their effects on breast cancer and chronic inflammation.

1.3. Breast cancer

In 2020 cancer incidence, breast cancer (BC) is the most prevalent and foremost reason for female fatalities (Figure 1.3). According to the world health organisation (WHO) reports globally, 685 000 persons died in 2020, and 2.3 million women had a diagnosis of BC. BC patients' survival rates differ significantly around the globe, with industrialised countries having an estimated 5-year survival rate of 80% and impoverished countries having a survival rate below 40% (Akram et al. 2017). As per

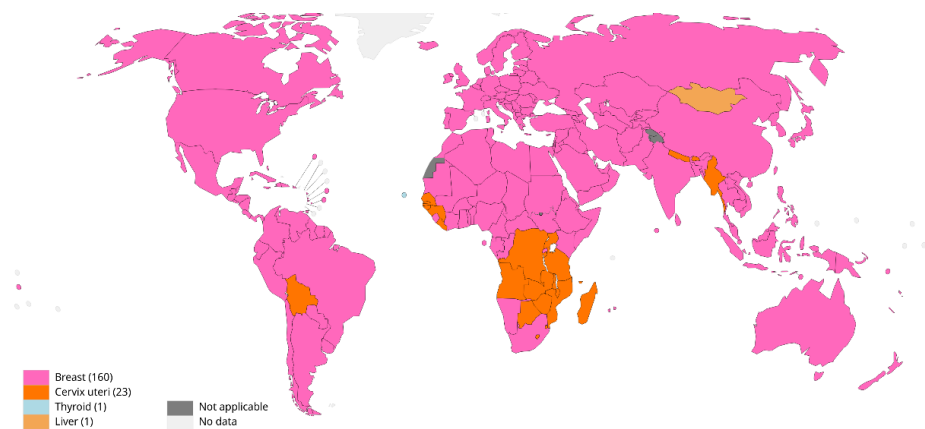


Figure 1.3: Breast cancer incidence in world population. Top cancer per country, estimated age-standardized incidence rates (world) in 2020, females, all ages Data source: GLOBOCAN 2020.WHO

the epidemiology in India, there will be an increase in the number of cancers between 2020 and 2040 from the current 1,80,000 cases to 3,70,000 cases. (Rai et al., 2022). According to Globocan 2020 statistics, BC caused 10.6% of fatalities in India. Mumbai was the leading site of BC, around 30.3%, followed by Thiruvananthapuram (28.5%), Chennai (22.4%), Bangalore (15.6%), and Dibrugarh (14.8%) (ICMR, 2012).

1.3.1. Lifestyle and risk factors of breast cancer

The breast is an estrogen-sensitive organ. Early menarche, absence of breastfeeding, and late menopause could be the risk factors for breast cancer. Single women are more likely to get breast cancer than married women. Many ladies who have used birth control pills or estrogen replacement therapy have discovered that their breasts swell and frequently become painful, significantly increasing the risk of breast cancer. Breast cancer may develop as a result of this medication's effects. (Huber et al., 2020). Breast cancer risk increases when certain benign tumour types are present. It could reduce by surgical removal of the tumour. Women over 50 had a greater incidence of breast cancer, with two per 1000 documented in this age range. Additionally, epidemiological studies have revealed that those women's age-related risk grows slowly throughout post-menopausal life and significantly during premenopausal life. Around 10% of cancer cases are hereditary and connected with a family history, albeit this varies significantly by ethnicity and between countries. BRCA1/2 are tumour-suppressor genes that repair DNA double-strand breaks by homologous recombination repair (HRR) to maintain genomic stability. BRCA1/2 mutations are associated with more than a 69% chance of having BC by age 80 (Yoshida 2021). Environmental conditions, cultures, lifestyles, and initiatives contribute to variances in breast cancer epidemiology patterns among nations. A growing body of research suggests that specific environmental toxins influence estrogenic activity and may be a factor in the high occurrence of breast issues in industrialised nations. According to studies, 20% of breast cancer cases are caused by controllable risk factors like obesity, inactivity, and alcohol consumption (Deglise et al., 2008). Drinking alcohol increases the chance of developing BC because alcohol raises the number of hormones in the blood and increases cell proliferation. The Western diet's high fat, low fibre intake overstimulates breast tissue. In obese women, the adipose tissue may supply the oestrogen. This disease burden could reduce by encouraging a healthy lifestyle (Deglise et al., 2008).

1.3.2. Pathogenicity

The unique way BC starts at the cellular level is unknown; there has been a significant effort to identify BC and describe its development and progression molecularly such as the clonal evolution concept (whereby mutations build up, epigenetic alterations in tumour cells take place, and the "fittest" cells survive) and the cancer stem cell model (in which the precursor cancer cells initiate and maintain progression). Cancer stem cells will also develop clonally (Akram et al. 2017). According to evidence at the molecular level, BC progresses along two distinct molecular pathways, mostly connected to estrogen receptor expression and human epidermal growth factor type-2

receptors (HER2). Molecular level, based on a series of early BCs, the genes tumour protein P53 (41% of tumours), PIK3CA (30%), MYC (20%), PTEN (16%), CCND1 (16%), ERBB2 (13%), FGFR1 (11%) and GATA3 (10%) are the most often altered or amplified in the tumour cells. These genes produce cell-cycle regulators that are either suppressed (like p53) or activated (like cyclin D1). They also maintain apoptosis, blocking active oncogenic pathways like MYC, HER2, FGFR1, and blocking components that are no longer regulated (PTEN) (Harbeck et al. 2019). The development of cancer is classified into four stages. The fourth metastatic stage is the most detrimental. The survival chance is significantly less compared to other stages. The stages of breast cancer are given in Figure 1.4.

STAGES OF BREAST CANCER

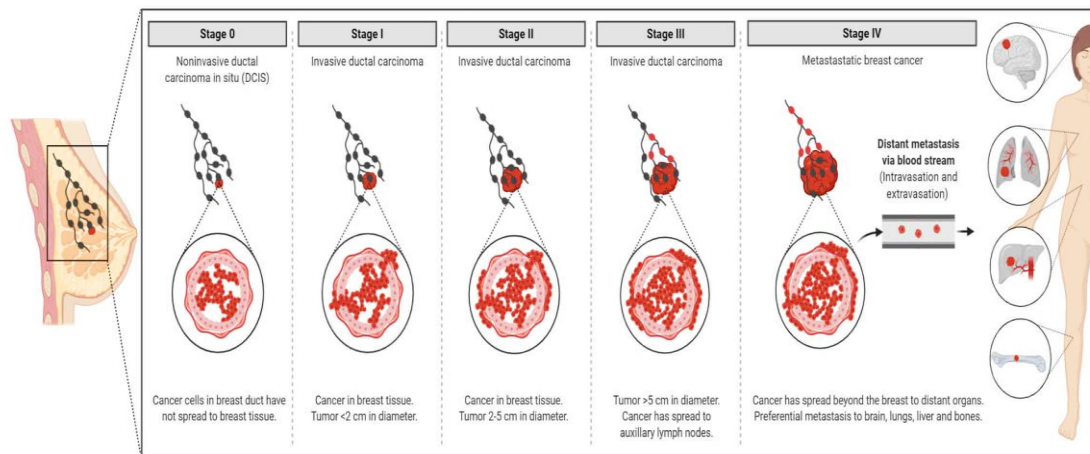


Figure 1.4: Stages of breast cancer. Data source: <https://thebiologynotes.com/breast-and-breast-cancer>

1.3.3. The most aggressive Triple-negative breast cancer

Among the breast cancer subtypes triple-negative breast cancer (TNBC) cells are most aggressive and highly metastatic in nature. TNBC is deficient in estrogen, progesterone and ERBB2 receptor expression, presenting a particularly challenging therapeutic target due to their highly invasive nature and a relatively low response to therapeutics (K. Wang et al. 2012). There is an absence of specific treatment strategies for this tumour subgroup. Hence, TNBC is managed with conventional therapeutics, often leading to systemic relapse notch, Hedgehog, Wnt/b-Catenin, and TGF-beta signalling pathways. Additionally, many epidermal growth factor receptor (EGFR), poly (ADP-ribose) polymerase (PARP) and mammalian target of rapamycin (mTOR) inhibitors effectively inhibit the TNBCs. However, they face challenges of either resistance to drugs or relapse. The resistance of TNBC to conventional therapeutic agents has helped advance TNBC therapeutic approaches, including hyperthermia, photodynamic therapy, and nanomedicine-based targeted therapeutics of drugs,

miRNA, siRNA, and aptamers. Artificial intelligence is another tool presented to enhance the diagnosis of TNBC (Medina et al. 2020).

1.3.4. Emergence of bioactive peptides against cancer

Chemotherapy is the systemic option to treat TNBC. It is an aggressive medicinal treatment designed to kill the proliferating cells having extreme adverse side effects. Bioactive peptides may be cytotoxic to several cancer cell lines with negligible adverse effects in anticancer medications. Peptides may exert their cytotoxic effects in a variety of ways. Moreover, the bioactive peptide may serve as a cytotoxic agent that mainly targets cancer cells without harming healthy cells. Peptides may block particular molecular signalling pathways of cancer cells to stem cells, differentiation, and oncogenesis. A few of the anticancer peptides are given in Table 1.3.

Source	Peptide	Activity	Cancer cell type/animal model	Reference
Soybean	Lunasin	Cell cycle-arrest at G1 phase, caspase-3, and cleavage of PARP	HCT-116 colorectal cancer	(Fern et al., 2020)
		Inhibition of cell cycle at the G1/S phase interface. Increased p27, reduction pAkt, and inhibition pRB (retinoblastoma protein)	NSCLC H661 non-small cell lung cancer cells	(McConnell et al., 2015)
		Reduced levels of pFAK, p Akt and pERK1/2	NSCLC H661 non-small cell lung cancer cells	(Inaba et al., 2014)
		Reduced adenoma progression, Hepatocyte proliferation through inhibition of β -catenin signalling	Male C57Bl/6 mice	(Mercer et al)
		Reduced activating pFAK and AKT as well as reduced histone acetylation of H3 and H4 histones.	A375 and B16-F10 cells	(Shidal et al., 2017)

	Vglycin	G1/S phase cell cycle arrest. Bax, Bcl-2 and Mcl-1, and caspase-3 activity	CT-26, SW480, and NCL-H716 colon cancer cells	(Gao et al., 2017)
Pea	Lectin	Increased levels of intrinsic caspases, p53 and decreased PARP1 protein. G2/M and G0/G1 cell cycle arrest	SW480 and SW48 colorectal cancer cell lines	(Islam et al., 2018)
Egg yolk protein	EYGF-23	caspase 3/7 activity	Caco-2 Colon Cancer Cells	(Yours et al., 2016)
Sepia esculenta	Sepia ink oligopeptide	S and G2/M phase cell cycle arrest. Bax/Bcl-2 expression ratio and caspase-3 were upregulated.	DU-145, PC-3 and LNCaP prostate cancer cell lines	(Huang et al., 2012)
Quinoa	Peptides FHPFPR, NWFPLP R, and HYNPYF PG	HDAC1, NFκB, IL-6, IL-8, Bcl-2 decreased, and caspase3 upregulated	Caco-2 Colon Cancer Cells	(Fan et al., 2022)
Camel milk	Whey protein	G2/M cell cycle arrest and modulated the expression of Cdk1, p-Cdk1, Cyclin B1, p-histone H3, p21 and p53	HCT-116 colorectal cancer	(Murali et al., 2021)
Amaranth seed		DNA fragmentation, membrane integrity loss, phosphatidylserine translocation and caspase 3 activity	MDA-MB 231 Breast cancer cells	(Taniya et al., 2020)

Table 1.3: List of anticancer bio-peptides

1.4. Inflammation

Since the early nineteenth century, inflammation has become one of biomedical researchers' most essential and fascinating fields of study. Inflammation is a universal defence mechanism that confines dangerous invaders, prevents excessive tissue damage, and activates healing systems. Inflammation is a broad range of physiological reactions against a foreign organism, including human diseases, dust particles, and viruses. The main tasks of the inflammation are isolating the damage factor, eliminating it, and finally regenerating or repairing (sclerosis) the wounded tissue. Inflammation was noticed and described even in the earlier period itself; ancient Roman doctors Celsus and Galen defined the most noticeable signs of inflammation, including redness (rubor), swelling (tumour), fever (calor), pain (dolor), and dysfunction (functio laesa)(Manabe 2011). The primary inflammatory response is defined by a temporally constrained activation of inflammatory processes that rises in the presence of a threat and subsides after it. Promoting a low-grade, non-infective systemic chronic inflammation, state is defined by the activation of immune components that are frequently different from those engaged during an acute immune response. The inflammatory response, short-lived to long-lived, can result in severe changes in all tissues and organs and abnormal cellular physiology, leading to the breakdown of immunological tolerance. (Furman et al., 2019).

1.4.1. Acute inflammation

Acute phases of inflammation are characterised by the recognition of pathogen-associated molecular patterns (PAMP) by tissue macrophages or mast cells, which activates the release of proinflammatory mediators to generate the immune response. These proinflammatory mediators will enhance vascular permeability, which causes a significant flow of plasma-carrying antibodies and other soluble components. Monocytes and lymphocytes build up at the inflammation sites as the inflammatory response intensifies to neutralise toxic chemicals. Inflammatory cells then experience apoptosis and are eliminated by tissue repair in the last step of the inflammatory cascade, reducing inflammation and restoring tissue homeostasis (Lawrence 2009).

1.4.2. Chronic inflammation

During inflammation, macrophages and dendritic cells stimulate the release of cytokines such as IL-1 and TNF- α . These cytokines trigger the release of Selectins and Integrins from the injury-site endothelial cells, which in turn stimulates the chemotaxis and diapedesis of the circulating leukocytes. Leukocytes produce cytokines and inflammatory mediators. In addition to attracting leukocytes to the injury site, cytokines activate the tissue macrophages and dendritic cells, which contribute to phagocytosis, cytokine production, and act as antigen-presenting cells. At that time, neutrophils release lysozyme, matrix metalloproteinases, and myeloperoxidase-rich granules for destroying antigens. Moreover, neutrophils phagocytose the antigen and produce cytokines and reactive oxygen species. The second line of defence is

composed of lymphocytes, which are essential in mediating inflammation via intricate processes, including the release of cytokines, costimulation of lymphocytes, formation of antibodies and immunological complexes. Circulating platelets can also contribute to inflammation by platelet aggregation, thrombus formation, and degranulation, which releases chemokines and inflammatory mediators. As a result of all these processes continuing longer than six weeks, and lack of homeostasis leads to chronic inflammation (Azab, Nassar, and Azab 2016; R. X. Wang et al. 2021).

1.4.3. Inflammation mediators

A very complex network of mediators operates the inflammatory processes. Based on the biochemical characteristics, inflammatory mediators are classified into seven groups: vasoactive amines, vasoactive peptides, cytokines, chemokines, fragments of complement components, lipid mediators, and proteolytic enzymes.

1.4.3.1. Vasoactive amines

Mast cells produce vasoactive amines like histamine and 5-hydroxytryptamine. These mediators affect the vascular system by enhancing vascular permeability and vasodilation.

1.4.3.2. Vasoactive peptides

Vasoactive precursors like Hageman factors, thrombin, or plasmin may be broken down into vasoactive peptides by proteolysis. These peptides will activate vascular permeability.

1.4.3.3. Cytokines

Cytokines are the main signalling molecules generated by inflammatory cells. IL-1, IL-6, IL-15, IL-17, IL-23, TNF- α and IFN are pro-inflammatory cytokines. IL-4, IL-10, IL-13, and TGF- are anti-inflammatory cytokines. Hence, IL-1 and IL-6 are well-known interleukins that activate the production of inflammatory molecules, reactive oxygen species (ROS), reactive nitrogen species and matrix metalloproteinase. Also, both of these IL-1 and IL-6 activate the JAK-STAT and NF- κ B signalling pathways. In addition, IL-6 has a significant role in T cell and B cell activation, proliferation, and differentiation.

1.4.3.4. Chemokines

Chemokines are a class of small signalling peptides essential for attracting inflammatory cells. They are divided into four categories based on the spacing of their N-terminal cysteines (C, CC, CXC and CX3C). The CC and CXC chemokines govern immune cell infiltration and leukocyte mobility, and they attach to G protein-coupled receptors (GPCRs) to cause cellular movements. Mostly neutrophils, mast cells, and eosinophils release chemokines. For instance, CCL2 is an essential chemokine;

vascular endothelial cells organise CCL2 gradients that guide monocytes to the site of inflammation in response to PAMPs. Another important chemokine is CXCL12, which promotes tissue repair by attracting mesenchymal stem cells to injury sites.

1.4.3.5. Fragments of complement components

Small soluble peptide fragments (complement C3a, C4a, and C5a) play crucial roles in the control of inflammation. They are formed via many complement activation pathways. Complement fragments attach to their receptors and activate migration, antigen presentation and the production of inflammatory mediators. Many proteolytic enzymes especially elastin and cathepsin have diverse functions in inflammation, including destroying extracellular and basement membrane proteins.

1.4.3.6. Lipid mediators and proteolytic enzymes

Cytoplasmic phospholipase A2 converts phosphatidylcholine into arachidonic (AA) and lysophosphatidic acids in cells. AA is broken down by either cyclooxygenase (COX1 and COX2) to make prostaglandins (PG) and thromboxane or lipoxygenases (LOXs) to make leukotrienes and lipoxins. Vasodilatation results from the prostaglandins E2 (PGE)₂ and prostacyclin I2 (PGI)₂; PGE₂ is also a potent inducer of fever and hyperalgesia.

1.4.4. Major receptors in inflammation

Plasma membrane receptors are essential to the inflammatory response; their presence controls the strength and persistence of inflammation. Most cytokine receptors are made up of chains connected to various non-receptor kinases. A signalling cascade like MAPK, NF- κ B, JAK, and STAT in the cells is started when a ligand binds to the receptors (TLR4, GM-CSFR, TNFR-1 and 2, etc.) which initiates synchronised phosphorylation processes. A new signalling cycle can begin if the receptor recycles to the cell surface, resulting in a continual transmission of the inflammatory stimulation to the cell's interior. An alternative way is for the cell to direct the receptor to the lysosomal pathway, ending inflammation and allowing the cell to begin self-regeneration. The receptor was found in recycling endosomes when the inflammatory response was still in progress. Results unambiguously demonstrate that inflammation ends when receptors are removed from cell surfaces, and regeneration may begin. It demonstrates that the intracellular destiny of the receptors should be a critical factor in determining the course of the inflammation (L. Kiss 2022).

1.4.5. Major activated pathways during inflammation- TLR and NF-κB signalling pathways

Toll-like receptors (TLRs) are key players in innate immune responses because they can identify specific PAMP. There are now 11 members of the TLR family known, with TLR3, TLR7, TLR8, and TLR9 being confined to the endosomal/lysosomal compartment, and TLR1, TLR2, TLR4, TLR5, TLR6, and TLR11 on the cell surface. The cytoplasmic Toll/IL-1 receptor (TIR) domain, associated with the TIR domain-containing adaptor MyD88, is the source of the TLR signalling pathway's activation. MyD88 interacts with the death domains of IL-1 receptor-associated kinase-4 (IRAK-4) to recruit it with TLRs in response to ligand stimulation. IRAK-1 is phosphorylated and interacts with TRAF6, activating the IKK complex and enabling the activation of MAP kinases and NF-κB. Nuclear factor-κB (NF-κB)/Rel proteins comprises NF-κB2 p52/p100, NF-κB1 p50/p105, RelA/p65, c-Rel, and RelB are the most common. These proteins act as dimeric transcription factors that control gene expression, affecting various biological processes, including innate and adaptive immunity, stress responses, B-cell development, and lymphoid organogenesis. IκB proteins bind to and inhibit NF-κB/Rel proteins in the conventional pathway. IKK complex (IKK, IKK, and NEMO) activation leads to the phosphorylation of IκB proteins by proinflammatory cytokines, LPS, growth factors, and antigen receptors. Phosphorylation of IκB leads to its ubiquitination and proteasomal destruction, releasing NF-κB/Rel complexes and activating proinflammatory mediators transcription (R. X. Wang et al. 2021).

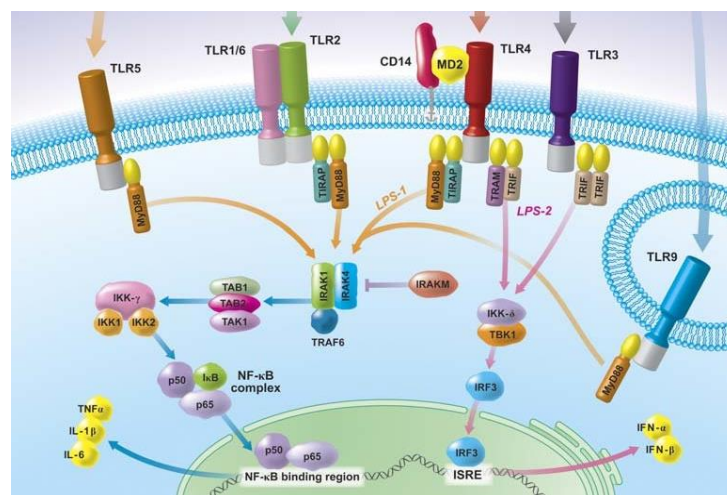


Figure 1.5: TLR and NFκB Pathways during inflammation. Data source: Martin and Frevert 2005

1.4.6. Aetiology

Chronic inflammation can develop in many ways, but it frequently happens when the substance that initially caused acute inflammation is not eliminated or pathogenic microorganisms and foreign substances that the body cannot clear by phagocytosis and

enzymatic digestion. The immune system mistakenly views a healthy body part as a foreign antigen and destroys it, leading to autoimmune diseases including systemic lupus erythematosus and rheumatoid arthritis. Moreover, a cell abnormality will mediate inflammation and cause it to persist or relapse. In certain situations, inflammatory and metabolic triggers, such as increased generation of free radical molecules, oxidised lipoproteins, advanced glycation end products, homocysteine, urate, and others (Duan et al. 2021).

1.4.7. Chronic inflammation diseases

Chronic inflammation is recognised globally as the root cause of many disorders, such as cardiovascular, neurological, and gastrointestinal diseases, diabetes, arthritis, fibrosis, and cancer.

1.4.7.1. Neurological diseases

Nervous system inflammation is referred to as neuroinflammation. Various stimuli, such as infection, severe brain injury, toxic metabolites, or autoimmune, may trigger it. Microglia are the innate immune cells in the central nervous system (CNS), brain and spinal cord and are activated in response to these cues. Peripheral immune cells are normally restricted by the blood-brain barrier (BBB), a specialised structure made up of astrocytes and endothelial cells. A weakened BBB, however, may allow circulating peripheral immune cells to pass through and come into contact with glial cells and neurons that exhibit the major histocompatibility complex components, sustaining the immune response. It leads to chronic inflammation via sustained activation of glial cells and recruitment of other immune cells into the brain, activating neurological diseases like Alzheimer's and Parkinson's. (Lucas, Rothwell, and Gibson 2006).

1.4.7.2. Obesity

Obesity and inflammation are mutually reinforcing, with inflammation causing obesity and obesity causing inflammation. Markers for inflammation include IL-6, CRP, and adiponectin. Stress and autoimmune conditions can have an impact on both inflammation and obesity. Adipose tissue is the primary source of pro-inflammatory cytokines in obesity; although adipocytes play a role, they are produced mainly by invading macrophages. It reduces the levels of these cytokines in the blood after weight loss. Moreover, obese people's adipocytes produce free fatty acids that activate the NF- κ B signalling cascade and TLR4, which induce inflammation (Rodríguez-Hernández et al. 2013).

1.4.7.3. Fibrosis

Persistent inflammation frequently leads to fibrosis in the organ. Fibrosis is crucial to the process of tissue repair. Myofibroblasts are the principal cells that produce connective tissue components. They are produced by fibroblasts, macrophages, and

endothelial cells, among many other cell types, in response to inflammatory stimuli. Inflammatory cytokines promote the conversion of the aforementioned cells into myofibroblasts. Long-term inflammatory stimuli and uncontrolled chronic inflammation increase the amplitude of connective tissue component synthesis and deposition, resulting in chronic fibrosis in many organs particularly the heart, kidney and liver (Lee and Olefsky 2021).

1.4.7.4. Post-Covid illnesses

Post-Covid illnesses have recently brought attention to the widespread impact of inflammation. During SARS-COV-2 viral infection, epithelial cells in the lung can create large amounts of cytokines creating a "cytokine storm". Due to inflammatory cytokines, many cells, including epithelial cells located in blood vessels, lung alveoli, and the pleura, can easily transdifferentiate into myofibroblasts. The extracellular matrix and connective tissue fibres produced by myofibroblasts later lead to localised lung fibrosis. The blood carries inflammatory cytokines throughout the body, influencing all organs; depending on a person's susceptibility, they will cause numerous chronic illnesses (Fernández-Quintela et al. 2020).

1.4.7.5. Asthma

Asthma is a complicated and chronic inflammatory condition characterised by airway hyperresponsiveness and airway tissue remodelling. First contact with the allergen activates the helper T cells (Th) that are specialised for it and produce IgE. Inflammatory cells are recruited, activated, and mediators are released in response to subsequent allergen exposures. Histamine, leukotrienes, and cytokines are released during degranulation by IgE-sensitized mast cells that express the high-affinity IgE receptor (FcRI). These mediators help to increase vascular permeability, smooth muscle contraction, and mucus formation. Eosinophils and Th2 cells are inflammatory cells recruited directly by chemokines produced by resident and inflammatory cells. Leukotrienes, simple proteins, and mediators like IL-5 are among the proinflammatory substances that are released by eosinophils. A lack of distinct "stop" signals for inflammatory reactions may lead to persistent inflammation. This help to explain the chronic character of allergy illness when combined with the ongoing presence of allergens. The dynamic process of natural inflammation resolution necessitates the elimination of the stimulus, the down-regulation of mediators and the clearance of dead cells. Asthma's development and progression can be aided by the failure of all these mechanisms, which hinders a return to equilibrium (George and Brightling 2016).

1.4.7.6. Inflammatory bowel disease (IBD)

IBD can be divided into two main pathogenic subtypes: ulcerative colitis (UC) and Crohn's disease (CD). UC is a non-specific, long-term inflammatory condition that primarily affects the colon and rectum's large intestinal mucosa and submucosa. A

chronic inflammatory granuloma known as CD typically develops in the terminal ileum and the colon next to it. However, it can affect the whole digestive system and has a segmental distribution. The CD is an inflammation-related illness dominated by Th-1 cells, which create a lot of IFN-gamma and TNF after being induced by IL-12, while UC is connected to Th-2 cells, which produce more IL-4, IL-5, and IL-13. Intestinal wall integrity is lost due to chronic mucosal inflammation caused by Th1 or Th2 cells. It hinders the regeneration of the epithelial barrier, allowing intestinal contents like bacteria and food antigens to readily infiltrate the gut and trigger an immune reaction that ultimately results in IBD (Duan et al. 2021).

1.4.7.7. Cancer

Many studies have demonstrated that chronic inflammation might boost the development of cancer. The "snowball" effect of inflammation brought to accelerates tumour growth. Up to 20% of malignancies are brought by chronic inflammation. Inflammatory cytokines and cells have been widely studied in malignancies of the stomach, colon, skin, liver, breast, lung, head, and neck, which are linked to carcinogenesis and tumour development in the majority of locations. NF-kB, cytokines, prostaglandins, and microRNA levels are enhanced in the inflammatory microenvironment, which has an impact on angiogenesis, cellular senescence, DNA mutation rates, cell death, and cell proliferation. Biomolecules created during inflammation contribute to the development and sustenance of tumour growth. On the other hand, low-grade inflammation brought on by obesity, hyperglycemia, and inappropriate lipid buildup is typical of a systemic type, which increases the risk of various cancers, notably liver, pancreatic, colon, breast and certain other cancers (Korniluk et al. 2017).

1.4.8. Anti-inflammatory medications

Anti-inflammatory medications have the potential to alter the pathophysiology of inflammation while trying to minimise tissue injury and enhance patient comfort. The two main categories of anti-inflammatory medications are glucocorticoids and nonsteroidal anti-inflammatory medicines (NSAIDs). In essence, glucocorticoids block prostaglandins and inflammatory proteins like corticosteroids, which are used to treat asthma and autoimmune diseases. Nonsteroidal medications work by inhibiting cyclooxygenase. The most frequently prescribed medications worldwide are NSAIDs, which are used to treat both acute and chronic pain brought on by an inflammatory process. NSAIDs' primary mechanism of action is the central and peripheral inhibition of COX (Cyclooxygenase), which prevents arachidonic acid from being converted to prostaglandins E2, prostacyclins, and thromboxanes. Enzymes involved in NSAIDs work are categorised into COX-1 and COX-2, which act in various body parts. Most cells, including foetal and amniotic fluid, contain COX-1, which is involved in regulation and protective effects, and COX-2 stimulates proinflammatory cytokines and inflammation. NSAIDs can be divided into non-selective NSAIDs, preferred COX-2 inhibitors, and highly selective COX-2 inhibitors. Non-selective NSAIDs

include ketoprofen, aspirin, naproxen, flunixin, and meglumine (coxib) (Zhao et al. 2021). In terms of structure, COX-2 selective medicines lack a carboxylic group and instead, sulfonamide groups or sulfones, which are essential for the enzyme's selectivity. As a result, they may target the COX-2 enzyme specifically; the scientific community has concentrated its efforts on looking for selective COX-2 inhibitors. Despite their initial effectiveness, adverse consequences appeared immediately after selective COX-2 medicines were introduced. In light of recent findings suggesting a significant danger of stroke, heart problems, renal failure, and arterial hypertension, the safety of using NSAIDs has come under scrutiny (Azab, Nassar, and Azab 2016).

1.4.9. Secondary metabolites- anti-inflammatory agents

From the dawn of time, secondary metabolites of plants have served as a significant source of medicines. Today, around half of all currently used pharmaceuticals come from natural sources. People are becoming more aware of the issues related to the overuse and overprescribing of synthetic anti-inflammatory medications. Significant anti-inflammatory capabilities are found in phenolic substances. Polyphenolic compounds, including flavonoids, condensed tannins and gallotannins, have been shown to block several proinflammatory mediators' molecular targets during inflammatory reactions. Many people are interested in using plant-based substances to treat inflammation. As a result, numerous research is focused on anti-inflammatory compounds from natural sources (Table 1.4).

Secondary metabolites	Plant	Targets	Reference
Proanthocyanidin	<i>Oryza sativa L.</i>	TNF- α , IL-1 β and IL-6	(Kangwan et al., 2023)
Gallotannins	<i>Protea simplex</i>	iNOS, COX-2 and	(Fawole et al., 2009)
Quercetin	<i>Capparis spinosa L. and Capparis orientalis</i>	NF κ B	(Piacente, 2023; Speisky et al., 2023)
Hesperidin	<i>Citrus aurantifolia</i>	NOX4	(Phucharoenrak et al., 2022; Syed et al., 2023)
Rutin	<i>Pimenta dioica</i>	TNF- α , IL-1 β , IL-2, IL-10 and G-CSF.	(El Gizawy et al., 2021)

Alkaloids	<i>Eclipta alba</i>	Decrease granuloma	(Kumar et al., 2005)
Saponins	<i>Chenopodium quinoa</i>	TNF- α and IL-6	(Yang Yao et al.2014)
Terpenoids	<i>Encostemma littorale</i>	NF- κ B and COX-2	(Indumathi et al., 2014; Manoharan et al., 2015)

Table 1.4: Anti-inflammatory compounds from natural sources

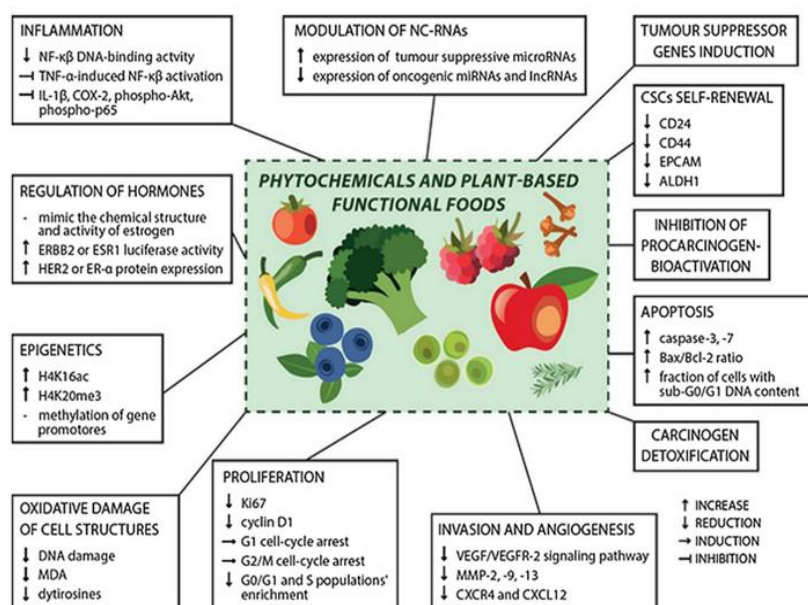


Figure 1.6: Mechanisms of action of functional foods on cancer and inflammation
Data source: Kapinova et al. 2017

Numerous pharmacological studies demonstrated that many food sources had anti-inflammatory properties. Food has potential impacts on the inflammatory pathways in the body. Food-derived compounds could represent innovative bioactive anti-inflammatory nutraceuticals and medicines since they are natural regulators of proinflammatory gene expression (Ricker & Haas, 2017). A growing body of research suggests that food-derived protein hydrolysates and phytochemicals have promising anti-breast cancer by inhibiting carcinogenesis, metastatic growth and supporting the immune system (Mazurakova et al., 2022). Functional foods can induce apoptosis,

invasion, and angiogenesis of tumour cells. Some of them can inhibit metabolic pro-carcinogens bioactivation (Figure 1.6). They can affect cell signalling, cell cycle regulation, oxidative stress and inflammation. In epigenetic processes (DNA methylation, modification of histone, non-coding RNA), and in this way may normalize altered cellular signalling in cancer cells. Importantly, they can act as modulators of noncoding RNAs (Kapinova et al. 2017). Every culture today has a solid understanding of food-based medicine due to the acquired knowledge of past generations. Thus, justifying the need for this work and illuminating the considerable attention that this field of study currently receives. Even though quinoa and amaranth are healthy alternatives to traditional grains, their biological processes must be thoroughly analysed.

1.5. Objective of the present study

In the current scenario, people with chronic diseases are much more common than healthy individuals. In that, chronic inflammation and triple-negative breast cancer are highly detrimental diseases. Currently, available medications for these diseases are having serious side effects. Here, we are attempting to investigate the effects of the bio-actives (peptides and phytochemicals) from amaranth and quinoa seeds against triple-negative breast cancer and inflammation. The broad objective of our study is to investigate the activity of biopeptides and phytochemicals from amaranth and quinoa seeds by screening and identification of bioactive isolates against breast cancer and inflammation. Nutrigenomic techniques are used to identify the genes and pathways responsible for the pharmacological effects. Additionally, their detailed molecular-level evaluation and experimental validation of identified peptides and extracts against breast cancer and inflammation. Major objectives are given as follows:

- Isolation of proteins from Amaranth and Quinoa seeds and their in vitro digestion for the preparation of peptide fractions.
- Preparation of solvent extract rich in secondary metabolites from Amaranth and Quinoa seeds.
- Screening of the isolated proteins/peptides/solvent extracts for their antioxidant, anti-breast cancer and anti-inflammatory properties.
- Nutrigenomic approaches to identify the responsible genes and pathways for the pharmacological effects.
- Detailed molecular-level evaluation of the identified peptides and extracts against breast cancer and inflammation.

1.6. Cell lines used for the present study

In this study, we used the MDA-MB-231 cells and RAW 264.7 cells for triple-negative breast cancer and inflammation studies respectively. The MDA-MB-231 cells were

isolated from human breast epithelial adenocarcinoma cells. These cells can be used for the model of late-stage breast cancer and triple-negative breast cancer (ER, PR, and E-cadherin negative, express mutated p53 and lack the growth factor receptor HER2) (Welsh. 2013). The RAW 264.7 cells were isolated from *Mus musculus*, mouse macrophage cells. The RAW 264.7 cell line is a frequently used model for inflammation because it generates strong and well-known inflammatory responses, particularly when challenged with inflammatory stimulants like lipopolysaccharide (LPS). Cell lines are widely utilised in in vitro screening for immunomodulators. Compounds that reduce the expression of pro-inflammatory cytokines or nitric oxide (NO) in LPS-stimulated RAW264.7 cells are frequently regarded as prospective anti-inflammatory medicines for humans (Bognar et al. 2013).

1.7. Standard drugs used for the present study

Ascorbic acid was utilised as the standard drug in the antioxidant investigation, while gallic acid was used to determine total phenolic content. Ascorbic acid is employed as a standard in antioxidant evaluation since it is an endogenous antioxidant that guards against free radicals, ROS, and other oxidants. Ascorbic acid can recover primary antioxidants by refilling hydrogen atoms, preventing the degradation of essential primary antioxidants. It promotes the biosynthesis and expression of genes that code for antioxidant proteins. It has been demonstrated that it may directly scavenge free radicals in cells and the circulatory system (Olszowy-Tomczyk, 2021). Gallic acid is a polyphenol extracted from plants that have anti-oxidant properties. It is often utilised for estimating polyphenol concentration, but it can also be used to assess antioxidant capability. Gallic acid is a powerful antioxidant that aids in the battle against oxidative stress (Abramovič et al., 2018). Curcumin was used as a positive control for TNBC and dexamethasone in anti-inflammatory investigations. The natural substance curcumin has demonstrated therapeutic potential in the treatment of cancer cell proliferation. Curcumin may work by inducing apoptosis and inhibiting cancer cell proliferation (Hu et al., 2018). Dexamethasone, a type of corticosteroid drug, is prescribed to treat diseases accompanied by inflammation. It operates by imitating the effects of cortisol, a hormone secreted by the adrenal glands that regulates metabolism and stress. Dexamethasone reduces inflammation and suppresses an overactive immune system (Kosutova et al., 2016).

1.8. References

1. Abramovič, Helena, Blaž Grobin, Nataša Poklar Ulrih, and Blaž Cigić. Relevance and Standardization of in Vitro Antioxidant Assays: ABTS, DPPH, and Folin–Ciocalteu. *Journal of Chemistry*. 2018. DOI:10.1155/2018/4608405.
2. Alonso-Miravalles, Loreto, and James A. O'Mahony. Composition, Protein Profile and Rheological Properties of Pseudocereal-Based Protein-Rich Ingredients. *Foods*. 2018;7(5). doi:10.3390/foods7050073

3. Barrio, Daniel Alejandro, and María Cristina Añón. Potential Antitumor Properties of a Protein Isolate Obtained from the Seeds of *Amaranthus Mantegazzianus*. *European Journal of Nutrition*.2010; 49(2): 73–82. doi:10.1007/s00394-009-0051-9.
4. Bogнар, E., Sarszegi, Z., Szabo, A., Debreceni, B., Kalman, N., Tucsek, Z., Sumegi, B., and Gallyas, F., Jr. Antioxidant and anti-inflammatory effects in RAW264.7 macrophages of malvidin, a major red wine polyphenol. *PloS one*.2013; 8(6), e65355. <https://doi.org/10.1371/journal.pone.0065355>
5. Caselato-Sousa, Valeria Maria, Michiko Regina Ozaki, Eros Antonio De Almeida, and Jaime Amaya-Farfan. Intake of Heat-Expanded Amaranth Grain Reverses Endothelial Dysfunction in Hypercholesterolemic Rabbits. *Food and Function*. 2014; 5(12): 3281–86.
6. Corzo-Ríos, L. J., Garduño-Siciliano, L., Sánchez-Chino, X. M., Martínez-Herrera, J., Cardador-Martínez, A., & Jiménez-Martínez, C. Effect of the consumption of amaranth seeds and their sprouts on alterations of lipids and glucose metabolism in mice. *International Journal of Food Science and Technology*. 2021; 56(7), 3269-3277. <https://doi.org/10.1111/ijfs.15014>
7. Diouf, Papa Niokhor, Tatjana Stevanovic, and Alain Cloutier. Study on Chemical Composition, Antioxidant and Anti-Inflammatory Activities of Hot Water Extract from *Picea Mariana* Bark and Its Proanthocyanidin-Rich Fractions. *Food Chemistry*. 2009; 113(4): 897–902. <http://dx.doi.org/10.1016/j.foodchem.2008.08.016>.
8. El Gizawy, H. A., Boshra, S. A., Mostafa, A., Mahmoud, S. H., Ismail, M. I., Alsfouk, A. A., Taher, A. T., and Al-Karmalawy, A. A. Pimenta dioica (L.) Merr. Bioactive Constituents Exert Anti-SARS-CoV-2 and Anti-Inflammatory Activities: Molecular Docking and Dynamics, In Vitro, and In Vivo Studies. *Molecules* (Basel, Switzerland). 2021; 26(19), 5844. <https://doi.org/10.3390/molecules26195844>
9. Fan, X., Guo, H., Teng, C., Zhang, B., Blecker, C., and Ren, G. Anti-Colon Cancer Activity of Novel Peptides Isolated from In Vitro Digestion of Quinoa Protein in Caco-2 Cells. *Foods* (Basel, Switzerland). 2022; 11(2), 194. <https://doi.org/10.3390/foods11020194>
10. Fawole, O. A., Ndhlala, A. R., Amoo, S. O., Finnie, J. F., and Van Staden, J. Anti-inflammatory and phytochemical properties of twelve medicinal plants used for treating gastro-intestinal ailments in South Africa. *Journal of ethnopharmacology*. 2009; 123(2), 237–243. <https://doi.org/10.1016/j.jep.2009.03.012>

11. Fernández-Tomé, S., Xu, F., Han, Y., Hernández-Ledesma, B., and Xiao, H. Inhibitory Effects of Peptide Lunasin in Colorectal Cancer HCT-116 Cells and Their Tumorsphere-Derived Subpopulation. *International journal of molecular sciences*.2020; 21(2), 537. <https://doi.org/10.3390/ijms21020537>
12. Gao, C., Sun, R., Xie, Y. R., Jiang, A. L., Lin, M., Li, M., Chen, Z. W., Zhang, P., Jin, H., and Feng, J. P. The soy-derived peptide Vglycin inhibits the growth of colon cancer cells in vitro and in vivo. *Experimental biology and medicine* (Maywood, N.J.).2017; 242(10), 1034–1043. <https://doi.org/10.1177/1535370217697383>.
13. García Fillería, Susan, and Valeria Tironi. Intracellular Antioxidant Activity and Intestinal Absorption of Amaranth Peptides Released Using Simulated Gastrointestinal Digestion with Caco-2 TC7 Cells. *Food Bioscience*. 2021; 41: 101086. <https://doi.org/10.1016/j.fbio.2021.101086>.
14. Hu, S., Xu, Y., Meng, L., Huang, L., and Sun, H. Curcumin inhibits proliferation and promotes apoptosis of breast cancer cells. *Experimental and therapeutic medicine*. 2018; 16(2), 1266–1272. <https://doi.org/10.3892/etm.2018.6345>
15. Huang, F., Yang, Z., Yu, D., Wang, J., Li, R., and Ding, G. Sepia ink oligopeptide induces apoptosis in prostate cancer cell lines via caspase-3 activation and elevation of Bax/Bcl-2 ratio. *Marine drugs*. 2012; 10(10), 2153–2165. <https://doi.org/10.3390/md10102153>
16. Inaba, J., McConnell, E. J., and Davis, K. R. Lunasin sensitivity in non-small cell lung cancer cells is linked to suppression of integrin signaling and changes in histone acetylation. *International journal of molecular sciences*. 2014; 15(12), 23705–23724. <https://doi.org/10.3390/ijms151223705>
17. Indumathi, C., G. Durgadevi, S. Nithyavani, and P. K. Gayathri. Estimation of Terpenoid Content and Its Antimicrobial Property in *Enicostemma Litorrale*. *International Journal of ChemTech Research* . 2014; 6(9): 4264–67.
18. Islam, Farhadul, Vinod Gopalan, Alfred K.Y. Lam, and Syed Rashel Kabir. Pea Lectin Inhibits Cell Growth by Inducing Apoptosis in SW480 and SW48 Cell Lines. *International Journal of Biological Macromolecules*. 2018; 117(2017): 1050–57. <https://doi.org/10.1016/j.ijbiomac>
19. Soriano Jorge, Raul Reyes-Bautista, Guerrero Legarreta Isabel, Ponce-Alquicira Edith, Escalona-Buendía Héctor, Almanza-Pérez Julio, César, Diaz-Godínez Gerardo and Román-Ramos Rubén. Dipeptidyl peptidase IV inhibitory activity of protein hydrolyzates from *Amaranthus hypochondriacus* L. Grain and their influence on postprandial glycemia in Streptozotocin-

- induced diabetic mice. *African Journal of Traditional, Complementary and Alternative Medicines*. 2015; 12. 90-98. 10.4314/ajtcam.v12i1.13.
20. Kangwan, N., Kongkarnka, S., Pintha, K., Saenjum, C., and Suttajit, M. Protective Effect of Red Rice Extract Rich in Proanthocyanidins in a Murine Colitis Model. *Biomedicines*, 11(2), 265. <https://doi.org/10.3390/biomedicines11020265>
 21. Kapinova, A., Stefanicka, P., Kubatka, P., Zubor, P., Uramova, S., Kello, M., Mojzis, J., Blahutova, D., Qaradakhi, T., Zulli, A., Caprnda, M., Danko, J., Lasabova, Z., Busselberg, D., and Kruzliak, P. Are plant-based functional foods better choice against cancer than single phytochemicals? A critical review of current breast cancer research. *Biomedicine and pharmacotherapy = Biomedecine and pharmacotherapie*. 2017; 96, 1465–1477. <https://doi.org/10.1016/j.biopha.2017.11.134>
 22. Kasozi, K. I., Namubiru, S., Safiriyu, A. A., Ninsiima, H. I., Nakimbugwe, D., Namayanja, M., and Valladares, M. B. Grain Amaranth Is Associated with Improved Hepatic and Renal Calcium Metabolism in Type 2 Diabetes Mellitus of Male Wistar Rats. *Evidence-based complementary and alternative medicine : eCAM*. 2018, 4098942. <https://doi.org/10.1155/2018/4098942>
 23. Kosutova, P., Mikolka, P., Balentova, S., Adamkov, M., Kolomaznik, M., Calkovska, A., and Mokra, D. Intravenous dexamethasone attenuated inflammation and influenced apoptosis of lung cells in an experimental model of acute lung injury. *Physiological research*. 2016; 65(Suppl 5), S663–S672. <https://doi.org/10.33549/physiolres.933531>
 24. Kumar, S. S., Sivakumar, T., Chandrasekar, M. J., and Suresh, B. Evaluation of Anti -Inflammatory Activity of *Eclipta alba* in rats. *Ancient science of life*. 2005; 24(3), 112–118.
 25. Lin, T. A., Ke, B. J., Cheng, C. S., Wang, J. J., Wei, B. L., and Lee, C. L. Red Quinoa Bran Extracts Protects against Carbon Tetrachloride-Induced Liver Injury and Fibrosis in Mice via Activation of Antioxidative Enzyme Systems and Blocking TGF- β 1 Pathway. *Nutrients*. 2019; 11(2), 395. <https://doi.org/10.3390/nu11020395>
 26. Maldonado-Cervantes, E., Jeong, H. J., León-Galván, F., Barrera-Pacheco, A., De León-Rodríguez, A., González de Mejía, E., de Lumen, B. O., and Barba de la Rosa, A. P. Amaranth lunasin-like peptide internalizes into the cell nucleus and inhibits chemical carcinogen-induced transformation of NIH-3T3 cells. *Peptides*. 2010; 31(9), 1635–1642. <https://doi.org/10.1016/j.peptides.2010.06.014>

27. Manoharan, S., Rajasekaran, D., Prabhakar, M. M., Karthikeyan, S., and Manimaran, A. Modulating Effect of *Enicostemma littorale* on the Expression Pattern of Apoptotic, Cell Proliferative, Inflammatory and Angiogenic Markers During 7, 12-Dimethylbenz (a) Anthracene Induced Hamster Buccal Pouch Carcinogenesis. *Toxicology international*. 2015; 22(1), 130–140. <https://doi.org/10.4103/0971-6580.172276>
28. McConnell, Elizabeth J., Bharat Devapatla, Kavitha Yaddanapudi, and Keith R. Davis. The Soybean-Derived Peptide Lunasin Inhibits Non-Small Cell Lung Cancer Cell Proliferation by Suppressing Phosphorylation of the Retinoblastoma Protein. *Oncotarget*. 2015; (7): 4649–62.
29. Montoya-Rodríguez, A., de Mejía, E. G., Dia, V. P., Reyes-Moreno, C., and Milán-Carrillo, J. Extrusion improved the anti-inflammatory effect of amaranth (*Amaranthus hypochondriacus*) hydrolysates in LPS-induced human THP-1 macrophage-like and mouse RAW 264.7 macrophages by preventing activation of NF- κ B signaling. *Molecular nutrition and food research*. 2014; 58(5), 1028–1041. <https://doi.org/10.1002/mnfr.201300764>
30. Mercer KE, Pulliam CF, Pedersen KB, Hennings L and Ronis MJ. Soy protein isolate inhibits hepatic tumor promotion in mice fed a high-fat liquid diet. *Experimental Biology and Medicine* (Maywood, N.J.). 2017; 242(6):635-644. DOI: 10.1177/1535370216685436. PMID: 28056552; PMCID: PMC5685258.
31. Murali, C., Mudgil, P., Gan, C. Y., Tarazi, H., El-Awady, R., Abdalla, Y., Amin, A., and Maqsood, S. Camel whey protein hydrolysates induced G2/M cellcycle arrest in human colorectal carcinoma. *Scientific reports*. 2021; 11(1), 7062. <https://doi.org/10.1038/s41598-021-86391-z>
32. Nana, Fernand W., Adama Hilou, Jeanne F. Millogo, and Odile G. Nacoulma. Phytochemical Composition, Antioxidant and Xanthine Oxidase Inhibitory Activities of *Amaranthus Cruentus* L. and *Amaranthus Hybridus* L. Extracts. *Pharmaceuticals*. 2012; 5(6): 613–28.
33. Noratto, Giuliana D., Kevin Murphy, and Boon P. Chew. Quinoa Intake Reduces Plasma and Liver Cholesterol, Lessens Obesity-Associated Inflammation, and Helps to Prevent Hepatic Steatosis in Obese Db/Db Mouse. *Food Chemistry*. 2019; 287: 107–14. <https://doi.org/10.1016/j.foodchem.2019.02.061>.
34. Olivera-Montenegro, L., Best, I., and Gil-Saldarriaga, A. Effect of pretreatment by supercritical fluids on antioxidant activity of protein hydrolyzate from quinoa (*Chenopodium quinoa* Willd.). *Food science and nutrition*. 2020; 9(1), 574–582. <https://doi.org/10.1002/fsn3.2027>

35. Olszowy-Tomeczyk, Małgorzata. How to Express the Antioxidant Properties of Substances Properly? *Chemical Papers*. 2021; 75(12): 6157–67. <https://doi.org/10.1007/s11696-021-01799-1>.
36. Ong, Eng Shi, Charlene Jia Ning Pek, Joseph Choon Wee Tan, and Chen Huei Leo. Antioxidant and Cytoprotective Effect of Quinoa (*Chenopodium Quinoa* Willd.) with Pressurized Hot Water Extraction (Phwe). *Antioxidants*. 2020; 9(11): 1–16.
37. Park, J. H., Lee, Y. J., Kim, Y. H., and Yoon, K. S. Antioxidant and Antimicrobial Activities of Quinoa (*Chenopodium quinoa* Willd.) Seeds Cultivated in Korea. *Preventive nutrition and food science*. 2017; 22(3), 195–202. <https://doi.org/10.3746/pnf.2017.22.3.195>
38. Paśko, P., Bartoń, H., Zagrodzki, P., Gorinstein, S., Fołta, M., and Zachwieja, Z. Anthocyanins, total polyphenols and antioxidant activity in amaranth and quinoa seeds and sprouts during their growth. *Food Chemistry*. 2009; 115(3), 994-998. <https://doi.org/10.1016/j.foodchem.2009.01.037>
39. Phucharoenrak, P., Muangnoi, C., and Trachootham, D. A Green Extraction Method to Achieve the Highest Yield of Limonin and Hesperidin from Lime Peel Powder (*Citrus aurantifolia*). *Molecules (Basel, Switzerland)*. 2022; 27(3), 820. <https://doi.org/10.3390/molecules27030820>
40. Ramkisson, Shanece, Depika Dwarka, Sonja Venter, and John Jason Mellem. In Vitro Anticancer and Antioxidant Potential of *Amaranthus Cruentus* Protein and Its Hydrolysates. *Food Science and Technology (Brazil)*. 2020; 634–39. DOI:10.1590/fst.36219
41. Sabbione, A. C., Ogutu, F. O., Scilingo, A., Zhang, M., Añón, M. C., and Mu, T. H. Antiproliferative Effect of Amaranth Proteins and Peptides on HT-29 Human Colon Tumor Cell Line. *Plant foods for human nutrition (Dordrecht, Netherlands)*. 2019; 74(1), 107–114. <https://doi.org/10.1007/s11130-018-0708-8>
42. Sandoval-Sicairos, E. S., Milán-Noris, A. K., Luna-Vital, D. A., Milán-Carrillo, J., and Montoya-Rodríguez, A. Anti-inflammatory and antioxidant effects of peptides released from germinated amaranth during in vitro simulated gastrointestinal digestion. *Food chemistry*. 2021; 343, 128394. <https://doi.org/10.1016/j.foodchem.2020.128394>
43. Sgadari, F., Cerulli, A., Schicchi, R., Badalamenti, N., Bruno, M., and Piacente, S. Sicilian Populations of *Capparis spinosa* L. and *Capparis orientalis* Duhamel as Source of the Bioactive Flavonol Quercetin. *Plants (Basel, Switzerland)*. 2023;12(1), 197. <https://doi.org/10.3390/plants12010197>

44. Shen, Y., Zheng, L., Peng, Y., Zhu, X., Liu, F., Yang, X., and Li, H. Physicochemical, Antioxidant and Anticancer Characteristics of Seed Oil from Three *Chenopodium quinoa* Genotypes. *Molecules* (Basel, Switzerland). 2022; 27(8), 2453. <https://doi.org/10.3390/molecules27082453>
45. Shidal, C., Inaba, J. I., Yaddanapudi, K., and Davis, K. R. The soy-derived peptide Lunasin inhibits invasive potential of melanoma initiating cells. *Oncotarget*. 2017; 8(15), 25525–25541. <https://doi.org/10.18632/oncotarget.16066>
46. Soriano-Santos, J., and Escalona-Buendía, H. Angiotensin I-Converting Enzyme inhibitory and antioxidant activities and surfactant properties of protein hydrolysates as obtained of *Amaranthus hypochondriacus* L. grain. *Journal of food science and technology*. 2015; 52(4), 2073–2082. <https://doi.org/10.1007/s13197-013-1223-4>
47. Speisky, H., Arias-Santé, M. F., and Fuentes, J. Oxidation of Quercetin and Kaempferol Markedly Amplifies Their Antioxidant, Cytoprotective, and Anti-Inflammatory Properties. *Antioxidants* (Basel, Switzerland). 2023; 12(1), 155. <https://doi.org/10.3390/antiox12010155>
48. Syed, A. A., Reza, M. I., Yadav, H., and Gayen, J. R. Hesperidin inhibits NOX4 mediated oxidative stress and inflammation by upregulating SIRT1 in experimental diabetic neuropathy. *Experimental gerontology*. 2023; 172, 112064. <https://doi.org/10.1016/j.exger.2022.112064>
49. Taniya, M.S., MV, Reshma, PS, Shanimol, Krishnan, Gayatri and Priya, Sulochana. Bioactive peptides from amaranth seed protein hydrolysates induced apoptosis and antimigratory effects in breast cancer cells. *Food Bioscience*. 2020; 35. 100588. [10.1016/j.fbio.2020.100588](https://doi.org/10.1016/j.fbio.2020.100588).
50. Vilcacundo, R., Barrio, D. A., Piñuel, L., Boeri, P., Tombari, A., Pinto, A., Welbaum, J., Hernández-Ledesma, B., and Carrillo, W. Inhibition of Lipid Peroxidation of Kiwicha (*Amaranthus caudatus*) Hydrolyzed Protein Using Zebrafish Larvae and Embryos. *Plants* (Basel, Switzerland). 2018; 7(3), 69. <https://doi.org/10.3390/plants7030069>
51. Welsh, Jo Ellen. *Animal Models for the Study of Human Disease Animal Models for Studying Prevention and Treatment of Breast Cancer*. Elsevier. 2013. <http://dx.doi.org/10.1016/B978-0-12-415894-8.00040-3>.
52. Yao, Y., Shi, Z., and Ren, G. Antioxidant and immunoregulatory activity of polysaccharides from quinoa (*Chenopodium quinoa* Willd.). *International journal of molecular sciences*. 2014; 15(10), 19307–19318. <https://doi.org/10.3390/ijms151019307>

53. Yao, Y., Yang, X., Shi, Z., and Ren, G. Anti-inflammatory activity of saponins from quinoa (*Chenopodium quinoa* Willd.) seeds in lipopolysaccharide-stimulated RAW 264.7 macrophages cells. *Journal of food science*. 2014; 79(5), H1018–H1023. <https://doi.org/10.1111/1750-3841.12425>
54. Yousr, M. N., Aloqbi, A. A., Omar, U. M., and Howell, N. K. Antiproliferative Activity of Egg Yolk Peptides in Human Colon Cancer Cells. *Nutrition and cancer*. 2017; 69(4), 674–681. <https://doi.org/10.1080/01635581.2017.1295087>.

CHAPTER 2

MATERIALS AND METHODS

2.1. MATERIALS

2.1.1. Cell lines and cell culture essentials

MDA-MB-231 (Human triple-negative breast cancer cell), and RAW 264.7 (Murine macrophage cell line) were purchased from NCCS, Pune, India. Low-glucose DMEM (Dulbecco's Minimal Essential Medium), RPMI (Roswell Park Memorial Institute) medium, FBS (Fetal bovine serum), Antibiotic Antimycotic Solution 100X Liquid w/10,000 U Penicillin, 10mg Streptomycin and 25 µg Amphotericin B per mL, and 10X Trypsin-EDTA solution were purchased from. Cell culture plastic wares were purchased from Himedia Laboratories Pvt. Ltd, India.

2.1.2. Chemicals and Biochemicals

Organic dried amaranth seeds (Super Grains, Organic Tattva Brand, Uttar Pradesh, India) and Quinoa seeds (Nourish you, R.R. district, Telangana, India.) were bought from Trivandrum, Kerala, India. Sodium phosphate buffer, Ammonium sulfate (ultrapure), phenylmethylsulfonylfluoride (PMSF), Ethylene diamine tetra acetic acid (EDTA), polyvinylpyrrolidone (PVP), pepsin (source-porcine stomach mucosa, 2500 U/mg), pancreatin (source-porcine pancreas, 75 U/mg), glycine, sodium bicarbonate, potassium chloride, ammonium molybdate and 2,2-diphenyl-1-picrylhydrazyl (DPPH) were purchased from Sisco Research Laboratory (Mumbai, India). Methanol, Hexane, and Ethylacetate were obtained from Spectrochem Pvt. Ltd., Mumbai, India. Dialysis sacks, curcumin, 3-(4,5-Dimethylthiazol-2-yl)-2,5-diphenyl tetrazolium bromide (MTT), bovine serum albumin (BSA, >99.9%), ethidium bromide, 4',6-diamidino-2-phenylindole (DAPI), and acridine orange were purchased from Sigma Aldrich (St Louis, MO, USA)., 2',7'-dichlorofluorescein diacetate (DCFDA), skim milk powder, radioimmunoprecipitation assay (RIPA) buffer, HPLC grade Methanol, Griess reagent for nitrite, Paraformaldehyde, N, N, N', N'-Tetramethyl ethylenediamine (TEMED), Dexamethasone, Lipopolysaccharide, Tween® 20 (Polysorbate) and glacial acetic acid were purchased from Sigma Aldrich-Merck, India. Glycerol, Normal Goat Serum, Dimethyl Sulfoxide (DMSO), Himedia laboratories Pvt.Ltd, Mumbai, India. The Immobilon polyvinylidene fluoride (PVDF) membrane was from Merck Millipore, Germany.

2.1.3. Antibodies

Anti-rabbit IgG (Alexa Fluor® 488 Conjugate), TLR-4, IκBα, MyD88, IL1, IL-6, IL-10, iNOS, COX-2, JNK, pJNK antirabbit mouse-specific antibodies were purchased from Geno Technology Inc., USA. NF-κB, β-actin antibodies, HRP-linked antibodies

and fluorescently labelled secondary antibodies were purchased from Cell Signalling Technology, Inc. USA.

2.1.4. Assay Kits

Annexin V CY3™ apoptosis detection kit and mitochondria staining kit were purchased from Sigma Aldrich-Merck, India. Caspase 3 fluorometric assay kit, BCA protein assay kit and RNaseZap™ RNase decontamination solution were purchased from Thermo Fisher Scientific, USA. Precision Plus Protein Dual Color Standard, and BD OptEIA TMB reagent substrate set (BD Biosciences, USA). Human Apoptosis Antibody Array Membrane:43 targets and Cytokine Array – Mouse Cytokine Antibody Array Membrane: 96 Targets (Abcam, UK), and RNeasy Mini Kit (QIAGEN, Germany). Other kits used for this study were Western BLoT Hyper HRP Substrate (Takara Bio Inc. Japan),

2.2. METHODOLOGY

2.2.1. Isolation of proteins by ammonium sulphate precipitation

In this process, protein is separated from complex constituents present in the seed. Ammonium sulphate is a commonly used salt for the protein isolation process due to low-cost, highly water-soluble salt and is capable of becoming more hydrated than any other ionic solvent. The ammonium sulphate precipitation method is based on the salting-out process. In the "salting-out" process the dissolved salt interacts with the proteins, raising the water's surface tension and driving the protein to fold more tightly. As there are reduced protein-water interactions and, increased hydrophobic interactions among protein molecules, which lead to protein aggregation and precipitation. Proteins can be concentrated by removing the residual ammonium sulphate solution, and then the protein pellet can be resolubilized in the conventional buffer. The protein solution can then be further purified using dialysis (Wingfield 1998). To inhibit protein degradation during isolation PVP, PMSF, EDTA and KCl were added to the buffer. PVP is used to remove phenolics from the solution because they can act as pro-oxidants and may harm proteins (Gayathri, Mohan, and Murugan 2007; Kakhrova, Khashimova, and Terenteva 2018). EDTA is used to prevent protein degradation during protein purification because it can interact with (divalent and trivalent) metal ions such as Mg^{2+} and Ca^{2+} to prevent the activation of protease enzymes. PMSF is used to inhibit the most common serine proteases found in plant tissues. KCl can improve the protein extraction process by maintaining the constant ionic condition. All these chemicals contribute an ideal condition for isolation and obtaining a high yield of protein (Sonawane and Arya 2018).

Amaranth and Quinoa seeds (200g) were rinsed in distilled water more than three times to eliminate the saponin contents from the seed surface. After straining, the seeds were ground and added to a 50 mM phosphate buffer. 50mM Phosphate buffer was prepared by adding 7.744 g of $Na_2HPO_4 \cdot 7H_2O$ and 2.913 g of $NaH_2PO_4 \cdot H_2O$ were

mixed with 800 mL of distilled water and the pH brought down to 7 using HCl or NaOH, then the total volume was brought to 1L using distilled water. Then the ground seed containing phosphate buffer was mixed with 8% PVP, 10mM PMSF, 0.1mM EDTA, and 30mM KCl. Then the solution was sieved through two layers of cheesecloth and centrifuged for 15 mins at 4 °C, 10,000 rpm, and the supernatant was collected. The 300 mL of supernatant underwent protein precipitation by ammonium sulphate. The supernatant solution was gradually dissolved 130.8 g of ammonium sulphate (saturation-70%), by continuously stir over a magnetic stirrer at 4 °C. The solution underwent overnight precipitation followed by a 25 mins centrifugation at 10,000 rpm. The pellets were collected and dissolved in 10 mL of 50 mM phosphate buffer. The ammonium sulphate was removed by overnight dialysis at 4 °C. Following dialysis, the crude protein extract was transferred to new tubes and kept at -80°C for further experiments. Lowry's method was used to estimate the protein content of the crude precipitate.

2.2.2. Estimation of proteins by Lowry method

The Lowry assay is a technique for calculating the amount of protein present in a sample. The test is based on the formation of a purple complex when copper ions interact with peptide bonds in the protein. The quantity of protein in the sample directly correlates with the colour intensity. It is a colourimetric test that measures protein contents in the sample, absorbance at 750 nm. The Lowry assay is a sensitive and precise technique for protein quantification. Protein estimation was performed according to the standard protocol with slight modifications (LOWRY et al. 1951). Before the experiment, the alkaline CuSO₄ reagent was freshly prepared by mixing reagents A and B in a 50:1 ratio. The reagent A contains 50mL of Na₂CO₃ and was mixed with 50mL of 0.1NaOH solution. Reagent B was prepared with 10mL of 1.56% CuSO₄ solution with 10mL of 2.37% Sodium potassium tartrate solution. After that the alkaline CuSO₄ reagent was prepared by mixing 50mL of reagent A and 1mL of reagent B. Sample protein solution (0.2mL) was added in a test tube and alkaline CuSO₄ reagent (2mL) was mixed into the solution well. Then, the half-diluted Folin Ciocalteu (0.2mL) was added to the mixture and incubated for 30 mins. Absorbance was measured at 660nm. Protein concentration was calculated by linear regression equation using the BSA calibration curve.

2.2.3. Simulated gastrointestinal digestion of proteins

In gastric digestion, the degradation of proteins is started in the stomach. The gastric fluids in the stomach contain pepsin and hydrochloric acid (HCl). HCl denatures the protein and transforms inactive pepsinogen into active pepsin. The major part of protein digestion takes place in the small intestine. After that, the chyme (partially digested protein) moves into the pancreatin, which contains major enzymes such as amylase, lipase, and protease and there further digestion occurs. When the protein reached the intestine, protease breaks down polypeptides into smaller peptides or single amino acids. Muscle contractions in the intestine allow for the absorption of

amino acids, dipeptides, and tripeptides into the intestinal cell wall (Gauthier, Vachon, And Savoie 1986).

Isolated amaranth and quinoa seed proteins (ASP and QSP) in the raw and heat-denatured (boiled at 100 °C for 10 mins) were subjected to simulated gastrointestinal digestion using pepsin and pancreatin according to a previously reported procedure (Wada and Lönnerdal 2015). 1 g of each protein sample was suspended in 50 Mm phosphate buffer pH 7 and was subjected to digestion. The simulated gastrointestinal digestion was performed by lowering the pH of the protein samples to 2.0 (stomach pH) using 1mol/L HCl. The protein sample was mixed with porcine pepsin (2% dissolved in 1 mmol/L HCl) in a 1: 12.5 ratio of pepsin and protein respectively, and the mixture was kept in a shaking incubator at 140 rpm for 15 mins at 37 °C. The pH of the digestion sample was then raised to 7.0 using 0.1 mol/L sodium bicarbonate, and pancreatin (0.4% in 0.1 mol/L sodium bicarbonate) was added to mimic intestine digestion. The pancreatin and protein ratio was 1:62.5, and again the samples were kept in the shaking incubator at 140 rpm at 37 °C for 5 mins. After that, the enzymes were heat inactivated in a water bath at 85 °C for 3 mins. The digested protein samples were kept at -80 °C for further analysis.

2.2.4. Essential amino acid analysis

Essential amino acids (EAA) are only supplied through food because the body cannot synthesise itself. The EAA content in food samples is a very important criteria for measuring the quality of protein. The EAA can be measured using amino acid analysis. This analysis helps to determine the released amino acids from the protein. Before being given for amino acid analysis, the hydrolysate was diluted and filtered. The hydrolysate was measured using a Shimadzu HPLC system equipped with an Agilent zorbax eclipse AAA column (4.6 x 150 mm,5 m) and pre-column derivatization with O-Phthalaldehyde (OPA). The mobile phases were Acetonitrile, Methanol, and Water (45:45:10 v/v/v), with a gradient. The elution of samples was conducted at a flow rate of 2.0 mL/min by gradient elution, and the total run time was 30 min. The reaction was performed at a buffering pH of 10.2, which enables the interaction of OPA with primary amino acids to form a fluorescent derivative with excitation at 340 nm and emission at 450 nm, which was detected by a fluorescence detector. Individual amino acid peaks were identified by comparing their retention times with those of standards. The quantity of EAA was estimated based on the regression equation obtained from the standard curve of standard amino acids.

2.2.5. Mass spectrometry and functional analysis of peptides

Advances in mass spectrometry technology increase the availability of large DNA/protein sequence databases, which enabled fast, sensitive protein identification processes. The principle of ESI-QTOF-MS for identifying proteins is based on the digestion of the protein with a specific protease produces a mixture of peptides distinct from that protein. The molecular masses of these peptides are measured and

given a specific dataset known as a peptide mass fingerprint. This data can be compared with theoretical peptide molecular masses that would be produced through the use of the same protease for the digestion of each protein in the sequence database to find the best match. According to a certain scoring system, the hits are rated. A candidate protein with a higher score can match observed masses and contains more proteolytic peptides. Proteins that are often identified receive the highest scores (Webster & Oxley, 2009).

The mass spectrometry data was acquired on a Q-TOF Maxis Impact mass spectrometer (Bruker Daltonics, Germany). Peptide samples were reconstituted in 0.1% of MS grade formic acid and injected into a reversed-phase C18 column (4.6 × 150 mm, 2.7 μm particle size, Agilent Technologies, USA). Samples were eluted using water, acetonitrile, and 0.1% formic acid as a mobile phase, with a flow rate of 200 μL min⁻¹. Conditions for mass spectral acquisitions included the following: an ion source, ESI; ion polarity, positive; m/z range, 40–1600; dry heater temperature, 220 °C; capillary voltage, 4000 V; end plate offset voltage, 500 V; charging voltage, 2000 V; nebulizer pressure, 2.4 bar; dry gas flow rate, 7.0 L min⁻¹. Collision-induced dissociation was used for MS2 fragmentations. Nitrogen was used as a collision gas. The collision energy for MS2 fragmentation was 10 Ev. Functional properties of the peptide were identified through Gene Ontology analysis (GO). GO was performed using the DAVID (database for annotation, visualization and integrated discovery), and the image was developed with FunRich software.

2.2.6. Isolation of secondary metabolites from amaranth and quinoa seeds

A. Sequential extraction (Soxhlet method)

The isolation of secondary metabolites from amaranth/quinoa seeds was done by sequential extraction, using different solvents based on increasing polarity for maximum yield (hexane, ethyl acetate, and methanol) by following the method described by Ling et al. (Ling et al. 2020). Hexane was used for isolating nonpolar compounds, ethyl acetate's biphasic actions enabled the extraction of both polar and nonpolar compounds, and methanol was used for polar organic substances. Samples were extracted successively using solvents in the following order: hexane, ethyl acetate, and methanol. 200 g of the powdered seeds (amaranth/quinoa) and 1000 mL of the solvent were loaded into the Soxhlet apparatus and refluxed for 10 h. The extract was pooled, and the residues were subsequently extracted with the higher polarity solvent using the same manner until the final solvent, methanol. The solvent was evaporated using a bench-top rotary evaporator (Heidolph, Germany.), and the extract was freeze-dried and stored in the refrigerator. Extract yield was calculated and expressed as a percentage (dry weight of solvent extracts/dry weight of sample) *100).

B. Direct extraction (Soxhlet method)

The isolation of secondary metabolites from amaranth/quinoa seeds was subjected to direct extraction, using 80% methanol. The extraction was conducted in the Soxhlet apparatus and the extract was isolated, freeze-dried and stored in a refrigerator, and the extract yield was calculated by following in the same manner as sequential extraction.

2.2.7. Assay of Total Antioxidant Capacity by Phosphomolybdenum method

The phosphomolybdenum assay was used to evaluate the antioxidant activity of amaranth and quinoa protein hydrolysates, and the standard procedure was followed with minor changes (Prieto, Pineda, and Aguilar 1999). The experiment was predicated on the extract's reduction capacity of Mo (VI) to Mo (V) and the formation of greenish phosphate/Mo (V) complexes at an acidic pH. A 300 μ L sample at various concentrations was mixed with 3 mL of reagent solution (0.6 M sulphuric acid, 28 mM sodium phosphate and 4 mM ammonium molybdate). Ascorbic acid was used as the positive control, and methanol (300 μ L) served as the blank. The reaction solution-containing tubes were sealed and incubated in a boiling water bath for 90 mins. The absorbance at 695 nm was measured after cooling to 25°C. The antioxidant capacity of the samples was calculated as mg equivalents of ascorbic acid/g extract.

2.2.8. Free radical scavenging activity Assay by DPPH method

DPPH can donate hydrogen or electrons and delocalize/stabilize the resultant phenoxyl radical inside their structure. The DPPH radical has a prominent absorption band with a centre wavelength of around 517 nm. The solution is a deep violet colour when neutralised, it turns colourless or light yellow.

Free radical scavenging activity was measured using the DPPH method (Chiu et al., 2005) with slight modifications. 100 μ L of samples were allowed to react with 100 μ L of 10 mM DPPH solution (19.7 mg of DPPH dissolved in 5 mL methanol solution). After 30 mins of incubation in the dark, the absorbance was measured at 517 nm. The percentage activity was determined using the formula.

$$= [(Absorbance\ of\ control - Absorbance\ of\ sample) / Absorbance\ of\ control] \times 100.$$

The results were expressed as IC₅₀ value (The quantity of protein samples required to scavenge 50% of the free radicals produced).

2.2.9. Analysis of total phenolic content

The Folin-C reagent will oxidise phenolic compounds (a complex mixture of heteropolyphosphotungstate and molybdate) in the presence of sodium carbonate to form a blue-coloured complex. The intensity of the blue colour is proportional to the amount of reactive phenolic compounds in the sample. The phenolic content is

determined by measuring the absorbance of the sample solution at 765 nm and comparing it with a calibration curve using gallic acid as a standard. The method can quantify the total polyphenolic content of about 5 w/w to 100% w/w in the extracts (Kupina et al. 2019).

The Folin-Ciocalteu technique was used to determine the total phenol content of amaranth and quinoa seed extracts (Colaco and Desai 2012). Samples (10mg) were dissolved in 1 mL of methanol. Homogenised solution was made with 5 mins of sonication. These samples (0.5 mL) were combined with 2.5 mL of the Folin-Ciocalteu reagent (diluted 10 times with distilled water) and 2 mL of an aqueous sodium carbonate solution (75 mg/mL). Results are reported in gallic acid equivalents (mg GA/g dry extract), with the calibration curve prepared using gallic acid.

2.2.10. Anticancer studies: Cell culture and maintenance

MDA-MB-231 cells were cultured and maintained in DMEM full growth medium comprising 1.0g/L glucose, 3.7g/L Sodium bicarbonate, supplemented with 10% FBS and antibiotic solution (penicillin (100units/L), streptomycin (100µg/mL) and Amphotericin B (25 µg/mL)) containing medium. Cells were cultured and maintained under 5% CO₂ at 37°C in a humidified incubator by following proper aseptic techniques. In a sterile condition, the required volume of DMEM full growth media was poured into the flask. The growth medium was replaced on alternate days and the cells were passaged in the log phase on reaching 80% confluence.

The subculturing was done by the cells were washed with 2 mL of PBS for removing FBS residues. Then the cells were incubated with 1 mL of 1X Trypsin for 3 mins in a CO₂ incubator. After checking the cell's morphology with the aid of a microscope, complete growth medium (3 mL) was added into the detached cells and centrifuged these cell suspensions at 3000 rpm for 3 min. The supernatant was discarded and the cell pellets were resuspended in 1m of fresh complete growth media and transferred to a new culture flask with full growth media. The hemocytometer was used for cell counting and then calculated the number of cells was according to the requirement of each experimental protocol.

Viable cells/ mL = The average count of live cells in 4 sets of haemocytometer × dilution factor × 10⁴.

2.2.11. Cytotoxicity analysis by MTT assay

Cytotoxicity of samples (peptides/secondary metabolites of amaranth and quinoa seeds) was evaluated by MTT assay. In 1983 Mosmann developed an MTT colourimetric assay for measuring the metabolic activity of viable cells. MTT assay was also used to analyse growth inhibition and toxicity of samples in cells. Metabolically active cells have the co-enzyme nicotinamide adenine dinucleotide (reduced form) (NADH), which reduces the MTT tetrazolium salt (yellow colour,

water-soluble) into formazan crystals (purple colour, water-insoluble). The colour intensity of the formazan crystal after solubilization in DMSO is then measured at 570 nm by the spectrophotometer (Buranaamnuay 2021).

The experimental condition was 5% CO₂ and 37°C, Cells were seeded in 96-well plates at a density of 1x10⁴ cells per well. After 24 hrs, the spent medium was aspirate and washed gently with PBS. Cells were treated with a 100µL medium containing various concentrations of samples and incubated for 24hrs. Later medium was replaced and introduced with medium with MTT dye (100µg/mL) for 3hrs at 37°C in dark conditions. Then, the medium was decanted 200µL of DMSO was directly added into the wells and incubated again for 20 min under gentle shaking at 37°C to dissolve the tetrazolium dye. Relative cell viability was calculated by determining the absorbance at 570 nm and untreated control cells using a multi-mode reader (BioTek, CA). The absorbance value is directly proportional to the number of viable cells and was used to estimate the percentage of growth inhibition.

Percentage of growth inhibition = [1-(absorbance of treated cells/absorbance of untreated cells)] x100.

2.2.12. Cellular morphology analysis using phase contrast microscopy

The morphology of the cells after treatment with the samples was examined using phase contrast microscopy. Phase contrast imaging was used to analyse the features of cell death (apoptosis or necrosis), such as shrinkage, blebbing, bloating, apoptotic bodies, etc. The cells were cultured in a 96-well plate at a density of 1×10⁴ cells/well for 24 hrs under standard culture conditions. The cells were treated with 100 µL samples for 24 hrs. Under a phase contrast microscope (Nikon Eclipse TS 100, Japan), the morphological alterations brought by these samples were examined, imaged, and compared to control cells.

2.2.13. Nuclear fragmentation analysis using DAPI staining

4, 6-Diamidino-2-phenylindole (DAPI) is a DNA-sensitive probe that may pass through an intact cell membrane which specifically binds to adenine-thymine-rich sections of the minor groove of double-stranded DNA (Kapuscinski 1995). Analysing nucleus morphology and nuclear fragmentation using DAPI enables the investigation of apoptosis (Wallberg, Tenev, and Meier 2016).

Cells were seeded at a density of 1×10⁴ cells/well in a black well plate. After removing the growth medium, cells were treated with 100 µL of ASP-HD (50 and 100 µg/mL) and the positive control curcumin (10 µM) for 24 hrs. Following that, the media was removed, and the cells were exposed to a 50 µL solution of DAPI (300 nM) for five min. After removing the DAPI solution, the cells were washed three times with 100µL PBS. The cells were suspended in 100 µL of 1X PBS at an excitation/emission of

358/461 nm, and nuclear morphology was studied using a spinning disc fluorescent microscope BD pathway bio-imaging system (BD Biosciences, San Jose, CA, USA).

2.2.14. Analysis of plasma membrane damage using Acridine orange/ethidium bromide (AO/EtBr) dual staining

The differential AO/EtBr staining distinguishes between viable and nonviable cells (dead and necrotic cells) based on the membrane integrity. AO can enter into both live and dead cells. When the cells are alive, the AO intercalates into the DNA, giving it a green colour. But, Ethidium bromide (EtBr) can only enter through the damaged cell membrane. When the cell is nonviable, it intercalates with DNA and emits red fluorescence. Because of this, early apoptotic cells have vivid green patches, whereas late apoptotic cells with membrane damage have bright orange patches of condensed chromatin in the nucleus (Kasibhatla et al. 2006; Wallberg, Tenev, and Meier 2016).

In a black 96-well plate, cells were seeded at a density of 1×10^4 cells/well and incubated for 24 hrs. After aspirating the medium, cells were treated with ASP-HD (50 and 100 $\mu\text{g}/\text{mL}$) and the positive control curcumin (10 μM) for 24 hrs. Following treatment, the cells were incubated with an AO/EB solution (1 $\mu\text{g}/\text{mL}$) for 10 min, washed three times in PBS to remove the excess stain, and then suspended in 100 μL of PBS. The cells were examined with the help of a spinning disc fluorescent microscope for membrane integrity at an excitation/emission of 500/526 nm.

2.2.15. Phosphatidylserine translocation assay by Annexin V staining

An early event in apoptosis can determine and measure using phosphatidylserine (PS) exposure on the cell surface. PS are concealed within the plasma membrane of live cells. During apoptosis, PS will shift from the cytoplasmic face of the plasma membrane to the cell surface. Annexin V can be used for detecting apoptosis because of its high, Ca^{2+} -dependent affinity for PS. The annexin V-Cy3 apoptosis detection kit was used to analyse phosphatidyl serine (PS) translocation following the manufacturer's instructions. The non-fluorescent substance 6-carboxyfluorescein diacetate (6-CFDA) enters the viable cell, and esterases hydrolyze into the fluorescent substance 6-carboxyfluorescein. 6-CFDA dyes viable cells green, and Annexin V binds to the exposed PS on the cell surface to emit red fluorescence. When these two factors are present, it is possible to distinguish between early-stage apoptotic cells (annexin V positive, 6-CFDA positive), necrotic cells (annexin V positive, 6-CFDA negative), and viable cells (annexin V negative, 6-CFDA positive).

Cells were seeded at a density of 1×10^4 cells/well in a black 96-well microplate and cultured for 24 hrs. The cells were treated with ASP-HD (50 and 100 $\mu\text{g}/\text{mL}$) and positive control curcumin (3.6 $\mu\text{g}/\text{mL}$) for 24 hrs. Then, the cells were gently rinsed twice with 50 μL 1X binding buffer. Stained the cells with 50 μL of dual stain [1 $\mu\text{g}/\text{mL}$ Annexin Cy3 (20 μL) and 6-CFDA (20 μL) in 1.96 mL 1X binding buffer] 10 min. The stain was removed by washing three times with 50 μL of 1X binding buffer. Cells

were suspended in 35 μL of 1X binding buffer and observed using a spinning disc fluorescent microscope (BD Biosciences USA) with rhodamine (Excitation/Emission = 543 nm/ 570 nm) and FITC (Excitation/Emission = 495 /517 nm) filters.

2.2.16. Caspase 3 assay

Caspases are Cysteine-requiring Aspartate proteases and caspase 3 belongs to the protease family that mediates apoptosis. Caspase 3 executes the vast number of proteolysis that causes apoptosis (Nicholson et al. 1995). This assay is based on caspase 3 hydrolysis of the peptide substrate Ac-DEVD-AMC (acetyl-Asp-Glu-Val-Asp-7-amido-4-methyl coumarin), which results in the release of the fluorescent AMC (7-amino-4-methyl coumarin) moiety. The AMC has an excitation/emission wavelength of 360/460 nm. As per the manufacturer's recommendations, the activity of caspase 3 was investigated using a standard kit.

Cells were enumerated, and 0.3×10^6 cells/well were seeded on a 6-well plate for 24 hrs. The medium was aspirated, and cells were treated with 1.5 mL of growth media containing ASP-HD (50 and $100 \mu\text{g}/\text{mL}$) hydrolysate and positive control curcumin ($3.6 \mu\text{g}/\text{mL}$) for 24 hrs. Then, the media were aspirated and re-suspended in 50 μL of cold cell lysis solution on ice for 10 min. 50 μL of 2X reaction buffer and 5 μL of 1 mM substrate were added to each sample and incubated for 2 hrs at 37 °C. Cell lysates from the control and protein hydrolysate-treated cells were incubated with the fluorescent substrate Ac-DEVD-AMC. Using a SynergyTM 4 microplate fluorescent reader, the fluorescence was measured at an excitation/emission of 360/460 nm (BioTek Instruments).

2.2.17. Scratch wound assay

The scratch wound assay is a method to analyse cell motility. Making a scratch wound in a confluent dish and monitoring the migration of cells as they close a scratch and this assay can be used to study cancer and metastasis (Bobadilla et al. 2019).

On 6-well plates, 1×10^6 cells/well were seeded. Growth media was changed every day until a monolayer (70–80% confluence) was produced in the well. A straight wound was mechanically created in the monolayer's centre using a sterile micropipette tip. 1mL PBS wash was given after removing the spent media, and the cells were treated with ASP-HD hydrolysates (50 and $100 \mu\text{g}/\text{mL}$) and positive control curcumin ($3.6 \mu\text{g}/\text{mL}$). The degree of migration was determined by imaging the wound closure using a phase contrast microscope (Nikon, Japan) at various time intervals (0 and 24 hrs) and also compared with positive control curcumin.

2.2.18. Human apoptosis antibody array analysis

Antibody arrays are an ELISA-like antibody-pair-based test that uses a membrane as the substrate rather than a plate. A human apoptosis antibody array membrane kit was employed for studying the expression of samples on the simultaneous detection of 43

apoptotic markers. The package included a membrane with a panel of 43 capture spots (Bad, Bax, Bcl-2, Bcl-w, BID, BIM, Caspase3, caspase8, CD40, CD40L, cIAP-2, cytoC, DR6, Fas, FasL, HSP27, HSP60, HSP70, HTRA, IGF-I, IGF-II, IGFBP-1, IGFBP-2, IGFBP-3, IGFBP-4, IGFBP-5, IGFBP-6, IGF-1sR, livin, p21, p27, p53, SMAC, Survivin, sTNF-R1, sTNF-R2, TNF-alpha, TNF-beta, TRAILR-1, TRAILR-2, TRAILR-3, TRAILR-4 and XIAP in duplicate) along with positive and negative controls. The provided capture antibodies were spotted on a membrane, with each pair of spots representing a distinct analyte.

In T-75 flasks, cells were seeded at a density of 2×10^6 and allowed to attach for 24 hrs. After that, ASP-HD (50 $\mu\text{g}/\text{mL}$) was administered as a treatment for 24 hrs. After treatment, gently rinsed the cells twice with cold PBS, and 1 mL of lysis solution was added and incubated for 30 min at 4 °C while gently rocking the dish. After centrifuging the lysates at 14000 x g for 10 mins, the supernatants were transferred to new tubes. Each lysate's total protein concentration was calculated using a BCA kit, and the equalisation process was performed using a blocking buffer to provide a final volume of 2 mL per membrane containing 400–600 μg of total protein. The membrane was positioned in the provided 8-well tray with its printed side facing up and 2 mL blocking buffer was gently poured on the membrane. The membrane was gently shaken for 30 mins at RT. After aspirating blocking buffer and membrane in a closed tray were incubated with 1.2 mL of lysate overnight at 4°C with gentle shaking. After incubation, the samples were aspirated, and the membrane was washed three times (5 mins each) using 2 mL of wash buffer I, and then the membrane was washed two times (5 mins each) with 2 mL of wash buffer II.

After aspirating the wash buffer, the membrane was gently shaken at 4°C incubated with 1 mL of biotin-conjugated antibody cocktail overnight. The reagent was aspirated, and the membrane was washed using wash buffers I and II following the earliest description. The membrane is treated with 2 mL of HRP-Streptavidin for 2 hrs at RT with gentle shaking. The HRP-streptavidin was aspirated, and the membrane was washed with the previously indicated Wash buffer I and Wash buffer II.

The membrane was then put on the provided plastic sheet, protein side facing up, and the excess water was blotted out by lightly wiping one edge of the membrane with filter paper. 250 μL of detection buffer was added to the membrane, and a second plastic sheet was carefully slipped over it to ensure that the detection mixture covered the membrane thoroughly and bubble-free. Remove the top plastic sheet to drain the excess buffer after 2 mins of RT incubation of the membrane. The top plastic sheet was replaced, and any air bubbles on the membrane surface were gently smoothed out. ChemiDoc™ MP System (Bio-Rad, Hercules, CA, USA) and IMAGE LAB™ Software enabled the chemiluminescence detection to be completed in 20 mins. corresponding control membrane.

The control sample membrane was used as the "reference," and the following formula was used to calculate the normalised values:

$$X(Ny) = X(y) \times P1/P(y)$$

Where:

P1 = mean signal density of Positive Control spots on reference array

P(y) = mean signal density of Positive Control spots on Array "y"

X(y) = mean signal density for spot "X" on Array for sample "y"

X(Ny) = normalized signal intensity for spot "X" on Array "y"

2.2.19. Anti-inflammatory studies: Cell culture maintenance and treatment

Raw 264.7 cells were cultured in RPMI complete growth medium comprising L-Glutamine, 4.5g/L glucose, 3.7g/L Sodium bicarbonate supplemented with 10% FBS and penicillin (100units/L), streptomycin (100µg/mL) and Amphotericin B (25 µg/mL) containing medium. Following proper aseptic techniques, cells were cultured and maintained under 5% CO₂ at 37°C in a humidified incubator. The growth medium was replaced on alternate days. Cells were subcultured after 80% confluence and detached with a cell scraper. RPMI complete growth medium was added to the detached cells, and the cell suspensions were centrifuged at 1500 rpm for 3 mins. After discarding the supernatant, the cell pellets were reconstituted in 1 ml of complete growth media and transferred to a new culture flask containing RPMI complete growth media. The hemocytometer was used to count the cells, and the number of cells for each experimental protocol was computed.

According to each treatment required number of Raw 264.7 cells were cultured for 24 hrs and pre-treated with different concentrations of samples for 4 hrs. Inflammatory conditions were generated in Raw 264.7 cells by incubating them with LPS (1 µg/mL) for 24 hrs. Dexamethasone(20µM) was used as a positive control in addition.

2.2.20. Nitric Oxide analysis

Nitric oxide (NO) is a signalling molecule that plays a key role in vascular regulation, vertebrate biological messenger, neurotransmission, immune responses and apoptosis. In contrast, NO acts as a pro-inflammatory mediator due to overproduction in abnormal situations. The synthesis and release of NO into the endothelial cells by iNOS convert arginine into citrulline. NO is intricate in the pathogenesis of inflammatory disorders of the joint, gut and lungs. Therefore, NO inhibitors have a significant role in the management of inflammatory diseases. NO content is measured using Griess reagent. This reagent reacts with nitrite in samples to form a purple azo product, the absorbance of which is measured at 546nm (J.N. Sharma, A. Al-Omran & S.S. Parvathy. (2007).

The nitrite levels in the culture medium were assessed by Griess reaction. RAW 264.7 macro-phage cells (5×10^3 cells/well) were cultured for 24 hrs in a 96-well plate and pre-treated with different concentrations of samples for 4 hrs. Dexamethasone (8 $\mu\text{g}/\text{mL}$) was taken as a positive control. Cellular NO production was stimulated by adding LPS (1 $\mu\text{g}/\text{mL}$), followed by incubation for 24 hrs. The conditioned medium (50 μl) was then mixed with the same volume of Griess reagent and incubated for 15 mins. The absorbance of the mixture at 546 nm was measured using a microplate reader (TECAN infinite 200Pro). The values were compared with those from standard concentrations of sodium nitrite and then levels of nitrite in the conditioned media of treated cells were calculated (Dhanasekar, Kalaiselvan, and Rasool 2015).

2.2.21. RNA sequencing (RNA-Seq) and Analysis

RNA sequencing (RNA-Seq) is revolutionising the study of the transcriptome. It is sensitive and accurate for assessing expression across the transcriptome. RNA-Seq is opening a new window for research into previously undetected areas of diseases in response to therapies and across a wide range of other study designs. Researchers can depend on transcriptome data without the restriction of prior knowledge because RNA-Seq detects both well-known and new features in a single test. RNA-seq is a broadly used screening technique active in inflammation research for identifying the whole expression of genes via next-generation sequencing (NGS).

A. RNA Isolation

High-quality RNA is crucial for gene expression. The RNeasy Mini kit (QIAGEN) was used to isolate and purify RNA effectively and according to the manufacturer's recommendations. This method combines the speed of micro spin technology with the selective binding capabilities of a silica-based membrane. The RNeasy silica membrane can bind up to 100 μg of RNA longer than 200 bases thanks to a specific high-salt buffer system. To ensure the purification of intact RNA, biological materials are first lysed and homogenised in the presence of a highly denaturing solution that contains guanidine-thiocyanate. This quickly inactivates RNases. After adding ethanol to create the proper binding conditions, the sample is put into an RNeasy Mini spin column, where complete RNA binds to the membrane and impurities are effectively removed. The next step is to elute high-quality RNA in 30-100 μl of water. The RNeasy method purifies all RNA molecules longer than 200 nucleotides.

Cells were grown in a monolayer (1×10^7 cells), the medium was aspirated after 24 hrs of treatment, and cells were washed twice with PBS. The cells were then carefully scraped out of the flask and transferred into an RNase-free polypropylene centrifuge tube centrifuged at 300 x g for five mins, the supernatant was discarded. Cells were disrupted by adding 600 μL of buffer RLT and vortexed for 5 mins. 1 volume of 70% ethanol was added to the lysate and mixed well by pipetting. 700 μL of the sample were transferred to the 2 mL collection tube and centrifuged for 15 s at 8000 x g, flow-through discarded. RNeasy spin column was filled with 700 μL of Buffer RW1, and

the mixture was centrifuged for 15 seconds at 8000 x g to clean the spin column membrane. Then, the flow-through was discarded. The RNeasy spin column was filled with 500 μ L of buffer RPE, centrifuged for 15 seconds at 8000 x g to wash the spin column membrane, and the flow-through was discarded. This process was carried out twice. The RNeasy spin column was placed in a new 1.5 mL collection tube. After adding 40 μ L of RNase-free water straight to the spin column membrane, the RNA was eluted by centrifuging for one minute at 8000 x g.

B. RNA Integrity Check

The RNA quality assessment was carried out using the RNA ScreenTape System (Agilent) in a 4150 TapeStation System (Agilent), which is specialized for analysing eukaryote and prokaryote RNA molecules from 50 to 6000 nt to compute the RINe values, on which the RNA quality is measured. The RNA sample was mixed with 5 μ L of RNA ScreenTape Sample buffer, heat denatured for 3 mins at 72 °C, and then promptly chilled for 2 mins before being loaded into the Agilent 4150 TapeStation instrument. The programme assigns an RNA integrity number (RINe), which indicates the consistency of the RNA. RINe values ranged from 1 to 10, with values between 1 and 5 indicating fully degraded RNA, 5 and 7 indicating moderately degraded RNA, and values above 8 indicating high-quality RNA.

C. RNA Quantification

The RNA concentration was evaluated using the Qubit® 3.0 Fluorometer and the Qubit™ RNA BR Assay Kit, which comprises RNA reagents, a dye that specifically binds to RNA with linear fluorescence detection in the range of 1-1000 ng/ μ L, and two RNA standards. A 1:200 dilution of the dye and buffer was used, and then 1 μ L of the RNA sample was added to the mixture and incubated at RT for 2 mins. The readings were collected using a Qubit.3 Fluorometer. The equipment was calibrated using the two standards included in the kit. RNA integrity and quality were assessed by Clevergene Biocorp Private Limited, Bengaluru, India.

D. Enrichment of mRNA and development of libraries

250ng of Total RNA has been utilised for enriching the mRNA using NEBNext Poly (A) mRNA magnetic isolation module. The NEBNext® Ultra™ II RNA Library Prep Kit for Illumina was used to prepare the libraries from the enriched mRNAs. In a nutshell, the NEBNext Random Primers were used to prime the enriched mRNAs, and then they were chemically fragmented at 94°C for 7 mins to obtain an insert of about 200 nucleotides. Reverse transcription was used to create cDNA from the fragmented mRNAs. First-strand cDNA reaction products were transformed into ds DNA. 1.8X of AMPure XP beads were used to clean up the resulting double-stranded cDNA fragments. The cDNA passes through end repair, where the mix turns the overhangs left over from fragmentation into blunt ends. The end-repair mix has 3' to 5' exonuclease activity that eliminates 3' overhangs and polymerase activity that fills in

5' overhangs. Adenylation was carried out by adding a single 'A' nucleotide to the 3' ends of the blunt-ended fragments. A uracil-specific excision reagent (USER) enzyme was used to ligate and cleave adenylated fragments attached to the loop adapters. NEBNext Ultra II Q5 master mix and "NEBNext® Multiplex Oligos for Illumina" were also added to the cDNA throughout the seven cycles of PCR to aid in multiplexing the sequencing process. The final DNA library was created by purifying the amplified products with 0.9X AMPure XP beads. The final DNA library was eluted in 15 l of 0.1X TE buffer after the amplified products were purified using 0.9X AMPure XP beads.

E. Quantification of Libraries

The concentration of the library was evaluated using a Qubit.3 Fluorometer (Life Technologies) and The Qubit dsDNA HS (High Sensitivity) Assay Kit. The DNA HS Assay Kit comprises buffers, high-sensitivity DNA reagents, as well as two DNA standards. The DNA HS assay reagent is one of the most sensitive detection dyes for precise quantification of DNA/library in solution, having linear fluorescence detection in the range of 10pg/l to 100ng/l of DNA.

A 1:200 dilution of the dye and the buffers was used, and 1 µl of the library was combined with the dye mixture before being incubated at RT for 2 min. The Qubit.3 Fluorometer was used to record the readings. The equipment was calibrated using the two included standards in the kit before measuring the sample.

F. Validation of Libraries

The library quality assessment was performed using an Agilent D5000 ScreenTape System and an Agilent D1000 ScreenTape System in an Agilent 4150 TapeStation System designed for analysing DNA molecules from 100 to 5000bp. The purified library was combined with 10 µL of D5000 sample buffer, 1 µL of each was added, and the mixture was vortexed using an IKA vortexer at 2000 rpm for 1 minute to collect the sample at the strip's bottom. After that, the strip was placed into the Agilent 4150 TapeStation device.

G. Next-generation sequencing analysis

NGS systems were created in the 2000s, and they transformed the genomics science. On general NGS platforms, library preparation, library amplification, and sequencing are standard procedures. Either RNA or DNA can serve as the starting point for the library preparation process. RNA has to be transcribed into cDNA. NGS platforms must meet specified length requirements. Genomic DNA must be fractionated and size-selected via sonication, nebulization, or enzymatic methods, followed by gel electrophoresis and excision. The typical fragment size for the Illumina NGS platform is between 300 and 550 bp, including adapters. These adapters make it easier to adhere library pieces to a glass slide's surface. The amplification of library fragments by emulsion is possible during the sequencing process thanks to known adaptor

sequences. NGS often takes use of bridge PCR parallelism in a ratio of 10,000 to billions of library pieces. This is often accomplished by repeating cycles of nucleotide addition utilising DNA polymerases or ligases, detecting integrated nucleotides, and washing procedures. Even though they are automated, the lengthy cleaning and repeated procedures may thus need hrs or even days to sequence. Base calling is the process of using an algorithm to identify the nucleotide that has been integrated from the signal intensities that have been discovered during the sequencing process (Hari and Parthasarathy 2018).

H. Alignment and Expression analysis

NGS Data analysis procedure requires careful human attention to detect problems and verify the reliability of the experiment model. The QC passed reads were mapped onto indexed *mus musculus* genome (GRCm39) using STAR v2 aligner. Expression similarity between biological replicated was checked by Spearman Rank correlation and Principal Components Analysis.

I. Differential expression analysis

The variability between biological replicates was grouped into control, inflammation and quinoa-treated groups and was compared based on differentially expressed genes using multivariate graphical tools. After normalising the data using the TMM values, differential expression analysis was performed using the edge R programme. 29057 features (52.44%) were eliminated from the study after normalisation because they lacked at least 0.1 counts-per-million in at least 3 samples. Heatmaps and volcano plots are used to display the expression profile of genes that differ in expression across samples.

J. Heatmap generation

A data visualisation technique uses colour to depict a phenomenon's magnitude in two dimensions in a heatmap, the information is shown as a rectangular grid, with each row denoting a gene and each column a sample.

K. Volcano plot generation

A volcano plot is used to show important genes with significant fold changes. The results were presented as a scatter plot, which was created by showing the fold change on the X-axis and the negative logarithm of the p-value on the y-axis.

L. Protein-protein interaction (PPI) networks visualisation and cluster detection

A PPI network was created using Search Tool for the Retrieval of Interacting Genes (STRING) with a high confidence score of 0.7 to display the functional relationships of proteins represented by the discovered differentially expressed genes. STRING is a database of observed and anticipated protein-protein interactions. The relationships

are both direct (physical) and indirect (functional), and they are the result of computer prediction, information transmission across species, and interactions collected from other primary databases. The PPI network was then visualised using Cytoscape software version 3.10 and clustered using MCODE plug-in with default parameters (Degree cut-off, 2; cluster finding, haircut; node score cut-off, 0.2; k-core, 2; and max depth, 100) to discover intensively connected regions called clusters/modules.

M. Discovery of hub genes

The tightly linked protein hubs, in the PPI network, were found using the cytohubba version 0.1 plug-in of the Cytoscape software. The maximal clique centrality (MCC) approach was used to rank the top 10 upregulated and downregulated hub genes separately.

N. Gene Enrichment analysis

Enrichment analysis was done for studying the biological process, molecular function, and cellular components. Gene ontology and pathway analysis were carried out to examine the mechanistic features of these upregulated and downregulated genes. KEGG Pathway was performed using the Cluster Profiler R package.

O. Gene ontology

Gene ontology (GO) and pathway enrichment analyses were performed using the genes that had noticeably differing levels of expression. The ClusterProfiler R package was used to perform enrichment analysis for biological processes, molecular function, cellular components, and KEGG pathway. GO plot R software was utilised to display the GO enrichment. The following formula is used by the GO plot package to determine the z-score:

$$Z\ Score = \frac{(up - down)}{\sqrt{count}}$$

where the number of upregulated genes in a GO phrase is represented by up, and the number of downregulated genes GO term is represented by down. A general idea of a gene's expression profile inside a GO word is provided by the z-score.

P. Pathway analysis

The pathways were visualised using the Pathview programme and the Kyoto Encyclopedia of Genes and Genomes (KEGG pathway) database was used to study the upregulation and downregulation of proteins in different signalling pathways.

2.2.22. Enzyme-linked immunosorbent assay

Enzyme-linked immunosorbent assay, developed by Engvall and Perlmann, for qualitative and quantitative analyses. Easily quantify cytokines, antigens, antibodies,

glycoproteins, and growth factors from small amounts of test samples. In ELISA, the antigen is coated on a solid phase to trap a targeted antibody, then reported through a secondary antibody conjugated with an enzyme, where signals will be generated in the presence of its corresponding substrate. The ELISA procedure results in a coloured end product, which correlates to the amount of analyte in the original sample.

In a standard cell culture condition, cells were 4 hrs pretreated with extract and then incubated for 24 hrs with LPS. The medium was collected for further study. 100 µl of medium coated in 96-well immunoplates and at 4°C overnight incubation was conducted. The medium was aspirated after the incubation and washed three times with PBST. Then, the cells were blocked with 200 µl of 5% skim milk for 1 hr. Then the cells were washed using PBST (thrice) and kept on a shaker for 10 mins after each wash. Followed by cells were incubated with primary antibody at 4°C with gentle agitation overnight. Again, PBST wash (thrice) was done. Then the cells were incubated in a shaker with 100 µl of HRP-conjugated secondary antibody for 2 hrs. Three times PBST wash was done to eliminate unbound antibodies. Cells were incubated with 100 µl of substrate solution for 15 mins. After that, the reaction was stopped using 50 µl of 1M sulphuric acid. The absorbance at 540 nm was measured using a microplate reader (TECAN infinite 200Pro) and quantity was measured in optical density units of protein present in the treated medium.

2.2.23. ROS analysis

Reactive oxygen species (ROS) have a role in the onset, development, and resolution of the inflammatory response. The ROS is functioning as a second messenger and microbicidal agent during intracellular signalling. Excessive ROS production can cause tissue and cell damage and chronic inflammation that underlies many neurodegenerative, cardiovascular, and metabolic illnesses (Hancock, Desikan, and Neill 2001; Chelombitko 2018). The intracellular ROS formation was analyzed using DCFDA (2',7' -dichlorofluorescein diacetate), which is a fluorogenic used for detecting ROS. The cellular esterases are deacetylated into a product. Cellular ROS oxidise the product into a highly fluorescent DCF, which can be visualised by standard broad pass filters for FITC.

Cells were seeded in a 96-well black plate for the test at a density of 1×10^4 cells per well and attachment was allowed to occur under standard conditions for 24 hrs. After a 4 hrs preincubation with the extracts and dexamethasone (20 µM), cells were treated with 100µL medium with LPS (1µg/mL for 24 hrs. After aspirating the medium, the wells were washed twice with PBS. The wells were treated with 100 µL of DCFDA working solution, which was then incubated for 20 mins at 37°C in a CO₂ incubator. The stain was aspirated, and the wells were gently washed two times with PBS washes. The wells were filled with 100 L of PBS, and fluorescence was seen using a fluorescent microscope (ex 488 nm/em 525 nm) on a BD Pathway™ 855 High-Content BioImager (AttoVision software; BD Biosciences, San Jose, CA, USA).

2.2.24. Cell lysate preparation

Effective cell lysis is necessary for isolating the cellular proteins without causing protein breakdown. RIPA was chosen as the cell lysis solution because it allows quick protein extraction, effectively solubilizes proteins, and does not adversely interact with proteins. Furthermore, protease inhibitors were added to the lysis solution to inhibit proteolytic activity. Detergent act as reducing agents and are used to denature the proteins in the sample.

The media was aspirated, and two times cell washed with ice-cold PBS. An appropriate amount (300 μ L for 1×10^7 cells) of RIPA lysis buffer (RIPA lysis buffer- 10 mL RIPA buffer, 1 mL PIC, and 10 μ L Triton X 100 mixed) was added into the cell culture dish. After 30 mins of incubation, cells were separated using a cell scraper from the culture plate and lysed the remaining cells. after 5 mins of sonication, the lysate was centrifuged at 12000 rpm for 20 mins at 4°C. The supernatant was collected and kept at -80°C for later use.

2.2.25. Immunoprecipitation

Immunoprecipitation is a technique that uses an antigen-antibody interaction to separate a particular protein from a mixture. Affinity purification of antigens is accomplished by immobilising bacterial proteins, Protein A or Protein G, to a solid matrix. These bacterial proteins effectively interact with antibodies. The bacterial proteins in the matrix are bound by the antibody that is specific to the target protein. The target protein binds to the antibody during the subsequent incubation of the sample. It is possible to separate the proteins coupled to the antibody and obtain a concentrated protein sample. The manufacturer, MagGenome Technologies, supplied a standard protocol that was followed when experimenting. This procedure was utilised to precipitate the low-concentration proteins in the cell lysate. Cell lysate protein concentrations were normalised. Each sample of cell lysate was incubated with 2 μ L of primary antibody at 4 °C overnight. The magnetic nanoparticles were pre-cleared by washing them three times in PBS. 50 μ L of magnetic nanoparticles were added to each lysate-antibody mixture and then incubated at 4°C for two hrs with constant agitation. A magnetic platform was used to collect the nanoparticles, and after multiple washes, 50 μ L of 1X SDS-PAGE reducing sample buffer (1.25mL of 0.5M Tris HCl (pH-6.8), 2.5mL glycerol, 2 mL 10% SDS and a pinch of bromophenol blue added and the total volume of the solution made up to 10mL. Before the experiment β -mercaptoethanol was added into the solution (around a 4:1 ratio) was added to the mixture. After five mins of heating the sample at 100°C, the supernatant was extracted. After purification, the material was utilised for western blot analysis.

2.2.26. Western blot analysis

Western blotting is widely for researchers to isolate individual proteins from a complicated mixture of proteins using a western blot. Western blot is frequently used

to separate and identify proteins. In this method, a mixture of proteins is sorted by type and molecular weight using gel electrophoresis. These findings are subsequently transferred to a membrane, resulting in a band for each protein. Next, labelled antibodies that are specific to the target protein are incubated on the membrane (Mahmood and Yang 2012). The expression of proteins involved in immune response was analyzed using this technique according to a standard protocol. The samples were subjected to SDS-PAGE gel electrophoresis. The proteins were transferred from the gel to a PVDF membrane. To ensure protein transfer, the membrane was dyed with Ponceau S. The membrane was shaken in a 5% skim milk solution for one hour at RT for blocking the protein in the membrane. The membrane was washed three times for 10 mins with PBST (0.1% Tween 20 was added to PBS). After that, the membrane was incubated with the primary antibody in a shaker overnight at 4°C. To get rid of the unbound antibody, the membrane was once again washed three times for ten mins with PBST. Then, the membrane was incubated in a secondary antibody with a conjugated enzyme at RT for two hrs. The protein bands are detected by chemiluminescence utilising a ChemiDoc™ MP System (BioRad, Hercules, CA, USA). The substrate interacts with the enzyme conjugated to the secondary antibody to produce light; it was captured using a digital imaging device based on a charge-coupled device CCD. The protein was identified by the position of the band in the image, and densitometry (IMAGELAB™ Software) was used to analyse the protein's expression levels.

2.2.27. Immunofluorescence analysis

Immunofluorescence (IF) is a method that makes it possible to visualise most of the cell components. This broad capacity is due to the utilisation of the specific combination of fluorophore-labelled antibodies. An indirect IF technique was employed to analyse the nuclear translocation of NF- κ B and I κ B α expression.

On black 96-well plates, 1×10^4 cells were seeded and cultivated for 24 hrs. After attachment, the cells were 4 hrs pre-treated with extracts and then exposed to LPS for 24 hrs. Following the treatment, the cells were washed with PBS and then fixed in 100 μ L of 4% paraformaldehyde in PBS at RT for 15 mins. After aspiration of the fixative, the cells were incubated in 100 μ L of permeabilization buffer (0.1% Triton X100 in PBS) for 10 mins. Then the cells were washed with 200 μ L PBS three times (10 mins each) with mild agitation on a shaker. After that, the cells were incubated for 1 hr with gentle shaking in a blocking buffer (5% normal goat serum, 0.3% Triton X 100). The blocking buffer was removed, and the cells underwent three times PBS wash and then incubated with 100 μ L of primary antibody solution overnight at 4°C. After three times PBS, the cells were treated with 100 μ L of Alexa fluor-labelled secondary antibody. After 2 hrs of incubation in dark conditions, the secondary antibody was aspirated, and the cells were gently washed(3x) with PBS. The cells were incubated with DAPI solution for 5 mins on a shaker in a dark condition. After that, 100 μ L of PBS was

added to the cells, which were then viewed and imaged under a fluorescent microscope.

2.2.28. Cytokine array analysis

Cytokine is a broad name for secreted proteins that play key roles in inflammatory modulation. As pathogens invade, cytokines are produced to activate and multiply immune cells. The two types of cytokines are pro-inflammatory and anti-inflammatory. They are essential for coordinating cell-mediated immune responses. To manage inflammation, cytokines often influence immune cell proliferation, activity, differentiation, and home to the sites of infection.

Cytokine arrays are antibody-pair-based assays similar to ELISA, a membrane as a substrate. In this array technique, the simultaneous detection of 96 Mouse Cytokine proteins in serum, cell culture medium, plasma, and other liquid sample types is possible. The spotted cytokine proteins are Axl, Bfgf, BLC (CXCL13), CD30 Ligand (TNFSF8), CD30 (TNFRSF8), CD40 (TNFRSF5), CRG-2, CTACK (CCL27), CXCL16, CD26 (DPPIV), Dtk, Eotaxin-1 (CCL11), Eotaxin-2 (MPIF-2/CCL24), E-Selectin, Fas Ligand (TNFSF6), Fc gamma RIIB (CD32b), Flt-3 Ligand, Fractalkine (CX3CL1), GCSF, GITR (TNFRSF18), GM-CSF, HGFR, ICAM-1 (CD54) IFN-gamma, IGFBP-2, IGFBP-3, IGFBP-5, IGFBP-6, IGF-1, IGF-2, IL-1 beta (IL-1 F2), IL-10, IL-12 p40/p70, IL-12 p70, IL-13, IL-15, IL-17A, IL-17 RB, IL-1 alpha (IL-1 F1), IL-2, IL-3, IL-3 R beta, IL-4, IL-5, IL-6, IL-7, IL-9, I-TAC (CXCL11), KC (CXCL1), Leptin, Leptin R, LIX, L-Selectin (CD62L), Lungkine (CXCL15), Lymphotactin (XCL1), MCP-1 (CCL2), MCP-5, M-CSF, MDC (CCL22), MIG (CXCL9), MIP-1 alpha (CCL3), MIP-1 gamma, MIP-2, MIP-3 beta (CCL19), MIP-3 alpha (CCL20), MMP-2, MMP-3, Osteopontin (SPP1), Osteoprotegerin (TNFRSF11B), Platelet Factor 4 (CXCL4), Pro-MMP-9, P-Selectin, RANTES (CCL5), Resistin, SCF, SDF-1 alpha (CXCL12 alpha), Sonic Hedgehog N-Terminal (Shh-N), TNF RI (TNFRSF1A), TNF RII (TNFRSF1B), TARC (CCL17), I-309 (TCA-3/CCL1), TECK (CCL25), TCK-1 (CXCL7), TIMP-1, TIMP-2, TNF alpha, Thrombopoietin (TPO), TRANCE (TNFSF11), TROY (TNFRSF19), TSLP, VCAM-1 (CD106), VEGF-A, VEGFR1, VEGFR2, VEGFR3, VEGF-D. Undoubtedly, the simultaneous detection of several cytokines is a potent tool for unravelling the roles of multiple cytokines.

In T-75 flasks, cells were seeded at a density of 2×10^6 and allowed to attach for 24 hrs. After that, pre-treated with Q80-M for 4 hrs and LPS was administered for 24 hrs. After treatment, the medium was collected and kept at -20°C . Each media's total protein concentration was calculated using a BCA kit, and the protein was equalised using a blocking buffer to a final volume of 2 mL per membrane containing 400–600 μg of total protein. The membrane was positioned in the provided 8-well tray with its printed side facing up.

The membrane was placed in the 8-well tray and 2 mL blocking buffer was gently poured on top of the membrane. The membrane was kept for 30 mins at RT on a shaker. After aspirating blocking buffer and membrane were incubated with 1 mL of lysate overnight at 4°C with gentle shaking. After incubation, the samples were aspirated, and the membrane was washed three times (5 mins each) using 2 mL of wash buffer I, and then the membrane was washed two times (5 mins each) with 2 mL of wash buffer II.

After aspirating the wash buffer, the membrane was gently shaken at 4°C incubated with 1 mL of biotin-conjugated anti-cytokines overnight. After aspirating the reagent, the membrane was washed using wash buffers I and II following the earliest description. The membrane is treated with 2 mL of HRP-Streptavidin for 2 hrs at RT with gentle shaking. The HRP-streptavidin was aspirated, and the membrane was washed with the previously indicated wash buffer I and II.

The membrane was placed on the provided plastic sheet, the protein side facing up, and the excess water was blotted out by lightly wiping one edge of the membrane with filter paper. 250 L of detection buffer was added to the membrane, and another plastic sheet was placed over it to ensure that the detection mixture covered the membrane thoroughly and bubble-free. The top plastic sheet was removed to drain the excess buffer and after, 2 mins the chemiluminescence image of the membrane was taken using ChemiDoc™ MP System (Bio-Rad, Hercules, CA, USA) and IMAGE LAB™ Software.

The control solution added membrane was used as the "reference," and the following formula was used to calculate the normalised values:

$$X(Ny) = X(y) \times P1/P(y)$$

Where:

P1 = mean signal density of Positive Control spots on reference array

P(y) = mean signal density of Positive Control spots on Array "y"

X(y) = mean signal density for spot "X" on Array for sample "y"

X(Ny) = normalized signal intensity for spot "X" on Array "y"

2.2.29. Statistical Analysis

All experiments were performed three times except for NGS, apoptosis membrane array and cytokine membrane array (duplicate). In NGS analysis, differentially expressed genes with absolute log₂ fold change ≥ 1 and adjusted p-value ≤ 0.05 were considered significant. All the other data were displayed as mean \pm standard deviation (SD). SPSS software version 24.0 (IBM Corp., USA) was used to compare treatments

utilising one-way Analysis of Variance (One-way ANOVA), then Duncan's multiple range tests. The statistical significance of the difference in means, a p-value of less than 0.05, was considered statistically significant.

2.2.30. References

1. Bobadilla AVP, Arévalo J, Sarró E, Byrne HM, Maini PK, Carraro T, Balocco S, Meseguer A, Alarcón T. “In Vitro Cell Migration Quantification Method for Scratch Assays.” *Journal of the Royal Society Interface*. 2019; 16(151). doi: 10.1098/rsif.2018.0709. PMID: 30958186; PMCID: PMC6408363.
2. Buranaamnuay, Kakanang. “The MTT Assay Application to Measure the Viability of Spermatozoa: A Variety of the Assay Protocols.” *Open veterinary journal*. 2021; 11(2): 251–69. doi: 10.5455/OVJ.2021.v11.i2.9. Epub 2021 May 8. PMID: 34307082; PMCID: PMC8288735.
3. Chelombitko, M. A. “Role of Reactive Oxygen Species in Inflammation: A Minireview.” *Moscow University Biological Sciences Bulletin*. 2018; 73(4): 199–202. doi:10.3103/S009639251804003X
4. Dhanasekar C, Kalaiselvan S, Rasool M. “Morin, a Bioflavonoid Suppresses Monosodium Urate Crystal-Induced Inflammatory Immune Response in RAW 264. 7 Macrophages through the Inhibition of Inflammatory Mediators, Intracellular ROS Levels and NF- κ B Activation.” *PLoS One*. 2015; 10(12), doi:10.1371/journal.pone.0145093.
5. Gauthier, S. F., C. Vachon, and L. Savoie. “Enzymatic Conditions of an In Vitro Method to Study Protein Digestion.” *Journal of Food Science*. 1986; 51(4): 960–64, doi:10.1111/j.1365-2621.1986.tb11208.x.
6. Gayathri, T., T. C. Kishor Mohan, and K. Murugan. “Purification and Characterization of Polygalacturonase-3 from Jamaica Cherry (*Muntingia calabura* Linn).” *Journal of Plant Biochemistry and Biotechnology*. 2007;16(2): 127–30. doi:10.1007/bf03321987
7. Hancock, J. T., R. Desikan, and S. J. Neill. “Role of Reactive Oxygen Species in Cell Signalling Pathways.” *Biochemical Society Transactions*. 2001; 29(2): 345–50.
8. Hari, Ranjeev, and Suhanya Parthasarathy. 1–3 *Encyclopedia of Bioinformatics and Computational Biology: ABC of Bioinformatics Next Generation Sequencing Data Analysis*. 2018; 1. <http://dx.doi.org/10.1016/B978-0-12-809633-8.20093-9>.
9. Kakhorova, Komola A., Zaynat S. Khashimova, and Ekaterina O. Terenteva. “Studies on Cytotoxicity and Antioxidant Activities of Lectin-like Proteins from Phytoparasites (*Cuscuta Europaea*).” *Asian*

- Journal of Pharmacy and Pharmacology. 2018; 4(3): 265–70. doi:10.3109/10520299509108199.
10. Kapuscinski, Jan. “DAPI: A DMA-Specific Fluorescent Probe.” *Biotechnic and Histochemistry* 1995; 70(5): 220–33. doi:10.3109/10520299509108199.
 11. Kasibhatla S, Amarante-Mendes GP, Finucane D, Brunner T, Bossy-Wetzel E, Green DR. “Acridine Orange/Ethidium Bromide (AO/EB) Staining to Detect Apoptosis.” *Cold Spring Harbor Protocols* 2006(3):doi:10.1101/pdb.prot4493.
 12. Lowry, O. H., N. J. Rosebrough, A. L. Farr, and R. J. Randall. “Protein Measurement with the Folin Phenol Reagent.” *The Journal of biological chemistry*. 1951; 193(1): 265–75. [http://dx.doi.org/10.1016/S0021-9258\(19\)52451-6](http://dx.doi.org/10.1016/S0021-9258(19)52451-6).
 13. Mahmood, Tahrin, and Ping Chang Yang. “Western Blot: Technique, Theory, and Trouble Shooting.” *North American Journal of Medical Sciences*. 2012; 4(9): 429–34. doi:10.4103/1947-2714.100998.
 14. Sonawane, Sachin K, and Shalini S Arya. “Current Research in Nutrition and Food Science Plant Seed Proteins : Chemistry, Technology and Applications.” *Current Research in Nutrition and Food Science*. 2018; 06(2).
 15. Wada, Yasuaki, and Bo Lönnerdal.. “Bioactive Peptides Released from in Vitro Digestion of Human Milk with or without Pasteurization.” *Pediatric Research*. 20157; 7(4): 546–53. doi:10.1038/pr.2015.10.
 16. Wallberg, Fredrik, Tencho Tenev, and Pascal Meier. “Analysis of Apoptosis and Necroptosis by Fluorescence-Activated Cell Sorting.” *Cold Spring Harbor Protocols* 2016(4): 347–52.
 17. Webster, J., & Oxley, D. Protein Identification by Peptide Mass Fingerprinting using MALDI-TOF Mass Spectrometry In: Walker, J.M. (eds) *The Protein Protocols Handbook*.2009. 1117–1129. doi:10.1007/978-1-59745-198-7_120
 18. Wingfield, Paul. “Protein Precipitation Using Ammonium Sulfate.” *Current Protocols in Protein Science*, 1998; A.3F.1-A.3F.8. doi:10.1002/0471140864.psa03fs13.

CHAPTER 3

Isolation of bioactive peptides and secondary metabolites from Amaranth and Quinoa seeds and their screening for *in vitro* antioxidant, anti-breast cancer and anti-inflammatory effects

3.1. Introduction

Amaranth and quinoa grains have gained popularity recently due to their high nutritional value and potential health advantages. In light of this, the United Nations FAO designated 2013 as "The International Year of Quinoa" to encourage the growth and research of this pseudocereal (Abdelaleem and Elbassiony, 2021). Recently the research attention has been changed to phytochemicals and biopeptides of amaranth and quinoa due to their potential significance in reducing the risk of chronic diseases. Major phytochemicals in amaranth and quinoa seeds are carotenoids, flavonoids and polyphenols. Based on both *in vitro* and *in vivo* research, these phytochemicals are reported to impact human health positively. They are natural antioxidants with various biological attributes, such as anti-inflammatory and anti-cancer properties (Tang and Tsao, 2017).

Also, amaranth and quinoa are the sources of various bioactive peptides. Many research articles discuss the possible benefits of biopeptides for various disease conditions. Bioactive peptides are typically small (3–20 amino acid) peptides generated from proteins that have biological effects in addition to their intended nutritional value. They are generated during food processing (heating, fermentation, and ripening) and enzymatic proteolysis (gastrointestinal digestion, *in vitro* hydrolysis using proteolytic enzymes). Food-based biopeptides are currently the main focus of research due to their capacity to act like synthetic pharmaceuticals. The bioactive peptides and peptide-rich protein hydrolysates have the potential to enter the cells due to their dietary origins and the absence of harmful side effects. They serve as an alternative to natural ingredients and as a vital regulator of cell mechanisms. Therefore, there is a real need to concentrate on the connection between biopeptides and their biological functionalities. Biopeptides are significantly contributing to various biological processes including antihypertensive, antimicrobial, antithrombotic, immunomodulatory, hypocholesterolaemia, and antioxidative activities. Some peptide fragments may also exhibit multiple biological functions (Daliri et al., 2017)(Saadi et al., 2015).

Recent studies show that polyphenols and biopeptides are promising compounds that may help to control oxidative stress, cancer and inflammatory diseases. Oxidative damage is thought to be one of the causes of cancer and chronic inflammatory diseases (Wang et al., 2021). Abundant studies over the past 20 years have identified the mechanism by which persistent oxidative stress can cause chronic inflammation, which may mediate most chronic diseases. Oxidative stress can activate several transcription factors, including NF- κ B, AP-1, p53, HIF-1 α , PPAR- γ , β -catenin/Wnt,

and Nrf2. Activating these transcription factors can produce over 500 different genes, including those for growth factors, inflammatory mediators, and cell cycle regulatory molecules. Inflammation and even cancer can result from oxidative stress (Reuter et al., 2010). Oxidative stress influences the formation of cancer by causing cancer cells to become resistant to antiproliferative signals and apoptosis, anchorage-independent cell growth, and epigenetic modification of cancer cell invasion and migration (Zhao et al., 2021). Therefore, drug candidates with ameliorative effects on oxidative stress are considered suitable alternatives for treating chronic inflammation and associated diseases. The advantages of antioxidant supplements in health and disease have been sparked by the connection between inflammation and oxidative damage. Dietary antioxidants exert antioxidant properties through various mechanisms of action, including the scavenging of free radicals and the inhibition of the generation of reactive species during normal cell metabolism. This prevents the damage of lipids, proteins, nucleic acids, and cell damage (Iddir et al., 2020)(Zhang et al., 2018).

Numerous health benefits have been linked to this amaranth and quinoa seeds due to the presence of both biopeptides and phytochemicals. They positively impact human health and prevent diseases. In the present study, protein and phytochemicals of amaranth and quinoa seeds were isolated and studied for their activity as an antioxidant, anti-breast cancer and antiinflammation activity.

3.2. Methodology

Proteins and bioactive-rich solvent extracts isolated from amaranth and quinoa seeds. The protein isolates from amaranth and quinoa seeds underwent simulated gastrointestinal digestion to release peptides. Concurrently, using the Soxhlet extraction method, bioactive-rich solvent extracts were isolated. The peptides and extracts were tested for their antioxidant, anti-breast cancer, and anti-inflammatory properties. The peptide fraction and bioactive-rich extract with the necessary activity were ultimately chosen for additional in-depth research.

1. Protein isolation by Ammonium sulphate precipitation
2. *In vitro* gastrointestinal digestion for isolating peptides from amaranth and quinoa seeds
3. Isolation of bioactive molecules from amaranth and quinoa seeds by Sequential and direct Soxhlet extraction
4. DPPH assay for identifying the free radical scavenging activity of amaranth and quinoa protein hydrolysates and extracts.
5. Phosphomolybdenum Assay for measuring total antioxidant capacity amaranth and quinoa protein hydrolysates and extracts
6. The total phenol content analysis of solvent extracts.
7. MTT assay for cytotoxicity analysis amaranth and quinoa protein hydrolysates and extracts

8. Nitric Oxide analysis for examining the anti-inflammatory activity of amaranth and quinoa protein hydrolysates and extracts

All the assays were performed in triplicate, and the detailed procedures are described in Chapter 2. The positive control used in this chapter were ascorbic acid as an antioxidant, gallic acid in total phenol content analysis, curcumin for their anticancer and dexamethasone for antiinflammation study.

3.3. Results

3.3.1. Protein isolation by Ammonium sulphate precipitation

The crude proteins from amaranth and quinoa seeds (ASP and QSP) were efficiently precipitated using 70% ammonium sulphate as indicated by the protocol described in the methods. Amaranth and quinoa seeds were found to have protein contents of 21 ± 0.57 and 20 ± 0.47 mg protein/1g of seed, respectively. The protein yield from amaranth and quinoa seeds was 10.5% and 10%, respectively.

3.3.2. In vitro gastrointestinal digestion of isolating peptides from amaranth and quinoa seeds

The isolated proteins from amaranth and quinoa seeds were subjected to simulated gastrointestinal digestion in the raw and heat-denatured form as described in the methods. The different protein samples screened for the study are given in the list and Figure 3.1.

- ASP-Amaranth seed crude protein
- ASP-D- Amaranth seed protein digested
- ASP-HD- Amaranth seed protein digested after heat denaturation
- QSP- Quinoa seed crude protein
- QSP-D- Quinoa seed protein digested
- QSP-HD- Quinoa seed protein digested after heat denaturation

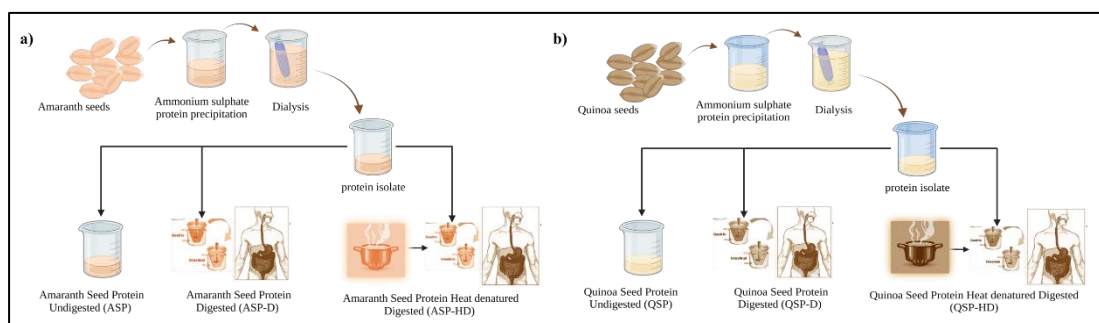


Figure 3.1: Protein isolation and in vitro simulated gastrointestinal digestion (a). Amaranth seed protein isolation and digestion method and (b). Quinoa seed protein isolation and digestion method

3.3.3. Isolation of bioactive molecules rich extract from amaranth and quinoa seeds by sequential extraction and direct soxhlet extraction

Amaranth and quinoa seed bioactive-rich extracts were prepared by direct and sequential extraction as described in the methods. The different solvent extracts screened for the study are given in the list and Figure 3.2.

- A-80M- Amaranth seed 80% methanol extract (direct extraction)
- AH-Amaranth seed hexane extract (sequential)
- AEA- Amaranth seed ethyl acetate extract (sequential)
- AM- Amaranth seed methanol extract (sequential)
- Q-80M- Quinoa seed 80% methanol extract (direct extraction)
- QH- Quinoa seed hexane extract (sequential)
- QEA- Quinoa seed ethyl acetate extract (sequential)
- QM- Quinoa seed methanol extract (sequential)

The total yields were reported as a percentage of both amaranth and quinoa seed extracts (Figure 3.2). In the direct method, A-80M (Amaranth seed 80% methanol extract) and Q-80M (Quinoa seed 80% methanol extract) have yields of 4.95% and 6.58%, respectively. The sequential extraction technique was chosen to elute the maximum number of molecules from the sample. Three different organic solvents were employed based on their polarities: hexane, ethyl acetate, methanol, and 80% methanol. In amaranth seed extract, higher yields were observed in AH (Amaranth seed hexane extract) (5.438% yield) and AM (Amaranth seed methanol extract) (2.785%). A far lower yield was registered for AEA (Amaranth seed ethyl acetate extract) (0.132%). The quinoa seed yield was slightly higher than the amaranth extraction yield. The lowest yield was recorded in QEA (Quinoa seed ethyl acetate extract), at 0.092%. QH (Quinoa seed hexane extract) and QM (Quinoa seed methanol extract) have good yields in the extraction process: 6.3% and 6.885%, respectively.

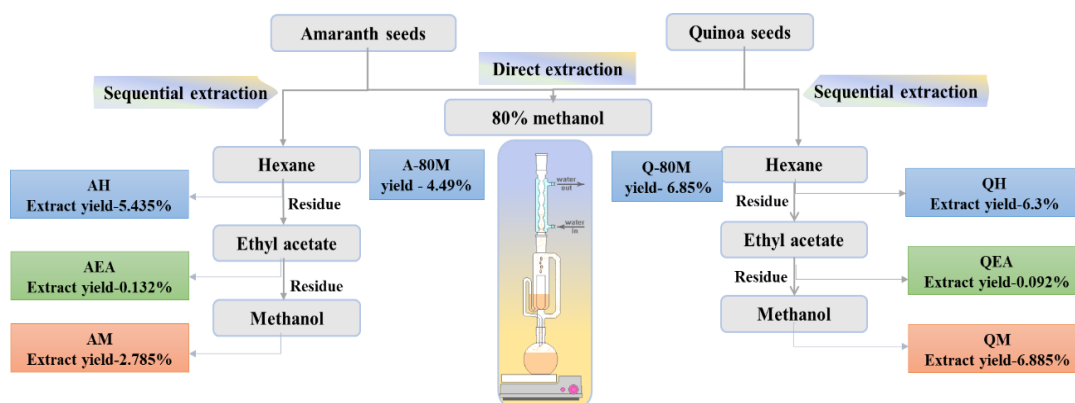


Figure 3.2: Direct and sequential extraction of amaranth and quinoa seeds using Soxhlet extraction method.

3.3.4. Antioxidant analysis of protein isolates and solvent extracts of amaranth and quinoa seeds

3.3.4.1. DPPH free radical scavenging analysis of protein isolates of amaranth and quinoa seeds

The protein hydrolysates had better DPPH[•] scavenging activity than the intact protein (Figure 3.3). EC₅₀ value of ASP and QSP in free radical scavenging potential was found to be 64 mg and 77mg, respectively, which decreased to 19 ± 0.5 mg in ASP-D and 48± 0.6 mg in QSP-D with the simulated digestion conditions (ASP-D). There was a significant decrease in the EC₅₀ value when the digestion was done after heat denaturation (1.9 ± 0.03 mg for ASP-HD and 41± 0.47mg for QSP-HD). The positive control of ascorbic acid gave an EC₅₀ value of 5.6 ± 0.1µg.

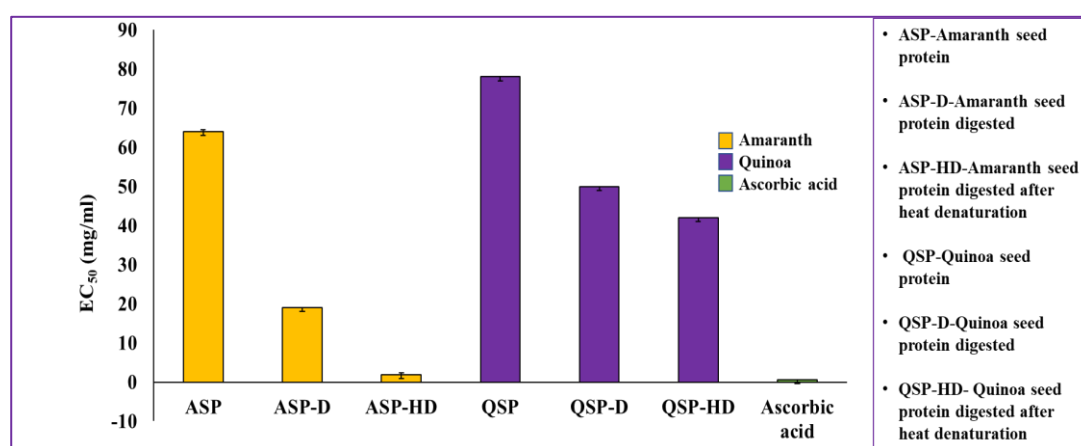


Figure 3.3: The effective concentration at which the DPPH radicals were scavenged 50% by Amaranth/Quinoa seed protein undigested, digested(D) and heat denatured digested (HD) samples. Each value represents a mean ± SD (n=3).

3.3.4.2. Total antioxidant activity of protein isolates of amaranth and quinoa seeds

Amaranth and quinoa protein isolates were both found to have antioxidant activity (Figure 3.4). The maximum overall antioxidant activity is seen in the ASP-HD and QSP-HD with 121± 0.52 and 99± 0.52 mg Ascorbic acid/g, respectively. The undigested seed protein isolates of amaranth and quinoa, ASP-16mg Ascorbic acid/g and QSP-13mg ascorbic acid/g, had the lowest antioxidant activity.

3.3.4.3. DPPH free radical scavaging analysis of solvent extracts of amaranth and quinoa seeds

The concentration needed to reduce the level of half-free radicals is known as the half-maximal effective concentration (EC₅₀). It evaluates a substance's ability to block biological or biochemical processes. In amaranth seed extracts, the AM extracts showed the highest free-radical scavenging activity with EC₅₀ values of 0.36± 0.014 mg/mL followed by AEA, A-80M and AH (0.4, 0.46±.001 and 0.75±014 mg/mL, respectively) (Figure 3.5). Among quinoa extracts, Q-80M showed the best antiradical EC₅₀ value (0.2mg/ mL), followed by QEA, QM, and QH (0.25, 0.25 and 0.5 ± 0.003 mg/mL, respectively)

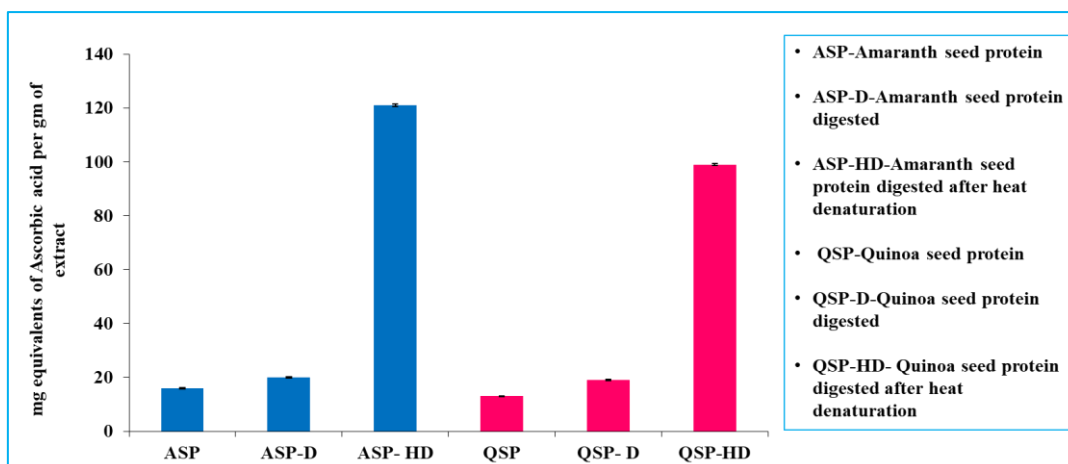


Figure 3.4: Total antioxidant capacity of Amaranth/Quinoa seed protein undigested, digested(D) and heat denatured (HD) by Phosphomolybdate assay. Each value represents a mean \pm SD ($n=3$).

3.3.4.4. Total antioxidant activity of solvent extracts of amaranth and quinoa seeds

Antioxidant activity was discovered in both amaranth and quinoa seed extracts (Figure 3.6). Amaranth seed extracts AM and AEA extract showed high total antioxidant activity, 37 ± 0.42 and 29 ± 0.61 mg Ascorbic acid/g, respectively. Among the quinoa seed extracts, QEA and Q80-M extract had high TAC 48 ± 0.21 and 40 ± 0.48 mg ascorbic acid/g, respectively.

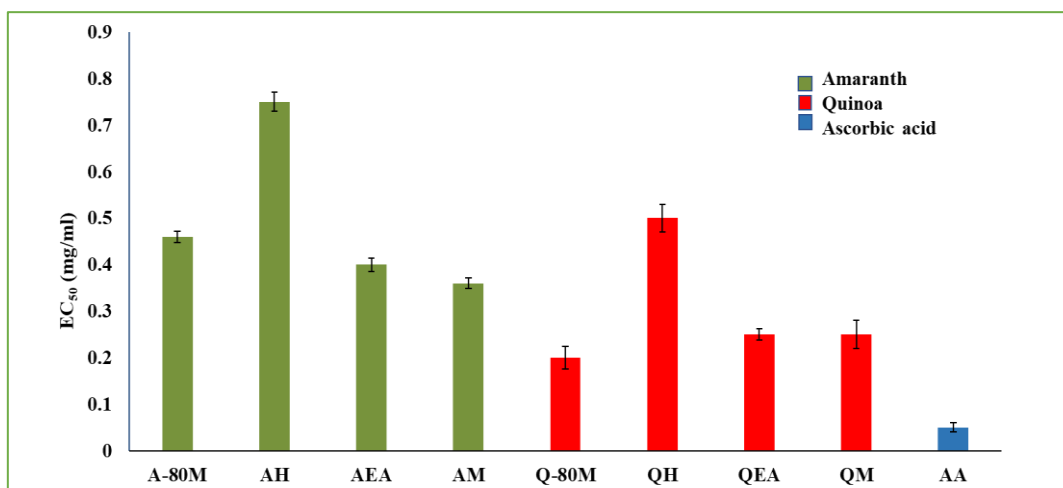


Figure 3.5: The effective concentrations at which 50% of DPPH radicals were scavenged by amaranth and quinoa solvent extracts. Values are average of three independent experiments \pm SD.

3.3.4.5. Phenolic contents in solvent extracts of amaranth and quinoa seeds

Phenolic compound contents of amaranth and quinoa extracts were determined using the Folin–Ciocalteu assay (Figure 3.7). Amaranth seed extract total phenolics ranged from 0.13 to 0.30 mg Gallic Acid Equivalent (GAE)/100 mg. The highest phenolic content was obtained in AM 0.30 mg GAE/100 mg, followed by AEA, A-80M, and

AH. The phenolic content of quinoa seeds ranges from 0.21 to 0.37 mg GAE/100 mg, significantly higher than that of amaranth seeds. The lowest phenolic concentration was found in QH at 0.21 mg GAE/100 mg, while Q-80M had a high phenolic level of 0.37 mg GAE/100 mg.

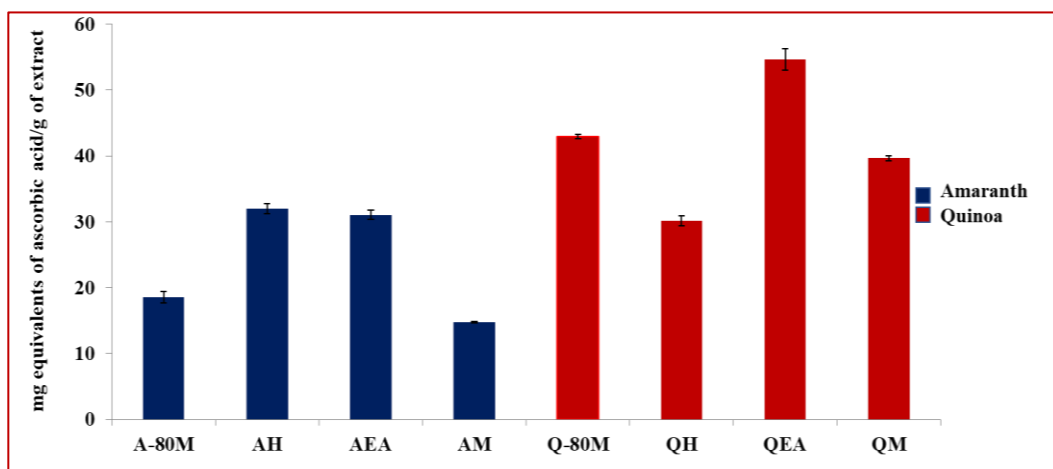


Figure 3.6: Total antioxidant activity of amaranth and quinoa solvent extracts. Values are average of three independent experiments \pm SD.

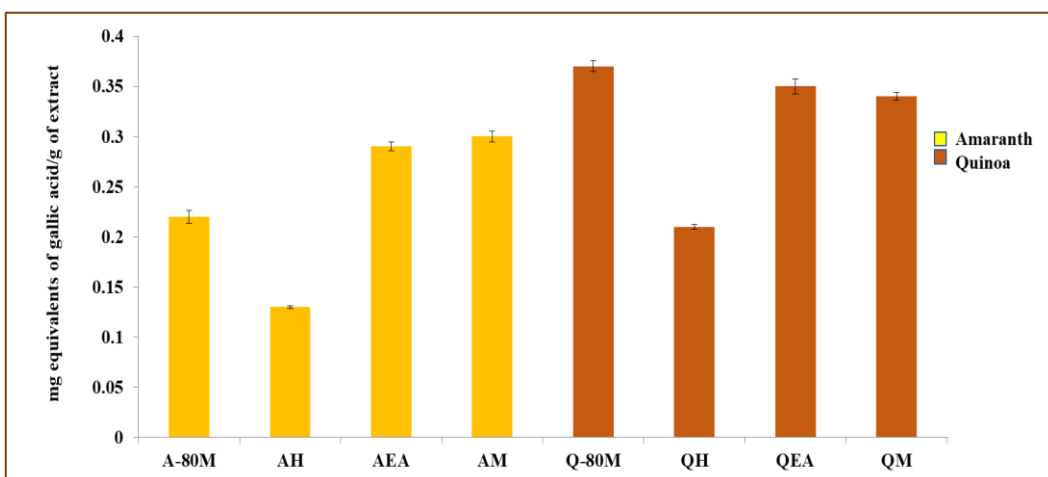


Figure 3.7: Total polyphenol content in amaranth and quinoa solvent extracts. Values are average of three independent experiments \pm SD.

3.3.5. Anti-breast cancer analysis of protein isolates and solvent extracts of amaranth and quinoa seeds

3.3.5.1. Cytotoxicity analysis of protein isolates of amaranth and quinoa seeds

Amaranth and quinoa protein hydrolysates were subjected to cytotoxicity evaluation using an MTT assay in MDA-MB-231 cells. Cells were exposed to varying concentrations of the hydrolysates (20, 50, 100, 200 and 500 μ g/mL) for 24 hours, and the percentage of growth inhibition for each compound was calculated by the formula given in section 2.2.4. The results indicated that ASP-HD exhibited significant

cytotoxicity towards MDA-MB-231 cells. GI50 (concentration at which 50% of growth inhibition is achieved) ASP-HD were found to be $48.3 \pm 0.2 \mu\text{g/ml}$ in MDA-MB-231 cells. ASP-HD were non-toxic towards normal L6 cells. The GI50 values of all the amaranth and quinoa hydrolysates are displayed in Table 3.1.a.

3.3.5.2. Cytotoxicity analysis of solvent extracts of amaranth and quinoa seeds

Solvent extracts from amaranth and quinoa seeds were also tested for cytotoxicity against breast cancer using an MTT assay in MDA-MB-231 cells. Following the procedure described in section 2.2.4, cells were exposed to solvent extracts (25, 50, 100, 250, and 500 $\mu\text{g/mL}$) concentrations. The results showed that the extracts were not significantly cytotoxic to MDA-MB-231 cells up to 500 $\mu\text{g/mL}$ (GI ranged from 4 ± 0.04 to $29 \pm 0.05\%$) Table 3.1.b.

a) Protein hydrolysates

Samples	Conc. ($\mu\text{g/ml}$)	% of cytotoxicity against MDA-MB cell lines
Protein isolates from Ammonium sulphate precipitation		
Amaranth seeds		
ASP	120 ± 0.61	50
ASP-D	100 ± 0.54	50
ASP-HD	$48.3 \pm 0.2 \mu\text{g/ml}$	50
Quinoa seeds		
QSP	500 ± 0.84	8
QSP-D	500 ± 0.91	15
QSP-HD	500 ± 0.88	26

b) Solvent extracts

Samples	Conc. ($\mu\text{g/ml}$)	% of cytotoxicity against MDA-MB cell lines
Amaranth seeds		
A-80M	500 ± 0.74	12
AH	500 ± 0.91	20
AEA	500 ± 0.85	29
AM	500 ± 0.72	11
Quinoa seeds		
Q-80M	500 ± 0.83	9
QH	500 ± 0.77	8
QEA	500 ± 0.87	12
QM	500 ± 0.96	4

Table 3.1: a) Cytotoxicity of amaranth and quinoa seed protein isolates against MDA-MB-231 cells. b) Cytotoxicity of amaranth and quinoa seed solvent extracts against MDA-MB-231 cells.

3.3.5.3. Morphology analysis of protein hydrolysates and solvent extracts of amaranth and quinoa seeds

Apoptotic cells show significant morphological alteration such as cell shrinkage, membrane blebbing and development of apoptotic bodies. Morphological alteration of amaranth and quinoa protein hydrolysates and extracts were analysed. The morphology of MDA-MB-231 cells was analysed after treatment with amaranth and quinoa protein hydrolysates and extracts using phase contrast microscopy. According to the results of morphological analyses, except for ASP-HD (Figure 4.2), all other protein isolates and extracts do not exhibit apoptotic evidence in their morphology (Figure 3.8). The ASP-HD-treated cells triggered severe shrinkage and development of small disintegrating cellular bodies similar to apoptotic bodies, with a considerable loss in the number of cells. In contrast, the control cells displayed spindle-shaped morphology within an intact membrane structure.

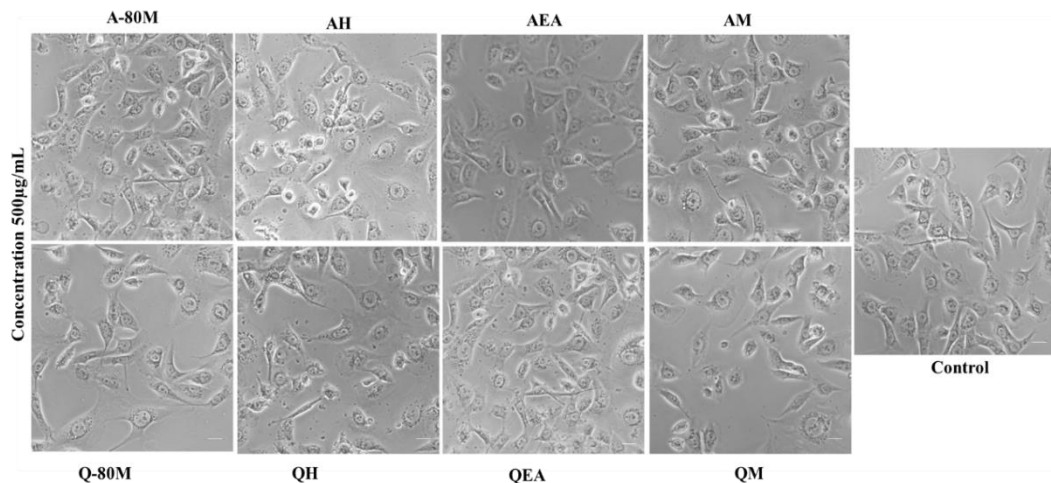


Figure 3.8: Phase contrast image showing the morphological alterations in breast cancer cells on treatment with amaranth and quinoa seed extracts (500µg/ml). Magnification-10x, Scale bar-5µm.

3.3.6. Anti-inflammatory activity of protein isolates and solvent extracts of amaranth and quinoa seeds

The anti-inflammatory activity of the protein hydrolysates and solvent extracts of amaranth and quinoa seeds were studied in the LPS-stimulated RAW cells as described in the methods. The reduction in NO production in extract pre-treated cells stimulated with LPS was assessed as the anti-inflammatory capacity. Dexamethasone was used as the standard drug for comparison.

3.3.6.1. The effects of protein hydrolysates of amaranth and quinoa seeds on anti-inflammatory activity

First, the cytotoxicity of amaranth and quinoa protein hydrolysates was evaluated using an MTT assay to see whether this hydrolysate causes any toxicity in Raw 264.7 cells. The result indicates (Table 3.2) that hydrolysates up to 200 µg/mL were nontoxic towards raw 264.7 cells.

Samples	Conc. (µg/ml)	% of cytotoxicity against RAW 264.7 cell lines
Protein isolates from Ammonium sulphate precipitation		
Amaranth seeds		
ASP	200	10±0.2
ASP-D	200	9±0.05
ASP-HD	200	8±0.14
Quinoa seeds		
QSP	200	10
QSP-D	200	10±0.08
QSP-HD	200	9±0.01

Table 3.2: Cytotoxicity of amaranth and quinoa seed protein isolates against RAW 264.7 cell.

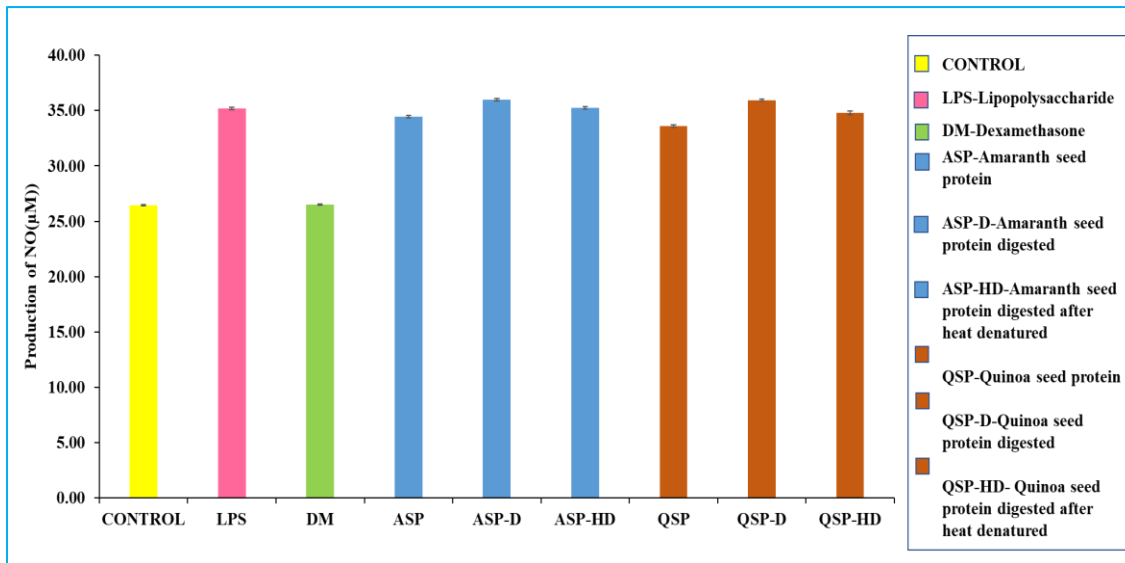


Figure 3.9: NO reduction capacity of amaranth and quinoa seed protein isolates (200µg/ml) in RAW 264.7 cells induced by LPS(1µM) and Dexamethasone (20µM) taken as a standard drug. Data are mean values ±standard deviations of 3 independent experiments.

3.3.6.2. The effects of solvent extracts of amaranth and quinoa seeds on anti-inflammatory activity

The cytotoxicity of amaranth and quinoa extracts was evaluated using an MTT assay to see whether this solvent extract causes toxicity in Raw 264.7 cells. The result indicates that except for QEA, all other extracts up to 50 µg/mL were nontoxic towards raw 264.7 cells (Figure 3.10). The effects of solvent extracts (50 µg/mL) in NO production were measured for assessing the anti-inflammatory activity. Compared to LPS-only treated cells, NO production was considerably reduced in AM and Q-80M treated cells (Figure 3.11).

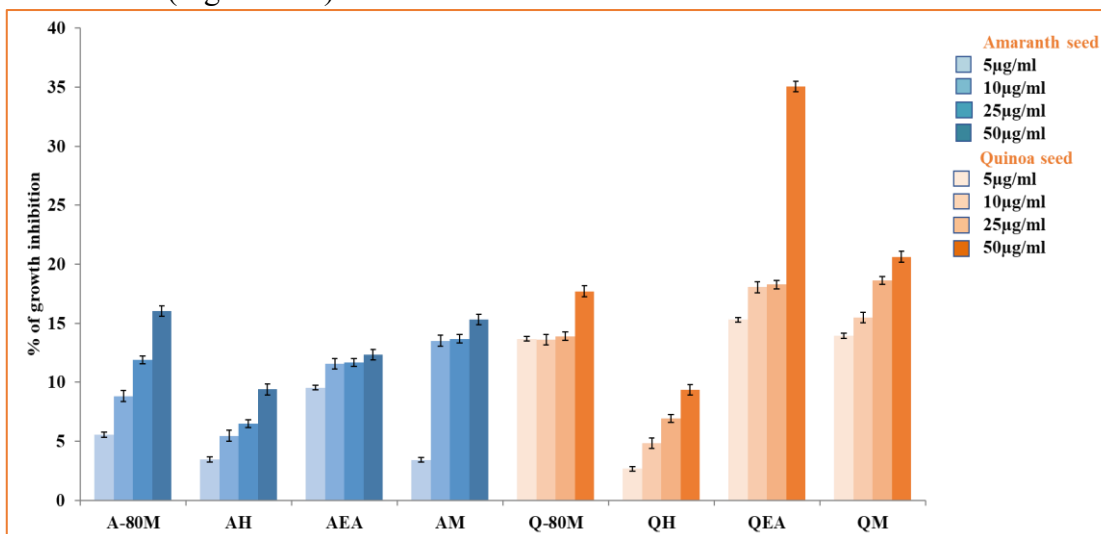


Figure 3.10: Cytotoxicity assay of amaranth and quinoa solvent extracts. Data are mean values ±standard deviations of 3 independent experiments.

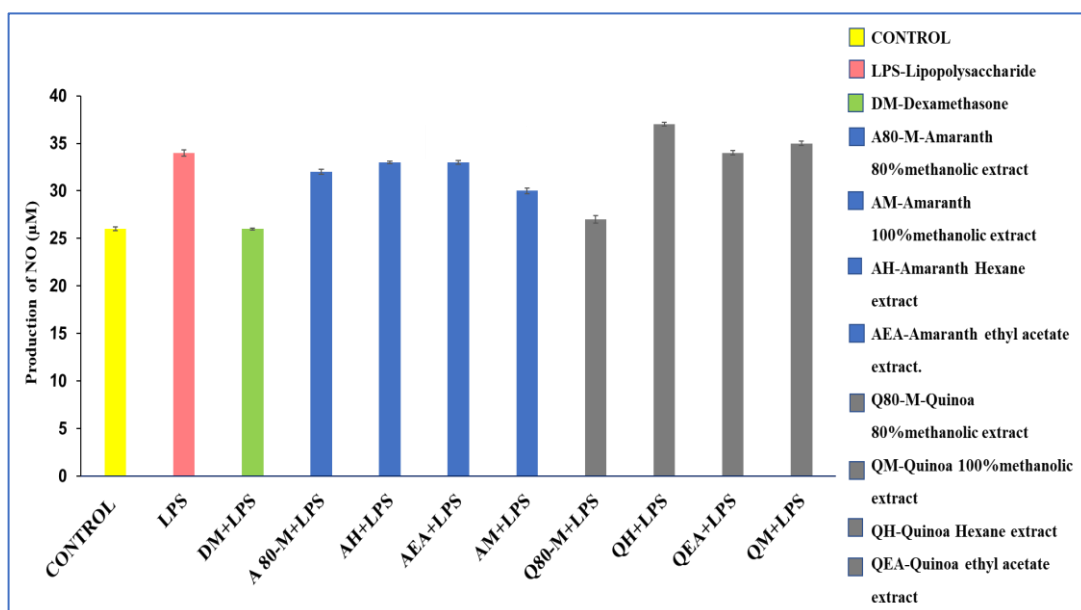


Figure 3.11: NO reduction assay of Amaranth/Quinoa seed extract (50µg/ml) in RAW 264.7 cells induced by LPS(1µM) and Dexamethasone(20µM) taken as a standard drug. Data are mean values ±standard deviations of 3 independent experiments.

Since AM and Q-80M showed considerable anti-inflammatory activity, these two extracts were further explored at higher concentrations. Their cytotoxicity was evaluated at different concentrations (25, 50, 100, 250, 500, 750 and 1000 µg/mL) and

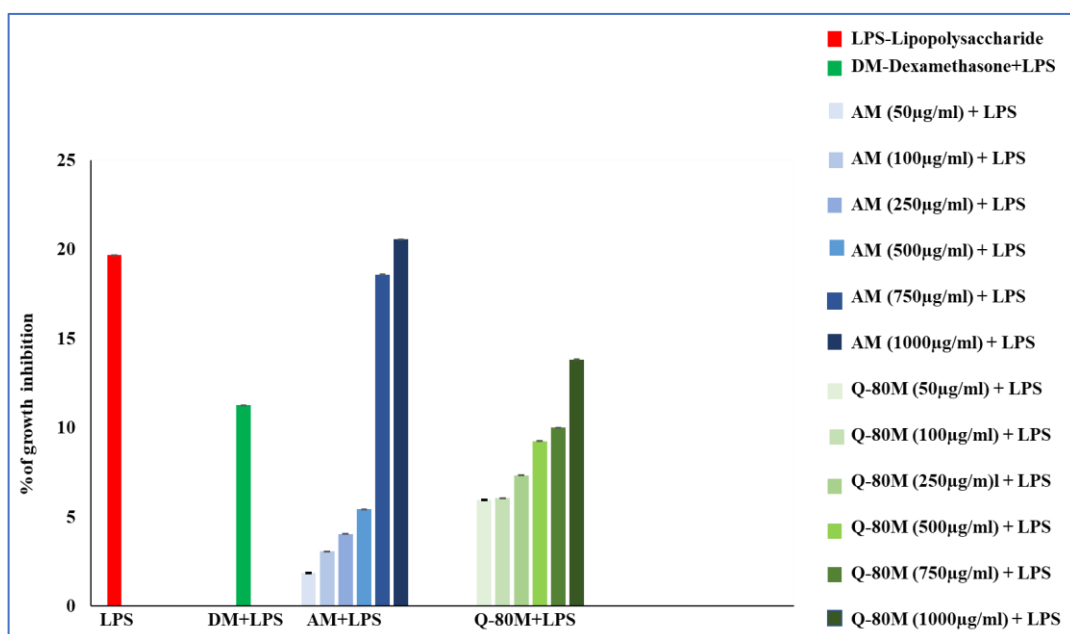


Figure 3.12: Cytotoxicity of amaranth methanolic extract and quinoa 80% methanolic extract in RAW 264.7 cells. RAW cells pre-treated with various concentrations (50, 100, 250, 500, 750 and 1000µg/ml) for 4h were treated with LPS for 24h and cell cytotoxicity was determined by MTT assay. Values are mean ± SD of three independent trials.

found that they were nontoxic up to 1 mg/ml (Figure 3.12). Different concentrations (25, 50, 100, 250, 500, 750 and 1000 µg/mL) of AM and Q-80M were measured for their action on reducing NO production in LPS-treated cells. The result showed that the Q-80M effectively reduced the NO production in concentration depending manner (Figure 3.13) compared to AM. Therefore, Q-80M was chosen for further in-depth investigation of its anti-inflammatory effects.

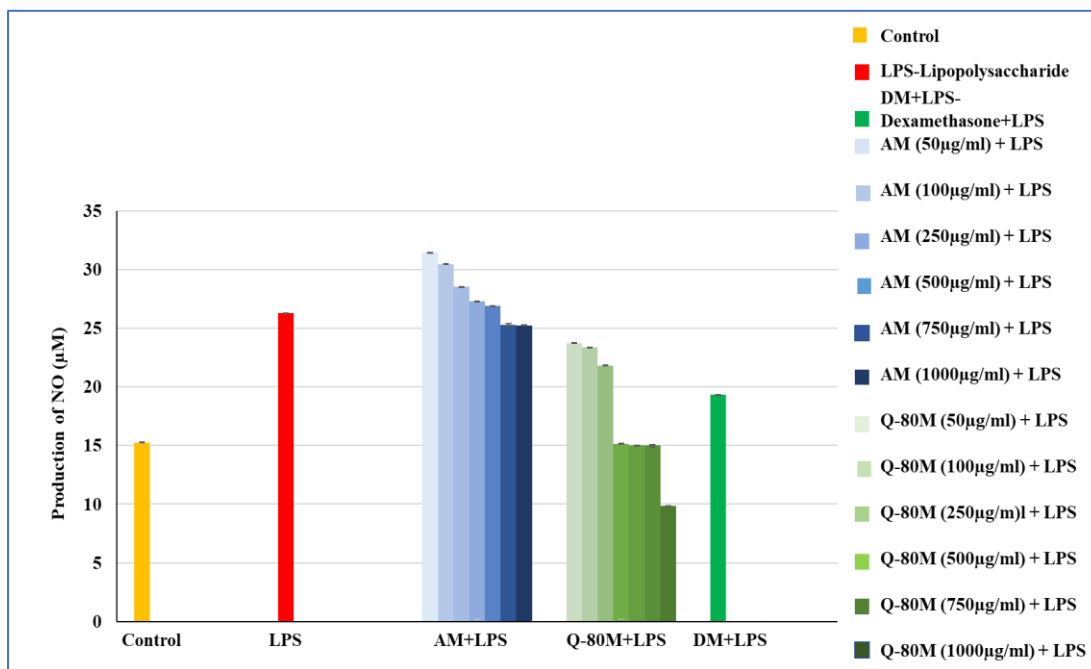


Figure 3.13: Effect of AM and Q-80M extracts on NO production in LPS-induced RAW 264.7 cells. RAW cells pre-treated with various concentrations (25, 50, 100, 250, 500, 750 and 1000µg/ml) for 4h were treated with LPS for 24 h. Values are mean ± SD of three independent trials.

3.4. Discussion

The primary attractive features of amaranth and quinoa seeds are their essential amino acid-rich protein and phytochemical contents (Jan et al., 2023). Recently, biopeptides were introduced as a novel treatment strategy with minimal side effects and significant therapeutic potential (Saadi et al., 2015). Food-derived bioactive peptides have excellent potential for treating or preventing various chronic diseases. Like biopeptides, phytochemicals serve as essential antioxidants with various physiological effects that lessen oxidative stress and guard against cell damage, helping to prevent cancer. Phytochemicals are also helpful in both the prevention and treatment of inflammatory diseases. The regulation of cell signalling pathways such as NF-κB, MAPK, signal transducer and activator of transcription 3 (STAT3), cyclooxygenase-2 (COX-2), 5-lipoxygenase (5-LOX), and phosphatidylinositol of 4 3-kinases (PI3K)/Akt are some of the mechanisms by which phytochemicals act in the prevention of cancer and the regulation of inflammation. Thus, the beneficial effects of phytochemicals in their capacity to regulate signalling pathways are crucial for modulating the interactions (Zaky et al., 2022).

We isolated the protein and phytochemicals-rich solvent extracts to explore the bioactivity of amaranth and quinoa seed. The ammonium sulphate (AS) technique was used to isolate the proteins, which is non-toxic and aids in preventing protein deterioration. The AS remains the gold standard for protein precipitation. Because AS precipitation doesn't cause widespread protein denaturation or activity loss, it is currently the least aggressive protein precipitation method. Additionally, AS has a stabilizing effect on the proteins and concentrates the target protein (Du et al., 2022). Direct and Soxhlet extraction techniques were used to separate the extracts from the amaranth and quinoa seeds.

Protein isolates and solvent extracts from amaranth and quinoa were tested for their antioxidant capacity. In this work, the antioxidant capacity of protein hydrolysate and solvent extracts was estimated by their ability to scavenge free radicals (DPPH) and evaluated the total antioxidant capacity. The heat-denatured digested proteins demonstrated significantly higher overall antioxidant activity and free radical scavenging capability than the undigested and digested (without heat denaturation) protein samples. The peptides of ASP-HD and QSP-HD improve digestibility and show promise as antioxidants and free radical scavengers. Wistar rats fed a high-fat diet were given amaranth protein isolate as a dietary supplement; this improved antioxidant status, decreased blood pressure, and increased faecal cholesterol excretion (Sisti et al., 2019). White germinated quinoa was reported to have antioxidant activity in the gastric and duodenal digest, with a DPPH value of 167.98 μmol Trolox equivalent/g of digest (Piñuel et al., 2019).

Results from the DPPH radical scavenging assay with relatively low IC_{50} values are linked to higher antioxidant activity. Comparing DPPH to the data reported by Oteri et al. in *A. hypochondriacus* seed, the range appears quite similar (0.30–0.54 mg/mL). Similar results were also found by Gresta et al. in *A. cruentus* (0.30-0.50 mg/mL) (Gresta et al., 2020). Previous studies discovered that quinoa seed extract (0.58 mg /mL) had a marginally higher IC_{50} value than the present study (Lim et al., 2020). Additionally, the DPPH scavenging activity of Brazilian quinoa (4.39 mg/ml) was lower than the result of the present investigation (Nickel et al., 2016). These findings support the total antioxidant capacity results and indicate that quinoa had a little more antioxidant capacity than amaranth seeds.

The total polyphenol content of amaranth seed agreement with specifically Indian and Pennsylvania varieties of *A. hypochondriacus* (0.30 mg GAE/g) also agreed to the study of four varieties of amaranth seeds (Oteri et al., 2021). Regarding the TPC content of quinoa seeds, similar results were obtained in the Puno variety of quinoa (31.7 mg GA/100 g-1) on its ultrasonic sound-assisted methanolic extraction. Compared to the literature, the TPC values of both varieties were lower than those found by Han et al. (Han et al., 2019). A strong association between total polyphenol and overall antioxidant activity was found in both amaranth and quinoa, similar to the findings of Akin-Idowu et al. and Enciso-Roca et al. ((Akin-Idowu et al., 2017; Enciso-Roca et al., 2021)).

According to recent research reports, peptides in whole-grain foods significantly lower the chance of developing several types of cancer. The current study revealed that amaranth seeds, upon heat denaturation, followed by simulated gastrointestinal digestion, release peptides with good cytotoxicity on MDA-MB-231 breast cancer cells. Similar to the results found in MCF-7 cells treated with *A. cruentus*, pepsin hydrolysate had a GI₅₀ of 3.87 µg/mL. Also, this study indicates that enzymatically digested protein hydrolysate has more cytotoxicity towards cancer cells than undigested protein. MCF-7 cell viability was reduced more in treatment with *A. cruentus* hydrolysate than in undigested protein isolates (Ramkisson et al., 2020). The amaranth plant is also reported to have cytotoxicity towards MDA-MB-231 cells. The methanolic extract of aerial parts from *A. spinosus* has anticancer activity against MDA-MB-231 cells (GI₅₀- 82.11±7.02 mg/mL)(Nivedya et al. 2020).

Macrophages play a critical role in inflammation. The activation of macrophage-derived inflammatory mediators is regarded as the key producer of inflammation. Thus, they are usually chosen as parameters to investigate the effect of anti-inflammatory materials. One of the most well-known phenomena in inflammation progress is the increase of NO, a reactive molecule originating from the guanidine nitrogen of l-arginine, catalysed by inducible NO synthase (iNOS) inactivated inflammatory cells. The overproduction of NO is harmful to the host, leading to the development of many inflammatory-related diseases. LPS induces NO production in RAW 264.7 cells than the LPS untreated control cells. One of the primary criteria of an anti-inflammatory drug could downregulate the overproduction of NO. In the present study, quinoa seed methanolic extract reduced the NO production without causing any cytotoxicity to macrophage cells. Similar to the current study quinoa saponin fraction testified to have anti-inflammatory activity. In LPS-induced RAW264.7 cells, quinoa saponin fractions dose-dependently reduced NO generation and prevented the release of inflammatory cytokines such as tumour necrosis factor and interleukin-6 (Yao, Yang, et al.2014). Foucault et al. reported that quinoa extract-treated mice exhibited marked attenuation of mRNA levels of several inflammation markers (monocyte chemotactic protein-1, CD68) and insulin resistance (osteopontin, plasminogen activator inhibitor-1) (Foucault et al., 2012).

3.5. Conclusion

Bioactive peptides and solvent extracts from amaranth and quinoa seeds were isolated and their preliminary screening against inflammation and breast cancer proliferation was conducted. Amaranth and quinoa seed proteins were isolated by ammonium sulphate precipitation. Isolated proteins were subjected to simulated gastrointestinal digestion in the raw and heat-denatured forms. The isolation of bioactive-rich solvent extracts from amaranth and quinoa seeds was carried out by direct (using 80% methanol) and sequential (using hexane, ethyl acetate and methanol) extraction methods. Different solvent extracts and digested protein samples from amaranth and quinoa seeds were screened for their in vitro antioxidant, anti-inflammatory and anti-breast cancer effects. The free radical scavenging and antioxidant activity were

significantly higher in the digested proteins after heat denaturation from amaranth seeds. In the case of solvent extracts, the free radical scavenging activity and the antioxidant activity were found to be more in Q-80M when compared to other extracts. The total polyphenol content was higher in the Q-80M and in sequentially extracted ethyl acetate and methanol fractions. The anti-breast cancer effects of different protein hydrolysates and solvent extracts were tested in MDA-MB-231 cells, and the results indicated that significant activity was found in ASP-HD. The anti-inflammatory potential was maximum for Q-80M (quinoa seed 80% methanol extract, direct extraction).

So, in the subsequent chapters, we have taken ASP-HD for detailed analysis of anti-breast cancer effects and Q-80M for anti-inflammatory studies.

3.6. References

1. Abdelaleem, M A, and K R A Elbassiony. "Evaluation of phytochemicals and antioxidant activity of gamma irradiated quinoa (Chenopodium quinoa)." *Brazilian journal of biology Revista brasleira de biologia*. 2021: 81,3: 806-813. doi:10.1590/1519-6984.232270.
2. Pamela E. Akin-Idowu, Olufemi T. Ademoyegun, Yemisi O. Olagunju, Ayodeji O. Aduloju, Usifo G. Adebó. Phytochemical Content and Antioxidant Activity of Five Grain Amaranth Species. *American Journal of Food Science and Technology*. 2017;5:249-255. <http://pubs.sciepub.com/ajfst/5/6/51>.
3. Daliri, Eric Banan Mwine, Deog H. Oh, and Byong H. Lee.. "Bioactive Peptides." *Foods*. 2017;6(5): 1–21 doi:10.3390/foods6050032.
4. Du M, Hou Z, Liu L, Xuan Y, Chen X, Fan L, Li Z, Xu B. ¹Progress, applications, challenges and prospects of protein purification technology. *Frontiers in Bioengineering and Biotechnology* 2022 Dec 6; 10:1028691. doi: 10.3389/fbioe.2022.1028691. PMID: 36561042; PMCID: PMC9763899
5. Enciso-Roca EC, Aguilar-Felices EJ, Tinco-Jayo JA, Arroyo-Acevedo JL, Herrera-Calderon O. Biomolecules with Antioxidant Capacity from the Seeds and Sprouts of 20 Varieties of *Chenopodium quinoa* Willd. (Quinoa). *Plants (Basel)*. 2021 9;10(11):2417. doi: 10.3390/plants10112417. PMID: 34834779; PMCID: PMC8618655
6. Foucault AS, Mathé V, Lafont R, Even P, Dioh W, Veillet S, Tomé D, Huneau JF, Hermier D, Quignard-Boulangé A. Quinoa extract enriched in 20-hydroxyecdysone protects mice from diet-induced obesity and modulates adipokines expression. *Obesity (Silver Spring)*. 2012; 20(2):270-7. doi: 10.1038/oby.2011.257. Epub 2011 Aug 25. PMID: 21869758.
7. Gresta F, Meineri G, Oteri M, Santonoceto C, Lo Presti V, Costale A, Chiofalo B. Productive and Qualitative Traits of *Amaranthus Cruentus* L.: An Unconventional Healthy Ingredient in Animal Feed. *Animals (Basel)*. 2020;

- 14;10(8):1428. doi: 10.3390/ani10081428. PMID: 32824062; PMCID: PMC7459667
8. Han, Y., Chi, J., Zhang, M., Zhang, R., Fan, S., Dong, L., Huang, F., Liu, L., Changes in saponins, phenolics and antioxidant activity of quinoa (*Chenopodium quinoa willd*) during milling process, *LWT - Food Science and Technology*. 2019. doi: <https://doi.org/10.1016/j.lwt.2019.108381>.
 9. House, Nivedya Cheerakuzhy, Drisya Puthenparampil, Dhilna Malayil, and Arunaksharan Narayanankutty. "Variation in the Polyphenol Composition, Antioxidant, and Anticancer Activity among Different *Amaranthus* Species." *South African Journal of Botany* .2020;135: 408–12. <https://doi.org/10.1016/j.sajb.2020.09.026>.
 10. Iddir M, Brito A, Dingo G, Fernandez Del Campo SS, Samouda H, La Frano MR, Bohn T. Strengthening the Immune System and Reducing Inflammation and Oxidative Stress through Diet and Nutrition: Considerations during the COVID-19 Crisis. *Nutrients*. 2020 ;12(6):1562. doi: 10.3390/nu12061562. PMID: 32471251; PMCID: PMC7352291.
 11. Jan, Nusrat, Syed Zameer Hussain, Bazila Naseer, and Tashooq A. Bhat. "Amaranth and Quinoa as Potential Nutraceuticals: A Review of Anti-Nutritional Factors, Health Benefits and Their Applications in Food, Medicinal and Cosmetic Sectors." *Food Chemistry*.2023: X 18: 100687. <https://doi.org/10.1016/j.fochx.2023.100687>.
 12. Lim JG, Park HM, Yoon KS. Analysis of saponin composition and comparison of the antioxidant activity of various parts of the quinoa plant (*Chenopodium quinoa* Willd.). *Food Science and Nutrition*. 2019 ;8(1):694-702. doi: 10.1002/fsn3.1358. PMID: 31993193; PMCID: PMC6977472.
 13. Nickel J, Spanier LP, Botelho FT, Gularte MA, Helbig E. Effect of different types of processing on the total phenolic compound content, antioxidant capacity, and saponin content of *Chenopodium quinoa* Willd grains. *Food Chemistry*. 2016; 209:139-43. doi: 10.1016/j.foodchem.2016.04.031. Epub 2016 Apr 13. PMID: 27173545.
 14. Orona-Tamayo D, Valverde ME, Paredes-López O. Bioactive peptides from selected latin american food crops - A nutraceutical and molecular approach. *Critical Reviews in Food Science and Nutrition*. 2019;59(12):1949-1975. doi: 10.1080/10408398.2018.1434480. Epub 2018 Feb 26. PMID: 29388805.
 15. Oteri M, Gresta F, Costale A, Lo Presti V, Meineri G, Chiofalo B. *Amaranthus hypochondriacus* L. as a Sustainable Source of Nutrients and Bioactive Compounds for Animal Feeding. *Antioxidants (Basel)*. 2021;10(6):876. doi: 10.3390/antiox10060876. PMID: 34070822; PMCID: PMC8229450.

16. Piñuel L, Boeri P, Zubillaga F, Barrio DA, Torreta J, Cruz A, Vásquez G, Pinto A, Carrillo W. Production of White, Red and Black Quinoa (*Chenopodium quinoa* Willd Var. Real) Protein Isolates and Its Hydrolysates in Germinated and Non-Germinated Quinoa Samples and Antioxidant Activity Evaluation. *Plants (Basel)*. 2019;8(8):257. doi: 10.3390/plants8080257. PMID: 31366118; PMCID: PMC6724106.
17. Ramkisson, Shanece, Depika Dwarka, Sonja Venter, and John Jason Mellem. “In Vitro Anticancer and Antioxidant Potential of *Amaranthus Cruentus* Protein and Its Hydrolysates.” *Food Science and Technology (Brazil)* .2020;40: 634–39. DOI: <https://doi.org/10.1590/fst.36219>
18. Reuter, S., Gupta, S. C., Chaturvedi, M. M., & Aggarwal, B. B. Oxidative stress, inflammation, and cancer: How are they linked? *Free Radical Biology and Medicine*. 2010; 49(11), 1603–1616. <https://doi.org/10.1016/j.freeradbiomed.2010.09.006>
19. Saadi S, Saari N, Anwar F, Abdul Hamid A, Ghazali HM. Recent advances in food biopeptides: production, biological functionalities and therapeutic applications. *Biotechnology Advances*. 2015 ;33(1):80-116. doi: 10.1016/j.biotechadv.2014.12.003. Epub 2014 Dec 12. PMID: 25499177.
20. Sisti MS, Scilingo A, Añón MC. Effect of the Incorporation of Amaranth (*Amaranthus Mantegazzianus*) into Fat- and Cholesterol-Rich Diets for Wistar Rats. *Journal of Food Science*. 2019;84(11):3075-3082. doi: 10.1111/1750-3841.14810. Epub 2019 Oct 10. PMID: 31599971.
21. Tang Y, Tsao R. Phytochemicals in quinoa and amaranth grains and their antioxidant, anti-inflammatory, and potential health beneficial effects: a review. *Molecular Nutrition and Food Research*. 2017 Jul;61(7). doi: 10.1002/mnfr.201600767. Epub 2017 Apr 18. PMID: 28239982.
22. Wang RX, Zhou M, Ma HL, Qiao YB, Li QS. The Role of Chronic Inflammation in Various Diseases and Anti-inflammatory Therapies Containing Natural Products. *ChemMedChem*. 2021;16(10):1576-1592. doi: 10.1002/cmdc.202000996. Epub 2021 Mar 7. PMID: 33528076.
23. Zaky AA, Simal-Gandara J, Eun JB, Shim JH, Abd El-Aty AM. Bioactivities, Applications, Safety, and Health Benefits of Bioactive Peptides from Food and By-Products: A Review. *Frontiers in Nutrition*. 2022; 8:815640. doi: 10.3389/fnut.2021.815640. PMID: 35127796; PMCID: PMC8810531.
24. Zhang Y, Liu Y, Zhu K, Dong Y, Cui H, Mao L, Xu X, Zhou H. Acute Toxicity, Antioxidant, and Antifatigue Activities of Protein-Rich Extract from *Oviductus ranae*. *Oxidative Medicine and Cellular Longevity*.2018 Feb 25;2018:9021371. doi: 10.1155/2018/9021371. PMID: 29991975; PMCID: PMC5845489.

25. Zhao, H., Wu, L., Yan, G., Chen, Y., Zhou, M., Wu, Y., & Li, Y. Inflammation and tumor progression: signaling pathways and targeted intervention. *Signal Transduction and Targeted Therapy*. 2021; 6(1). <https://doi.org/10.1038/s41392-021-00658-5>.

CHAPTER 4

***In vitro* evaluation of the anti-breast cancer potential of Amaranth bioactive peptides (ASP-HD) against MDA-MB-231 cells**

4.1. Introduction

Breast cancer (BC) is the most common malignancy in women and the main cause of cancer-related mortality worldwide. The most metastatic and aggressive form of breast cancer subtype is triple-negative breast cancer (TNBC), in which the human epidermal growth factor receptor-2 (HER2), progesterone receptor (PR), and oestrogen receptor (ER) were negatively expressed. According to gene expression profiling data, TNBC is categorised as a basal-like breast cancer subtype (Li et al., 2022). Based on epidemiological data, TNBC primarily affects premenopausal women under 40. TNBC patients have a shorter life expectancy than those with other breast cancer subtypes, and their mortality rate is 40% in the first five years after diagnosis. TNBC is extremely invasive. Only 13.3 months on average remain alive after metastasis, and up to 25% of cases relapse after surgery. The brain and visceral organs are frequently affected by metastases. In non-TNBC patients, the typical time to relapse is 35–67 months; however, in TNBC patients, it is just 19–40 months. About 75% of TNBC patients die within three months of the recurrence. TNBC is not susceptible to endocrine therapy or molecular targeted therapy because of its distinct molecular profile.

As a result, chemotherapy is the primary systemic treatment. Chemotherapeutic drugs, which usually target rapidly dividing cancer cells lead to harmful side effects because they cause damage to healthy cells and tissues. In some nations bevacizumab and chemotherapeutic medications have been utilised to treat TNBC; however, this has not appreciably increased patient survival time. Additionally, cancer cells become resistant to these medications due to the overexpression of multidrug resistance proteins, which flush the drugs out of cells and render them ineffective. Therefore, investigating and developing more potent and less harmful anticancer drugs has become essential (Yin et al., 2020).

Anticancer peptides have gained attention recently as possible replacements for existing chemotherapy medicines. Due to their various physiological functions, peptides are a viable alternative for creating medicinal substances (Liao et al., 2016). Depending on their kind, quantity, sequence, and amino acid characteristics, bioactive peptides have been observed to exhibit various types of physiological activity. Peptides have a higher bioavailability than proteins from a dietary perspective. Also, they have numerous therapeutic advantages, which make them more effective than conventional drugs. For instance, bioactive peptides are more effective even at low concentrations and have fewer or no adverse effects on the target tissue due to their highly specialised activities. This characteristic is helpful in the treatment of chronic disorders (Akbarian et al., 2022). Various proteins from both plant and animal sources

are digested to produce bioactive peptides. Proteolytic hydrolysis is used to release these peptides, which are inactive inside the parent proteins. Since bioactive peptides can be absorbed in the intestine and enter the bloodstream directly, this guarantees their bioavailability *in vivo* and a physiological effect at the target site. Once such bioactive peptides are released, they may exhibit various bio-functional activities depending on their structural, compositional, and sequential properties (Kim et al., 2012). Numerous studies have been conducted on human lactoferrin's anticancer properties. Lactoferrin was given to patients with resistant solid tumours in phase I clinical research, and it was found to be nontoxic with a dosage tolerance of 1.5–9 g/day. It has been demonstrated that bovine lactoferrin has anticancer action, suppressing tumours both *in vitro* and *in vivo* (Hayes et al., 2006). *Phaseolus vulgaris* L. dietary Peptides reduced colitis-associated colon carcinogenesis in Balb/c Mice (Luna-Vital et al., 2017). A growing body of research shows that peptides derived from milk and soy proteins help to prevent cancer. Previous findings suggested that residual walnut protein can be hydrolysed by papain to generate a unique bio-peptide CTLEW that induces apoptosis and autophagy in MCF-7 cells (Ma et al., 2015). The biopeptide exhibits specific immunomodulatory action and growth suppression of cancer cells. Intense anticancer activities were present in the peptide from *Enteromorpha prolifera* (Lin et al., 2022). Scientific studies also indicate that Vglycin, a new natural polypeptide derived from pea seeds, markedly increased apoptosis and G1/S phase cell cycle arrest in colon cancer cells (Gao et al., 2017). The results reported *in vitro* or *in vivo* models are equivocal, and there are only limited human clinical studies to support them, thus necessitating additional research on biopeptides anticancer investigations.

Preliminary testing in the preceding chapter found that the amaranth protein hydrolysate ASP-HD (protein sample heat denatured followed by simulated digestion) has cytotoxic effects on breast cancer MDA-MB-231 cells. So, this chapter deals with the detailed analysis of the anti-breast cancer effects as well as the identification of peptides in ASP-HD and their functional analysis.

4.2. Methodology

Detailed investigations of the mechanism behind the observed cytotoxic potential of ASP-HD in MDA-MB-231 cells and the identification and functional analysis of peptides in ASP-HD were studied using the following assay methods:

1. Cell viability evaluation using MTT assay.
2. Cellular morphology analysis using phase contrast microscopy.
3. Nuclear fragmentation analysis using DAPI staining
4. Phosphatidylserine translocation studied using annexin V staining
5. Caspase-3 activity examined by fluorometric analysis

6. Simultaneous detection of 43 human apoptotic markers using human apoptosis antibody array membrane
7. Cell migration was evaluated using scratch wound assay.
8. Essential amino acid content identified using HPLC
9. Peptide identification and their functional annotation using ESI-QTOF-MS and gene ontology.

All the assays were performed in triplicate and the detailed procedures are described in chapter 2. Curcumin 3.6µg/ml was used as the positive control for the study.

4.3. Results

4.3.1. Effects of ASP-HD on the cell viability of MDA-MB-231

We have investigated the cytotoxic effects of amaranth protein hydrolysates (ASP, ASP-D, and ASP-HD) on MDA-MB-231 cells for 24 hrs in a concentration-dependent manner. The results indicated that the ASP-HD had dose-dependent growth inhibitory effects, with a GI_{50} value of 48.3 ± 0.2 µg/ml. The results are given in Figure 4.1.

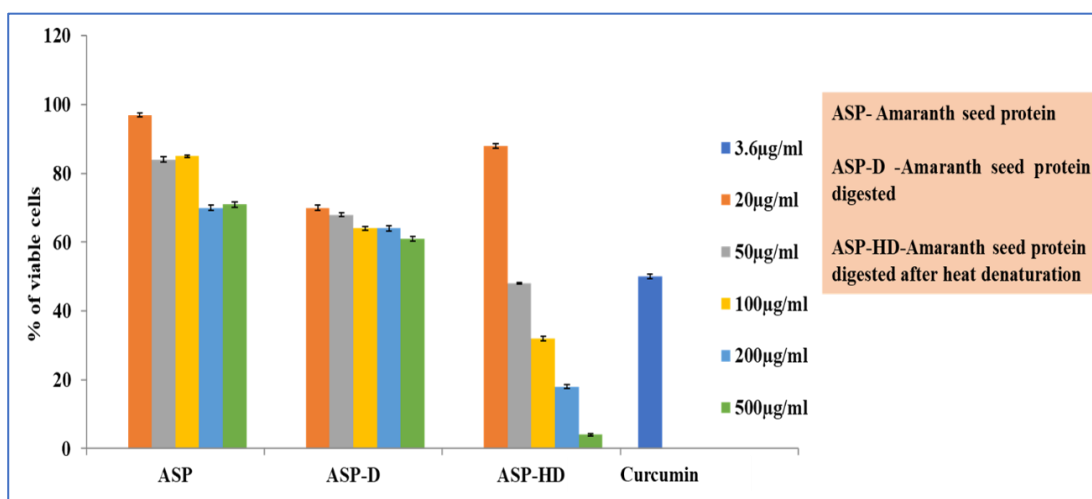


Figure 4.1: MTT assay showing the percentage cell viability of ASP treated breast cancer cells. ASP-HD showed concentration dependent effects on cell viability and GI_{50} was found to be 48 ± 0.681 µg/ml. Positive control taken as Curcumin (3.6µg/ml). Values expressed are the average of three independent experiments \pm SD.

4.3.2. Effect of ASP-HD on cellular morphology of MDA-MB-231

The morphology of the ASP-HD-treated cells was also examined and the findings depicted in Fig. 4.2, revealed that the treatment resulted in notable alterations such as a reduction in viable cell number, cell blebbing, loss of attachment and membrane rupture, which were comparable to those seen in the case of curcumin (positive control)-treated cells.

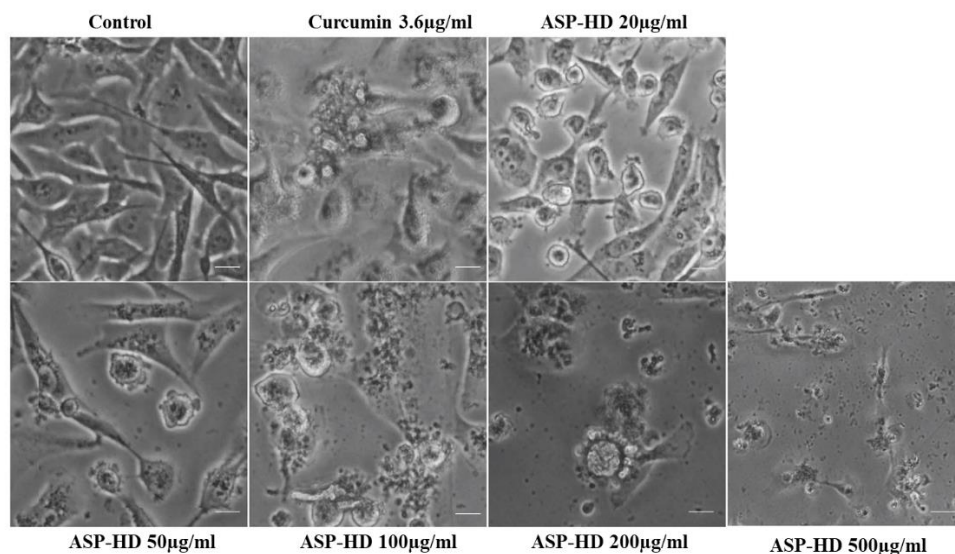


Figure 4.2: Phase contrast image showing the morphological alterations in breast cancer cells on treatment with ASP-HD. From 20 µg/ml forward, morphological changes were seen in cells treated with ASP-HD. Magnification-10x, Scale bar-

4.3.3. Effects of ASP-HD on nuclear fragmentation

Nuclear fragmentation is a critical event in apoptosis, and the impact of ASP-HD on nuclear fragmentation was investigated using DAPI staining. The findings are depicted in Figure. 4.3 shows significant alterations to nuclear morphology, including condensation and fragmentation in ASP-HD treatment, denoted by white arrows. The

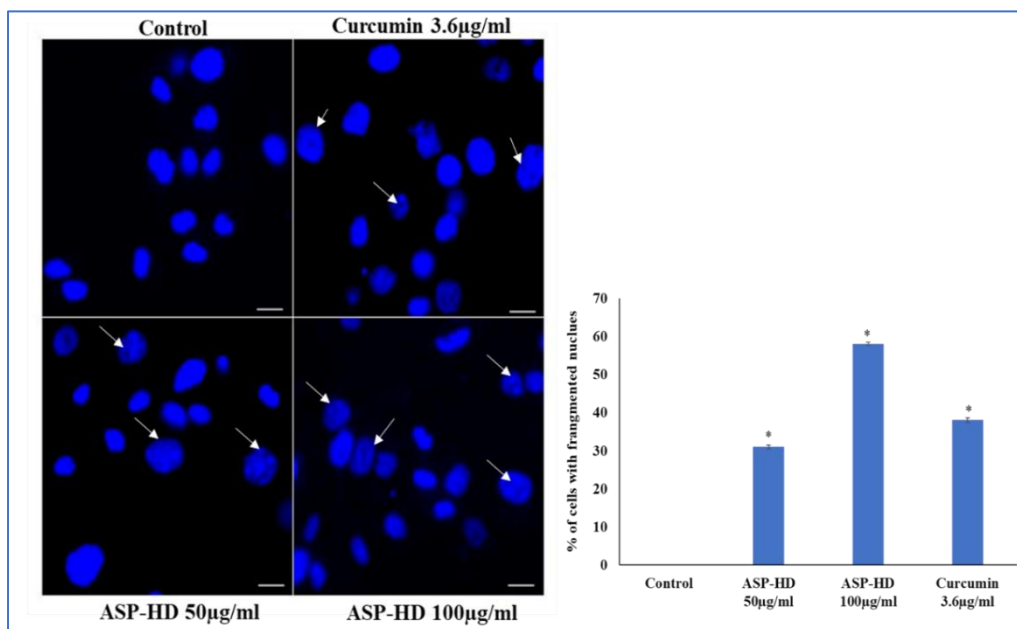


Figure 4.3: DAPI staining - fluorescent images showing the nuclear fragmentation in the control and treated cells. White arrows in the treated cells indicate fragmentation of the nucleus. The nucleus of control cells appeared to be normal. The percentage of fragmented nucleus in a field of 100 cells were counted and plotted as a bar diagram. Values are the average of three independent experiments±SD and * $p < 0.05$ when compared with control. Magnification-20x, Scale bar-20µm

nucleus of control cells appeared to be normal. The graph depicts the percentage of cells with a fragmented nucleus.

4.3.4. Effects of ASP-HD on the loss of membrane integrity

Apoptotic cells undergo membrane damage, and the intensity of this has been analysed using acridine orange/ethidium bromide co-staining. The findings in Figure 4.4 demonstrated a considerable loss in membrane integrity, which was visible as orange with the co-staining of ethidium bromide (red) and acridine orange (green) in the ASP-HD treated cells. The control cells were green due to their intact membrane structure. The percentage of treated cells with membrane distortion is represented on the graph.

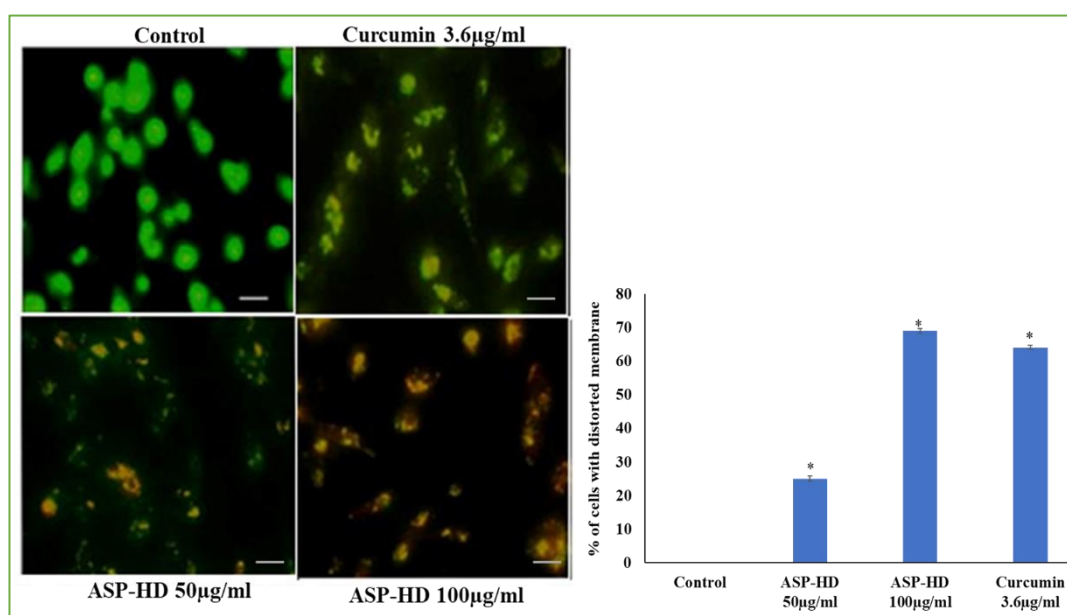


Figure 4.4: AO/EtBr staining - The membrane integrity studies using co-staining with AO and EtBr. The control cells with intact cell membrane only took up AO and appeared as green. The ASP-HD treated orange-coloured cells showed the membrane damage due the incorporation of EtBr along with AO. Magnification-20x, Scale bar-20µm. The number of cells with damaged membrane was counted from a field of 100 cells and plotted as the bar diagram. Values are the average of three independent experiments±SD and * $p < 0.05$ when compared with control.

4.3.5. Effects of ASP-HD on phosphatidylserine translocation

The translocation of phosphatidylserine (PS) was evident as red fluorescent spots on the plasma membrane's outer surface of ASP-HD-treated cells after annexin V labelling. Healthy cells are stained green by 6-CFDA, whereas Annexin V binds to the PS exposed on the cell surface and fluoresces red (Fig. 4.5). These modifications were seen to be enhanced in a dose-dependent way on ASP-HD treatment. They were comparable to those of cells treated with curcumin. A graph displaying the percentage of annexin V-positive cells in a colony of 100 cells was calculated.

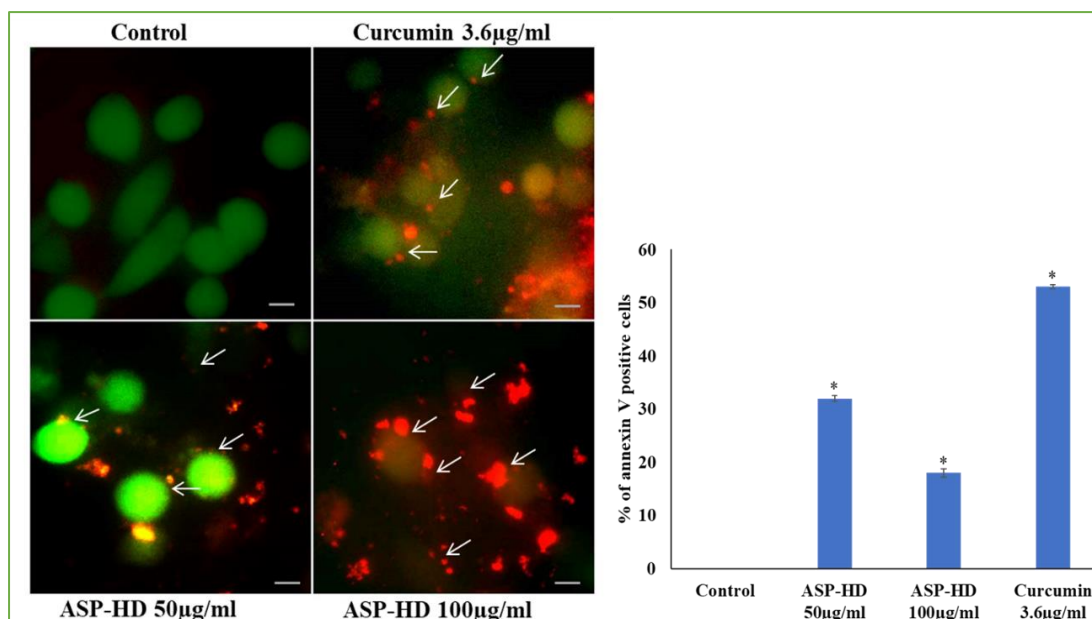


Figure 4.5: Annexin V staining - Translocated phosphatidyl serine was stained with annexin V labelled with Cy3 (indicated by white arrows) in the treated cells. Magnification-20x, Scale bar-20µm. The percentage of annexin V cells are shown in the bar diagram. Values are the average of three independent experiments±SD and * $p < 0.05$ when compared with control.

4.3.6. Effects of ASP-HD on caspase3 activation

The induction of apoptosis in MDA-MB-231 cells was also evaluated by detecting caspase-3 activation. A class of proteases known as caspases has been suggested to be extremely important in apoptosis. Among these, caspase-3 is a frequently activated death protease necessary for some typical apoptotic hallmarks, such as DNA fragmentation and apoptotic chromatin condensation. The impact of ASP-HD on the caspase-3 activity of MDA-MB-231 breast cancer cells is shown in Figure 4.6 at two

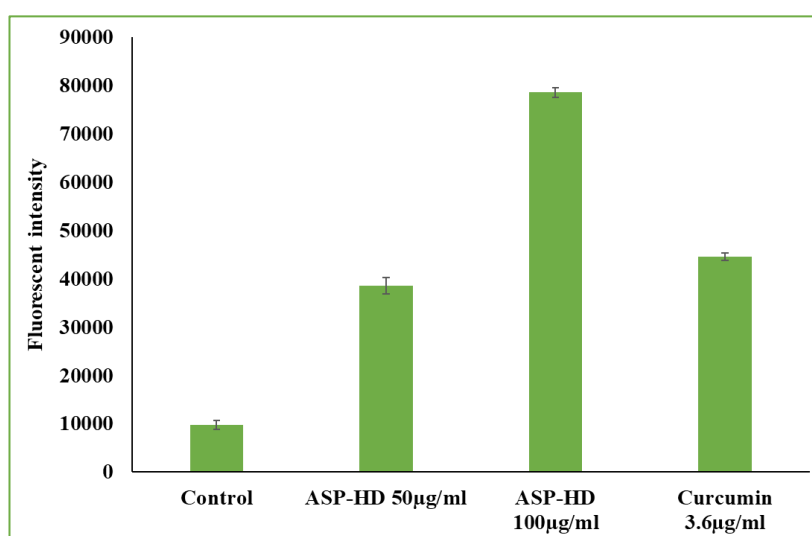


Figure 4.6: Caspase 3 activity assay - Increased caspase activity was observed in the treated cells compared with control. Values are the average of three independent experiments±SD and * $p < 0.05$ when compared with control.

different concentrations (50 and 100 µg/mL). Additionally, caspase-3 activity was substantially higher in ASP-HD than in controls. These findings imply that ASP-HD treatments led to the induction of apoptosis.

4.3.7. Effects of ASP-HD on the expression of apoptotic proteins

A human apoptosis antibody array kit, which includes 43 human apoptosis-related proteins, was used to determine the underlying mechanisms of ASP-HD-induced regulation of apoptosis in cells. The treatment with ASP-HD decreased the expression levels of the proteins Bcl2, Livin, and Survivin and elevated the expression levels of the pro-apoptotic proteins Bax, caspase 3 and 8, HSP70, P27, P53, SMAC, XIAP, and TNF. These findings imply that ASP-HD may prevent apoptosis in MDA-MB-231 cells by controlling the apoptotic protein's expression. Figure 4.7 displays the human apoptosis array membrane and the summary of the results. The signal intensities of antibody spots were compared using densitometry analysis.

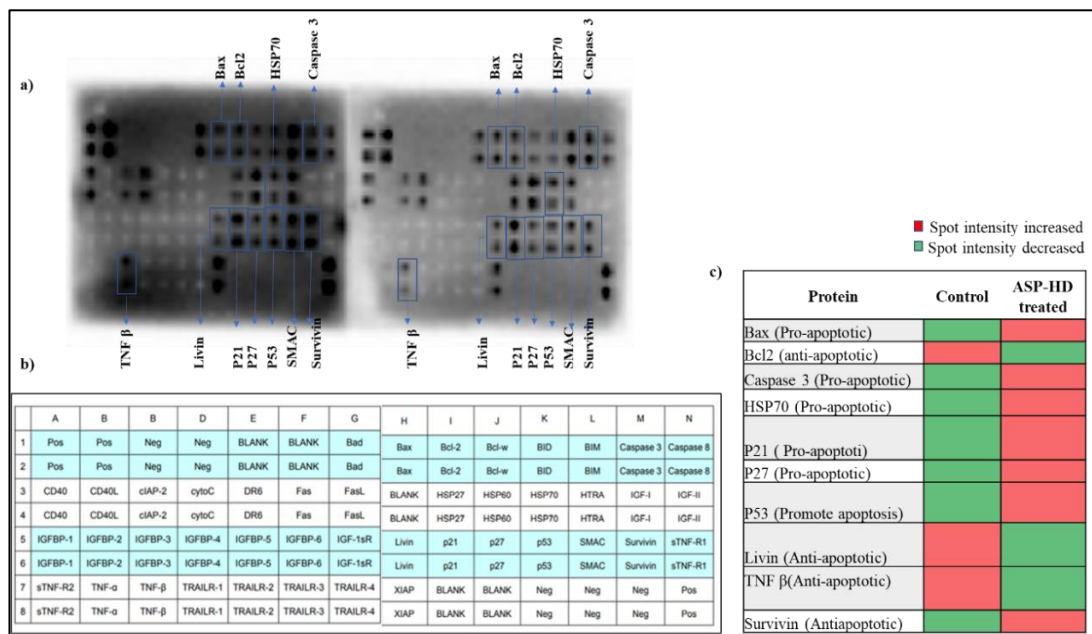


Figure 4.7: The protein antibody kit showed that the expression levels of apoptotic proteins ASP-HD treated group compared with control group. a) Chemidoc image of antibody membrane array, b) Membrane array map, c) Relative difference in the apoptotic marker proteins.

4.3.8. Effects of ASP-HD on cellular migration

A scratch wound assay was performed to investigate the ability of ASP-HD to hinder the cellular migration of TNBC cells on an artificial wound. The results of the experiment are displayed in Figure 4.8. Within 24 hrs, more than 50% of cell migration and wound closure were seen in control cells, compared to 10% in treated cells. The percentage of dead cells in the control cells was zero after 24 hrs, whereas it was greater than 50% in the treated cells. These findings suggested that ASP-HD had similar anti-metastatic potential to curcumin.

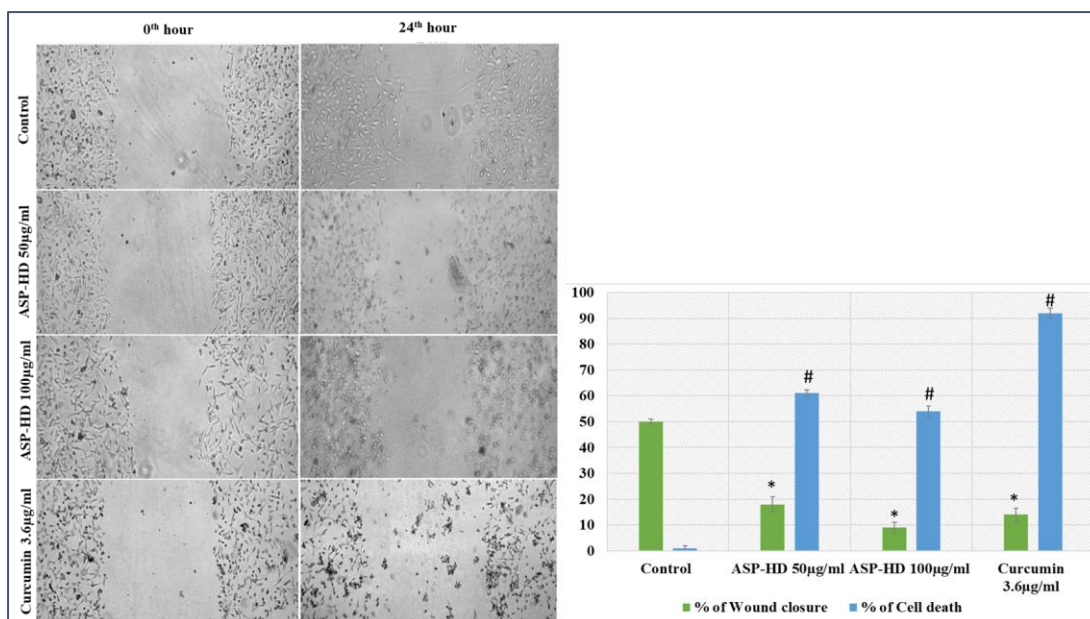


Figure 4.8: Cell migration assay - The anti-migratory effects of ASP-HD and curcumin were evaluated using wound closure over a period of 24 h. ASP-HD prevent wound closures in a concentration-dependent manner. Magnification-4x, Scale bar-100µm. The bar diagram indicated the percentages of wound closures and cell deaths that occurred with treatment. Values are the average of three independent experiments \pm SD and * $p < 0.05$ when compared with the control.

4.3.9. Comparison of the essential amino acid contents in ASP, ASP-D and ASP-HD

The essential amino acid content of amaranth protein hydrolysate (ASP, ASP-D and ASP-HD) was done using HPLC and the results are shown in Figure. 4.9. The amino acid profile showed that the amount of free EAA in the undigested amaranth proteins was relatively small. Leucine, threonine, and lysine release were all significantly boosted by simulated digestion. However, the release of amino acids like Leu, Thr, and Trp was considerably improved. The current study demonstrated that amaranth proteins, particularly Leu and Lys, release higher EAA after heat denaturation and simulated gastrointestinal digestion.

4.3.10. Peptide sequencing of ASP-HD and functional analysis by Gene Ontology

A total of 4606 peptides were identified from ASP-HD by mass spectrometry analysis. The DAVID software was used to assign functional GO annotation regarding biological processes, molecular function, and cellular component categories based on each protein accession ID. The results are given in Figure 4.10. Thus, utilising Funrich software, a functional annotation chart was created. Protein metabolism (40%), cell development and maintenance (20%), and energy pathways (20%) were discovered to be the most important biological processes of the ASP-HD peptide. Primary molecular functions of the ASP-HD protein include its activity as a ligase (20%), a serine-type peptidase (20%), and a protein inhibitor (20%). The major

cellular components of ASP-HD interact with are lysosomes (60%), exosomes (60%), nucleus (40%), cytoplasm (40%), and other organelles.

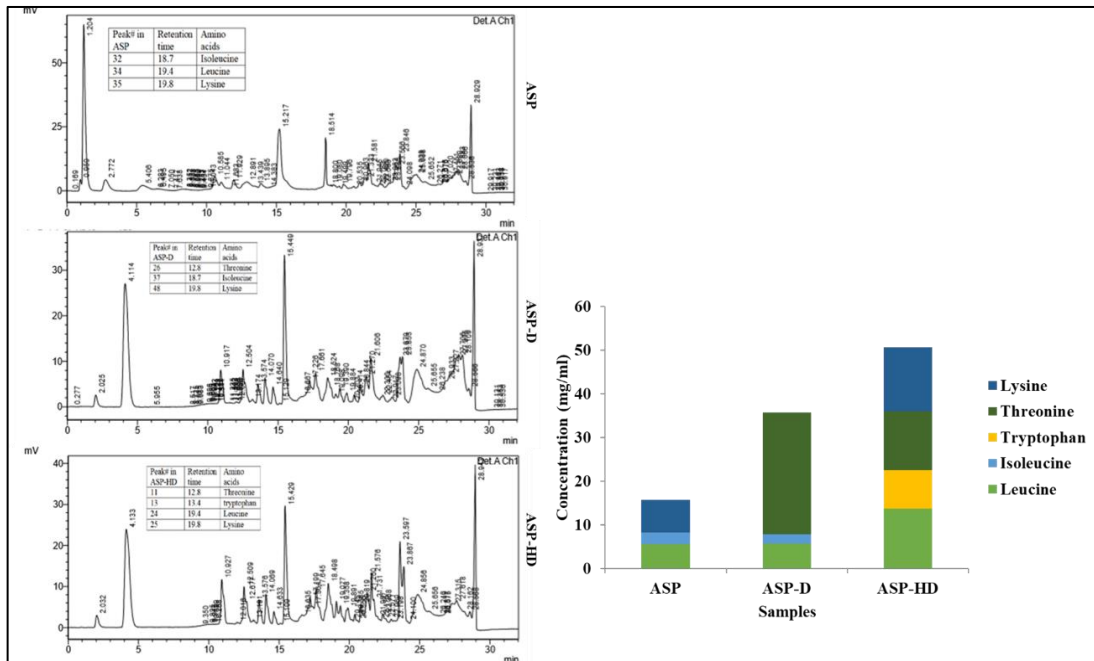


Figure. 4.9. (a) Chromatogram showing the separation of amino acids ASP, ASP-D and ASP-HD with retention time of standard essential amino acids and peak number (b) Amount of different essential amino acids present (mg/ml) in the samples ASP, ASP-D and ASP-HD.

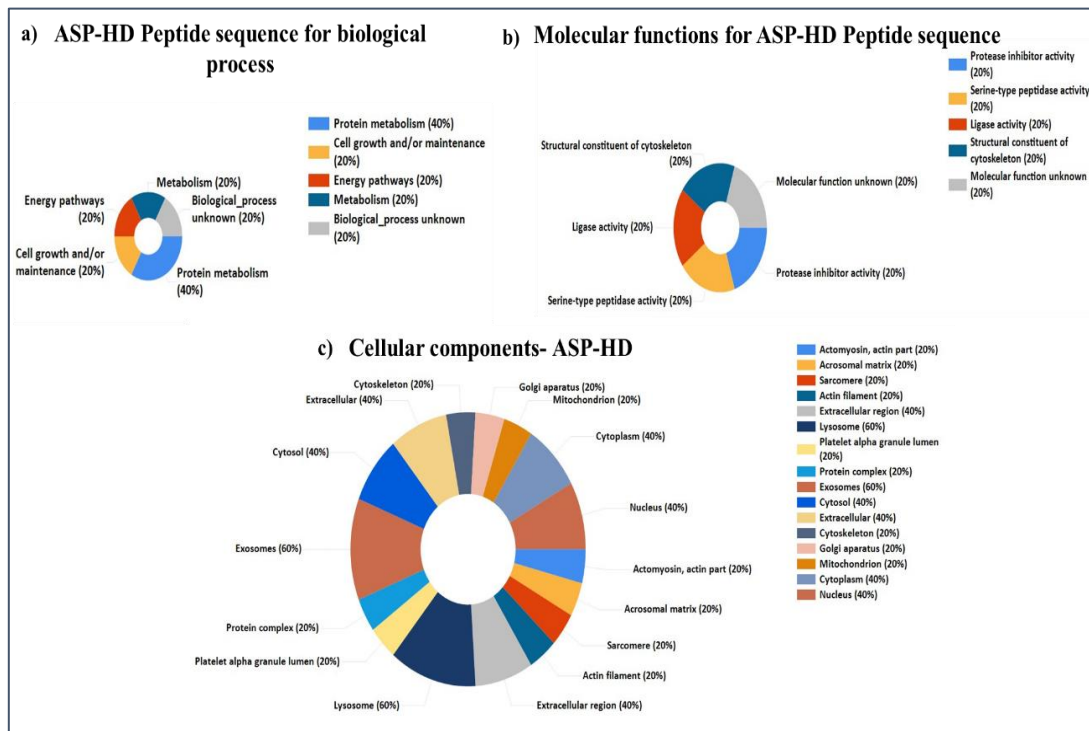


Figure. 4.10. Functional annotation analysis of ASP-HD (a) Biological process (b) Molecular function (c) Cellular components.

4.4. Discussion

Recent research has shown that consuming whole-grain food with proteins, peptides, and AA in them plays a significant role to lower the chance of developing many types of cancer. In conventional cereals, maize bioactive peptides have been reported to exhibit anticancer properties and numerous other health-enhancing qualities (Díaz-Gómez et al., 2017). According to the preliminary investigation in the previous chapter, amaranth protein hydrolysate (ASP-HD) significantly decreased MDA-MB-231 cell survival. In this chapter, we chose ASP-HD for our anti-breast cancer investigation because it showed significant cytotoxicity in a dose-dependent manner against MDA-MB-231 cells. The cell morphology analysis also revealed the cytotoxic effect of ASP-HD, as evidenced by the loss of cell attachment and the occurrence of round and swollen cells. Additionally, there were fewer viable cells and a higher percentage of apoptotic cells. Sabbione et al. also found that *Amaranthus mantegazzianus* proteins and peptides released after simulated gastrointestinal digestion inhibited HT-29 colon cancer cells' ability to proliferate (IC₅₀ values of 1.35± 0.12 mg soluble protein/mL) (Sabbione et al., 2019). Quiroga et al. found similar results while studying the effect of amaranth protein isolates on UMR106 rat osteosarcoma-derived cells (Quiroga et al., 2015).

Apoptosis has a crucial role in tumour regression. Further research was conducted to evaluate whether the cytotoxic effects of ASP-HD are induced by apoptosis. In the initial phases of apoptosis, the caspase protein family is activated, along with possibly additional proteases. These proteases break down the structural proteins in the cytoskeleton and nuclear proteins. The emergence of morphological alterations in the cell and widespread DNA cleavage are the outcomes of these biochemical processes. Nucleosomal and oligonucleosomal DNA fragments (180 bp and multiples of 180 bp) are the end products of DNA degradation and cause a specific alteration in the cell similar to nuclear condensation and fragmentation that can be seen by DAPI staining (Riccardi & Nicoletti, 2006). In the present work, we discovered that ASP-HD causes nuclear fragmentation in breast cancer cells and may induce these TNBC cells to undergo apoptosis. Dual AO/EB fluorescence labelling in apoptotic cells can identify basic morphological alterations. It also permits the differentiation of necrotic cells, early and late apoptotic cells, and normal cells. As a result, AO/EB staining provides a qualitative and quantitative approach to identifying apoptosis. We speculate that AO, which fluoresces green when attached to DNA, entered healthy and early apoptotic cells with intact membranes. EB only entered cells with broken membranes, such as late apoptotic and dead cells, and released an orange-red fluorescent signal when bound to concentrated DNA fragments or apoptotic bodies. Dual AO/EB staining can also find minor DNA damage (Liu et al., 2015). In the current investigation apoptosis induction research using (AO-EB) dual staining revealed that treatment with ASP-HD (50 µg/mL) increases the proportion of cells with deformed membranes and induces apoptosis in cancer cells. PS exposure was chosen as our potential marker because it is a reliable indicator of programmed cell death in its early phases. PS is a crucial component of the plasma membrane that is

actively restricted to the inner membrane leaflet in healthy cells. During apoptosis, PS translocate to the plasma membrane's outer leaflet, detected by fluorescently labelled annexin V conjugates. The strong, calcium-dependent affinity and specificity of annexin V make it an ideal probe for PS exposure (Kupcho et al., 2019). The current study's findings showed a significantly higher proportion of PS translocation in ASP-HD-treated cells than in control cells.

Caspase-3 is a crucial molecule for triggering cancer cell apoptosis. Cleaved caspase-3 served as the main cleavage enzyme to promote apoptosis. Among apoptotic marker proteins, Bax is a proapoptotic protein whereas, Bcl-2 suppresses caspase-3 activation (W. Wang et al., 2019). When MDA-MB-231 cells were treated with ASP-HD, the expression of Bcl-2 was reduced, and the activity of caspase-3 and Bax was enhanced. Our results highlight the intricate relationship between ASP-HD and apoptotic proteins. Since external stress is a constant for cancer cells, upregulating and expressing HSPs is crucial for their survival by maintaining protein structure and function. It was discovered that HSP60 activates cytoprotective pathways that stabilise survivin levels in the mitochondria and generate HSP60-p53 complexes that block p53 activity in tumour cells, both of which prevent cancer cells from apoptosis. HSP70 improves tumour antigen presentation by forming an HSP70-antigen complex that is transferred to antigen-presenting cells for cross-presentation and eventually activation of cytotoxic CD8 T cells (Eric C et al., 2018). ASP-HD-treated MDA-MB-231 cancer cells can effectively activate HSP70, P53, and downregulate survivin and induce apoptosis in TNBC cells. Anti-estrogen therapy, such as tamoxifen or fulvestrant, causes down-regulation of p21 and p27 also the cell cycle arrest in endocrine-sensitive breast cancer (Moore et al., 2022). Similarly, in the current study, ASP-HD activated the CDK inhibitors p21 and p27 which may cause the cell cycle arrest of cancer cells. Additionally, ASP-HD causes Livin to decrease within cells. According to reports, Livin's anti-apoptosis pathways bind to Caspase-3 either directly or indirectly by controlling the Caspase signal pathway to suppress apoptosis (Gu et al., 2015). Our research suggests that ASP-HD might regulate the expression of apoptotic and antiapoptotic proteins in MDA-MB-231 breast cancer cells to inhibit tumour growth.

Inhibiting cellular migration is crucial in searching for new cancer treatments since cancer cells must invade and spread (Bravo-Cordero et al., 2013). The capacity of ASP- HD to prevent breast cancer cells from migrating over an artificial wound was investigated through experiments. These findings suggested that ASP-HD had similar anti-metastatic potential to curcumin.

Amino acid profiling was performed on raw and heat-denatured amaranth seed proteins to understand the EAA found in amaranth protein isolates. According to the amino acid profile, the free EAA content of the undigested amaranth proteins was extremely low. The release of amino acids like leucine, threonine, and lysine was significantly boosted by simulated digestion. However, heat denaturation followed by simulated digestion markedly boosted the release of amino acids like Leu, Thr, and

Trp. The protein and EAA content of pseudocereals has previously been investigated and reported to be around 16 g of crude protein/100 g seeds with a high leucine content (Mota et al., 2014). To gain a comprehensive understanding of the types of proteins discovered, the MS analysis results were divided into three major categories by Gene Ontology (GO) (using the DAVID software system): cellular component, molecular function, biological process, and protein class. ASP-HD has a major role in the molecular functions of serine-type peptidase, Ligase, protease inhibitor and structural constituent of the cytoskeleton. The major biological process was protein metabolism, cell growth and maintenance and ASP-HD can interact with every cellular component especially high interaction with in Lysosome, Exosome, Nucleus and Cytoplasm. These findings shed light on the ASP-HD peptide's fundamental roles and significant cellular connections.

4.5. Conclusion

This chapter deals with a detailed analysis of the anti-breast cancer effects of amaranth seed protein hydrolysates. We have tested different concentrations of ASP, ASP-D, and ASP-HD samples in MDA-MB-231 cells and the potential cytotoxicity was observed for ASP-HD samples with a GI₅₀ value of 48.3 ± 0.2 µg/ml. ASP-HD can induce apoptosis in MDAMB-231 cells, which was examined through DNA fragmentation, phosphatidylserine translocation, membrane integrity loss, and caspase 3 activity analysis. Apoptosis array results demonstrated that ASP-HD could activate proapoptotic proteins such as Bax, caspase 3, HSP 70, P21, P27, P53, SMAC, and TNF-β and inhibited antiapoptotic proteins like Bcl2 and Livin. ASP-HD impeded the migration of cells by reducing the healing of artificial wounds in a cell monolayer. We have also done the amino acid analysis (through HPLC) of ASP, ASP-D and ASP-HD and the results indicated that the ASP-HD sample contained the maximum number of essential amino acids like lysine, threonine, tryptophan, isoleucine, phenylalanine and leucine. These results indicated that amaranth proteins upon heat denaturation followed by simulated digestion released maximum essential amino acids. Also, we have identified around 4606 peptides in ASP-HD and the GO analysis revealed various functional properties of these peptides.

4.6. References

1. Akbarian, M., Khani, A., Eghbalpour, S., & Uversky, V. N. Bioactive Peptides: Synthesis, Sources, Applications, and Proposed Mechanisms of Action. *International Journal of Molecular Sciences*.2022; 23(3). <https://doi.org/10.3390/ijms23031445>
2. Bravo-Cordero, J. J., Magalhaes, M. A. O., Eddy, R. J., Hodgson, L., & Condeelis, J. Functions of cofilin in cell locomotion and invasion. *Nature Reviews Molecular Cell Biology*. 2013; 14(7), 405–417. <https://doi.org/10.1038/nrm3609>
3. Díaz-Gómez, J. L., Castorena-Torres, F., Preciado-Ortiz, R. E., & García-Lara, S. Anti-cancer activity of maize bioactive peptides. *Frontiers in Chemistry*. 2017; 5(June), 1–8. <https://doi.org/10.3389/fchem.2017.00044>

4. Eric C. Meyers, Bleyda R. Solorzano, Justin James, Patrick D. Ganzer, Elaine S., Robert L. Rennaker, Michael P. Kilgard and Seth Hays. *Physiology & Behavior*. 2018; 176(1), 100–106. <https://doi.org/10.1016/j.urolonc.2018.09.007>.Heat
5. Gao, C., Sun, R., Xie, Y. R., Jiang, A. L., Lin, M., Li, M., Chen, Z. W., Zhang, P., Jin, H., & Feng, J. P. The soy-derived peptide Vglycin inhibits the growth of colon cancer cells in vitro and in vivo. *Experimental Biology and Medicine*. 2017; 242(10), 1034–1043. <https://doi.org/10.1177/1535370217697383>
6. Gu, J., Ren, L., Wang, X., Qu, C., & Zhang, Y. Expression of livin, survivin and caspase-3 in prostatic cancer and their clinical significance. *International Journal of Clinical and Experimental Pathology*. 2015; 8(11), 14034–14039.
7. Hayes, T. G., Falchook, G. F., Varadhachary, G. R., Smith, D. P., Davis, L. D., Dhingra, H. M., Hayes, B. P., & Varadhachary, A. Phase I trial of oral talactoferrin alfa in refractory solid tumors. *Investigational New Drugs*. 2006; 24(3), 233–240. <https://doi.org/10.1007/s10637-005-3690-6>
8. Kim, E. K., Joung, H. J., Kim, Y. S., Hwang, J. W., Ahn, C. B., Jeon, Y. J., Moon, S. H., Song, B. C., & Park, P. J. Purification of a novel anticancer peptide from enzymatic hydrolysate of *Mytilus coruscus*. *Journal of Microbiology and Biotechnology*. 2012; 22(10), 1381–1387. <https://doi.org/10.4014/jmb.1207.07015>
9. Kupcho, K., Shultz, J., Hurst, R., Hartnett, J., Zhou, W., Machleidt, T., Grailer, J., Worzella, T., Riss, T., Lazar, D., Cali, J. J., & Niles, A. A real-time, bioluminescent annexin V assay for the assessment of apoptosis. *Apoptosis*. 2019; 24(1–2), 184–197. <https://doi.org/10.1007/s10495-018-1502-7>
10. Li, Y., Zhang, H., Merkher, Y., Chen, L., Liu, N., Leonov, S., & Chen, Y. Recent advances in therapeutic strategies for triple-negative breast cancer. *Journal of Hematology and Oncology*. 2022; 15(1), 1–30. <https://doi.org/10.1186/s13045-022-01341-0>
11. Liao, W., Zhang, R., Dong, C., Yu, Z., & Ren, J. Novel walnut peptide–selenium hybrids with enhanced anticancer synergism: Facile synthesis and mechanistic investigation of anticancer activity. *International Journal of Nanomedicine*. 2016; 11, 1305–1321. <https://doi.org/10.2147/IJN.S92257>
12. Lin, X., Dong, L., Yan, Q., Dong, Y., Wang, L., & Wang, F. Preparation and Characterization of an Anticancer Peptide from Oriental Tonic Food *Enteromorpha prolifera*. *Foods*. 2022; 11(21). <https://doi.org/10.3390/foods11213507>
13. Liu, K., Liu, P. cheng, Liu, R., & Wu, X. Dual AO/EB staining to detect apoptosis in osteosarcoma cells compared with flow cytometry. *Medical Science Monitor Basic Research*. 2015; 21, 15–20. <https://doi.org/10.12659/MSMBR.893327>
14. Luna-Vital, D. A., González de Mejía, E., & Loarca-Piña, G. Dietary Peptides from *Phaseolus vulgaris* L. Reduced AOM/DSS-Induced Colitis-Associated Colon Carcinogenesis in Balb/c Mice. *Plant Foods for Human Nutrition*. 2017; 72(4), 445–447. <https://doi.org/10.1007/s11130-017-0633-2>

15. Ma, S., Huang, D., Zhai, M., Yang, L., Peng, S., Chen, C., Feng, X., Weng, Q., Zhang, B., & Xu, M. Isolation of a novel bio-peptide from walnut residual protein inducing apoptosis and autophagy on cancer cells. *BMC Complementary and Alternative Medicine*. 2015; 15(1), 1–14. <https://doi.org/10.1186/s12906-015-0940-9>
16. Mota, C., Santos, M., Mauro, R., Samman, N., Sofia, A., Torres, D., & Castanheira, I. Protein content and amino acids profile of pseudocereals. *food chemistry*. 2014. <https://doi.org/10.1016/j.foodchem.2014.11.043>
17. Riccardi, C., & Nicoletti, I. Analysis of apoptosis by propidium iodide staining and flow cytometry. *Nature Protocols*. 2006; 1(3), 1458–1461. <https://doi.org/10.1038/nprot.2006.238>
18. Wang, L., Dong, C., Li, X., Han, W., & Su, X. Anticancer potential of bioactive peptides from animal sources (Review). *Oncology Reports*. 2017 38(2), 637–651. <https://doi.org/10.3892/or.2017.5778>
19. Wang, W., Zhu, M., Xu, Z., Li, W., Dong, X., Chen, Y., Lin, B., & Li, M. Ropivacaine promotes apoptosis of hepatocellular carcinoma cells through damaging mitochondria and activating caspase-3 activity. *Biological Research*. 2019; 52(1), 36. <https://doi.org/10.1186/s40659-019-0242-7>
20. Yin, L., Duan, J. J., Bian, X. W., & Yu, S. C. Triple-negative breast cancer molecular subtyping and treatment progress. *Breast Cancer Research*, 2020; 22(1), 1–13. <https://doi.org/10.1186/s13058-020-01296-5>

CHAPTER 5

Identification of genes and pathways responsible for the anti-inflammatory activity of Quinoa extract (Q-80M) through NGS analysis

5.1. Introduction

Over the past few decades, researchers, nutritionists, and health professionals have become interested in learning about healthy diets. Humans have used plant-based food as remedies for thousands of years. Since they have recognized that environment and diet may affect a person's health. As research progressed, scientists began to wonder about the interplay between genes and food-bio actives that can cause either a positive or negative effect on an individual's health (Sales et al., 2014).

Nutritional genomics is an emerging area of science that deals with the connection between food bioactive and the genome. It comprises nutrigenetics and nutrigenomics. Nutrigenomics refers to the influence of nutrients on gene expression, whereas Nutrigenetics refers to the diverse response of gene variations to nutrients. Nutrigenetics can tailor a person's nutritional intake for optimum health and disease prevention. Food tolerances among humans vary based on genetics, opening the door to individualized dietary recommendations for optimum health and disease prevention. Nutrigenomics investigates the interactions between food bio-actives and their impact on the genome. This field of science will uncover the best diet through a series of dietary modifications. Thus, nutrigenomics refers to the application of biochemistry, physiology, nutrition, genomics, proteomics, metabolomics, transcriptomics, and epigenomics. It will help to investigate and explain the existing reciprocal connections between genes and nutrients at the molecular level. Nutrigenomics will make it easier to prescribe diet plans based on the genotype (Milner, 2006).

At the cellular level, nutrients may bind to transcription factor receptors or undergo primary or secondary metabolism. This changes the number of substrates or intermediates and ultimately can regulate signal pathways. Nutrients can act as transcription factors (TFs) and alter gene expression. Nuclear receptors experience a conformational shift upon ligand binding that causes coordinated corepressor dissociation and recruitment of coactivator proteins to set up transcriptional activation. These TFs serve as nutrient sensors in metabolically active organs (liver, gut, and adipose tissue) by adjusting the transcription of particular genes in response to nutrient levels. Epidemiological research demonstrates a link between dietary intake and the prevalence of chronic diseases (B. Liu & Qian, 2011). As a result, it will be feasible to treat or prevent disease, particularly in the domain of Nontransmissible Chronic Diseases (NTCDs). Currently, the NTCDs are considered a significant global public health issue (Daimiel et al., 2012).

Globally, disorders associated with chronic inflammation continue to rank among the leading causes of morbidity and mortality. Optimal nutrition would promote immune

cell functioning, enabling them to launch efficient responses against infections. It can resolve the reaction promptly and avoid any underlying, persistent inflammation. Some micronutrients and dietary components have critical roles in the development and maintenance of a functional immune system throughout life, as well as in reducing chronic inflammation. For instance, the micronutrients vitamin A and zinc regulate a proper proliferative response within the immune system, and the amino acid arginine is essential for producing nitric oxide by macrophages. Some foods, especially long-chain omega-3 polyunsaturated fatty acids, can prevent TLR4 from being activated and reduce the inflammatory signal. The Mediterranean diet is full of fish, 'good' dietary fats, vegetables, fruit, nuts, and legumes, in contrast to the Western diet. Mediterranean diet can reduce the risk of chronic diseases (cancer, cardiovascular disease, and Alzheimer's disease) (Román et al., 2019). The protective effect of diets with fruits and vegetables lowers the risk of getting non-communicable diseases due to the bioactive compounds in fruits and vegetables. Dietary polyphenols are one family of chemicals that are recognized to play a part in the control of inflammation (Minihane et al., 2015). The evidence regarding dietary polyphenols' potential to lower the risk of cancer, several neurological illnesses, and cardiovascular disease, as well as the processes by which they can be immunomodulatory and anti-inflammatory. There is interest in determining whether specific dietary interventions can improve immune function even further in preclinical settings, thereby delaying the onset of infections or chronic inflammatory disorders (Vauzour et al., 2010).

The molecular-based analysis of nutrients has grown in popularity recently because it offers high resolution and accuracy. Next-generation sequencing (NGS), often referred to as massively parallel sequencing or high-throughput sequencing, is a technology that enables the simultaneous sequencing of millions of DNA or RNA sequences. NGS has several benefits over conventional sequencing techniques, including better throughput with sample multiplexing, higher sensitivity in finding low-frequency variations, a quicker turnaround for large sample volumes, and reduced cost (G. Liu et al., 2021). After Sanger sequencing, NGS marks a real revolution in sequencing technology. NGS can be used for a variety of purposes. A recent investigation used whole-genome transcriptomics analysis to determine the impact of nutrients at the genomic and proteomic levels. We can investigate a wide range of biomarkers using NGS technology in chronic inflammation (Xu et al., 2021). RNA-seq is generally used to identify differentially expressed genes, determine statistically enriched pathways, and identify hub genes that are principally responsible for the observed phenotype (Chen et al., 2020).

In the preliminary screening for anti-inflammatory studies, we found that Q-80M (quinoa seed 80% methanol extract, direct extraction) showed significant anti-inflammatory effects in RAW 264.7 cells. So, in this chapter, we have elucidated the major genes and pathways responsible for the anti-inflammatory activity of Q-80M through whole-transcriptome analysis.

5.2. Methodology

The following methodologies were adopted in this chapter

1. RNA was isolated using an RNeasy Mini kit (QIAGEN) from control, LPS stimulated, and Q-80M (250 µg/ml) pretreated LPS stimulated RAW cells.
2. The RNA quality was assessed by RNA ScreenTape System (Agilent) in a 4150 Tape Station System (Agilent).
3. RNA concentration was determined using the Qubit™ RNA BR Assay Kit on Qubit® 3.0 Fluorometer.
4. mRNA Enrichment was done using NEBNext Poly (A) mRNA magnetic isolation module.
5. The library was prepared using the NEBNext® Ultra™ II RNA Library Prep Kit.
6. The library concentration was evaluated by Qubit dsDNA HS (High Sensitivity) Assay Kit using a Qubit.3 Fluorometer (Life Technologies).
7. The library quality assessment was performed using an Agilent D5000 ScreenTape System and an Agilent D1000 ScreenTape System in an Agilent 4150 TapeStation System.
8. Paired-end sequencing on the Illumina NovaSeq and data quality were examined using FastQC and MultiQC software.
9. Alignment and expression of reads were analyzed using the STAR v2 aligner.
10. Statistically significant DEGs were identified using a volcano plot and heatmap.
11. The PPI network of DEGs was constructed using the STRING database and visualized by Cytoscape. Gene clusters were identified using the MCODE cytoscape app 2.0.0.
12. The hub genes identified with CytoHubba.
13. Enrichment analysis for biological process, Molecular function, Cellular component and KEGG Pathway was performed using the ClusterProfiler R package.

The workflow is Reference-based mRNA-seq data analysis and functional annotation given in Figure 5.1. RNA isolation was performed in triplicate, and the detailed procedures are described in Chapter 2.

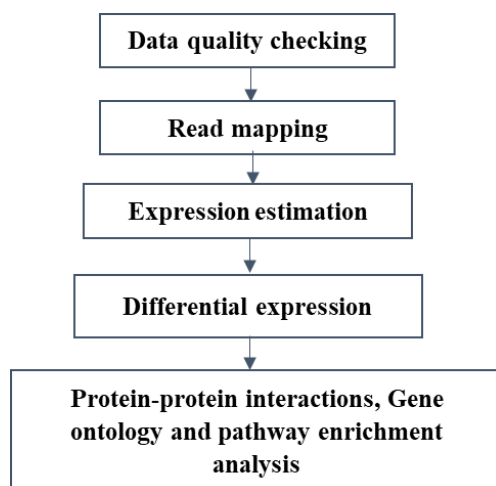


Figure 5.1. Workflow of mRNA-seq data analysis and functional annotation

5.3. Results

5.3.1. Total RNA and quality checking

RNA samples were extracted from control cells, LPS-induced cells and Q-80M pre-treated LPS-induced cells. The RNA quality was evaluated using an RNA ScreenTape System (Agilent) in a 4150 TapeStation System (Agilent). The RNA concentration was determined using the Qubit™ RNA BR Assay Kit on a Qubit® 3.0 Fluorometer (ThermoFisher Scientific). Table 5.1 summarizes the findings. According to the findings, the recovered RNA was of sufficient amount and quality to move forward with the sequencing.

Sl. No :	Sample ID	RIN	28D/18D Ratio	Conc.(ng / μ L)	The volume of RNA available(μ L)	Total RNA mass(n g)	QC status
1	Control 1	8.9	2.5	668	20	13360	Pass
2	Control 2	9.4	2.6	558	20	11160	Pass
3	LPS 1	9.5	3.1	2120	20	42400	Pass
4	LPS 2	9.2	3	2001	20	40354	Pass
5	Q-80M+LPS 1	6.7	1	2160	8	17280	Pass
6	Q-80M+LPS 1	8	1.9	666	20	13320	Pass

Table 5.1: Complete quality checking status of total RNA

5.3.2. mRNA Enrichment and Library Preparation and quality checking

250ng of total RNA has been utilised for enriching the mRNA using NEBNext Poly (A) mRNA magnetic isolation module. The libraries from the enriched mRNAs were prepared using the NEBNext® Ultra™ II RNA Library Prep Kit for Illumina. The concentration of the library was evaluated according to the Qubit dsDNA HS (High

Sensitivity) Assay Kit using a Qubit.3 Fluorometer (Life Technologies). The library quality assessment was performed using an Agilent D5000 ScreenTape System and an Agilent D1000 ScreenTape System in an Agilent 4150 TapeStation System designed for analysing DNA molecules from 100 to 5000bp. The library qualification criteria are based on the presence of a broad peak in the region of 300bp to 1000bp, with an average size of 400bp-600bp in the Agilent 4150 TapeStation system and a qubit concentration of more than 2ng/1 or 10nmol. The findings confirmed that all the samples were qualified for the library qualification criteria (Table 5.2.).

Sl.No:	Sample ID	Qubit conc. (ng/μl)	Size (bp)	Conc. (nmol)	QC status
1	Control 1	15.1	337	67.89	Qualified
2	Control 2	7.98	333	36.31	Qualified
3	LPS 1	5.58	339	24.94	Qualified
4	LPS 2	10.6	333	48.23	Qualified
5	Q-80M+LPS 1	8.36	326	38.85	Qualified
6	Q-80M+LPS 2	12.4	339	55.42	Qualified

Table 5.2: The complete library validation report of samples

5.3.3. NGS data quality checking

The sequence data were generated using an Illumina NovaSeq. Data quality was examined using FastQC and MultiQC software. The data were assessed for base call quality Distribution, % bases above Q20, Q30, %GC, and sequencing adaptor contamination (Table 5.3). Each sample complied with the QC requirements (Q20>95%). Adaptor motifs and poor-quality bases were removed from the raw sequencing reads using Fastp.

Samples	Number of reads	% of Bases>Q30
Control 1	37112708	94.51
Control 2	40499372	94.05
LPS 1	32695790	94.15
LPS 2	47957800	94.5
Q-80M+LPS 1	41287382	94.53
Q-80M+LPS 2	22119216	94.18

Table 5.3: Summarizes the raw sequence data and its quality.

5.3.4. Alignment and Expression Analysis

The quality-checked reads were mapped to the indexed *mus musculus* genome (GRCm39) using the STAR v2 aligner. 99.69% on average of the readings matched with the reference genome (Table 5.4).

Sample ID	Reads after QC	Mapped reads	Mapped reads%	Unmapped reads	Unmapped reads%	Uniquely mapped reads%
Control 1	34907202	34783886	99.65	123316	0.35	93.17
Control 2	39026956	38842672	99.53	184284	0.47	92.29
LPS 1	31719360	31680818	99.88	38544	0.12	93.46
LPS 2	46916210	46879874	99.92	36336	0.08	94.9
Q-80M +LPS 1	39767628	39498898	99.32	268730	0.68	91.72
Q-80M +LPS 2	21405468	21381722	99.89	23746	0.11	92.59

Table 5.4: Read alignment statistics

5.3.5. Functional annotation of differentially expressed genes

5.3.5.1. Screening of differentially expressed genes

The data were normalised using the trimmed mean of M (TMM) values before differential expression analysis was carried out with the help of the edgeR programme. During normalisation, 29057 features (52.44%) were removed from the analysis because they lacked at least 0.1 counts per million across at least three samples. Genes that exhibited an absolute log₂ fold change of 1 with a corrected p-value of 0.05 were considered significant (Table 5.5).

A volcano plot is a scatterplot that displays statistical significance (P value) vs magnitude of change (fold change). It enables the quick detection of large-fold changed statistically significant genes. In a volcano plot, the upregulated genes are on the right, the downregulated ones are on the left, and the statistically significant ones are at the top. In the control and inflammatory conditions, higher scattering was observed in upregulated genes (Figure 5.2(a)). More excellent dispersion on the upregulated gene side suggests LPS induce more genes than control cells. In contrast, in inflammation versus Q-80M treatment, more dispersion was seen in the downregulated genes (Figure 5.3(a)). This indicates that Q-80 can downregulate more genes from inflammatory conditions.

A heatmap was created using the Euclidean distance formula. The gene (row) and sample (column) clusters can be seen using the heatmap. The colour represents the fold-change value and shows downregulation as green and upregulation as red. The resulting heat map and volcano plot of control versus inflammation and inflammation versus Q-80M treatment are shown in the Figures. 5.2(b) and 5.3(b). DEGs with significant expression variation were extracted using a cut-off (p-value 0.05 and fold change >2), yielding 2174 genes that differed between control and inflammation, with 777 downregulated and 1397 upregulated. In LPS-induced inflammation versus Q-80M pre-treatment, 615 genes were expressed, 481 of which are downregulated and 139 of which are upregulated.

Condition	Tested genes	Significantly expressed genes	Upregulated genes	Down-regulated genes
Control Vs. Inflammation (LPS treatment)	27146	2174	1397	777
Inflammation (LPS treatment) Vs. LPS+ Q-80M treatment	27146	615	134	481

Table 5.5: Number of Differentially expressed genes

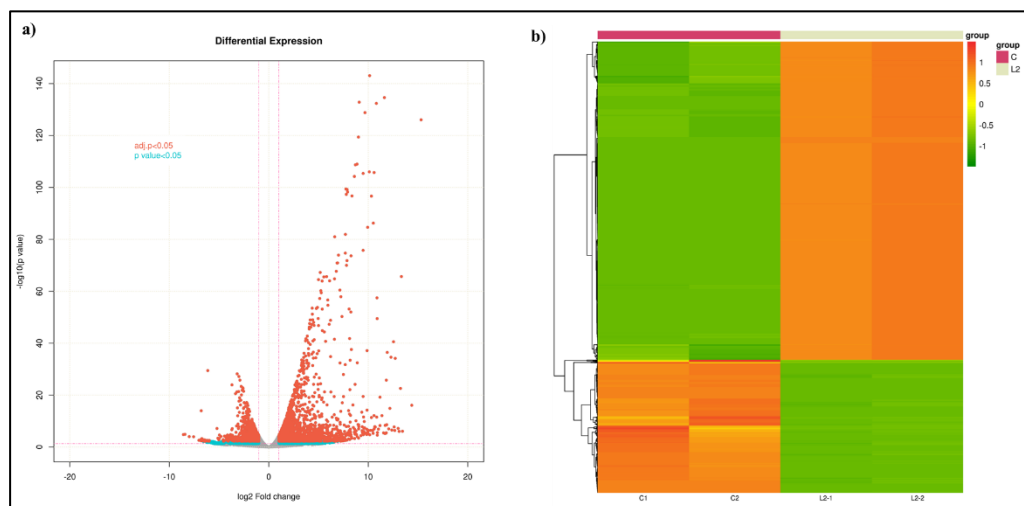


Figure 5.2: Control versus Inflammation. a). Volcano plot showing Differential expression profile of genes. Blue dots indicate \log_2 fold change ≥ 1 and P value ≤ 0.05 . Red dots indicate \log_2 fold change ≥ 1 and adjusted P value ≤ 0.05 . b). Heatmap: Expression profile of the significant differentially expressed genes across the samples. Upregulated genes-red colour and down regulated genes-green colour. Column 1 and 2 – Control, Column 3 and 4- Inflammation.

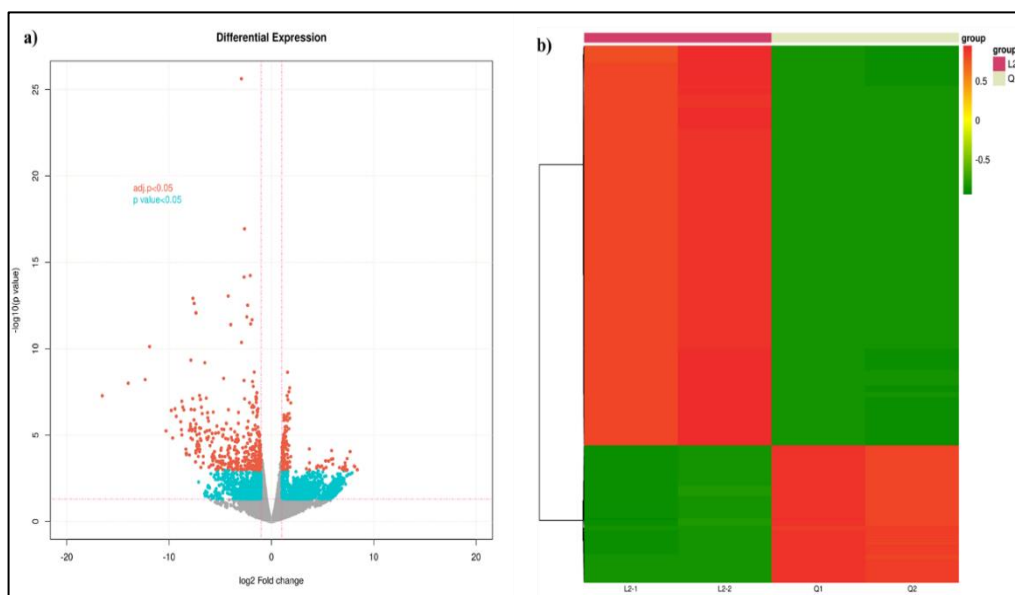


Figure 5.3: Inflammation versus Q80-M treatment. a). Volcano plot showing Differential expression profile of genes. Blue dots indicate \log_2 fold change ≥ 1 and P value ≤ 0.05 . Red dots indicate \log_2 fold change ≥ 1 and adjusted P value ≤ 0.05 . b). Heatmap: Expression profile of the significant differentially expressed genes across the samples. Upregulated genes-red colour and down regulated genes-green colour. Column 1 and 2 – Inflammation, Column 3 and 4- Q-80M treatment.

5.3.5.2. Protein-protein interaction network and topological analysis

The PPI network of the control versus inflammation and the inflammation versus Q-80M treatment group was constructed with STRING and visualised using Cytoscape version 3.10. In the control versus inflammatory group, the upregulated PPI network had 1495 nodes and 20509 edges. There were 643 nodes and 6553 edges in the downregulated PPI network (Figure 5.4(a)). In inflammation versus Q-80M pretreatment, the upregulated PPI network contained 107 nodes and 2716 edges. The downregulated PPI networks were discovered to have 328 nodes and 2231 edges (Figure 5.5(a)). Every PPI network was constructed with an enrichment p-value of $1.0e-16$.

Gene clusters were identified using the MCODE plugin (v1.6.1) with default parameters (Degree cut-off, 2; cluster finding, haircut; node score cut-off, 0.2; k-core, 2; and max depth, 100) to discover intensively connected regions called clusters. We found clusters in this network that were upregulated and downregulated under control versus inflammatory conditions (Figure 5.4(b)). The upregulated cluster has 116 nodes, 3220 edges, and a score of 56. The downregulated cluster has 96 nodes, 4307 edges, and a score of 56. We discovered upregulated and downregulated clusters in the inflammation versus Q-80M treatment (Figure 5.5(b)). The upregulated cluster contained 2078 edges and 66 nodes, a score of 63. The downregulated cluster has 25 nodes, 281 edges, and a score of 23.

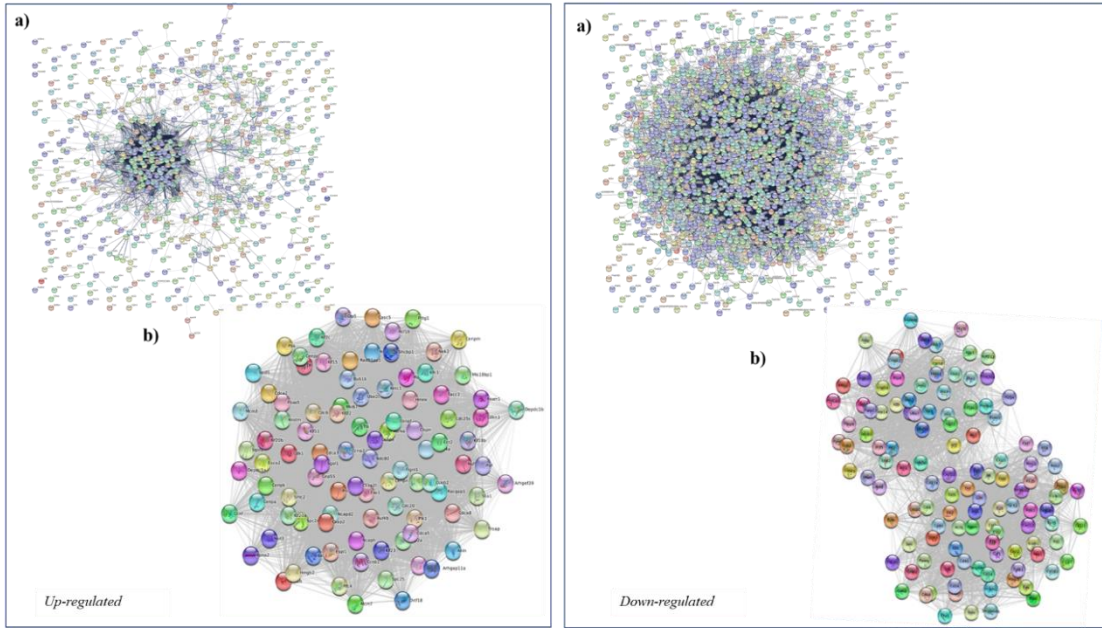


Figure 5.4: a) Protein-protein interaction networks of the Control versus inflammation were constructed using the STRING database. Each node represents a protein, and each edge indicates a protein-protein interaction. b) The cluster was constructed from the PPI network using the MCODE.

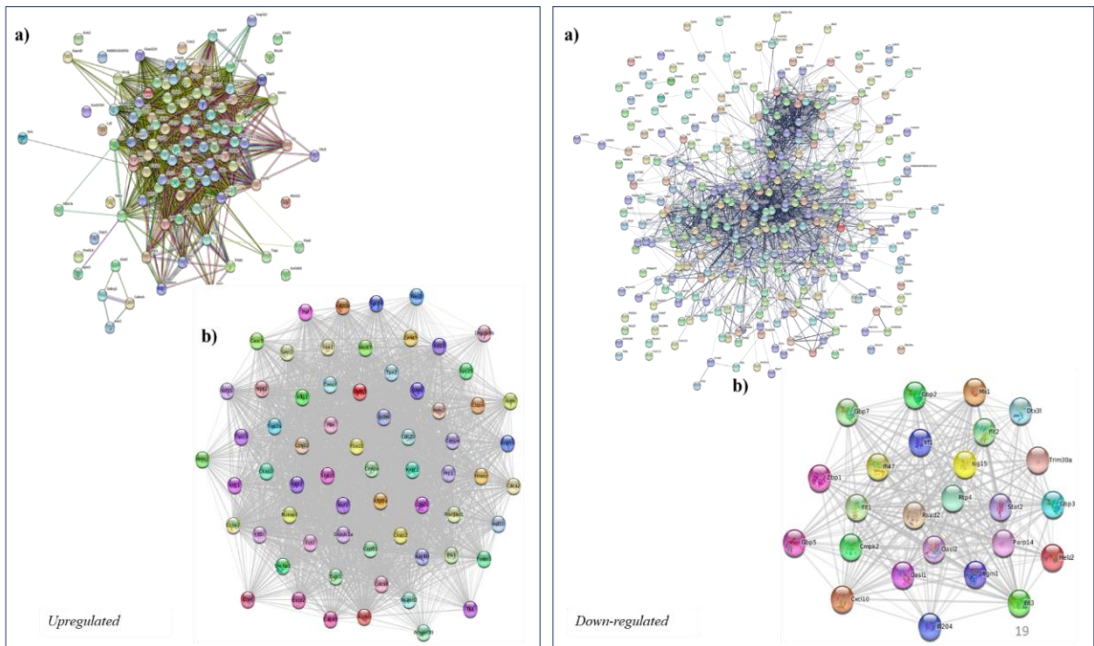


Figure 5.5: a) Protein-protein interaction networks of the inflammation versus Q80-M were constructed using the STRING database. Each node represents a protein, and each edge indicates a protein-protein interaction. b) The cluster was constructed from the PPI network using the MCODE.

The highly interconnected protein hubs in the PPI network were identified using the cytohubba version 0.1 plug-in of the Cytoscape software. The maximal clique centrality (MCC) approach was used to rank the top 10 upregulated and downregulated hub genes separately. MCC captures more critical proteins in the top-ranked list for both high-degree and low-degree proteins. The top 10 upregulated and downregulated hub nodes were identified in control versus inflammation (Figure 5.6). Similarly, the top 10 upregulated and downregulated hub nodes of inflammation versus Q-80M pre-treatment were identified (Figure 5.7).

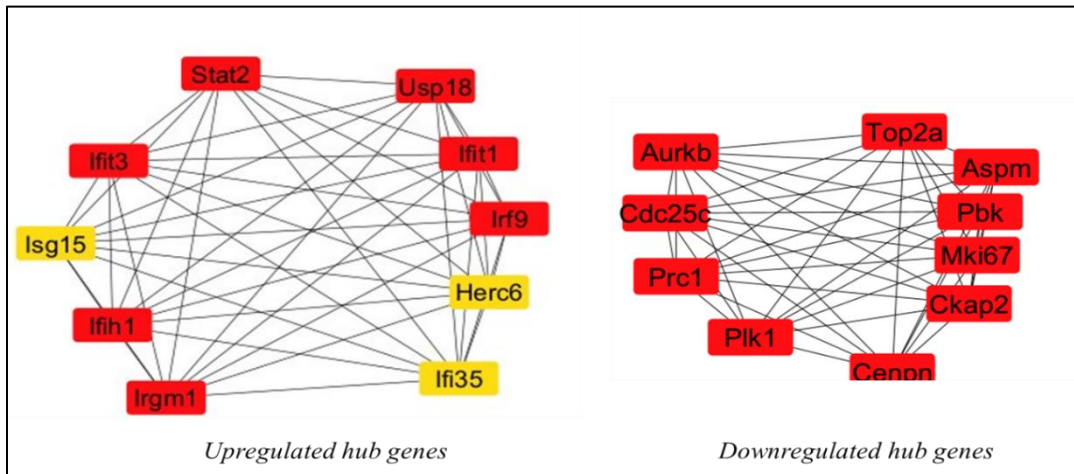


Figure 5.6: Control versus Inflammation The hub genes were screened from the PPI network using the MCC algorithm of CytoHubba plugin.

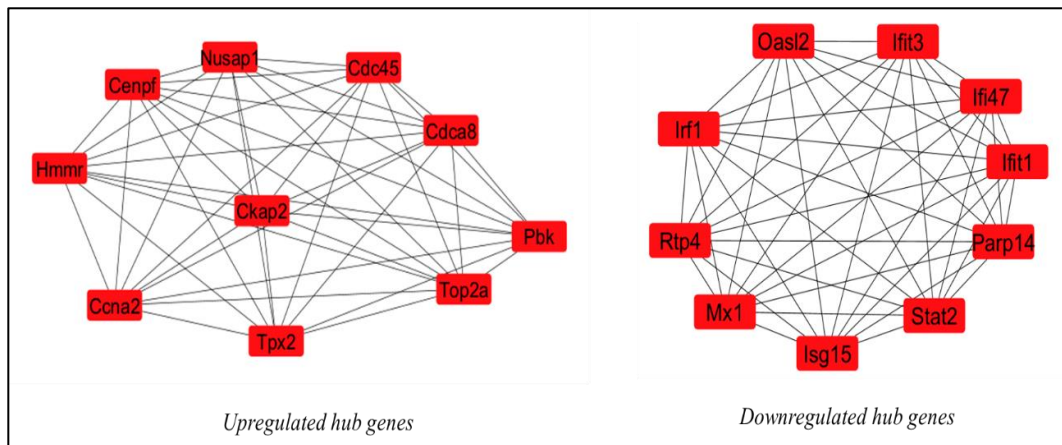


Figure 5.7: Inflammation versus Q80-M - The hub genes were screened from the PPI network using the MCC algorithm of CytoHubba plugin.

5.3.5.4. Analysis of GO Function and KEGG Enrichment of Related Targets

GO enrichment analysis illustrates gene function on three levels: biological process (BP), cellular component (CC), and molecular function (MF). In control verse inflammation, BP mostly involves aspects of response to positive regulation of cytokine production, adaptive immune response, positive regulation of response to external stimulus, and positive regulation of immune response. CC is mainly related to the external side of the plasma membrane, MHC protein complex, lytic vacuole,

lytic vacuole, and NLRP1 inflammasome complex. MF is largely involved in Cytokine receptor binding, chemokine activity, T cell receptor binding, and MHC class II protein complex binding. The data is given in Figure 5.8. In inflammation verse Q-80M treatment, BP primarily involves aspects of response negative regulation of response to external stimulus, negative regulation of immune response, and negative regulation of defence response. CC is the most related external side of the plasma membrane, chromosome, and centromeric region. MF is mainly involved in antioxidant activity peptidase regulator activity, and scavenger receptor binding. The results are given in Figure 5.9.

Further studies have revealed the underlying mechanism of Q-80M in chronic inflammation, a comprehensive pathway model of control versus inflammation compared with inflammation versus Q-80M pretreatment. The effect of Q-80M on inflammation was analysed based on pathways through KEGG pathway analysis. According to KEGG enrichment results, Q-80M exerts anti-inflammatory by regulating the cytokine cytokine receptor interaction pathway (Figure 5.10), TNF signalling pathway (Figure 5.11), chemokine signalling pathway (Figure 5.12), NOD-like receptor signalling pathway (Figure 5.13), and NFκB signalling pathway (Figure 5.14). The list of downregulated genes in each signalling pathway on Q-80M treatment is in Figure 5.15.

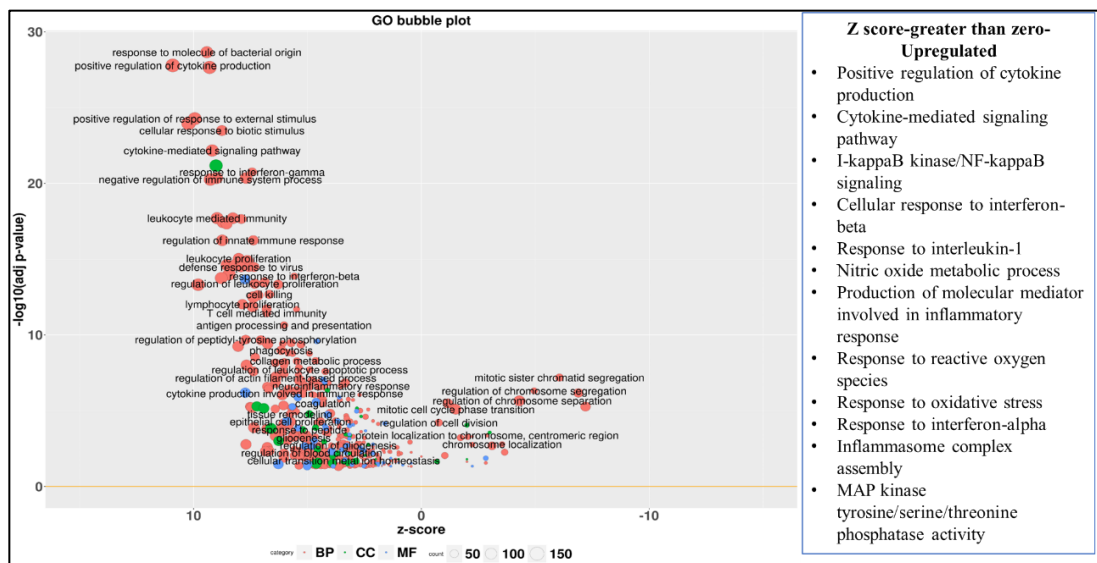


Figure 5.8: Control versus Inflammation- Bubble plot of the enriched GO terms using significantly expressed genes. The orange line represents the p-value threshold (Benjamini-Hochberg p-value 0.05). The size of the bubble is proportionate to the number of genes involved in the GO term.

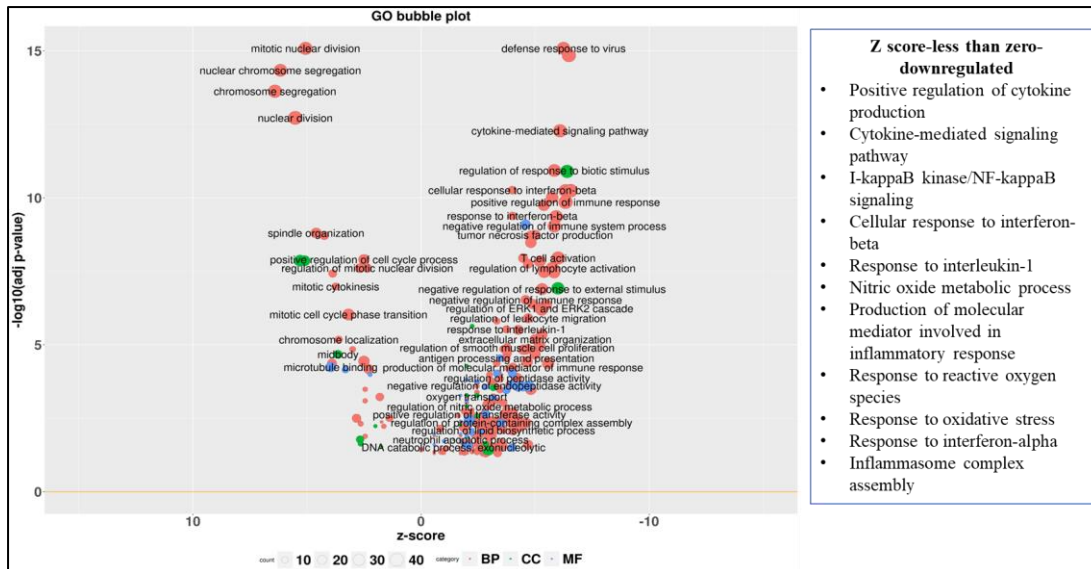


Figure 5.9: Inflammation versus Q-80M pretreatment- Bubble plot of the enriched GO terms using significantly expressed genes. The orange line represents the p-value threshold (Benjamini-Hochberg p-value 0.05). The size of the bubble is proportionate to the number of genes involved in the GO term.

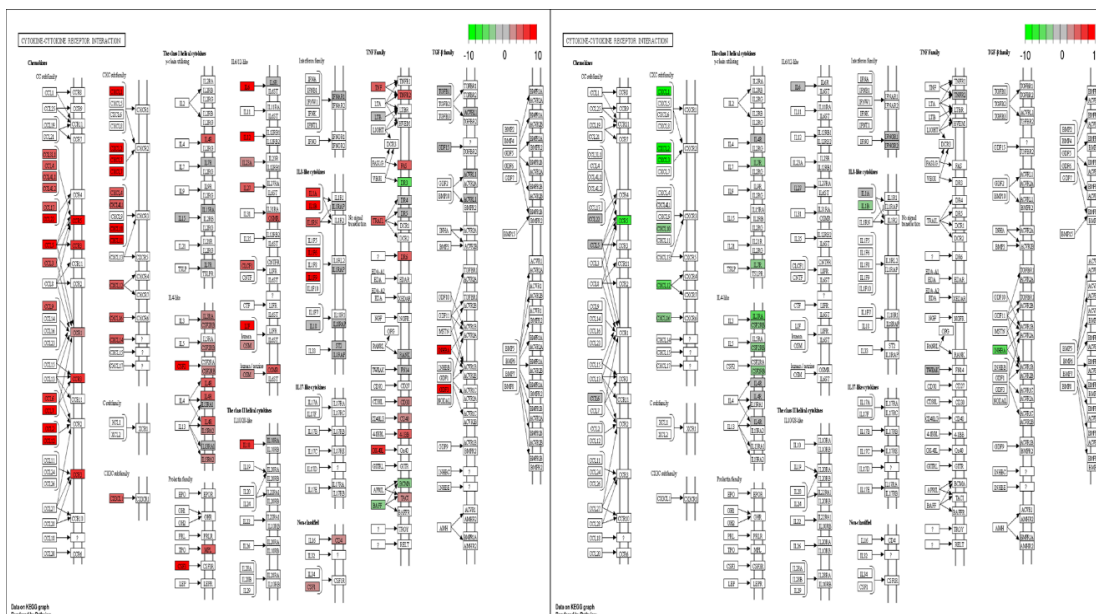


Figure 5.10: Cytokine-cytokine receptor interaction pathway of significant genes. The scale is set as log2 fold change (-10 to 10) where up and down regulated genes are shaded red and green respectively.

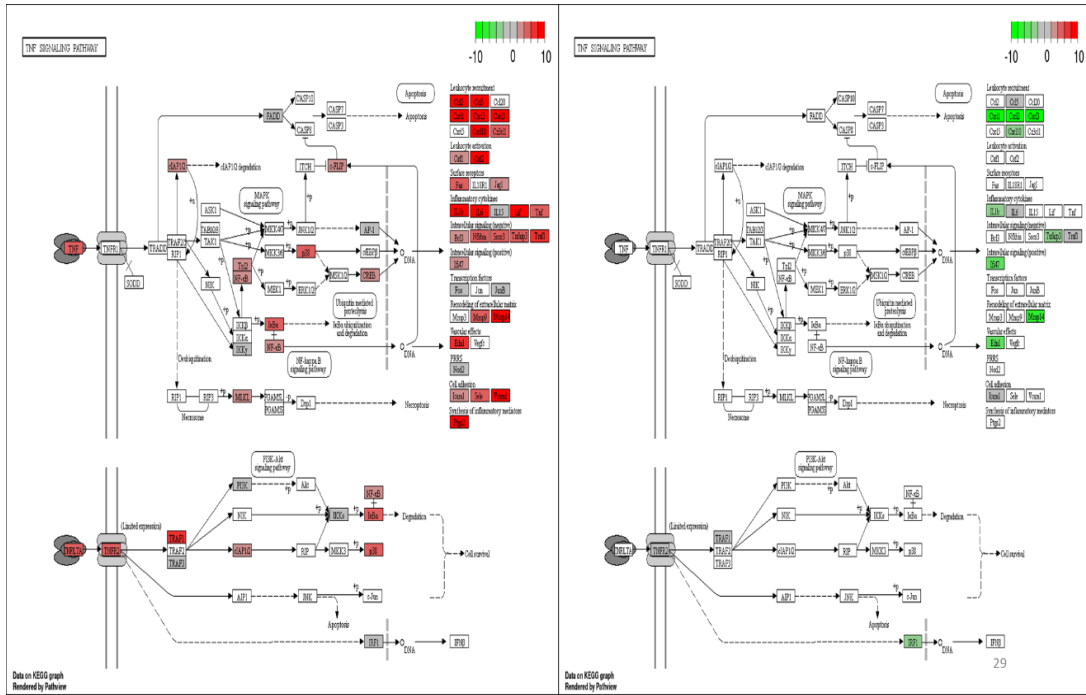


Figure 5.11: TNF signalling pathway of significant genes. The scale is set as log2 fold change (-10 to 10) where up and down regulated genes are shaded red and green respectively.

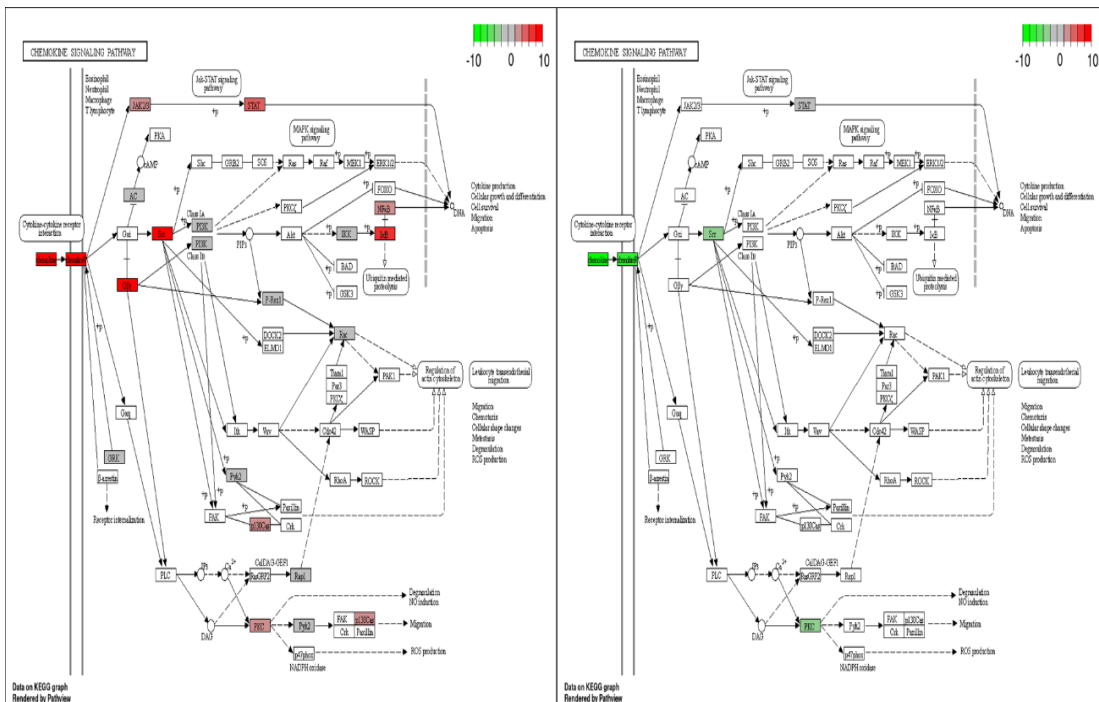


Figure 5.12: Chemokine signalling pathway of significant genes. The scale is set as log2 fold change (-10 to 10) where up and down regulated genes are shaded red and green respectively.

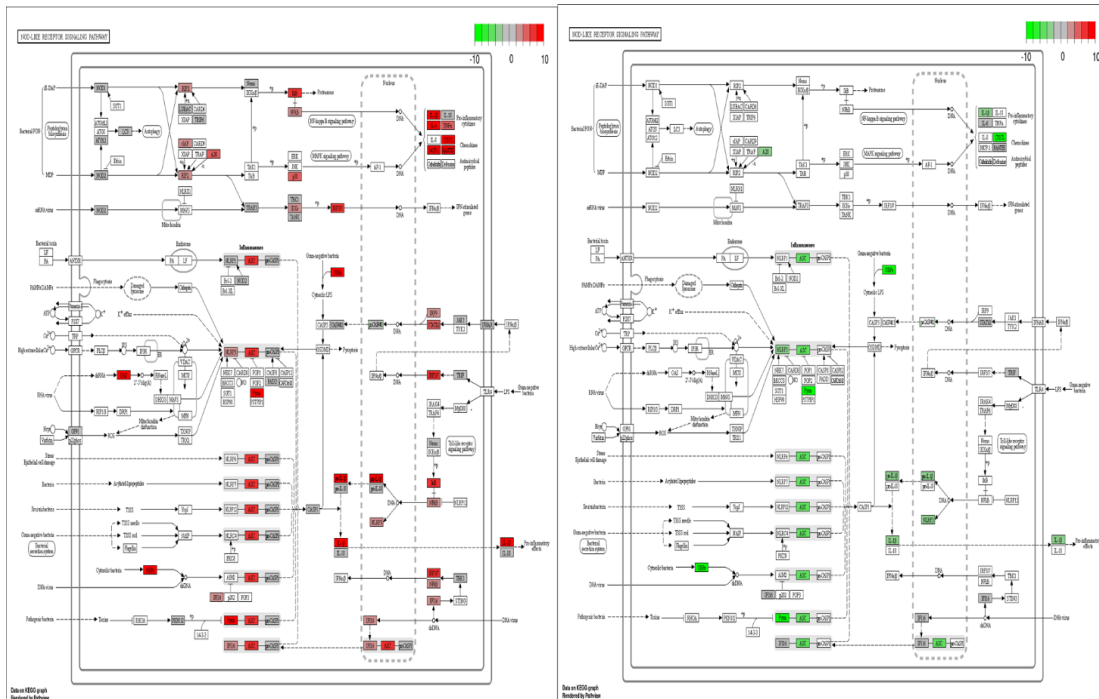


Figure 5.13: NOD-like receptor signalling pathway of significant genes. The scale is set as log₂ fold change (-10 to 10) where up and down regulated genes are shaded red and green respectively.

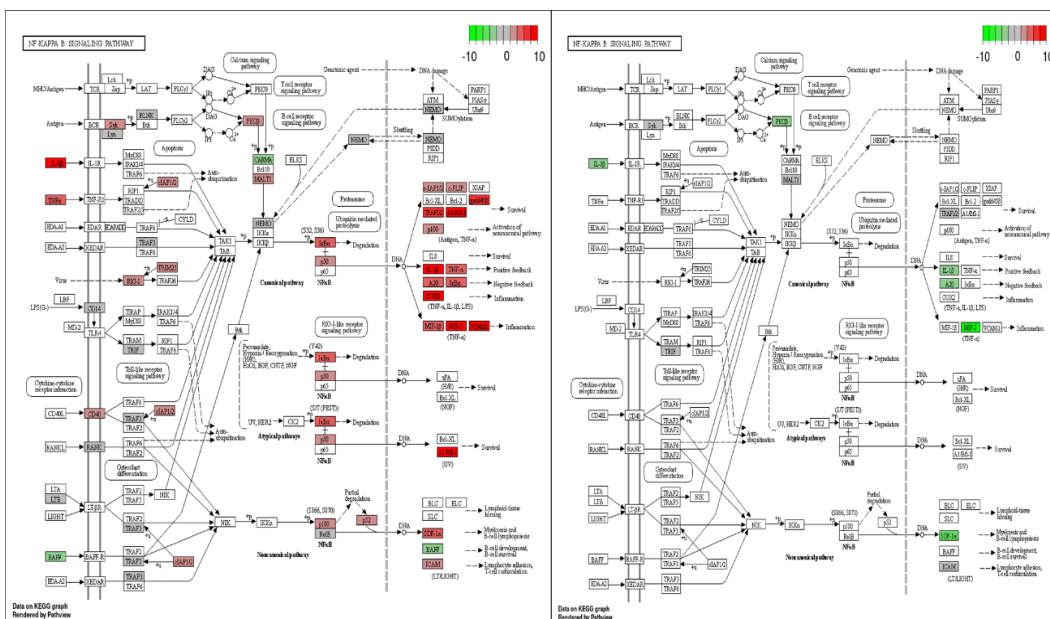


Figure 5.14: NF-κB signalling pathway of significant genes. The scale is set as log₂ fold change (-10 to 10) where up and down regulated genes are shaded red and green respectively.

Cytokine-Cytokine receptor interaction Pathway CCR5 CXCL1 CXCL2 CXCL3 CXCL10 CXCL12 CXCL16 IL-7R IL-1 β	TNF Signaling pathway Cxcl1 Cxcl2 Cxcl3 Cxcl10 IL-1 β MMP-14 Ifi47 Edn1
NFκB Signaling pathway IL-1 β PKC β A20 MMP-2 SDF-1 α	NOD-Like receptor Signaling pathway NLRP3 OPB3 ASC IL-1 β PKC β A20 CXCL
Chemokine Signaling pathway SRC STAT PKC	

Figure 5.15: Significantly down regulated genes in Inflammation versus Q-80M pretreatment

5.4. Discussion

Inflammation is the body's defence mechanism, a biological response of the immune system to potentially harmful stimuli such as different pathogens (viruses, bacteria), poisons, toxic chemicals, and tissue injury. These damaging stimuli create a chain of chemical reactions that activate leukocytes, which then secrete and generate inflammatory cytokines. These cytokines interact and stimulate one another. When a receptor is activated, many signalling molecules are phosphorylated, then activate different transcription factors. The level of inflammatory mediators in resident tissue cells is controlled by this coordinated activation of signalling molecules, which also attract inflammatory cells from circulation. As a result, acute inflammation serves as a protective mechanism, removing harmful stimuli and starting a repair process that returns the organism to its normal state of homeostasis. However, uncontrolled acute inflammation tends to progress into chronic disease. Chronic inflammation is the foundation for an array of diseases (tumours, various neurodegenerative conditions like Alzheimer's disease, Parkinson's disease, multiple sclerosis, lateral sclerosis, autoimmune diseases, diabetes, cardiovascular disorders, fibrosis, etc.). Although the pathophysiology of various diseases differs, the inflammatory mediators, regulatory, and signalling mechanisms are consistent in most cases (L. Kiss, 2022). Inflammation has recently been the subject of a plethora of studies, with RAW264.7 cells triggered by LPS being the most widely used in vitro model. The most popular in vitro study method for evaluating the anti-inflammatory efficacy of natural substances is RAW 264.7 cells. LPS is a common inducer from Escherichia coli O111:B4. During an

inflammatory response, LPS can upregulate a variety of inflammatory mediators in RAW264.7 cells, including nitric oxide (NO), cyclooxygenase-2 (COX-2), tumour necrosis factor (TNF- α), interleukin 6 (IL-6), and others (Han et al., 2019). In the present study, we used the LPS-induced RAW264.7 cell as an inflammatory model.

For the first time, we were utilising transcriptome analysis for investigating the anti-inflammatory properties of quinoa seed extract to pinpoint DEGs. The heat map and volcano plot indicate that Q-80M may significantly reduce the high amount of DEG resulting from inflammatory conditions. A total of 10 hub genes were found to be upregulated and downregulated on LPS-induced inflammation by bioinformatic analyses. In addition, we identified the top 10 hub genes that were upregulated and downregulated in response to Q-80M treatment. In control vs an inflammatory state, the top 10 hub genes demonstrated interferon activation and the development of inflammation.

Furthermore, the GO analysis discovered that responses to positive regulation of cytokine production, adaptive immune response, positive regulation of response to external stimulation, and positive regulation of immune response were present in inflammatory conditions. Likewise, in inflammation, the cellular components are primarily connected to the NLRP1 inflammasome complex and MHC protein complex. Molecular function in LPS stimulation primarily participates was chemokine activity and cytokine receptor binding. However, according to the GO analysis of Q-80M treatment effectively reduces the expression of inflammatory cytokines such as I-kappaB kinase/NF- κ B signalling, the cytokine-mediated signalling pathway, interferon-beta cellular reaction, interleukin-1 response, nitric oxide metabolism, response to reactive oxygen species, production of a molecular mediator implicated in the inflammatory response to oxidative stress, interferon-alpha response assembly of the inflammasome complex. These findings provide solid evidence that Q-80M has potent anti-inflammatory properties.

A key gene that was downregulated in this signalling pathway on Q-80M pretreatment was additionally identified by the aforementioned analysis. Those downregulated key genes are CCR5, CXCL1, CXCL2, CXCL3, CXCL10, CXCL12, CXCL16, IL-7R, IL-1, PKC, MMP-2, Ifi47, Edn1, NLRP3, OPB3, ASC, SRC, and STAT. These key genes are reported to induce inflammation through various mechanisms. Recent research has shown that inflammation greatly increased the levels of chemokines. Chemokines are released by a variety of injured tissues, including those affected by autoimmunity, allergies, Alzheimer's disease, chronic inflammatory illness, cardiovascular disease, and cancer (Hughes & Nibbs, 2018). During tissue inflammation, the production of the chemokines CXCL1 and CXCL2 can recruit neutrophils (De Filippo et al., 2013). According to studies, the inflammatory chemokine CXCL10 binds to CXCR3 and mediates immunological responses by activating and attracting leukocytes like T cells, eosinophils, monocytes, and NK cells (Ruffilli et al., 2014). As a member of the chemotactic cytokine superfamily and a chemokine produced by inflammatory cells, CXCL16 plays a significant role in the

development of rheumatoid arthritis, inflammatory bowel disease, SLE, gout disease, tissue damage, and fibrosis (Akyol et al., 2021). Recently, it has been proposed that CXCL12 plays a part in inflammation of the joints, lungs, brain, and intestines and is classified as a constitutive chemokine. Rheumatoid arthritis (RA) patients have higher levels of CXCR4 and CXCL12 expression (Dotan et al., 2010). According to studies, CCR5 is a potential therapeutic target for immunological disorders. Also crucial for the pathogenesis of the human immunodeficiency virus (HIV) by serving as the main coreceptor of the viruses (Zhang et al., 2021). We discovered that the molecular mechanism through which Q-80M affects inflammation may be connected to CXCL's regulation of inflammation. The most important conclusion of a study on the expression of IL-1 β -mediated disorders, which are sometimes referred to as "auto-inflammatory," is the release of the active form of IL-1 β , which is triggered by endogenous substances acting on monocytes and macrophages (Dinarello. 2011). The IL-7 receptor interacts with the IL-7 protein on the cell surface. IL-7 is a cytokine, a type of protein that controls the activity of immune system cells. A series of chemical signals are sent inside the cell, which initiate inflammatory responses (Bikker et al., 2012). Previous research centred on the phrase that in response to microbial infection and cellular injury, the NLRP3 inflammasome is a crucial part of the innate immune system that promotes caspase-1 activation and the release of proinflammatory cytokines IL-1 and IL-18 (Kelley et al., 2019). Large intracellular protein aggregates of the inflammasome adaptor ASC are a sign of autoinflammation and a hallmark of inflammasome activation. ASC specks and the strongly proinflammatory cytokine IL-1 are released into the extracellular environment by cells with activated inflammasomes (Wittmann et al., 2023). The B cell-produced GTP-binding protein IFI47 stimulates inflammatory responses (Cheluvappa et al., 2015). Signalling from EDN1 causes the stabilisation of hypoxia-inducible factor 1, allowing for prolonged proinflammatory expression (Solis et al., 2019). The studies have demonstrated that Src participates in a variety of processes that are involved in innate immunity that is mediated by macrophages, including phagocytosis, the production of inflammatory cytokines and mediators, and the induction of cellular migration. This strongly suggests that Src is essential for the functional activation of macrophages (Byeon et al., 2012). According to research, PKC regulates macrophage inflammatory responses in the process of developing diabetic atherosclerosis. The development of inflammatory diseases and immunity against infections depend heavily on STAT proteins. The significance of STATs in immunological responses, cellular development, and as targets for the treatment of immune-mediated disorders are discussed in six review articles by eminent researchers for this special focus on STAT Signalling in Inflammation(Kaplan, 2013). The current study's findings showed that Q-80M is capable of significantly regulating inflammatory pathways. Additionally, we made the first discovery that quinoa methanolic extract can considerably reduce an array of chemokines and cytokines in chronic inflammation.

5.5. Conclusion

In the preliminary screening for anti-inflammatory studies, we found that Q-80M (quinoa seed 80% methanol extract, direct extraction) showed significant effects in RAW 264.7 cells. Lipopolysaccharide (LPS) was used to stimulate inflammation in RAW cells. Before going for the cell-based assays and validation, we have done a whole transcriptome analysis to find out the genes and pathways responsible for the anti-inflammatory effects of Q-80M. We isolated the RNA samples from control, LPS stimulated, and Q-80M (250 µg/ml) pretreated LPS stimulated RAW cells. We did the next-generation sequence analysis using the Illumina platform. Using various bioinformatics tools, the differentially expressed genes were analysed and key pathways were identified as responsible for the anti-inflammatory effects of Q-80M. NGS analysis results showed that upon LPS stimulation, RAW cells upregulated 1990 genes and downregulated 817 genes which are responsible for inflammation regulation. The Q-80M pretreated RAW cells, upon stimulation with LPS, reduced these differentially expressed genes significantly. Here we have observed an upregulation of 134 genes and a downregulation of 481 genes. Protein-protein interaction (PPI) networks were built with upregulated and downregulated gene sets using STRING and visualized with Cytoscape. Gene clusters of upregulated and downregulated genes were identified using the MCODE plugin. The top 10 hub genes were identified for both upregulated gene sets and downregulated gene sets in inflammation, as well as Q-80M, pretreated LPS-stimulated RAW cells. Gene ontology analysis (top gene suite concerning cellular components, molecular function and biological processes) of the DEGs indicated that the downregulated genes performed functions like negative regulation to response to external stimuli, cytokine-mediated signalling, T cell and lymphocyte activation, response to TNF, IFN, IL-1 etc. which are responsible for the anti-inflammatory effects of Q-80M. Genes involved in the mitotic nuclear division, chromosomal segregation, and adverse immune system processes were increased after pretreatment with Q-80M in inflammation. KEGG pathway analysis revealed that Q-80M has the potential to regulate the key genes involved in inflammatory pathways (cytokine- cytokine receptor interaction, TNF, chemokine, NOD-like receptor and NFκB signalling pathway) and thereby reduce the inflammatory condition.

5.6. Reference

1. Akyol, T., Düzenli, T., & Tanoğlu, A. Evaluation of serum CXC chemokine ligand 16 (CXCL16) as a novel inflammatory biomarker or familial Mediterranean fever disease. *Turkish Journal of Medical Sciences*. 2021;51(2), 813–818. <https://doi.org/10.3906/sag-2010-64>
2. Bikker, A., Erik Hack, C., P.J.G. Lafèber, F., & A.G. van Roon, J. Interleukin-7: a key Mediator in T Cell-driven Autoimmunity, Inflammation, and Tissue Destruction. *Current Pharmaceutical Design*. 2012;18(16), 2347–2356. <https://doi.org/10.2174/138161212800165979>
3. Byeon, S. E., Yi, Y. S., Oh, J., Yoo, B. C., Hong, S., & Cho, J. Y. The role of

- Src kinase in macrophage-mediated inflammatory responses. *Mediators of Inflammation*. 2012. <https://doi.org/10.1155/2012/512926>
4. Charles A. Dinarello. A clinical perspective of IL-1b as the gatekeeper of inflammation. *European Journal of Immunology*. 2011. 41: 1203–1217 DOI 10.1002/eji.201141550
 5. Cheluvappa, R., Eri, R., Luo, A. S., & Grimm, M. C. Modulation of interferon activity-associated soluble molecules by appendicitis and appendectomy limits colitis-identification of novel anti-colitic targets. *Journal of Interferon and Cytokine Research*. 2015; 35(2), 108–115. <https://doi.org/10.1089/jir.2014.0091>
 6. Chen, R., Yin, C., Hu, Q., Liu, B., Tai, Y., Zheng, X., Li, Y., Fang, J., & Liu, B. Expression profiling of spinal cord dorsal horn in a rat model of complex regional pain syndrome type-I uncovers potential mechanisms mediating pain and neuroinflammation responses. *Journal of Neuroinflammation*. 2020; 17(1), 1–19.
 7. Daimiel, L., Vargas, T., & Ramírez de Molina, A. Nutritional genomics for the characterization of the effect of bioactive molecules in lipid metabolism and related pathways. *Electrophoresis*. 2012; 33(15), 2266–2289. <https://doi.org/10.1002/elps.201200084>
 8. De Filippo, K., Dudeck, A., Hasenberg, M., Nye, E., Van Rooijen, N., Hartmann, K., Gunzer, M., Roers, A., & Hogg, N. Mast cell and macrophage chemokines CXCL1/CXCL2 control the early stage of neutrophil recruitment during tissue inflammation. *Blood*. 2013; 121(24), 4930–4937. <https://doi.org/10.1182/blood-2013-02-486217>
 9. Dotan, I., Werner, L., Vigodman, S., Weiss, S., Brazowski, E., Maharshak, N., Chen, O., Tulchinsky, H., Halpern, Z., & Guzner-Gur, H. CXCL12 is a constitutive and inflammatory chemokine in the intestinal immune system. *Inflammatory Bowel Diseases*. 2010; 16(4), 583–592. <https://doi.org/10.1002/ibd.21106>
 10. Han, S., Gao, H., Chen, S., Wang, Q., Li, X., Du, L. J., Li, J., Luo, Y. Y., Li, J. X., Zhao, L. C., Feng, J., & Yang, S. Procyanidin A1 Alleviates Inflammatory Response induced by LPS through NF-κB, MAPK, and Nrf2/HO-1 Pathways in RAW264.7 cells. *Scientific Reports*. 2019; 9(1), 1–13. <https://doi.org/10.1038/s41598-019-51614-x>
 11. Hughes, C. E., & Nibbs, R. J. B. A guide to chemokines and their receptors. *FEBS Journal*. 2018; 285(16), 2944–2971. <https://doi.org/10.1111/febs.14466>
 12. Kaplan, M. H. STAT signaling in inflammation. *Jak-Stat*. 2013; 2(1), e24198. <https://doi.org/10.4161/jkst.24198>
 13. Kelley, N., Jeltema, D., Duan, Y., & He, Y. The NLRP3 Inflammasome: An Overview of Mechanisms of Activation and Regulation Nathan. *International Journal of Molecular Sciences*. 2019; 20(13), 1–24.
 14. L. Kiss, A. Inflammation in Focus: The Beginning and the End. *Pathology and Oncology Research*. 2022; 1–7. <https://doi.org/10.3389/pore.2021.1610136>
 15. Liu, B., & Qian, S. B. Translational Regulation in Nutrigenomics. *Advances*

- in Nutrition. 2011; 2(6), 511–519. <https://doi.org/10.3945/an.111.001057>
16. Liu, G., Zhang, S., Zhao, X., Li, C., & Gong, M. Advances and limitations of next-generation sequencing in animal diet analysis. *Genes*. 2021; 12(12). <https://doi.org/10.3390/genes12121854>
 17. Milner, J. Nutrigenomics and Nutrigenetics. *Nutritional Oncology*. 2006; 5, 15–24. <https://doi.org/10.1016/B978-012088393-6/50058-0>
 18. Minihane, A. M., Vinoy, S., Russell, W. R., Baka, A., Roche, H. M., Tuohy, K. M., Teeling, J. L., Blaak, E. E., Fenech, M., Vauzour, D., McArdle, H. J., Kremer, B. H. A., Sterkman, L., Vafeiadou, K., Benedetti, M. M., Williams, C. M., & Calder, P. C. Low-grade inflammation, diet composition and health: Current research evidence and its translation. *British Journal of Nutrition*. 2015; 114(7), 999–1012. <https://doi.org/10.1017/S0007114515002093>
 19. Román, G. C., Jackson, R. E., Gadhia, R., Román, A. N., & Reis, J. Mediterranean diet: The role of long-chain ω -3 fatty acids in fish; polyphenols in fruits, vegetables, cereals, coffee, tea, cacao and wine; probiotics and vitamins in prevention of stroke, age-related cognitive decline, and Alzheimer disease. *Revue Neurologique*. 2019; 175(10), 724–741. <https://doi.org/10.1016/j.neurol.2019.08.005>
 20. Ruffilli, I., Ferrari, S. M., Colaci, M., Ferri, C., Politti, U., Antonelli, A., & Fallahi, P. CXCR3 and CXCL10 in autoimmune thyroiditis. *Clinica Terapeutica*. 2014; 165(3). <https://doi.org/10.7417/CT.2014.1727>
 21. Sales, N. M. R., Pelegri, P. B., & Goersch, M. C. Nutrigenomics: Definitions and advances of this new science. *Journal of Nutrition and Metabolism*. 2014. <https://doi.org/10.1155/2014/202759>
 22. Solis, A. G., Bielecki, P., Steach, H. R., Sharma, L., Harman, C. C. D., Yun, S., de Zoete, M. R., Warnock, J. N., To, S. D. F., York, A. G., Mack, M., Schwartz, M. A., Dela Cruz, C. S., Palm, N. W., Jackson, R., & Flavell, R. A. Mechanosensation of cyclical force by PIEZO1 is essential for innate immunity. *Nature*. 2019; 573(7772), 69–74. <https://doi.org/10.1038/s41586-019-1485-8>
 23. Vauzour, D., Rodriguez-Mateos, A., Corona, G., Oruna-Concha, M. J., & Spencer, J. P. E. Polyphenols and human health: Prevention of disease and mechanisms of action. *Nutrients*. 2010; 2(11), 1106–1131. <https://doi.org/10.3390/nu2111106>
 24. Wittmann, N., Mishra, N., Gramenz, J., Kuthning, D., Behrendt, A.-K., Bossaller, L., & Meyer-Bahlburg, A. Inflammasome activation and formation of ASC specks in patients with juvenile idiopathic arthritis. *Frontiers in Medicine*. 2023; 10, 1–11. <https://doi.org/10.3389/fmed.2023.1063772>
 25. Xu, B., Dai, J., Bi, J., & Fu, Y. Application of next generation sequencing in 3 Waardenburg syndrome. *Lin Chuang Er Bi Yan Hou Tou Jing Wai Ke Za Zhi = Journal of Clinical Otorhinolaryngology, Head, and Neck Surgery*. 2021; 35(10), 25–43. <https://doi.org/10.13201/j.issn.2096-7993.2021.10.010>
 26. Zhang, H., Chen, K., Tan, Q., Shao, Q., Han, S., Zhang, C., Yi, C., Chu, X., Zhu, Y., Xu, Y., Zhao, Q., & Wu, B. Structural basis for chemokine

recognition and receptor activation of chemokine receptor CCR5. *Nature Communications*, 2021; 12(1), 1–12. <https://doi.org/10.1038/s41467-021-24438-5>

CHAPTER 6

***In vitro* validation studies of specific cytokines and regulatory molecules responsible for the anti-inflammatory activity of Q-80M extract**

6.1. Introduction

One of the most significant medical findings in the last two decades is the immune system and inflammatory processes that are implicated in a wide range of health problems. Indeed, it has been determined that chronic inflammatory diseases are the leading cause of death in the world today, with more than 50% of all fatalities. Examples of chronic inflammatory diseases include ischemic heart disease, stroke, cancer, diabetes mellitus, chronic kidney disease, non-alcoholic fatty liver disease (NAFLD), auto-immune, and neurodegenerative conditions (Furman et al., 2019).

Macrophages are significant inflammatory cells involved in the initiation of inflammatory reactions. They play crucial roles in the pathogenesis of many inflammatory diseases by secreting proinflammatory mediators and cytokines. Gram-negative bacteria's lipopolysaccharide (LPS) is a pathogen-associated molecular pattern (PAMP) that can result in severe inflammatory damage and even death. Anti-inflammatory mechanisms function through many pathways. LPS causes inflammatory damage by activating the TLR4/NF- κ B p65 inflammatory signalling pathway. TLR4 act as the LPS receptor. In response to LPS, TLR4 activates the MyD88-dependent signalling pathway, the NF- κ B p65 transcription response, and secretes proinflammatory cytokines. IL-10 and transforming growth factor (TGF)-1 are anti-inflammatory cytokines that reduce the synthesis and activity of proinflammatory cytokines (Cao et al., 2019). A crucial component in the initiation and maintenance of the inflammatory response is the nuclear factor B (NF- κ B). NF- κ B may target inflammation by increasing the expression of inflammatory cytokines, chemokines, and adhesion molecules. They also regulate cell proliferation and differentiation. An important process for preserving good health includes the complete resolution of an acute inflammatory response and restoration into homeostasis. Chronic inflammation is frequently characterised by increased NF- κ B activation. In light of this, NF- κ B activation downregulation may be a desirable strategy for anti-inflammatory treatments. Growing evidence points to nuclear factor-kappa B (NF- κ B) as a prime transcriptional regulator of inflammatory cytokines, such as tumour necrosis factor (TNF), interleukin (IL)-1, IL-6, nitric oxide (NO), and others (Fu et al., 2021). One of the most concerning inflammation mediators is NO synthesised by induced NO synthase (iNOS). As a result, TLR 4/NF-B may play critical roles in anti-inflammatory pathways (Li et al., 2018).

According to epidemiological and scientific research, consuming plenty of fruits and vegetables that are high in polyphenolic phytochemicals can help protect against diseases including diabetes, arthritis, and disorders of the cerebrovascular system and

the nervous system (Serino & Salazar, 2019). An alternative food source, quinoa seeds are rich in phytochemicals. The native Andean people of South America referred to quinoa (*Chenopodium quinoa Willd.*) as the "golden grain" and have used it as a vital food source for thousands of years. Quinoa seed has a wide range of secondary metabolites with diverse bioactivities. In the last 40 years, at least 193 secondary quinoa metabolites have been discovered. They primarily consist of steroids, phenolic acids, flavonoids, terpenoids, and nitrogen-containing substances. These metabolites have an ample range of biological activities, including antioxidant, cytotoxic, anti-diabetic, and anti-inflammatory capabilities. Moreover, too many physiological roles like insecticidal, molluscicidal, and antibacterial activity (Lin et al., 2019). The most encouraging results were seen when total saponins extracted from quinoa were used to reduce metabolic endotoxemia, systemic inflammation, visceral white adipose accumulation, body weight increase, and insulin resistance (W. Li et al., 2022). However, less idea about how quinoa seeds may affect immunological and inflammatory responses. In Chapter 1, it was demonstrated that Q80-M (80% methanolic extract of quinoa seeds) had anti-inflammatory effects. However, it is not quite clear how quinoa seed prevents inflammation. The current study advances our line of inquiry into the precise mechanism through which Q-80M might exert its anti-inflammatory effects. This study was specifically designed to look at the possible ability of Q-80M to impact the TLR4/NF- κ B pathway in a murine macrophage cell model after the inflammatory trigger.

6.2. Methodology

The preliminary screening experiments revealed that Q-80M extract has anti-inflammatory properties. A whole genome transcriptome investigation in the preceding chapter showed that Q-80M significantly reduced the genes and pathways related to inflammation. In this chapter, we employed two concentrations of Q-80M (Q-80M1 and Q-80M2) for the evaluation of inflammatory parameters to validate the anti-inflammatory action of Q-80M. The experimental groups of RAW264.7 cells were divided into the following five groups

- Control group
- LPS treated group- (treated with 1 μ g/mL LPS for 24 h),
- Q-80M1+LPS- (Q-80M (125 μ g/mL) for 4h pretreatment + LPS for 24 h),
- Q-80M2 +LPS- (Q-80M (250 μ g/mL) for 4h pretreatment + LPS (1 μ g/mL) for 24 h)
- D+LPS- (Dexamethasone (8 μ g/mL) for 4h pretreatment + LPS (1 μ g/mL) for 24 h).

The assay methods followed include,

1. The activity of pro/anti-inflammatory cytokines and enzymes (IL-1 β , IL-6, IL-10, TNF- α , COX2 and iNOS) in the cell-free culture supernatants were detected using the ELISA method.
2. The intracellular ROS formation was analyzed using DCFDA dye and visualized using a fluorescent microscope.
3. The protein expressions of COX2, iNOS, TLR4, TLR1, MyD88, JNK, pJNK, NF- κ B P65, and I κ B α were detected by western blotting.
4. The expression of I κ B α and NF- κ B P65 in the nucleus and cytosol was analyzed by immunofluorescence staining and visualized using a fluorescence microscope.
5. Analysis of 96 target-cytokines expressions was conducted using a membrane antibody array kit.
6. LCMS analysis of Q-80M (for identifying the major compounds) was done using LC/ESI-MS-thermo-ultimate™ 3000 standard dual system.

All the assays were performed in triplicate, and the detailed procedures are described in Chapter 2. Dexamethasone (8 μ g/mL) was used as the positive control for the antiinflammation study.

6.3. Results

6.3.1. Effects of Q-80M on the release of pro and anti-inflammatory cytokines in LPS stimulated RAW264.7 cells

The concentration of cytokines in cell culture supernatants was quantified using ELISA. According to the data, LPS-stimulated RAW264.7 cells had higher amounts of IL-1 α , IL-6 and TNF- α in their supernatants than the control group. However, treatment with two concentrations of Q-80M such as Q-80M1 (125 μ g/mL), Q-80M2 (250 μ g/mL), and positive control dexamethasone (8 μ g/mL) reduced the release of IL-1, IL-6, and TNF- α to lesser than that in the LPS group (Figure 6.1). IL-10 are an important anti-inflammatory cytokine that plays a key role in preventing the pathological process of inflammation. In comparison to the other three groups (Q-80M1, Q-80M2, and DM), the LPS group had a lower average level of IL-10. Pretreatment with Q-80M1 and Q-80M2 under an inflammatory condition significantly raised the concentration of IL-10. The results indicate that Q-80M inhibits the release of proinflammatory cytokines simultaneously activating anti-inflammatory cytokines in RAW264.7 cells.

6.3.2. Effects of Q-80M on LPS-induced iNOS and COX-2 overexpression in RAW 264.7 cells

iNOS and COX-2 are the primary inflammatory mediators. They have a crucial role in the assessment of inflammation intensity. The impact of Q-80M on both iNOS and

COX-2 was investigated using ELISA and western blotting. COX-2 as well as iNOS expression in RAW cells after a 24-hour LPS treatment were considerably increased. As shown in Figures 4a and b, pretreatment with Q-80M1 and Q-80M2 significantly reduced the overexpression of iNOS and COX-2. The LPS-induced overexpression of iNOS and COX-2 was also suppressed by dexamethasone (8 μ g/mL). The impact of two concentrations of Q-80M (Q-80M1 and Q-80M2) on Western blot analysis showed that LPS stimulated group significantly increased the expression of COX-2 and iNOS, but Q-80M1, Q-80M2 and dexamethasone pretreatment reduced the overexpression of these proteins. The LPS-induced phenomena were reversed by Q-80M treatment (Figure 6.2).

6.3.3. Effects of Q-80M on LPS-induced ROS generation in RAW cells

ROS is critical in the modulation of many inflammatory mediators and disorders associated with metabolic imbalance and inflammation (Yang et al., 2020). Cells treated with LPS (1 μ g/ml) showed a significant increase in intracellular ROS levels (Fig. 3a and b). As shown in Figure 6.3a and b, pretreatment with Q-80M1(125 μ g/mL), Q-80M2 (250 μ g/mL), and dexamethasone (8 μ g/mL) almost fully reversed the LPS-induced ROS generation (51.09% by Q-80M1, 61.8% by Q-80M2, and 64.4% by dexamethasone).

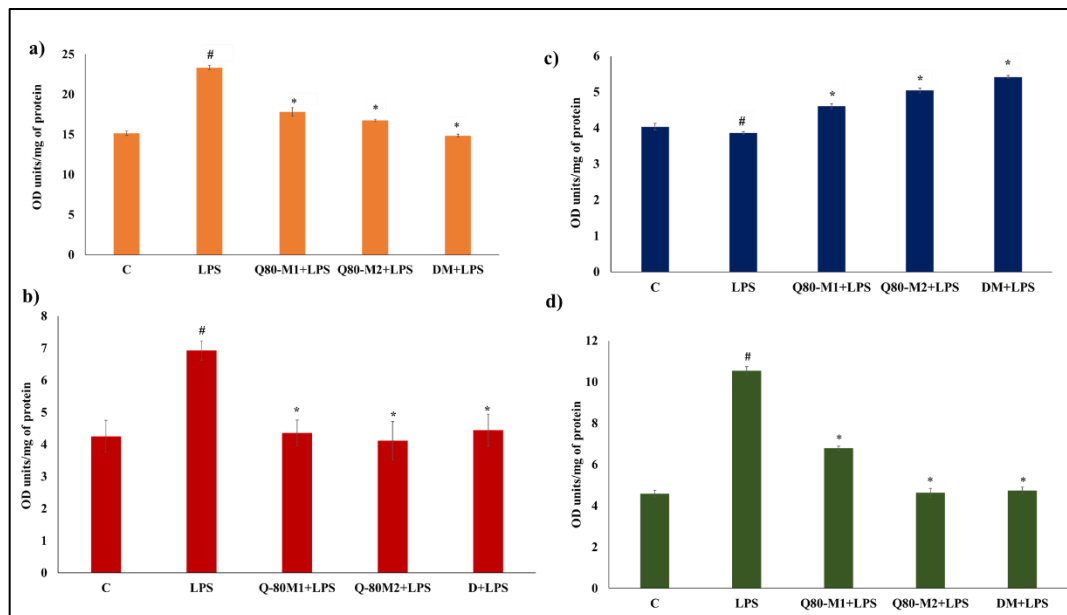


Figure 6.1: The effect of Q-80M on cytokines. RAW 264.7 cells were pretreated with two concentrations of Q-80M, such as Q80-M1 (125 μ g/mL), Q80-M2 (250 μ g/mL), and dexamethasone (8 μ g/mL) for 4 hrs followed by LPS (1 μ g/ml) for 24 hrs. Cytokines in the supernatant medium were analyzed by ELISA, a) IL1 α , b) IL-6, c) IL-10, (d) TNF- α . Values represent the mean \pm SD of three separate trials; # and * indicate significant differences between the control and LPS-treated groups, respectively ($p \leq 0.05$).

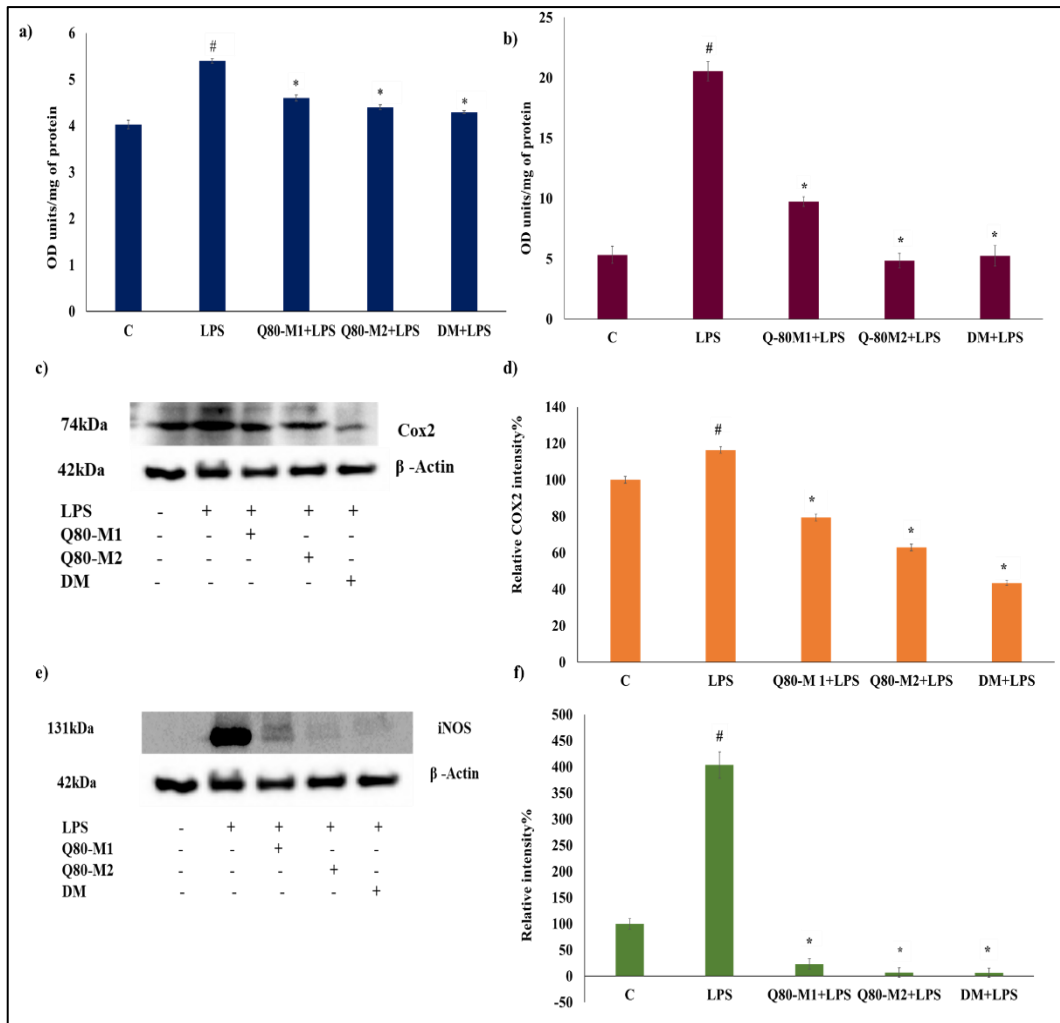


Figure 6.2: Effects of Q80-M on the overexpression of COX-2 and iNOS in LPS-simulated RAW cells. The cells were pretreated by two concentrations of Q-80M, such as Q80-M1 (125 µg/mL), Q80-M2 (250 µg/mL), and dexamethasone (8 µg/mL) for 4 hrs before being incubated with LPS (1 µg/mL) for 24 hrs. ELISA was used to detect COX-2 and iNOS in the culture supernatant. Western blotting analysis was used to examine the proteins expression, with β-actin serving as an internal reference. The relative band intensity was evaluated with densitometry. Values represent the mean ±SD of three separate trials; # and * indicate significant differences between the control and LPS-treated groups, respectively ($p \leq 0.05$). (a). ELISA results of COX-2, (b). ELISA results of iNOS, (c). Western blotting results of COX-2, (d). The effects of Q-80M pretreatment on the protein expression of COX-2, (e). Western blotting results of iNOS, (f). The effects of Q-80M pretreatment on the protein expression of iNOS.

6.3.4. Effects of Q-80M on the expression of Toll-like receptors

TLR4 is specifically present in numerous cells and has a significant impact on the inflammatory process. During an infection, TLR4 reacts to the LPS found in tissues and circulation. TLR4 dimerizes in the presence of LPS and activates the NF-κB, MAPK, and other signalling cascades. TLR4 induces pathogen-specific innate immune responses by producing pro-inflammatory cytokines (S. Han et al., 2019). To

investigate the effect of Q-80M on the TLR4/MyD88 pathway, the expression of TLR4 in LPS-stimulated RAW cells was identified by Western blot. The expression of MyD88 was detected by immunoprecipitation followed by western blotting analysis. LPS enhanced the expression of TLR4 and MyD88, as seen in Figure 6.4 a, b and c. On the other hand, Q-80M and dexamethasone pretreatment significantly reduced TLR4 and MyD88 expression. As shown in the results (Figure 6.4. a and d), pretreatment with Q-80M and dexamethasone significantly decreased the increase of JNK phosphorylation by LPS treatment.

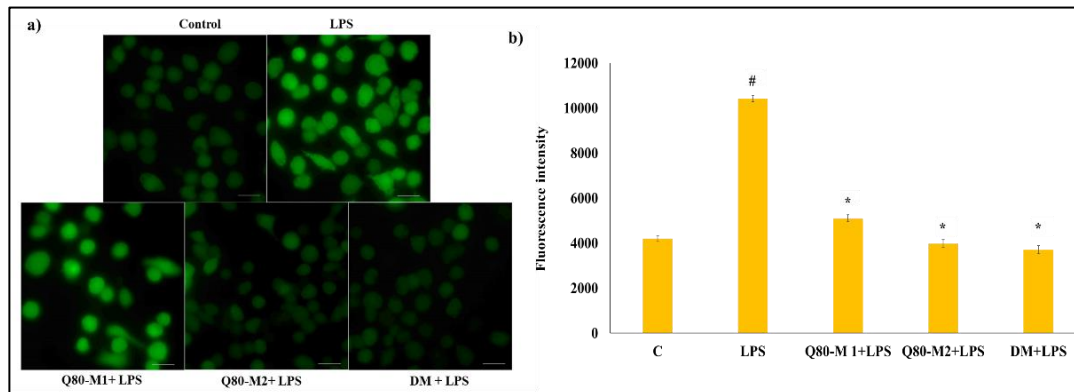


Figure 6.3: Effects of Q80-M on LPS-stimulated ROS production in RAW 264.7 cells. (a) ROS production in each experimental groups including Control, LPS (1 $\mu\text{g}/\text{mL}$), Q80-M1(125 $\mu\text{g}/\text{mL}$) + LPS (1 $\mu\text{g}/\text{mL}$), Q80-M2(250 $\mu\text{g}/\text{mL}$) + LPS (1 $\mu\text{g}/\text{mL}$), Dexamethasone (8 $\mu\text{g}/\text{mL}$) + LPS (1 $\mu\text{g}/\text{mL}$). (b) The graph depicts the relative fluorescence intensity of respective experimental group. Values represent the mean \pm SD of three independent experiments; # and * indicate significant differences between the control and LPS-treated groups, respectively ($p \leq 0.05$). Magnification-20x, Scale bar-10 μm

6.3.5. Effects of Q-80M on LPS-induced NF- κ B nuclear translocation

According to reports, LPS cause NF- κ B/p65 to move from the cytoplasm to the nucleus. The nucleus translocation of NF- κ B can govern the release of an enormous variety of inflammatory mediators such as TNF- α , IL-6, IL-1, NO, and iNOS (Wu et al., 2022). As demonstrated in Figure 6.5, LPS-induced RAW264.7 cells enhanced NF- κ B/p65 protein expression, whereas pre-treatment with the two concentrations of Q-80M (Q-80M1 and Q-80M2), and positive control dexamethasone (8 $\mu\text{g}/\text{mL}$) significantly reduced NF- κ B/p65 protein expression. Additionally, LPS facilitated NF- κ B nuclear translocation. However, Q-80M1 (125 $\mu\text{g}/\text{mL}$), Q-80M2 (250 $\mu\text{g}/\text{mL}$) and positive control dexamethasone (8 $\mu\text{g}/\text{mL}$) prevented the nuclear translocation of NF- κ B (Fig. 6.5c and d). Moreover, our immunofluorescence results demonstrated that LPS promoted NF- κ B nuclear translocation, this was inhibited by Q-80M (Figure 6.5a and b). In light of the findings, we can conclude that Q-80M suppressed NF- κ B nuclear translocation, thereby inhibiting the activation of proinflammatory cytokines.

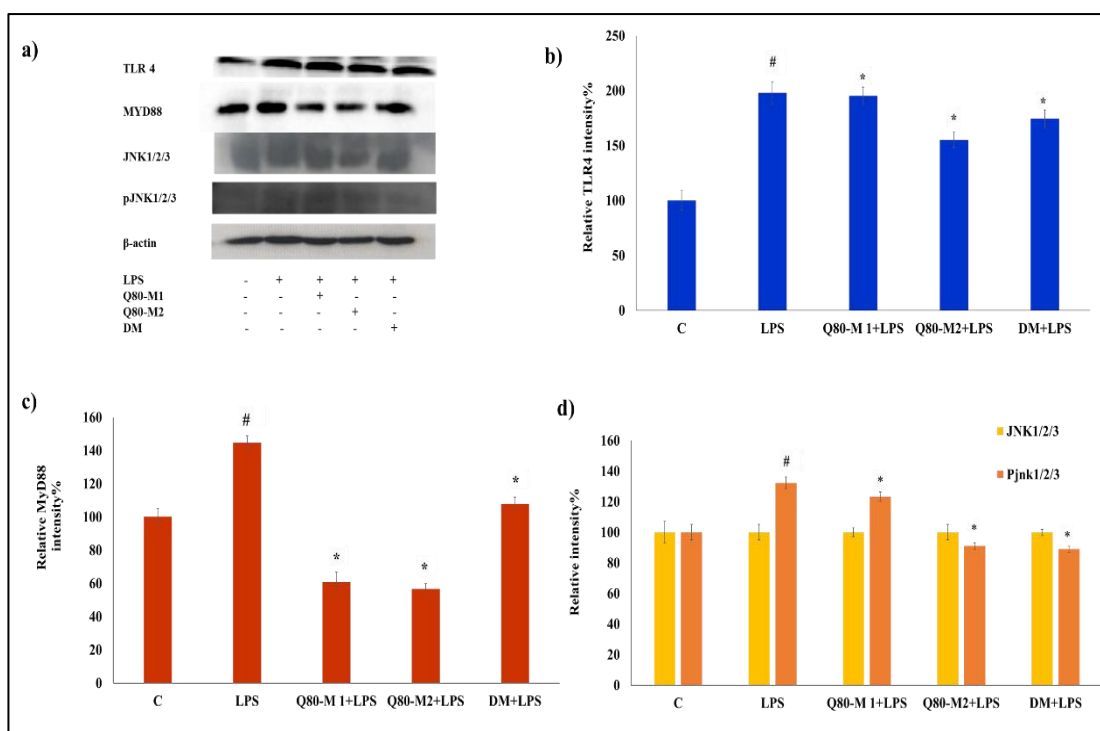


Figure 6.4: The effect of Q80-M on TLR4 activation in LPS-induced RAW 264.7 cells. The cells were pretreated with Q80-M1, Q80-M2 and dexamethasone (8 $\mu\text{g}/\text{mL}$) for 4 hrs before being cultured with LPS (1 $\mu\text{g}/\text{mL}$) for 24 hrs. (a) Western blotting (WB) was performed using the cell lysate, and TLR4, MyD88, JNK, and pJNK-specific antibodies were employed to express proteins. Total JNK acted as an internal control for their phosphorylated JNK. β -actin employed as an internal control for the TLR4 and MyD88. Densitometry was used to measure the relative band intensities of each band in comparison to the corresponding internal controls. The graph of relative intensity of band (b) TLR4, (c) MyD88, (d) pJNK & JNK. Values represent the mean \pm SD of three separate trials; # and * indicate significant differences between the control and LPS-treated groups, respectively ($p \leq 0.05$).

6.3.6. Effects of Q-80M on the degradation of I κ B- α

I κ B- α is a prototypical member of the seven-member IB family. I κ B- α , an inhibitory protein, forms an inactive complex in the cytoplasm with the transcription factor NF- κ B. I κ B- α , p50 and p65 are the three subunits that make up inactive NF- κ B. Following an inflammatory stimulation, the initial step in the activation of NF- κ B by the degradation of I κ B- α . (Jacobs & Harrison, 1998). Considering its role in inducing inflammation, we used immunofluorescence and Western blotting to monitor the degradation of I κ B- α after pretreatment with Q-80M and dexamethasone in LPS-stimulated RAW 264.7 cells (Figure 6.6). The LPS-induced degradation of I κ B- α was significantly decreased by Q-80M1(125 $\mu\text{g}/\text{mL}$), Q-80M2 (250 $\mu\text{g}/\text{mL}$), and dexamethasone (8 $\mu\text{g}/\text{mL}$).

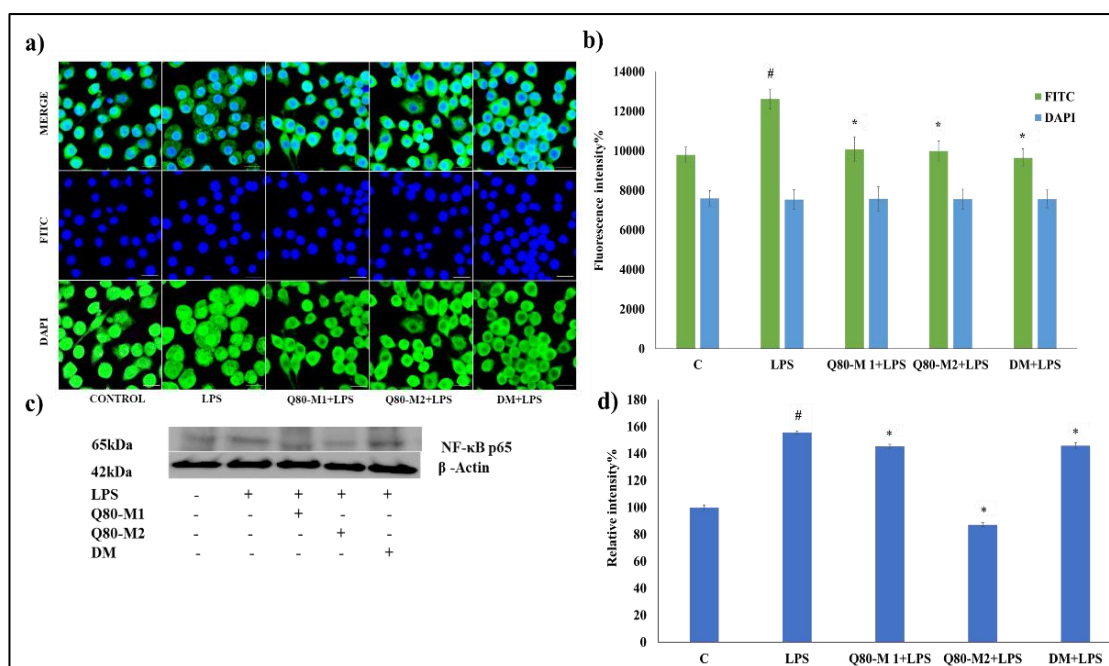


Figure 6.5: The effect of Q-80M on nuclear translocation of NF- κ B. (a) The nuclear translocation of NF κ B-p65 was determined using immunofluorescence staining with fluorescently labelled NF κ B-p65 (green colour) and the cell nucleus were stained by DAPI (blue colour). (b), The graph shows the relative fluorescent intensity of NF κ B-p65. (c), The NF κ B-p65 protein expression was detected using Western blotting. β -actin as internal controls. (d), The graph shows the relative band intensity of NF κ B-p65. Values represent the mean \pm SD of three separate trials; # and * indicate significant differences between the control and LPS-treated groups, respectively ($p \leq 0.05$). Magnification-20x, Scale bar-10 μ m.

6.3.7. Effects of Q-80M on anti-inflammatory and proinflammatory cytokines

Cytokine array analysis was performed to comprehensively profile the effect of cytokines on pretreatment with Q-80M on RAW cells. We used cell-free supernatant media for cytokine array analysis. The cytokine profiles of LPS and Q-80M were remarkably different (Figure 6.7). The production of pro-inflammatory cytokines was significantly enhanced by LPS LPS enhanced the release of pro-inflammatory cytokines. However, Q-80M successfully reduced the expression of many pro-inflammatory cytokines significantly GM-CSF, IL3Rb, GCSF, IL6, MMP-2, TRANCE, TROY, and TSLP. Anti-inflammatory cytokines such as Fit-3 Ligand, were found to be activated by Q-80M. These findings led us to hypothesise that Q-80M can regulate inflammatory cytokines and have antiinflammation activity.

6.3.8. Identification of bioactive compounds from Q-80M extract by LC-MS analysis

Quinoa seeds are rich source of secondary metabolites, such as phenolic acids, flavonoids, terpenoids, steroids, and nitrogen-containing compounds (Melini & Melini, 2021). Quinoa 80% methanol extract (Q-80M) was subjected to LC-MS analysis. The molecular mass and fragments of the identified compounds in the methanol extracts of Q-80M are presented in Figure 6.8c. Q-80M contains phenolics,

cinnamic and flavonoids derivatives given in Figure 6.8b. These extracts also contain partially identified chemicals, the results of which are shown in Table 6.8c. In addition, the LC-MS results revealed the presence of numerous unidentified peaks that need to be examined by further purification investigations.

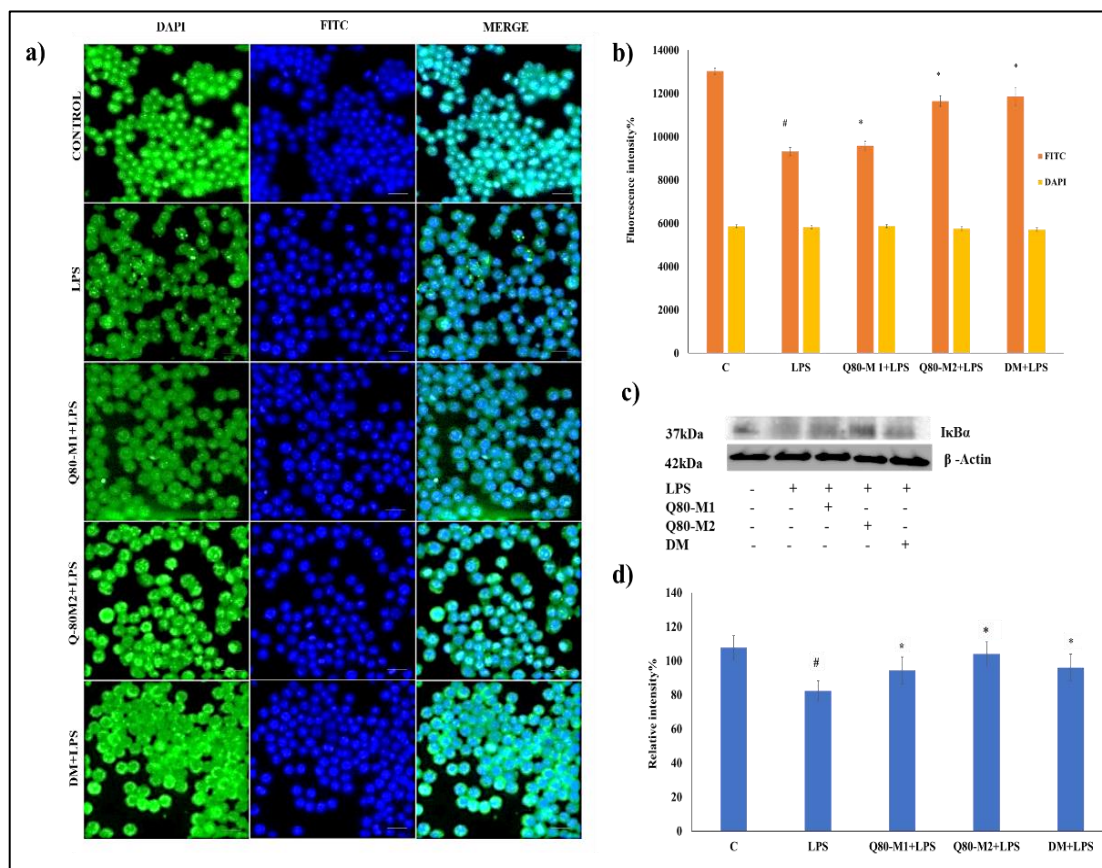


Figure 6.6: Effect of Q-80M on IkBa degradation. (a) The expression of IkBa was detected by immunofluorescence imaging using fluorescently labelled antibody IkBa (green colour) and the nucleus were stained by DAPI (blue colour). (b) The graph depicts the relative fluorescence intensity- IkBa, (c) Western blotting was performed to identify IkBa protein expression. β -actin as internal controls, (d) The graph shows the relative band intensity of IkBa. Values represent the mean \pm SD of three separate trials; # and * indicate significant differences between the control and LPS-treated groups, respectively ($p \leq 0.05$). Magnification-20x, Scale bar-10 μ m.

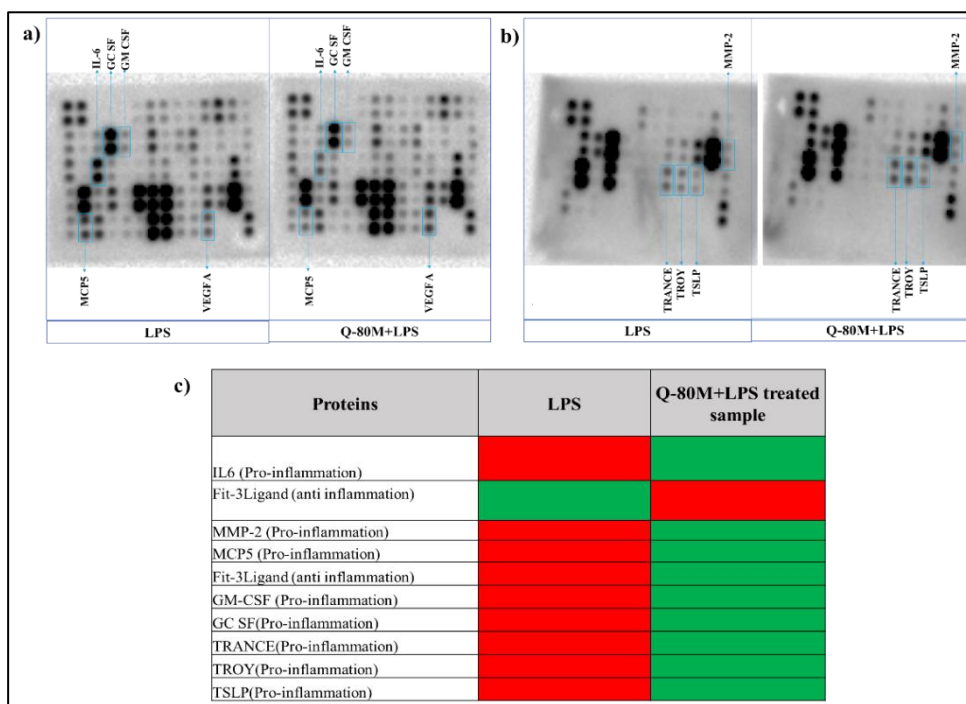


Figure 6.7: Effect of Q-80M on LPS-induced cytokine in RAW264.7 cell line by cytokine array experiment. The impact of Q-80M on LPS- stimulated cells was evaluated by comparing the spot intensity of cytokines. (a) Cytokine Antibody Membrane Array 1- LPS treatment versus and Q-80M, (b) Cytokine Antibody Membrane Array 2- LPS and Q-80M, LPS treatment versus and Q-80M (c) Excel Heat map of array proteins. Red colour-upregulation, green colour-

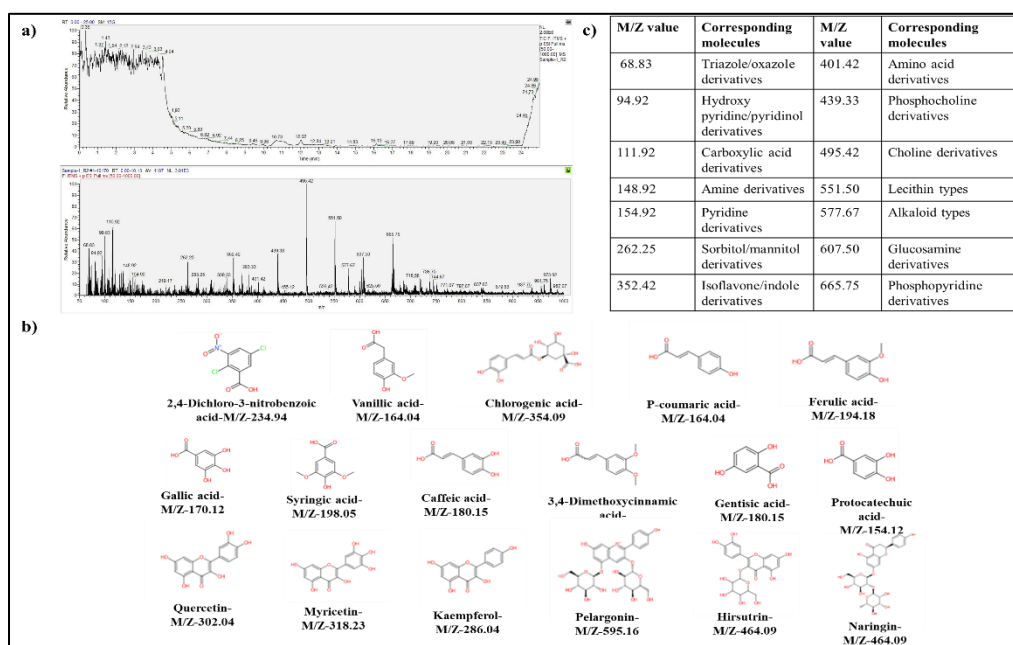


Figure 6.8: Bioactive compounds identified in Q-80M extract by LC/ESI-MS analysis. (a) Experimental LCMS spectrum of Q-80M. (b) Structures of major compounds identified from the Q-80M. (c) List of partially identified compounds from Q-80M.

6.4 Discussion

Chronic inflammatory disorders are the leading cause of death around the world. According to the World Health Organisation (WHO) reports, chronic diseases is the biggest threat to human health. Chronic inflammatory diseases, such as stroke, chronic respiratory conditions, heart problems, cancer, obesity and diabetes, claim the lives of 3 out of 5 individuals worldwide (Tsai et al., 2019). As a result, suppression of inflammation is crucial for treating these diseases. Enormous evidence support that natural products are unrivalled sources of active compounds for treating inflammatory diseases. The phytochemicals-rich food has powerful medicinal potential in reducing inflammation and associated diseases (Aswad et al., 2018). Quinoa seeds are a rich source of phytochemicals with anti-inflammatory potential like protocatechuic acid, syringic acid, vanillin, ferulic acid and others (Lin et al., 2019). It indicates that quinoa seed might be effective in reducing inflammatory diseases. Our previous research discovered that the 80% methanolic extract of quinoa seed has the effective potential to reduce LPS-induced NO production in RAW267.4 cells. The whole genome transcriptome analyses revealed that Q-80M extract effectively reduced inflammation. In this chapter, we validated the molecular mechanism-specific cytokines and regulatory molecules responsible for the anti-inflammatory activity of Q-80M extract.

In the current investigation, LPS-stimulated RAW 264.7 cells were employed as an inflammatory model. LPS as an inflammatory agent is an endotoxin isolated from gram-negative bacteria. The immune system lyses the bacteria and releases the lipid part of LPS into the body, which initiates the inflammatory process. LPS used to simulate inflammation similar to the real-life situation of bacterial infection. The pretreatment approach is advocated because the LPS tends to adhere to surfaces and preserve its structure, which could affect the test sample. LPS promotes the signalling pathway such as NF- κ B via activation of Toll-like receptor 4 (TLR4), which then releases pro-inflammatory cytokines and mediators such as IL-1, TNF, IL-6, and NO (Blunck et al., 2001). Cytokines and mediators have an essential role in inflammation because of their chemotactic and vasoactivator characteristics. Cytokines and mediators increase blood vessel permeability and recruit more inflammatory cells to the affected locations. Its main objective is to offer localization to the affected area, eliminate the harmful substance in the damaged tissue and speed up the healing process. They should be brought back to their original level otherwise; it leads to detrimental chronic inflammation. Cytokines and mediators also act as a stimulus to activate the inflammatory pathway (Lucas et al., 2006). Anti-inflammatory cytokines inhibit inflammation by regulating the response of pro-inflammatory cytokines. In the present study, Q-80M downregulate pro-inflammatory cytokines and upregulated anti-inflammatory cytokines.

The effects of LPS on the secretion of pro-inflammatory mediators (IL-1, IL-6, and TNF-) were successfully diminished by pretreatment with Q-80M1 (125 g/mL) and Q-80M2 (250 μ g/mL), while the release of an anti-inflammatory mediator, IL-10, was increased. The LPS-stimulated macrophage produces an enormous amount of nitric

oxide, which is synthesized from L-arginine by the enzymatic action of iNOS (inducible NOS). iNOS is overexpressed during inflammation (Prado et al., 2005). Another essential enzyme is COX-2, stimulated by LPS. COX-2 enhances prostaglandin E2 formation and accelerates LPS-induced IL-1 β secretion via increasing NF- κ B activation (Echizen et al., 2016). Therefore, a successful therapeutic approach to combat inflammation can involve lowering the production of both iNOS and COX-2. In the present study, Q-80M exerted inhibitory activity on the expression of both COX-2 and iNOS, which causes a decrease in the production of iNOS and COX-2, respectively.

ROS can operate as a secondary messenger in LPS-induced signal transduction pathways such as NF- κ B and MAPK that ultimately promote the synthesis of pro-inflammatory genes. Inhibiting ROS formation is also an important therapeutic target in inflammatory disorders (Yang et al., 2020). In this investigation, Q-80M considerably decreased the generation of ROS induced by LPS.

LPS is one of the TLR4 ligands and is a component of the cell membrane of Gram-negative bacteria. When LPS binds to TLR4, it activates MyD88, which causes the subsequent production of kinases. The MyD88-dependent TLR4 pathway activates JNK and NF- κ B. LPS induces the phosphorylation of JNK. These phosphorylated kinases are essential for regulating the expression of pro-inflammatory cytokines like iNOS, IL-1, IL-6, TNF- α , and COX-2. In this study, LPS was employed as a TLR4 activator. Therefore, inflammation can decrease by downregulating the TLR4/NF- κ B Signalling Pathway (Fu et al., 2021). The present study discovered that Q-80M treatment reduced the expression of primary inflammatory molecules TLR4, MyD88, and pJNK on LPS stimulation. These results suggest that Q-80M can downregulate chronic inflammation.

The NF- κ B complex initiates the transcription of genes implicated in immune-inflammatory responses and a cascade of pro-inflammatory cytokines, especially TNF-, IL-1, and IL-6. NF- κ B activation causes phosphorylation, ubiquitination, and eventual destruction of I κ B- α by specific I κ B- α kinases. The activated NF- κ B p65-p50 heterodimer translocates into the nucleus and initiates the production of inflammatory-promoting genes (Jacobs & Harrison, 1998; Han et al., 2019). Q-80M lowered the expression of NF- κ B downstream pro-inflammatory genes, which was reasonable to speculate that Q-80M may interfere with NF- κ B signalling activation. Therefore, we examined Q-80M's ability to prevent LPS-induced degradation of I κ B- α protein and nuclear translocation of NF- κ B. Our findings demonstrated that LPS treatment led to a significant decrease in I κ B- α . Also, NF- κ B concentration was high in the nucleus than in the cytoplasm on LPS stimulation. But that result could be fully reversed by pre-treating with Q-80M extract in a concentration-dependent manner. The current investigation demonstrates that Q-80M suppresses LPS-induced NF- κ B activation, in part by suppressing I κ B- α protein degradation, which results in NF- κ B retention in the cytoplasm of RAW264.7 macrophages.

We found that Q-80M shielded RAW264.7 from LPS-induced cell damage through *in vitro* tests, and we employed an inflammatory cytokine array to assess 96 cytokines. Q-80M has a major impact on nine cytokines (MCP5, IL-6, Fit-3Ligand, GM CSF, GC SF, TRANCE, TROY, TSLP and MMP-2). Q-80M downregulates major pro-inflammatory cytokines such as MCP-5, IL-6, GM CSF, GC SF, TRANCE, TROY, TSLP and MMP-2. These cytokines have a critical role in inflammation and are used as targets for treating chronic inflammatory diseases. MCP-5 are chemokines that can enhance macrophage recruitment to inflammation sites, and IL-6 is activated downstream of inflammatory cell infiltration (Chen et al., 2008). Previous research has shown that MMP-2 is directly engaged in the pathophysiological processes in inflammatory bowel disorders (Jakubowska et al., 2016). The present study discovered the importance of Q-80M anti-inflammatory activity by reducing MCP-5, IL-6 and MMP-2.

G-CSF and GM CSF are therapeutic targets in inflammatory joint diseases like rheumatoid arthritis (Lawlor et al., 2004; Bhattacharya et al., 2015). A study confirmed that TRANCE has an inflammatory effect and may contribute to the pathophysiology of inflammatory disease. TRANCE acts as an inflammatory mediator and its underlying signalling mechanism in the vascular wall. They caused NF- κ B activation, I κ B phosphorylation and generation of reactive oxygen in endothelial cells (Min et al., 2005). In the present study, Q-80M also inhibits the expression of TROY and TSLP, two pro-inflammatory cytokines. TROY, also known as TNFRSF19, is a member of the tumour necrosis factor receptor (TNFR) superfamily. TROY could promote inflammation by activating pathways involving NF- κ B or JNK. TROY may induce several diseases, including chronic inflammatory bowel disease and cancer (Schön et al., 2014)(Dien et al. & Pratik K. Mutha, Robert L. Sainburg, 2008). The epithelial cytokine thymic stromal lymphopoietin (TSLP) is a primary modulator in the immune response (Gauvreau et al., 2020). Q-80M enhances the activity of the anti-inflammatory cytokine Fit-3 Ligand. Animal studies reveal that Flt 3 Ligand lessens the severity of experimentally produced allergy inflammation (Edwan et al., 2004).

The LC-MS results supported Lin et al.'s findings that quinoa seed extracts contain a significant amount of secondary metabolites, including phenolic acids, flavonoids, alkaloids, and nitrogen-containing chemicals (Lin et al., 2019). The majority of these were derivatives of benzoic acid. Benzoic acid derivatives include benzoic acid, gallic acid, protocatechuic acid, syringic acid, vanillic acid, and their analogues. Earlier investigations reported that quinoa seeds were a rich source of benzoic acid derivatives. It was discovered that 2,4-Dichloro-3-nitrobenzoic acid, protocatechuic acid, gallic acid, syringic acid, and vanillic acid all had anti-inflammatory properties (Choi et al., 2016; Jung et al., 2008; Dłudla et al., 2019; Kakkar & Bais, 2014). The cinnamic acid derivatives in quinoa seeds include caffeic acid, P-coumaric acid, chlorogenic acid, and ferulic acid. The anti-inflammatory properties of these cinnamic acid derivatives have been described in many scientific reports (Antonio, 2021; Ji et al., 2022; Pragasam et al., 2013; Sakai et al., 1999). Earlier investigations on inflammation have claimed that flavonoids reduce inflammation. According to recent

findings, the flavonoids gentisic acid, quercetin, myricetin, and kaempferol in Q-80M extract have anti-inflammatory activities (Sun et al., 2021; Li et al., 2016; Rho et al., 2011). Related studies support the current investigation of the anti-inflammatory properties of quinoa seeds. In cultured colonic epithelial Caco-2 cells, quinoa polyphenols have been shown to downregulate the cytokines IL-1, IL-8, and TNF. They have also been shown to defend mice from obesity-induced inflammation and gastrointestinal health (Noratto G et al., 2015). Yao et al. indicate that quinoa saponin fractions reduced the response of inflammatory mediators and inflammatory cytokines in LPS-induced RAW264.7 cells (Yao et al., 2014).

6.5 Conclusion

This chapter focuses on the cytokines and regulatory molecules responsible for Q-80M extract's anti-inflammatory effect in LPS-stimulated RAW 264.7 cells. The effect of Q-80M on cytokines was studied using indirect ELISA and cytokine membrane array. The findings showed that Q-80M significantly decreased the proinflammatory cytokines IL-1, IL-6, and TNF. Anti-inflammatory IL-10 was markedly increased by Q-80M pretreatment. Additionally, we observed that cells pretreated with Q-80M showed downregulation of COX-2 and iNOS. Q-80M also inhibited the generation of ROS in inflammatory conditions, as demonstrated by DCFDA staining. Antibody array research showed that pretreatment of Q-80M in LPS-stimulated RAW cells resulted in the downregulation of proinflammatory molecules (MCP5, GM CSF, GC SF, TRANCE, TROY, and MMP-2) and an increase in fit-3 ligand anti-inflammatory cytokine. TLR-4, MyD88, and pJNK were found to be downregulated in Western blot analysis. The function of NF- κ B and I- κ B was

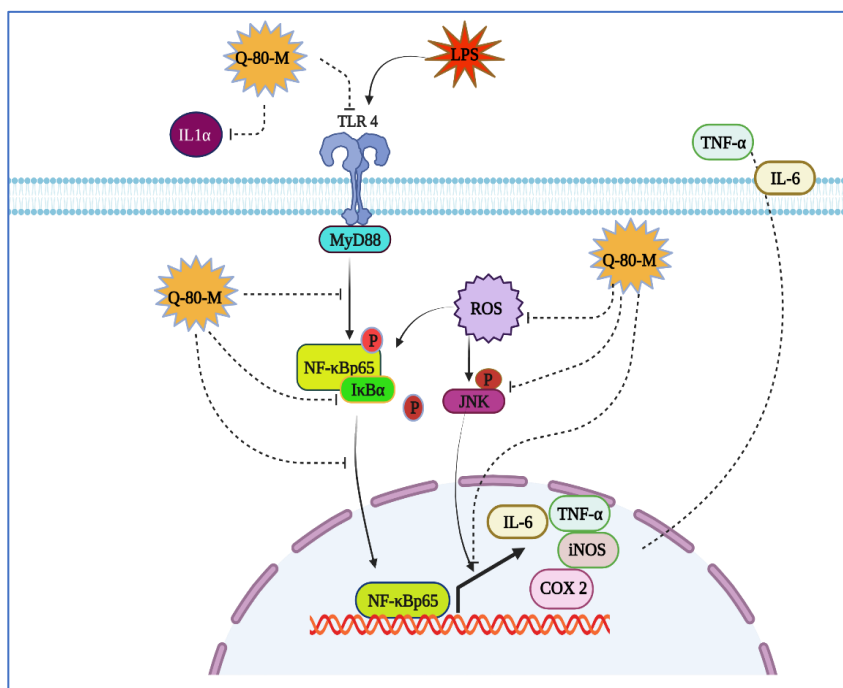


Figure 6.9: Summary of the effects of Q-80M on LPS-induced RAW264.7 cells

established by both western blot and immunofluorescence investigations. According to the Q-80M extract's LCMS study, it contains bioactive like phenolic, cinnamic, and derivatives of flavonoids. According to the research, the LPS-stimulated TLR-4 pathway, which MYD88 and NF- κ B mediate, is inhibited by the bioactive extract of Q-80M, which confirmed the anti-inflammatory capabilities.

6.6 References

1. Aswad, M., Rayan, M., Abu-Lafi, S., Falah, M., Raiyn, J., Abdallah, Z., & Rayan, A. (Aswad, M., Rayan, M., Abu-Lafi, S., Falah, M., Raiyn, J., Abdallah, Z., & Rayan, A. Nature is the best source of anti-inflammatory drugs: indexing natural products for their anti-inflammatory bioactivity. *Inflammation Research*. 2018; 67(1), 67–75. <https://doi.org/10.1007/s00011-017-1096-5>
2. Bhattacharya, P., Budnick, I., Singh, M., Thiruppathi, M., Alharshawi, K., Elshabrawy, H., Holterman, M. J., & Prabhakar, B. S. Dual Role of GM-CSF as a Pro-Inflammatory and a Regulatory Cytokine: Implications for Immune Therapy. *Journal of Interferon and Cytokine Research*. 2015; 35(8), 585–599. <https://doi.org/10.1089/jir.2014.0149>
3. Blunck, R., Scheel, O., Müller, M., Brandenburg, K., Seitzer, U., & Seydel, U. New Insights Into Endotoxin-Induced Activation of Macrophages: Involvement of a K⁺ Channel in Transmembrane Signaling. *The Journal of Immunology*. 2001; 166(2), 1009–1015. <https://doi.org/10.4049/jimmunol.166.2.1009>
4. Cao, Y., Chen, J., Ren, G., Zhang, Y., Tan, X., & Yang, L. Punicalagin prevents inflammation in lps-induced raw264.7 macrophages by inhibiting foxo3a/autophagy signaling pathway. *Nutrients* 2019; 11(11), 1–14. <https://doi.org/10.3390/nu11112794>
5. Chen, D., Carpenter, A., Abrahams, J., Chambers, R. C., Lechler, R. I., McVey, J. H., & Dorling, A. cProtease-activated receptor 1 activation is necessary for monocyte chemoattractant protein 1-dependent leukocyte recruitment in vivo. *Journal of Experimental Medicine*. 2008; 205(8), 1739–1746. <https://doi.org/10.1084/jem.20071427>
6. Choi, J. H., Song, Y. S., Lee, H. J., Hong, J. W., & Kim, G. C. Inhibition of inflammatory reactions in 2,4-Dinitrochlorobenzene induced Nc/Nga atopic dermatitis mice by non-Thermal plasma. *Scientific Reports*. 2016; 6(March), 1–11. <https://doi.org/10.1038/srep27376>
7. Dlodla, P. V., Nkambule, B. B., Jack, B., Mkandla, Z., Mutize, T., Silvestri, S., Orlando, P., Tiano, L., Louw, J., & Mazibuko-Mbeje, S. E. Inflammation and oxidative stress in an obese state and the protective effects of gallic acid. *Nutrients*. 2019; 11(1). <https://doi.org/10.3390/nu11010023>

8. Echizen, K., Hirose, O., Maeda, Y., & Oshima, M. Inflammation in gastric cancer: Interplay of the COX-2/prostaglandin E2 and Toll-like receptor/MyD88 pathways. *Cancer Science*. 2016; 107(4), 391–397. <https://doi.org/10.1111/cas.12901>
9. Edwan, J. H., Perry, G., Talmadge, J. E., & Agrawal, D. K. Flt-3 Ligand Reverses Late Allergic Response and Airway Hyper-Responsiveness in a Mouse Model of Allergic Inflammation. *The Journal of Immunology*. 2004; 172(8), 5016–5023. <https://doi.org/10.4049/jimmunol.172.8.5016>
10. Fu, Y. jun, Xu, B., Huang, S. wei, Luo, X., Deng, X. liang, Luo, S., Liu, C., Wang, Q., Chen, J. yan, & Zhou, L. Baicalin prevents LPS-induced activation of TLR4/NF- κ B p65 pathway and inflammation in mice via inhibiting the expression of CD14. *Acta Pharmacologica Sinica*. 2021; 42(1), 88–96. <https://doi.org/10.1038/s41401-020-0411-9>
11. Furman, D., Campisi, J., Verdin, E., Carrera-Bastos, P., Targ, S., Franceschi, C., Ferrucci, L., Gilroy, D. W., Fasano, A., Miller, G. W., Miller, A. H., Mantovani, A., Weyand, C. M., Barzilai, N., Goronzy, J. J., Rando, T. A., Effros, R. B., Lucia, A., Kleinstreuer, N., & Slavich, G. M. Chronic inflammation in the etiology of disease across the life span. *Nature Medicine* 2019; 25(12), 1822–1832. <https://doi.org/10.1038/s41591-019-0675-0>
12. Gauvreau, G. M., Sehmi, R., Ambrose, C. S., & Griffiths, J. M. Thymic stromal lymphopoietin: its role and potential as a therapeutic target in asthma. *Expert Opinion on Therapeutic Targets*. 2020; 24(8), 777–792. <https://doi.org/10.1080/14728222.2020.1783242>
13. Han, B., Dai, Y., Wu, H., Zhang, Y., Wan, L., Zhao, J., Liu, Y., Xu, S., & Zhou, L. Cimifugin inhibits inflammatory responses of RAW264.7 cells induced by lipopolysaccharide. *Medical Science Monitor*. 2019; 25, 409–417. <https://doi.org/10.12659/MSM.912042>
14. Han, S., Gao, H., Chen, S., Wang, Q., Li, X., Du, L. J., Li, J., Luo, Y. Y., Li, J. X., Zhao, L. C., Feng, J., & Yang, S. Procyanidin A1 Alleviates Inflammatory Response induced by LPS through NF- κ B, MAPK, and Nrf2/HO-1 Pathways in RAW264.7 cells. *Scientific Reports*. 2019; (1), 1–13. <https://doi.org/10.1038/s41598-019-51614-x>
15. Jacobs, M. D., & Harrison, S. C. Structure of an I κ B α /NF- κ B complex. *Cell*. 1998; 95(6), 749–758. [https://doi.org/10.1016/S0092-8674\(00\)81698-0](https://doi.org/10.1016/S0092-8674(00)81698-0)
16. Jakubowska, K., Prczynicz, A., Iwanowicz, P., Niewiński, A., Maciorkowska, E., Hapanowicz, J., Jagodzińska, D., Kemon, A., & Guzińska-Ustymowicz, K. Expressions of matrix metalloproteinases (MMP-2, MMP-7, and MMP-9) and their inhibitors (TIMP-1, TIMP-2) in inflammatory bowel diseases. *Gastroenterology Research and Practice*, 2016. <https://doi.org/10.1155/2016/2456179>

17. Ji, Q., Zhang, M., Wang, Y., Chen, Y., Wang, L., Lu, X., Bai, L., Wang, M., Bao, L., Hao, H., & Wang, Z. Protective effects of chlorogenic acid on inflammatory responses induced by *Staphylococcus aureus* and milk protein synthesis in bovine mammary epithelial cells. *Microbial Pathogenesis*. 2022; 171, 105726. <https://doi.org/10.1016/j.micpath.2022.105726>
18. Jung, H. J., Song, Y. S., Lim, C. J., & Park, E. H. Anti-angiogenic, anti-inflammatory and anti-nociceptive activities of vanillyl alcohol. *Archives of Pharmacal Research*. 2008; 31(10), 1275–1279. <https://doi.org/10.1007/s12272-001-2106-1>
19. Kakkar, S., & Bais, S. A Review on Protocatechuic Acid and Its Pharmacological Potential. *ISRN Pharmacology*. 2014, 1–9. <https://doi.org/10.1155/2014/952943>
20. Lawlor, K. E., Campbell, I. K., Metcalf, D., O'Donnell, K., Van Nieuwenhuijze, A., Roberts, A. W., & Wicks, I. P. Critical role for granulocyte colony stimulating factor in inflammatory arthritis. *Proceedings of the National Academy of Sciences of the United States of America*. 2004; 101(31), 11398–11403. <https://doi.org/10.1073/pnas.0404328101>
21. Li, S. T., Dai, Q., Zhang, S. X., Liu, Y. J., Yu, Q. Q., Tan, F., Lu, S. H., Wang, Q., Chen, J. W., Huang, H. Q., Liu, P. Q., & Li, M. “Ulinastatin attenuates LPS-induced inflammation in mouse macrophage RAW264.7 cells by inhibiting the JNK/NF- κ B signaling pathway and activating the PI3K/Akt/Nrf2 pathway.” *Acta pharmacologica Sinica*. 2018; 1294-1304. doi:10.1038/aps.2017.143
22. Li, Y., Yao, J., Han, C., Yang, J., Chaudhry, M. T., Wang, S., Liu, H., & Yin, Y. Quercetin, inflammation and immunity. *Nutrients*. 2016; 8(3), 1–14. <https://doi.org/10.3390/nu8030167>
23. Li, W., Song, Y., Cao, Y. N., Zhang, L. Le, Zhao, G., Wu, D. T., & Zou, L. Total saponins from quinoa bran alleviate high-fat diet-induced obesity and systemic inflammation via regulation of gut microbiota in rats. *Food Science and Nutrition*. 2022; 10(11), 3876–3889. <https://doi.org/10.1002/fsn3.2984>
24. Lin, M., Han, P., Li, Y., Wang, W., Lai, D., & Zhou, L. Quinoa secondary metabolites and their biological activities or functions. *Molecules*. 2019; 24(13). <https://doi.org/10.3390/molecules24132512>
25. Lucas, S. M., Rothwell, N. J., & Gibson, R. M. The role of inflammation in CNS injury and disease. *British Journal of Pharmacology*. 2006; 147(SUPPL. 1), 232–240. <https://doi.org/10.1038/sj.bjp.0706400>
26. Melini, Valentina & Melini, Francesca. Functional Components and Anti-Nutritional Factors in Gluten-Free Grains: A Focus on Quinoa Seeds. *Foods*. 2021; 10. 351. [10.3390/foods10020351](https://doi.org/10.3390/foods10020351).

27. Min, J.-K., Kim, Y.-M., Kim, S. W., Kwon, M.-C., Kong, Y.-Y., Hwang, I. K., Won, M. H., Rho, J., & Kwon, Y.-G. TNF-Related Activation-Induced Cytokine Enhances Leukocyte Adhesiveness: Induction of ICAM-1 and VCAM-1 via TNF Receptor-Associated Factor and Protein Kinase C-Dependent NF- κ B Activation in Endothelial Cells. *The Journal of Immunology*. 2005; 175(1), 531–540. <https://doi.org/10.4049/jimmunol.175.1.531>
28. Paulino, V. M., Yang, Z., Kloss, J., Ennis, M. J., Armstrong, B. A., Loftus, J. C., & Tran, N. L. TROY (TNFRSF19) is overexpressed in advanced glial tumors and promotes glioblastoma cell invasion via Pyk2-Rac1 signaling. *Molecular cancer research: MCR*. 2010; 8(11), 1558–1567. <https://doi.org/10.1158/1541-7786.MCR-10-0334>
29. Prado, C. M., Leick-Maldonado, E. A., Arata, V., Kasahara, D. I., Martins, M. A., & Tibério, I. F. L. C. Neurokinins and inflammatory cell iNOS expression in guinea pigs with chronic allergic airway inflammation. *American Journal of Physiology - Lung Cellular and Molecular Physiology*. 2005; 288(4 32-4). <https://doi.org/10.1152/ajplung.00208.2004>
30. Pragasam, S. J., Venkatesan, V., & Rasool, M. Immunomodulatory and anti-inflammatory effect of p-coumaric acid, a common dietary polyphenol on experimental inflammation in rats. *Inflammation* 2013; 36(1), 169–176. <https://doi.org/10.1007/s10753-012-9532-8>
31. Rho, H. S., Ghimeray, A. K., Yoo, D. S., Ahn, S. M., Kwon, S. S., Lee, K. H., Cho, D. H., & Cho, J. Y. Kaempferol and kaempferol rhamnosides with depigmenting and anti-inflammatory properties. *Molecules*. 2011; 16(4), 3338–3344. <https://doi.org/10.3390/molecules16043338>
32. Sakai, S., Kawamata, H., Kogure, T., Mantani, N., Terasawa, K., Umatake, M., & Ochiai, H. Inhibitory effect of ferulic acid and isoferulic acid on the production of macrophage inflammatory protein-2 in response to respiratory syncytial virus infection in RAW264.7 cells. *Mediators of Inflammation*. 1999; 8(3), 173–175. <https://doi.org/10.1080/09629359990513>
33. Schön, S., Flierman, I., Ofner, A., Stahringer, A., Holdt, L. M., Kolligs, F. T., & Herbst, A. β -catenin regulates NF- κ B activity via TNFRSF19 in colorectal cancer cells. *International Journal of Cancer*. 2014; 135(8), 1800–1811. <https://doi.org/10.1002/ijc.28839>
34. Serino, A., & Salazar, G. Protective role of polyphenols against vascular inflammation, aging and cardiovascular disease. *Nutrients*. 2021; 11(1), 1–23. <https://doi.org/10.3390/nu11010053>
35. Sun, W. L., Li, X. Y., Dou, H. Y., Wang, X. D., Li, J. Da, Shen, L., & Ji, H. F. Myricetin supplementation decreases hepatic lipid synthesis and inflammation

- by modulating gut microbiota. *Cell Reports*. 2021; 36(9), 109641. <https://doi.org/10.1016/j.celrep.2021.109641>
36. Tsai, D. H., Riediker, M., Berchet, A., Paccaud, F., Waeber, G., Vollenweider, P., & Bochud, M. Effects of short- and long-term exposures to particulate matter on inflammatory marker levels in the general population. *Environmental Science and Pollution Research* 2019; 26(19), 19697–19704. <https://doi.org/10.1007/s11356-019-05194-y>
 37. Wu, Z., Mehrabi Nasab, E., Arora, P., & Athari, S. S. Study effect of probiotics and prebiotics on treatment of OVA-LPS-induced of allergic asthma inflammation and pneumonia by regulating the TLR4/NF- κ B signaling pathway. *Journal of Translational Medicine*. 2022; 20(1), 1–14. <https://doi.org/10.1186/s12967-022-03337-3>
 38. Yang, H. L., Yang, T. Y., Gowrisankar, Y. V., Liao, C. H., Liao, J. W., Huang, P. J., Hseu, Y. C., Hseu, Y. C., Hseu, Y. C., & Hseu, Y. C. Suppression of LPS-Induced Inflammation by Chalcone Flavokawain A through Activation of Nrf2/ARE-Mediated Antioxidant Genes and Inhibition of ROS/NF κ B Signaling Pathways in Primary Splenocytes. *Oxidative Medicine and Cellular Longevity*, 2020. <https://doi.org/10.1155/2020/3476212>
 39. Yao, Y., Yang, X., Shi, Z., & Ren, G. Anti-inflammatory activity of saponins from quinoa (*Chenopodium quinoa* Willd.) seeds in lipopolysaccharide-stimulated RAW 264.7 macrophages cells. *Journal of food science*. 2014; 79(5), H1018–H1023. <https://doi.org/10.1111/1750-3841.12425>
 40. Zielińska D, Zieliński H, Laparra-Llopis JM, Szawara-Nowak D, Honke J, Giménez-Bastida JA. Caffeic Acid Modulates Processes Associated with Intestinal Inflammation. *Nutrients*. 2021 Feb 8;13(2):554. doi: 10.3390/nu13020554. PMID: 33567596; PMCID: PMC7914463.

CHAPTER 7

SUMMARY AND CONCLUSION

Global food demand is increasing as the world's population expands. The majority of the people depend on conventional cereals like rice, wheat and maize. But this Conventional cereal production is not sufficient to feed the world population. Recently pseudocereals have emerged as a preferable alternative to cereal. Amaranth and quinoa are the most commonly used pseudocereals. Amaranth and quinoa seeds are rich in proteins with all the essential amino acids, an abundance of phytonutrients, a high dietary fibre content, vitamins, and minerals. The demand for amaranth and quinoa seeds has markedly and steadily increased. According to research, amaranth and quinoa seeds have a substantial impact on disease therapy and prevention.

One of the finest discoveries in the last two decades is that every chronic disease is heavily influenced by inflammation. The immune system and inflammation cause mental and physical disorders leading to more than 50% mortality. World statistics indicate that one of the major chronic diseases is cancer because it results in more than 10 million death per year. Breast cancer (BC) is the most common cancer in women. Among the BC subgroups, triple-negative breast cancer (TNBC) is the most aggressive and metastatic. The sole treatment option used is chemotherapy. The currently used treatment methods for both inflammation and TNBC may cause numerous side effects. Many kinds of research are conducted with plant-based phytochemicals and biopeptides because of negligible side effects and ease of penetrating the cells. Although amaranth and quinoa have been consumed since ancient times, the full extent of their biological processes is yet unknown. In this work, we have done *in vitro* studies on the effects of bioactive from quinoa and amaranth seeds against breast cancer and inflammation.

Bioactive peptides and solvent extracts from amaranth and quinoa seeds were isolated. These isolates underwent preliminary testing against inflammation and breast cancer proliferation (Figure 7.1). Amaranth and quinoa seed proteins were isolated and subjected to simulated gastrointestinal digestion. The isolation of bioactive-rich solvent extracts from amaranth and quinoa seeds was carried out by direct (using 80% methanol) and sequential (using hexane, ethyl acetate and methanol) extraction methods. Different solvent extracts and digested protein samples from amaranth and quinoa seeds were screened for their *in vitro* antioxidant, anti-inflammatory and anti-breast cancer effects. The antioxidant activity was significantly higher in the ASP-HD. In the case of solvent extracts, antioxidant activity and phenolic content were found to be more in Q-80M when compared to other extracts. The anti-breast cancer effects of different protein hydrolysates and solvent extracts were examined in MDA-MB-231 cells. The cytotoxicity assay results revealed that ASP-HD showed significant anti-breast cancer activity. The anti-inflammatory potential was maximum for Q-80M (quinoa seed 80% methanol extract, direct extraction), compared to other isolates Q-80M significantly reduced the LPS-stimulated NO production in RAW cells.

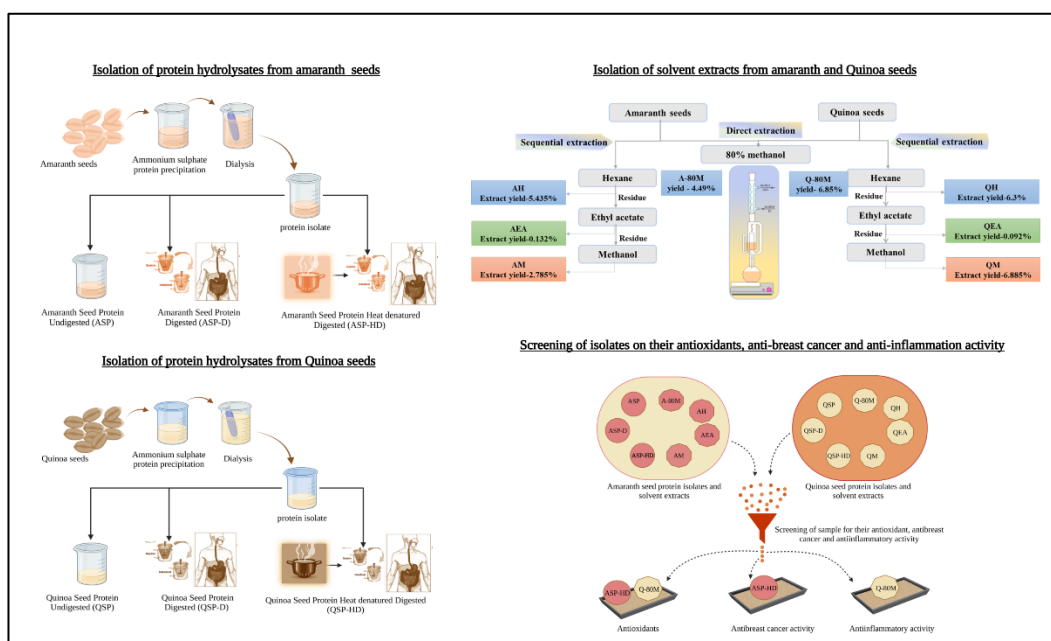


Figure 7.1: Diagrammatic representation of the isolation of bioactive peptides and solvent extracts from amaranth and quinoa seeds also their preliminary screening against inflammation and breast cancer proliferation

We have conducted a detailed analysis of the anti-breast cancer effects of ASP-HD in MDA-MB-231 cells. The potential breast cancer cell cytotoxicity was observed for ASP-HD. ASP-HD can induce apoptosis in MDA-MB-231 cells, which was examined through DNA fragmentation, phosphatidylserine translocation, membrane integrity loss, and caspase 3 activity analysis. Apoptosis array results demonstrated that ASP-HD activates proapoptotic proteins and inhibits antiapoptotic proteins. Also, ASP-HD impeded the migration of cancer cells. The amino acid analysis results indicated that the ASP-HD contained the maximum number of essential amino acids like lysine, threonine, tryptophan, isoleucine, phenylalanine and leucine. These results indicated that amaranth proteins upon heat denaturation followed by simulated digestion released maximum essential amino acids. Also, we have identified around 4606 peptides in ASP-HD. The GO analysis revealed various functional properties of ASP-HD, in that important biological processes were protein metabolism (40%), cell development (20%) and energy pathways (20%). Primary molecular functions of the ASP-HD protein include ligase activity (20%), serine-type peptidase (20%) and protein inhibitor (20%). The major cellular components of ASP-HD interact with lysosomes (60%), exosomes (60%), nucleus (40%), cytoplasm (40%), and other organelles. The schematic representation of ASP-HD anti-breast cancer activity is given in Figure 7.2.

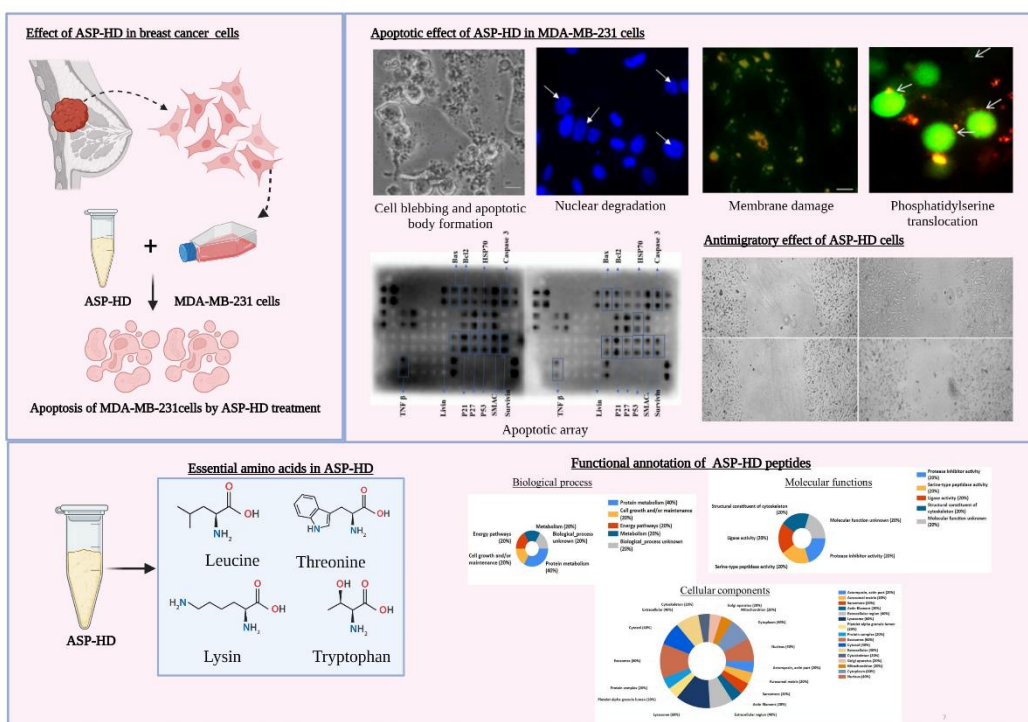


Figure 7.2: Diagrammatic representation of the anti-breast cancer activity of ASP-HD with the essential amino acids content and the functional annotation analysis of ASP-HD.

In the preliminary screening for anti-inflammatory studies, we found that Q-80M (quinoa seed 80% methanol extract, direct extraction) showed significant anti-inflammatory activity in LPS-stimulated RAW 264.7 cells. Whole transcriptome analysis results showed that LPS stimulation in RAW cells causes the upregulation of 1990 genes and the downregulation of 817 genes. The Q-80M pretreated in LPS-stimulated RAW cells shows significant changes like a downregulation of 481 genes and an upregulation of 134 genes. PPI networks, gene clusters and 10 hub genes were identified from both upregulated and downregulated gene sets in inflammation as well as Q-80M pretreated cells. Q-80M pretreatment regulated the inflammation by reducing the response to external stimuli, cytokine-mediated signalling, T cell and lymphocyte activation and cytokine response. Q-80M can normalize the principal genes involved in inflammatory pathways (cytokine- cytokine receptor interaction, TNF, chemokine, NOD-like receptor and NF- κ B signalling pathway) and thereby reduce the inflammatory condition. The diagrammatic representation of transcriptomic results is given in Figure 7.3.

Then we focused on the effect of Q-80M on the cytokines and regulatory molecules responsible for inflammation. Q-80M significantly decreased the proinflammatory cytokines (IL-1, IL-6, TNF- α , MCP5, GM CSF, GC SF, TRANCE, TROY, and MMP-2) and increased anti-inflammatory cytokine (IL-10 and fit-3 ligand). Additionally, we observed that LPS-stimulates RAW cells pretreated with Q-80M showed downregulation of COX-2 and iNOS. Q-80M also inhibited the generation of ROS in

inflammatory conditions. Furthermore, Q-80M pretreatment also inhibited the activation of the TLR4/MyD88/NF- κ B p65 pathway in LPS-induced RAW264.7 cells. Q-80M inhibited the NF- κ B translocation into the nucleus by preventing the degradation of I- κ B α . Q-80M extracts contain phytochemicals like phenolic, cinnamic and flavonoid derivatives. According to the experimental results, the LPS-stimulated TLR-4 pathway mediated by MYD88 and NF- κ B is inhibited by the bioactive extract of Q-80M. It confirms the anti-inflammatory capabilities of the extract. The anti-inflammatory activity of Q-80M is depicted in Figure 7.4.

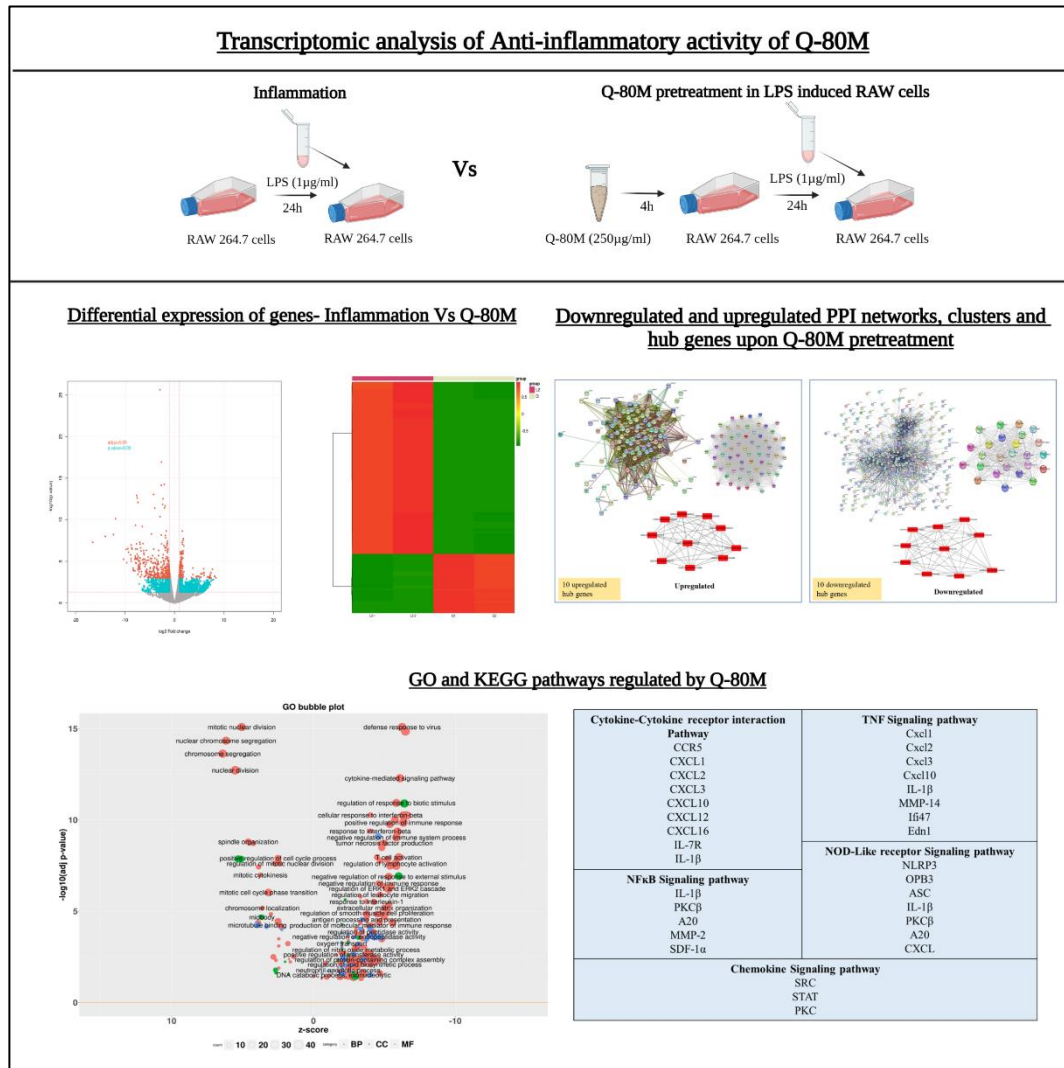


Figure 7.3: Diagrammatic representation of the anti-inflammatory activity of Q-80M by whole genome transcriptomic analysis.

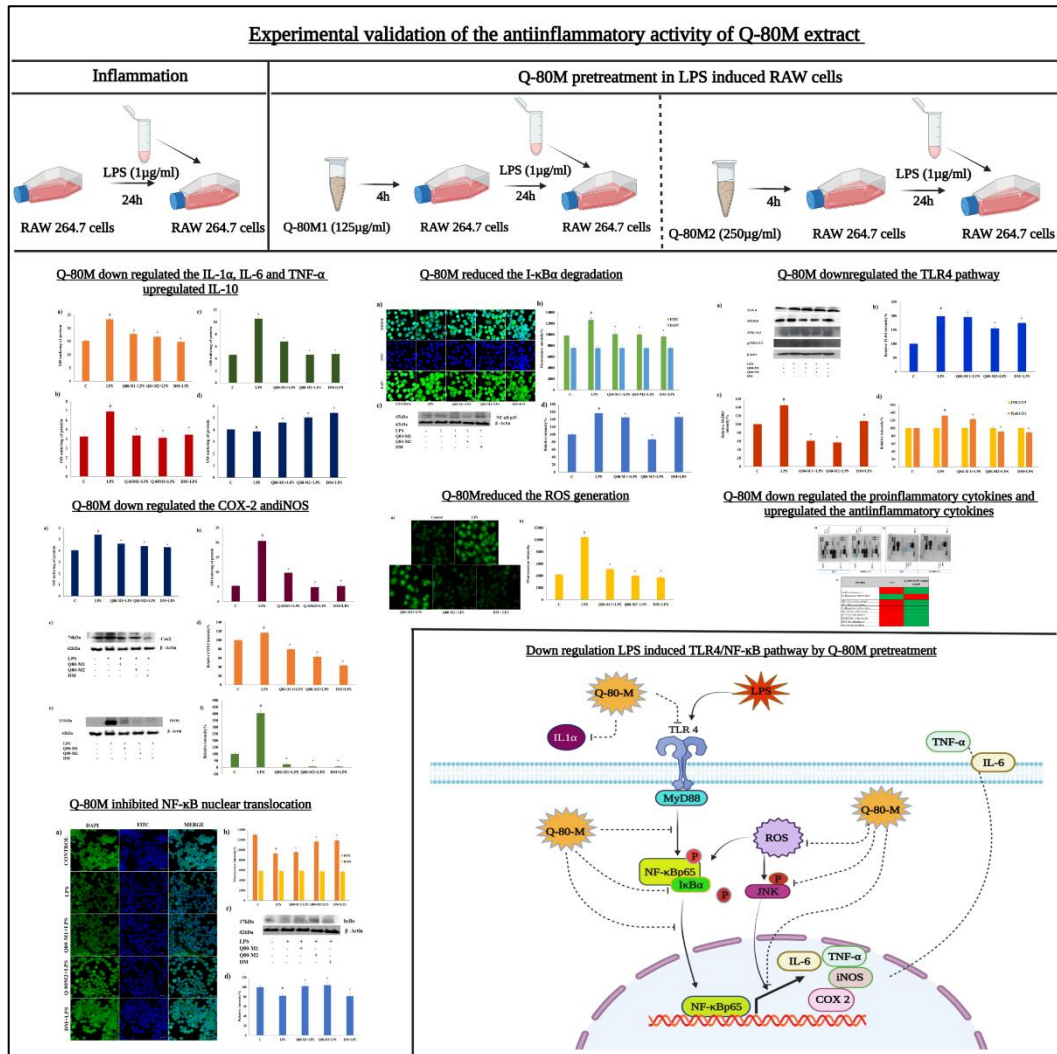


Figure 7.4: Diagrammatic representation of the anti-inflammatory activity of Q-80M by experimental validation.

From this study, it is revealed that amaranth and quinoa are having the capability to regulate breast cancer and chronic inflammation respectively. Amaranth protein isolate (ASP-HD) induces apoptosis and prevents cell migration, thereby it prevents the growth and metastasis of breast cancer. Quinoa methanolic extract inhibited chronic inflammation by regulating various inflammatory genes, pathways, cytokines and inflammatory mediators.

Future prospects of the study

From our study, the anti-breast cancer effect of ASP-HD and the anti-inflammatory activity of Q-80M were revealed. In the anti-breast cancer study, molecular-level evaluation of ASP-HD against breast cancer is required to identify the mode of action and further validation. Also, the Q-80M downregulated anti-inflammatory genes identified by NGS analysis still need to be confirmed by RT-PCR and the respective protein level validation needs to be confirmed by detailed proteome analysis. *In vivo*, validation of ASP-HD against breast cancer and Q-80M against inflammation are also required for further confirmation.

ABSTRACT

Name of the Student: Taniya. M. S
Faculty of Study: Biological sciences

Registration No.: 10BB17J39009
Year of Submission: 2023

AcSIR academic centre/CSIR Lab: NIIST

Name of the Supervisor(s): Dr Priya S

Title of the thesis: *In vitro* studies on the effects of bioactives from quinoa and amaranth seeds against breast cancer and inflammation

The Amaranth and quinoa seeds are well known for their nutritional qualities and emerged as an alternative to gluten-free cereals. Amaranth and quinoa are excellent sources of protein and bioactive phytochemicals. This study investigated the protein hydrolysates and phytochemicals of amaranth and quinoa seeds to assess their anti-breast cancer and anti-inflammatory activities. The hydrolysates were prepared using *in vitro* simulated gastrointestinal digestion (pepsin and pancreatin) with the native and heat-denatured proteins. The bioactive phytochemical-rich extracts of amaranth and quinoa seeds were isolated by sequential and direct solvent extraction. All these isolates were screened for their antioxidant activity, anti-breast cancer effects on MDA-MB-231 cells and anti-inflammatory activity in LPS-stimulated RAW cells. Further research was carried out with the selected isolate, which possesses anti-breast cancer activity. Then its apoptotic and anti-migratory properties on MDA-MB-231 cells were examined in detail. The essential amino acid content and functional annotation of the anti-breast cancer potent hydrolysate were performed with the HPLC and mass spectrometry analysis. Similarly, the extract with high anti-inflammatory activity and less cytotoxicity was evaluated by *in vitro* LPS-induced RAW264.7 macrophages. Then, NGS analysis with RNA isolates and functional analysis of DEGs were performed. The experimental confirmation of critical proteins and the inflammatory pathways of transcriptome analysis were evaluated. Also, LCMS analysis was done to elucidate the bioactive components of the extract. The results indicated that ASP-HD protein hydrolysate and solvent extract Q-80M have high antioxidant capacity. The anti-breast cancer results showed that ASP-HD could inhibit breast cancer cell growth by causing DNA fragmentation, membrane integrity loss, phosphatidylserine translocation, caspase-3 activity, upregulation of apoptotic proteins, and inhibition of cancer cell migration in MDA-MB-231 cells. The anti-inflammation activity analysis discovered that Q-80 M decreased LPS-induced NO production in macrophages without generating cytotoxicity. The RNA-Seq identified a total of 615 DEGs, a significant upregulation of 134 genes and a downregulation of 481 genes from inflammation conditions. The topological expression of the upregulated and downregulated gene sets was identified for both inflammation and Q-80M pretreatment. Gene ontology and pathway analysis of the DEGs revealed that the Q-80M downregulated the genes and inflammatory pathways. Further experimental results confirmed that the Q-80M was able to cut down the expression of the proinflammatory cytokine genes. Q-80M targeted the upstream elements of the inflammatory cascade by blocking the TLR4 /NF- κ B pathway. The Q-80M prevented the transcription of proinflammatory cytokines by inhibiting the nuclear translocation of NF- κ B and I κ B α degradation. LCMS analysis of the Q-80M showed the polyphenol and flavonoid derivatives in the extract. In a nutshell, this study showed that amaranth seed is an excellent source of biopeptides and can suppress the development and migration of highly aggressive triple-negative breast cancer cells. Our study also offers solid proof that quinoa seed extract (Q-80M) exerts its anti-inflammatory impact by regulating cytokines and inflammatory pathways. As a result, amaranth biopeptide and quinoa methanolic extracts may be promising sources of anti-breast cancer and anti-inflammatory action, respectively.

LIST OF PUBLICATIONS

Publications emanated from the thesis

- **Taniya MS**, Reshma MV, Shanimol PS, Gayatri Krishnan and Priya S. Bioactive peptides from amaranth seed protein hydrolysates induced apoptosis and antimigratory effects in breast cancer cells, J Food Bioscience, **2020**, 35, 100588. <https://doi.org/10.1016/j.fbio.2020.100588>

Other publications

- Veena KS, **Taniya MS**, Jaice R, Arun Kumar T, Priya S and Ravishankar L. Semi-synthetic diversification of coronarin D, a labdane diterpene, under Ugi reaction conditions. Nat Prod Res., 2020, 2020 Jun 25;1-7. doi: 10.1080/14786419.2020.1782406.



Contents lists available at [ScienceDirect](#)

Food Bioscience

journal homepage: www.elsevier.com/locate/fbio



Corrigendum to “Bioactive peptides from amaranth seed protein hydrolysates induced apoptosis and antimigratory effects in breast cancer cells” [Food Bioscience 35 (2020) 100588]

M.S. Taniya ^{a,b}, M.V. Reshma ^a, P.S. Shanimol ^c, Gayatri Krishnan ^c, S. Priya ^{a,b,*}

^a Agro-Processing and Technology Division, National Institute for Interdisciplinary Science and Technology (NIIST), Council for Scientific and Industrial Research (CSIR), Trivandrum, Kerala, 695 019, India

^b Academy of Scientific and Innovative Research (AcSIR), Ghaziabad, New Delhi, 201002, India

^c Department of Biotechnology and Bioinformatics, Kerala University of Fisheries and Ocean Studies, Kochi, Kerala, 682 506, India

The authors regret an error in one of the author affiliations. The correct affiliation “b” is as follows:

^b Academy of Scientific and Innovative Research (AcSIR), Ghaziabad,

201002, India.

The authors would like to apologise for any inconvenience caused.

DOI of original article: <https://doi.org/10.1016/j.fbio.2020.100588>.

* Corresponding author. Agro-Processing and Technology Division, CSIR-National Institute for Interdisciplinary Science and Technology (CSIR-NIIST), Trivandrum, Kerala, 695 019, India.

E-mail addresses: priyasulu@niist.res.in, priyasulu@gmail.com (S. Priya).

<https://doi.org/10.1016/j.fbio.2022.101927>

Available online 10 August 2022

2212-4292/© 2022 Elsevier Ltd. All rights reserved.



Bioactive peptides from amaranth seed protein hydrolysates induced apoptosis and antimigratory effects in breast cancer cells



M.S. Taniya^{a,b}, Reshma MV^a, Shanimol PS^c, Gayatri Krishnan^c, Priya S^{a,b,*}

^a Agro-Processing and Technology Division, National Institute for Interdisciplinary Science and Technology (NIIST), Council for Scientific and Industrial Research (CSIR), Trivandrum, Kerala, 695 019, India

^b Academy of Scientific and Innovative Research (AcSIR), Ghaziabad, New Delhi, 201002, India

^c Department of Biotechnology and Bioinformatics, Kerala University of Fisheries and Ocean Studies, Kochi, Kerala, 682 506, India

ARTICLE INFO

Keywords:

Amaranthus caudatus
Simulated digestion
Anticancer
Antimigration

ABSTRACT

Bioactive peptides are short chains of amino acids with positive health effects. Food proteins may be an important source of bioactive peptides. Pseudocereals contain a high amount of proteins. In the present study, proteins were isolated from the seeds of the pseudocereal, amaranth and the hydrolysates were prepared using simulated gastrointestinal digestion with the native and heat-denatured proteins. Heat denaturation increased the digestibility, released essential amino acids and peptides with antioxidant and free radical scavenging activity. Due to the high antioxidant activity of the protein hydrolysates prepared after heat denaturation followed by simulated digestion, the end product was used to measure the *in vitro* anticancer activity in human triple-negative breast cancer cells. The results indicated that the digested sample was capable of inhibiting cell growth with a GI₅₀ value of 48.3 ± 0.2 µg/ml. The protein hydrolysates also induced DNA fragmentation, membrane integrity loss, phosphatidylserine translocation and caspase 3 activity in the treated cells. It inhibited cell migration across an artificial wound created in the cell monolayer. Therefore, amaranth may be a good source of bioactive peptides with good antioxidant activity and promising anticancer activity.

1. Introduction

Pseudocereals or ancient grains are the edible seeds produced by the non-grass family of plants such as amaranth, quinoa and buckwheat. They have a high amount of protein with balanced essential amino acid (EAA) composition and are rich in constituents important for human health, such as dietary fiber, antioxidants, and vitamins. The high nutritional quality and interesting functional properties, make them an alternative to cereals. Pseudocereals are considered as one of the promising foods of the future, due to their high protein content and absence of gluten (Theethira & Dennis, 2015). The high calcium content of the seeds makes them suitable for individuals with sarcopenia and osteoporosis. They are also a viable source of vitamin E, C, Mg, K, P and Fe (Alvarez-Jubete, Arendt, & Gallagher, 2010).

Diets rich in protein help to maintain/lose weight, control blood sugar level, boost energy level, increase the ability to concentrate, support bone/muscle development and aid in the absorption of many nutrients (Pesta & Samuel, 2014). Food proteins can promote good health and food-derived peptides help to prevent many diseases

including cancer (Chakrabarti, Guha, & Majumdar, 2018). The peptides extracted from the common bean (*Phaseolus vulgaris*) reduced azoxymethane/dextran sodium sulfate (AOM/DSS)-induced colitis-associated colon carcinogenesis in the Balb/c mice model (Luna-Vital, Gonzalez de Mejia, & Loarca-Pina, 2017). There are differences in the digestion pattern and absorption of different proteins in the human body. Non-digestible proteins have immune reactions and cause allergies (Huby, Dearman, & Kimber, 2000). Simulated digestion is an effective way to study the digestibility of proteins *in vitro*. Pepsin and pancreatin convert proteins into amino acids and small peptides which may have biological activity. *In vitro* digestion of rice bran proteins released peptides < 3 kDa with alpha-glucosidase and angiotensin-converting enzyme inhibitory activity (Uraipong & Zhao, 2017). The pseudocereals like amaranth which contain 10–15% protein can be a sustainable replacement for animal based proteins (Janssen et al., 2017). The amount and percentage of EAA present in pseudocereals are better when compared to other plant sources (Alvarez-Jubete, Arendt, & Gallagher, 2009).

Amaranthus caudatus L. is one of the gluten free pseudocereals and

* Corresponding author. Agro-Processing and Technology Division, CSIR-National Institute for Interdisciplinary Science and Technology (CSIR-NIIST), Trivandrum, Kerala, 695 019, India.

E-mail addresses: priyasulu@niist.res.in, priyasulu@gmail.com (P. S).

<https://doi.org/10.1016/j.fbio.2020.100588>

Received 6 March 2019; Received in revised form 27 March 2020; Accepted 27 March 2020

Available online 03 April 2020

2212-4292/ © 2020 Elsevier Ltd. All rights reserved.

its protein contains a well-balanced composition of EAA. The antioxidant and antimicrobial activity of amaranth seed extracts has been reported previously (Al-Mamun, Husna, Khatun, & Ferdousi, 2016). Ether and ethyl acetate extracts of amaranthus leaves were studied for their antioxidant, anti-inflammatory (using RAW cells) and anticancer potential (using colon and liver cancer cells) and the results showed that the ethyl acetate extract gave better results (Jin et al., 2013). The anti-inflammatory activity of the ethanol and butanol extracts of amaranth leaves has also been studied (Sen et al., 2015). It modulated cholesterol metabolism by inhibiting HMG-CoA reductase and effectively inhibited hyaluronidase, lipoxygenase, and xanthine oxidase enzymes. The extract was also a good inhibitor of hydroperoxides, nitric oxide and ferric ion radicals (Salvamani et al., 2016).

The present study evaluated the antioxidant and anti-cancer activities of amaranth seed proteins after simulated gastrointestinal digestion in native and heat-denatured samples.

2. Materials and methods

2.1. Materials

Organic dried amaranth seeds (Super Grains, Organic Tattva Brand, Noida, Uttar Pradesh, India) were purchased from Trivandrum, Kerala, India. Ammonium sulfate (ultrapure), polyvinylpyrrolidone (PVP), sodium phosphate buffer, phenylmethylsulfonylfluoride (PMSF), ethylenediaminetetraacetic acid (EDTA), pepsin (from porcine stomach mucosa, 2500 U/mg), pancreatin (from porcine pancreas, 75 U/mg), glycine, sodium bicarbonate, 2,2-diphenyl-1-picrylhydrazyl (DPPH), ammonium molybdate and potassium chloride were purchased from Sisco Research Laboratory (Mumbai, India). Breast cancer MDA-MB 231 cells were purchased from the National Centre for Cell Science (Pune, India). 3-(4,5-Dimethylthiazol-2-yl)-2,5-diphenyl tetrazolium bromide (MTT), 4',6-diamidino-2-phenylindole (DAPI), dialysis sacks, bovine serum albumin (BSA, > 99.9%), curcumin, ethidium bromide, acridine orange and an annexin V staining kit were purchased from Sigma Aldrich (St Louis, MO, USA). A caspase 3 assay kit was purchased from BioVision Inc. (Milpitas, CA, USA). Dulbecco's modified Eagle medium (DMEM), fetal bovine serum (FBS), 100X antibiotic solution (10,000 units of penicillin and 5 mg/ml of streptomycin in 0.9% saline), 10X trypsin-EDTA solution (0.5% trypsin and 0.2% EDTA in 0.85% normal saline), phosphate buffer, phosphate buffered saline (PBS) and plastic wares for cell culture were purchased from Himedia (Mumbai, India).

2.2. Preparation of amaranth seed protein (ASP)

Amaranth seeds (200 g) were washed thoroughly in distilled water and this process was repeated 3–4 times (until the froth in the water ceased) to remove the saponin from the surface. After washing, the seeds were strained using a metal strainer (mesh size-10 mm) to remove the water. Extraction buffer (200 ml 50 mM phosphate buffer, pH 7 with 0.1 mM EDTA and 30 mM KCl) was added to the seeds along 16 g PVP and 10 mM PMSF. The mixture was blended using a mixer grinder (Preethi 110 V Eco Plus, Chennai, India) and filtered through double-layered cheesecloth, centrifuged at 15,900xg in a 50 ml tube (10,000 rpm in an AG-6512C rotor, Model 7780, Kubota Laboratory Centrifuges, Tokyo, Japan) for 15 min at 4 °C. The protein in the supernatant was precipitated using 130.8 g of ammonium sulfate (to 70% saturation) with stirring on a magnetic stirrer at 4 °C. After overnight precipitation, the solution was centrifuged at 15,900xg for 25 min and the pellet was dissolved in 10 mL 50 mM phosphate buffer. It was then dialysed (using dialysis sacks with a nominal MWCO of 12000 Da) against 100 ml of 50 mM phosphate buffer at 4 °C (2 h, 3x). After dialysis the crude protein extract was stored at -80 °C for a maximum period of 6 months. The total protein in the crude extract was estimated using Lowry's method (Lowry, Rosenbrough, Farr, & Randall, 1951)

using BSA (> 99.9%) as the standard and the results are expressed as BSA equivalents (E)/ml of solution.

2.3. In vitro simulation of gastrointestinal digestion

Simulated gastrointestinal digestion of proteins was carried out using pepsin and pancreatin following a previously published protocol (Wada & Lonnerda, 2014). Native and heat-denatured (100 °C for 10 min) amaranth proteins (1 g) were suspended in 10 ml phosphate buffer, pH 7. The simulated digestion was done by adjusting the pH to 2.0 with 1 mol/l HCl. Pepsin (2% in 1 mmol/l HCl) was added at a 1:12.5 ratio (pepsin:protein) and the samples were placed in an incubating shaker at 140 rpm at 37 °C for 15 min. After that, the pH of the sample was adjusted to 7.0 with 0.1 mol/l sodium bicarbonate and pancreatin (0.4% in 0.1 mol/l sodium bicarbonate) was added at a ratio of 1:62.5 (pancreatin:protein). The samples were returned to the incubator shaker at 140 rpm at 37 °C for 5 min. After incubation, the enzymes were inactivated in a water bath at 85 °C for 3 min.

After digestion, the three samples were: ASP, ASP-D (ASP after simulated digestion) and ASP-HD (ASP simulated digested after heat denaturation).

2.4. AA analysis

Analysis of the EAA was done using an AA analyzer Zorbax Eclipse (Agilent Technologies Pvt. Ltd., Gurgaon, India). Separation was done using a gradient mixture of mobile phase A (40 mM NaH₂PO₄, pH 7.8) and mobile phase B (CH₃CN/MeOH/H₂O, 45:45:10) at a flow rate of 2 ml/min and the detection was done using a fluorescence detector with excitation/emission 340/450 nm. The amount of amino acids were calculated based on the regression equation from the standard curve plotted for known amino acids.

2.5. Ninhydrin test for the quantitation of released peptides

The ninhydrin test was done following a previously published protocol (Moore & Stein, 1948). Different volumes (0.1 to 1 ml) of standard glycine solutions (1 mg/ml) and protein samples were pipetted and brought to 4 ml by adding distilled water. Distilled water served as the blank. Ninhydrin reagent (1 ml) was added and incubated in a boiling water bath for 15 min. The reaction mixture was cooled and the absorbance was measured at 570 nm. Peptides with free α -amino acids released were calculated from the OD values using the following equation:

$$\text{Peptides released (mg GlyE/g protein)} = \frac{[(\text{OD}_{\text{test}}) - (\text{OD}_{\text{blank}})] / (\text{OD}_{\text{std}} - (\text{OD}_{\text{blank}})] \times 100}$$

2.6. SDS-PAGE analysis

SDS-PAGE was done using the protocol of Laemmli (1970). Vertical slab polyacrylamide mini-gels (10%, 7 × 10 cm) were prepared by mixing 1.6 ml distilled water, 1.5 ml Tris-HCl, pH 8.8, 1 ml 40% acrylamide stock, 0.1 ml 2% SDS, 0.01 ml 3% ammonium persulphate and 0.004 ml TEMED. The protein samples (40 μ g/well) were loaded into the wells and were then subjected to separation using a Mini-PROTEAN electrophoresis apparatus (BioRad Laboratories, Hercules, CA, USA) at 90 V for 2 h. After electrophoresis, the gel was stained with Coomassie brilliant blue (0.25% solution in 1:3:6 ratio of acetic acid, ethanol and water) for 2 h and destained overnight. The visualization and imaging of the gel was done using the gel documentation system Gel Doc XR⁺ (BioRad Laboratories).

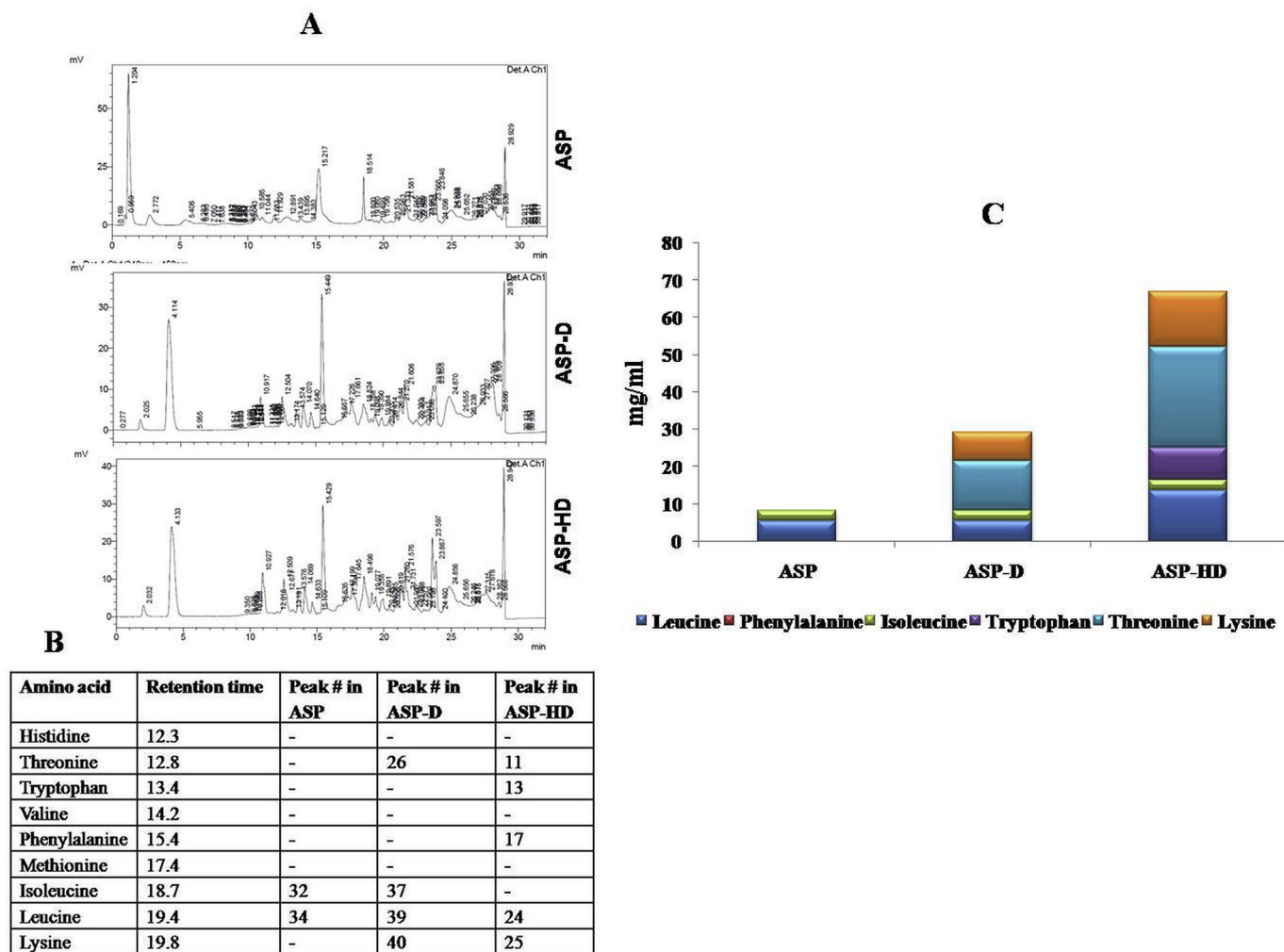


Fig. 1. (A) Chromatogram showing the separation of amino acids ASP, ASP-D and ASP-HD (B) Retention time of standard essential amino acids and peak number in the chromatogram representing the essential amino acids in ASP, ASP-D and ASP-HD (C) Amount of different essential amino acids present (mg/ml) in the samples ASP, ASP-D and ASP-HD.

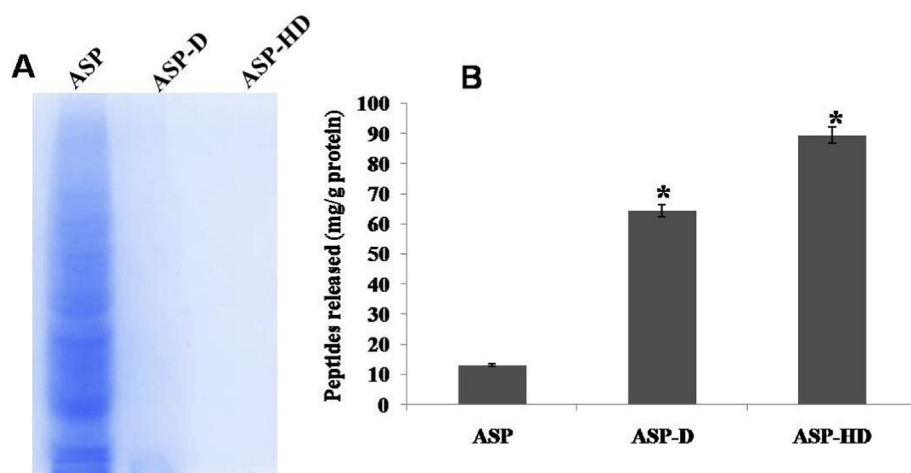


Fig. 2. (A) SDS-PAGE analysis of samples ASP, ASP-D and ASP-HD. (B) Ninhydrin test for the release of peptides with α -amino acids. More released peptides were seen in digested samples compared to undigested samples and heat denaturation increased the amount of peptides released. Values expressed are the average of three independent experiments \pm SD. * $p < 0.05$ when compared with untreated samples.

2.7. Free radical scavenging activity using the DPPH method

Free radical scavenging activity was measured using DPPH method (Chiu et al., 2005) with slight modifications. Sample (100 μ l) was allowed to react with 100 μ l of 10 mM DPPH solution (10 mM DPPH

solution in buffered methanol; 60% methanol and 40% 0.1 M citrate phosphate buffer pH 5.5). After adding the sample to the DPPH solution, the mixture was incubated in the dark for 30 min. The absorbance was measured at 517 nm. The percentage activity was determined using the formula:

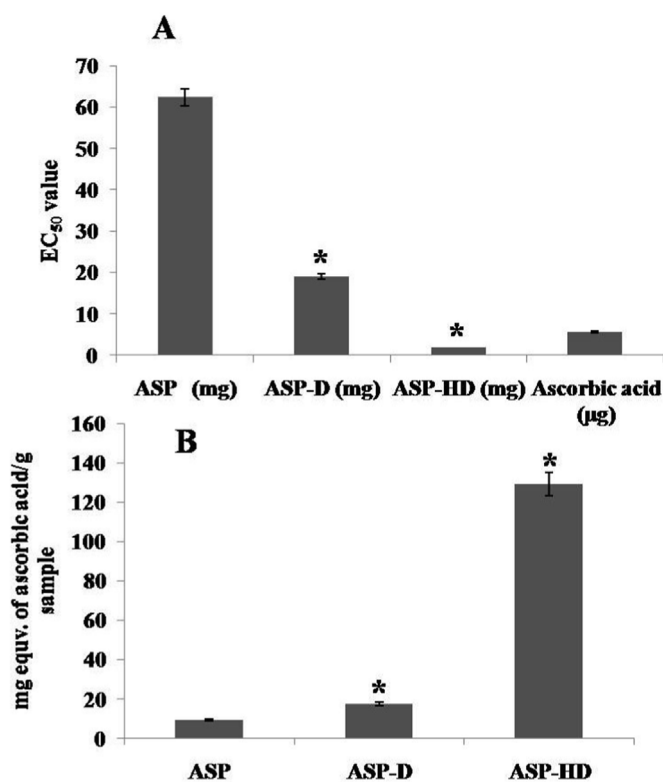


Fig. 3. (A) Free radical scavenging activity of digested and undigested samples of amaranth proteins. Values expressed are the average of three independent experiments \pm SD. * $p < 0.05$ when compared with undigested amaranth sample

(B) Total antioxidant activity of digested and undigested samples of amaranth proteins. Values expressed are the average of three independent experiments \pm SD. * $p < 0.05$ when compared with undigested amaranth sample.

Percentage activity = [(Absorbance of control - Absorbance of sample)/Absorbance of control] \times 100

The results were expressed as EC₅₀ value (the amount of protein sample required to scavenge 50% of the free radicals produced).

2.8. Total antioxidant capacity using the phosphomolybdenum method

The antioxidant activity was measured using the phosphomolybdenum method according to the standard protocol with slight modifications (Prieto, Pineda, & Aguilar, 1999). The assay is based on the reduction of Mo (VI) - Mo (V) by the extract and subsequent formation of a green phosphate/Mo (V) complex at acidic pH. A 300 μ l hydrolysate of varying concentrations (25, 50 and 100 μ g/ml) were combined with 3 ml of reagent solution (0.6 M sulfuric acid, 28 mM sodium phosphate and 4 mM ammonium molybdate). Methanol (300 μ l) served as a blank and ascorbic acid as the positive control. The tubes containing the reaction solution were capped and incubated in a boiling water bath for 90 min. After cooling to 25 $^{\circ}$ C, the absorbance of the solution was measured at 695 nm. The antioxidant capacity of samples was expressed as mg E of ascorbic acid/g extract.

2.9. In vitro anticancer activity studies

(a) Cell culture and Cytotoxicity studies

Human breast cancer cells (MDA-MB-231) were maintained in standard culture conditions at 37 $^{\circ}$ C in a 5% CO₂ incubator in DMEM with 10% fetal bovine serum and 10 mg/ml streptomycin and 100

units/l penicillin. Cells were sub-cultured at regular intervals (doubling time was found to be \sim 30 h) and monolayers of cells grown in culture plates were used for various assays.

The MTT assay was used for the cytotoxicity testing. Cells [1×10^4 cells/well, counted using a hemocytometer (Neubauer counting chamber, Mumbai, India)] were cultured in 96 well plates and after attachment of cells, different concentrations of protein hydrolysates (20, 50, 100, 200 and 500 μ g/ml) were added to the wells. The plate was kept at standard culture conditions for another 24 h. The percentage of viable cells in the control and treated conditions were monitored based on the purple color (formazan) produced as a result of the reduction of MTT by the viable cells which was measured at 570 nm using the microplate reader (SynergyTM⁴, BioTek Instruments, Winooski, VT, USA). The percentage of growth inhibition was calculated using the formula:

% of growth inhibition = [1-(absorbance of treated cells/absorbance of untreated cells)] \times 100

Also, the morphological changes of the cells (normal and treated conditions) were observed at a magnification of 20x using the phase-contrast microscope Nikon Eclipse^{TS}100 (Nikon Instruments Inc., Melville, NY, USA).

Curcumin (10 μ M) was used as the standard for all the anticancer studies.

(b) Nuclear fragmentation using DAPI staining

Nuclear fragmentation is an important event during the apoptosis process. DAPI is a fluorescent dye intercalating in the AT-rich regions of DNA and was used to check for nuclear DNA fragmentation. The cells were treated with two different concentrations of the protein hydrolysate (50 and 100 μ g/ml) for 24 h. After incubation, the medium was aspirated and the cells were treated with 300 nM DAPI solution for 20 min. The DAPI solution was removed and the cells were washed with PBS and the nuclear morphology was observed at an excitation/emission of 358/461 nm using a spinning disc fluorescent microscope BD pathway bio-imaging system (BD Biosciences, San Jose, CA, USA).

(c) Membrane integrity using acridine orange/ethidium bromide staining

The membrane damage associated with apoptosis was measured using acridine orange/ethidium bromide co-staining. Acridine orange is a vital dye which will be taken up by dead and live cells, whereas ethidium bromide can enter only if there is membrane breakage. As a result of co-staining (AO and EB), the apoptotic cells appear as orange due to membrane damage; live cells appear as green (no membrane breakage). After protein hydrolysate treatment (50 and 100 μ g/ml) for 24 h, the cells were incubated with AO/EB together (1 μ g/ml) solution for 10 min followed by 1 X PBS wash to remove the excess stain. The cells were observed for membrane integrity at an excitation/emission of 500/526 nm using the spinning disc fluorescent microscope.

(d) Annexin V staining for phosphatidylserine translocation

Translocation of phosphatidylserine (PS) from the inner leaflet to the outer side of the membrane is a typical feature associated with apoptosis and this was studied using an annexin V labeling kit by following the instructions from the manufacturer. 6-Carboxyfluorescein (6-CF) labeled the viable cells whereas the cy3-conjugated annexin V was bound to the translocated annexin V in the outer layer of the plasma membrane. The cells after treatment with the protein hydrolysate (50 and 100 μ g/ml) for 24 h, stained with the annexin V staining solution and were observed at an excitation/emission of 650/670 nm using the spinning disc fluorescent microscope.

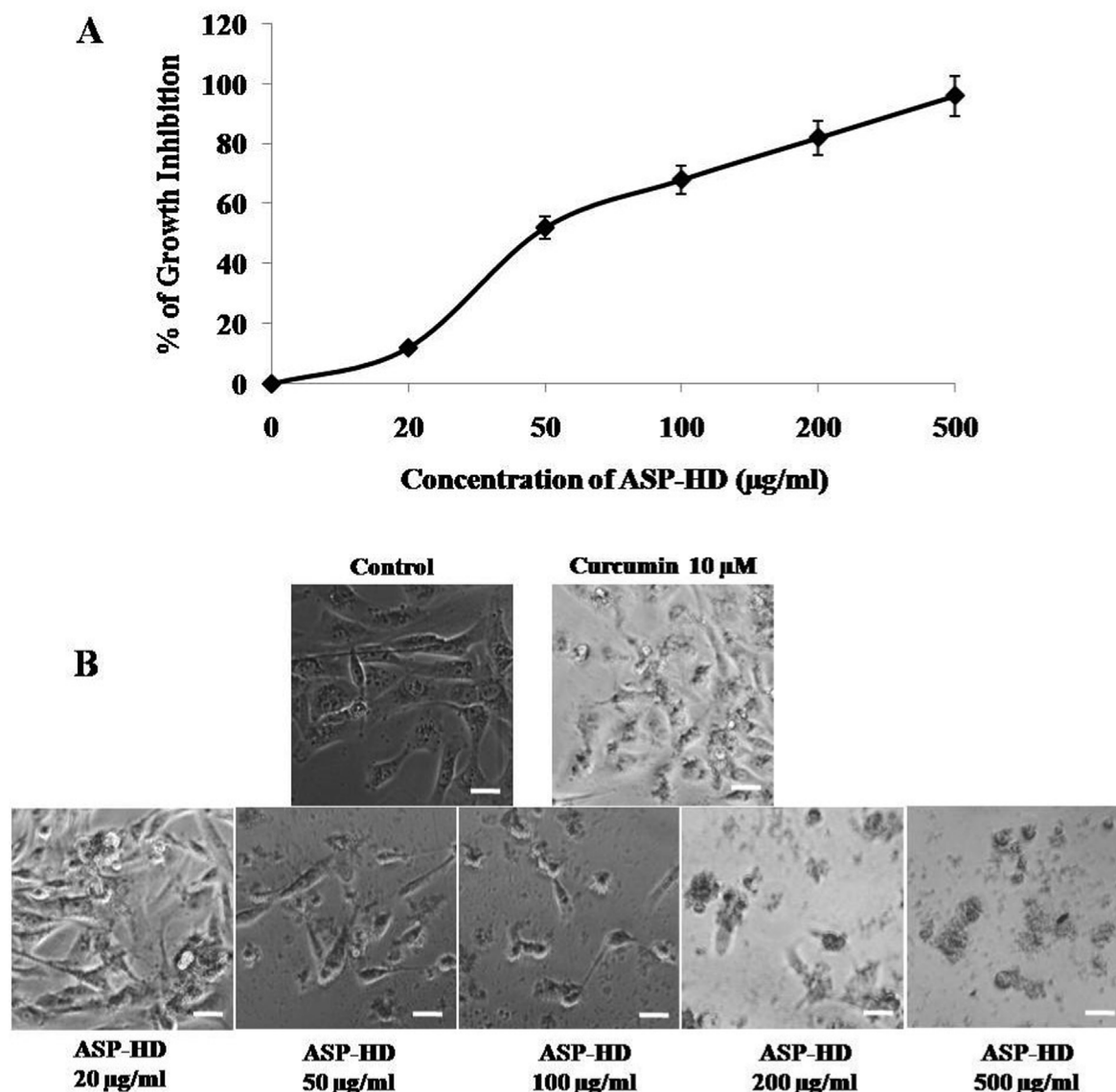


Fig. 4. (A) MTT assay showing the percentage growth inhibition of ASP-HD in breast cancer cells. ASP-HD showed concentration dependent effects on growth inhibition and the GI_{50} value was found to be $48.3 \pm 0.2 \mu\text{g/ml}$. Values are the average of three independent experiments \pm SD.

(B) Phase contrast image showing the morphological alterations in breast cancer cells on treatment with ASP-HD. Morphological alterations were observed in cells treated with ASP-HD from $20 \mu\text{g/ml}$ onwards.

(e) Caspase 3 activity assay

Caspase 3 is a cysteine protease activated during the apoptotic process. The caspase 3 activity was studied using a standard kit by following the manufacturer's instruction. Cell lysates were collected from the control as well as protein hydrolysate treated (50 and $100 \mu\text{g/ml}$) cells and incubated with the fluorescent substrate specific for caspase 3, Ac-DEVD-AMC (N-acetyl-Asp-Glu-Val-Asp-7-amido-4-methylcoumarin). The fluorescence developed as a result of the reactions was measured at an excitation/emission of $360/460 \text{ nm}$ using a microplate fluorescent reader Synergy™ 4 (BioTek Instruments).

(f) Cell migration assay

A scratch wound assay was done to study the effects of inhibition of cell migration by the protein hydrolysates. A monolayer of cells was grown in culture plates and an artificial line between the cells was created in the plate using a sterile pipette tip. After treatment with the protein hydrolysates (50 and $100 \mu\text{g/ml}$), the closing of the wound was

monitored for 24 h and compared with the untreated control. The observations were made using a phase contrast microscope Nikon Eclipse™100 at $4\times$ magnification (Nikon Instruments Inc.).

2.10. Statistical analysis

Results are expressed as average \pm standard deviation (SD) of three independent experiments. Data were analyzed using one way ANOVA using the Statistical Package for the Social Sciences (SPSS) 20.0 software (IBM, Armonk, NY, USA) and the differences were considered as statistically significant at $p < 0.05$.

3. Results and discussion

The raw and heat denatured proteins from amaranth seeds were subjected to simulated gastrointestinal digestion. The free EAA after simulated digestion of raw and heat denatured protein is given in Fig. 1. The amino acid profile indicated that the number of free EAA was negligible in the undigested amaranth proteins. Simulated digestion

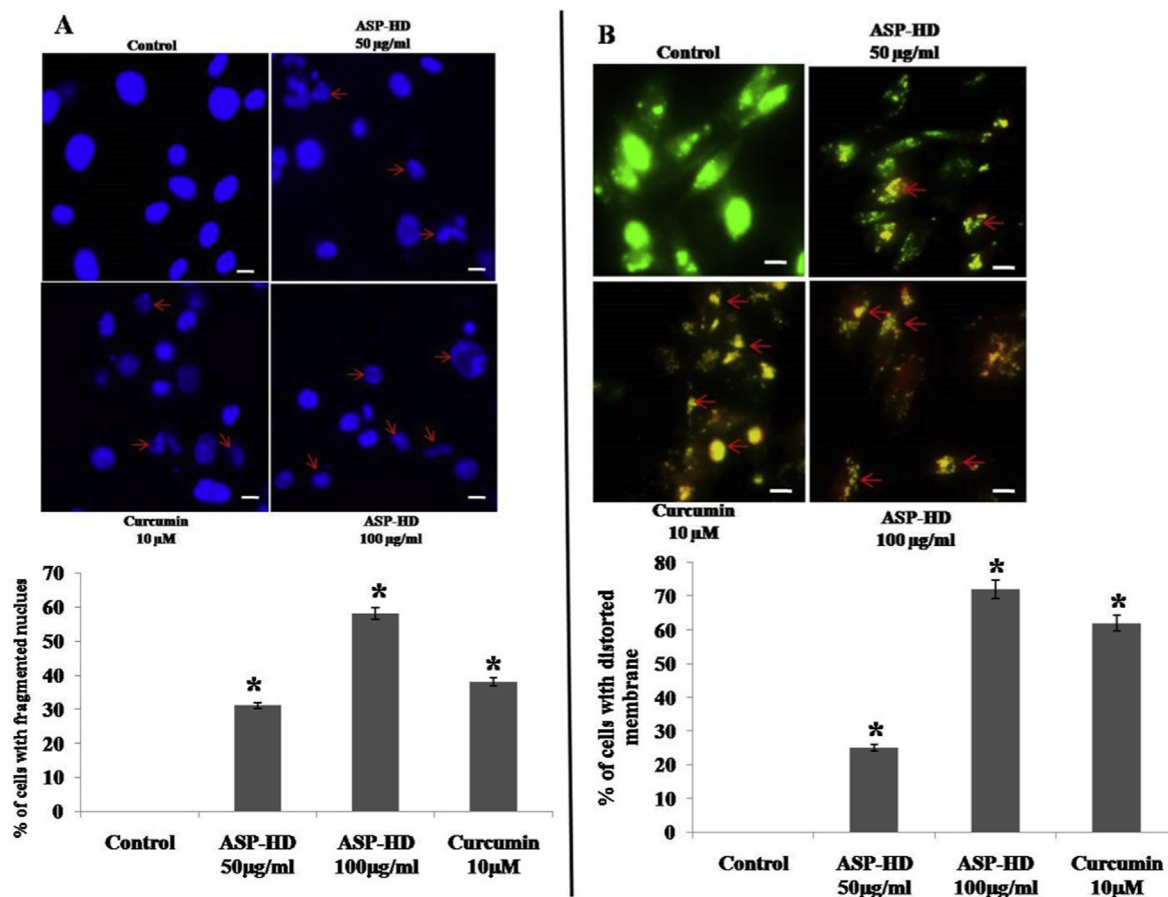


Fig. 5. (A) DAPI staining - Fluorescent images showing the nuclear fragmentation in the control and treated cells. Red arrows in the treated cells indicate fragmentation of the nucleus. The nucleus of control cells appeared to be normal. The percentage of fragmented nucleus in a field of 100 cells were counted and plotted as a bar diagram. Values are the average of three independent experiments \pm SD and * $p < 0.05$ when compared with control.

(B) AO/EtBr staining - The membrane integrity studies using co-staining with AO and EtBr. The orange colored cells (indicated by red arrows) showed the membrane damage due the incorporation of EtBr along with AO. The control cells with intact cell membrane only took up AO and appeared as green. The number of cells with damaged membrane was counted from a field of 100 cells and plotted as the bar diagram. Values are the average of three independent experiments \pm SD and * $p < 0.05$ when compared with control. (For interpretation of the references to color in this figure legend, the reader is referred to the Web version of this article.)

significantly increased the release of amino acids like leucine, threonine, and lysine. But heat denaturation followed by simulated digestion significantly increased the release of amino acids such as Lue, Thr, and Trp. The protein content and the EAA found in pseudocereals have been analyzed before and reported to be around 16 g of crude protein/100 g seeds with a high leucine content (Mota et al., 2016). The leucine in these seeds helps in muscle development by activating the mammalian target of rapamycin (mTOR). Moreover, the bioavailability of pseudocereal proteins is better than that of other plant proteins and is similar to animal proteins (Alvarez-Jubete et al., 2009). The present study showed that heat denaturation followed by simulated gastrointestinal digestion of amaranth proteins release more EAA especially leu and lys.

After digestion, the samples were run on SDS-PAGE and there were no bands in the lanes with digested samples. This may be due to the low molecular weight peptides formed as a result of digestion running out from the gel easily compared to undigested protein samples. The results are shown in Fig. 2A. The peptides with α -amino acids after digestion were quantitated using the ninhydrin test and the results are shown in Fig. 2B. Simulated digestion alone led to certain peptides but led to more in the heat denatured sample after digestion. These results indicated that the proteins from amaranth are easily digestible in the simulated gastric system and do not cause any irritation in the bowel due to indigestion of proteins.

The heat denatured digested proteins showed a significant increase in free radical scavenging potential and total antioxidant activity when

compared to the undigested and digested (without heat denaturation) protein samples. EC_{50} value of ASP in free radical scavenging potential was found to be 64 mg, which decreased to 19 ± 0.5 mg with the simulated digestion conditions (ASP-D). There was a significant decrease in the EC_{50} value (1.9 ± 0.03 mg) when the digestion was done after heat denaturation (ASP-HD). The positive control of ascorbic acid gave an EC_{50} value of 5.6 ± 0.1 μ g. ASP-HD had > 121 mg equivalents of ascorbic acid/g of BSA E protein. So the heat denaturation of ASP aids the digestibility and the peptides released as a result of this showed promising free radical scavenging and antioxidant activity. The results are shown in Fig. 3A and 3B. The nutritional benefits of amaranth along with several other pseudocereals have been reported before (Orona-Tamayo, Valverde, & Paredes-Lopez, 2018). Dietary addition of amaranth protein isolate increased the antioxidant status, decreased blood pressure and increased fecal cholesterol excretion in high fat-fed Wistar rats (Lado, Burini, Rinaldi, Anon, & Tironi, 2015). Antithrombotic and antioxidant activity of amaranth hydrolysate was obtained by using endogenous activation of aspartic protease indicating its potential cardiovascular protecting effects (Sabbione, Ibañez, Martínez, Añón, & Scilingo, 2016). Bioactive peptides exerted their antioxidant activity by targeting various signaling molecules and transcription factors including nuclear factor kappa B (Liang et al., 2018).

Recent studies indicated that the consumption of whole-grain food products reduces the risk of various types of cancer and the proteins, peptides and AA present in them are major contributors (Bouglé &

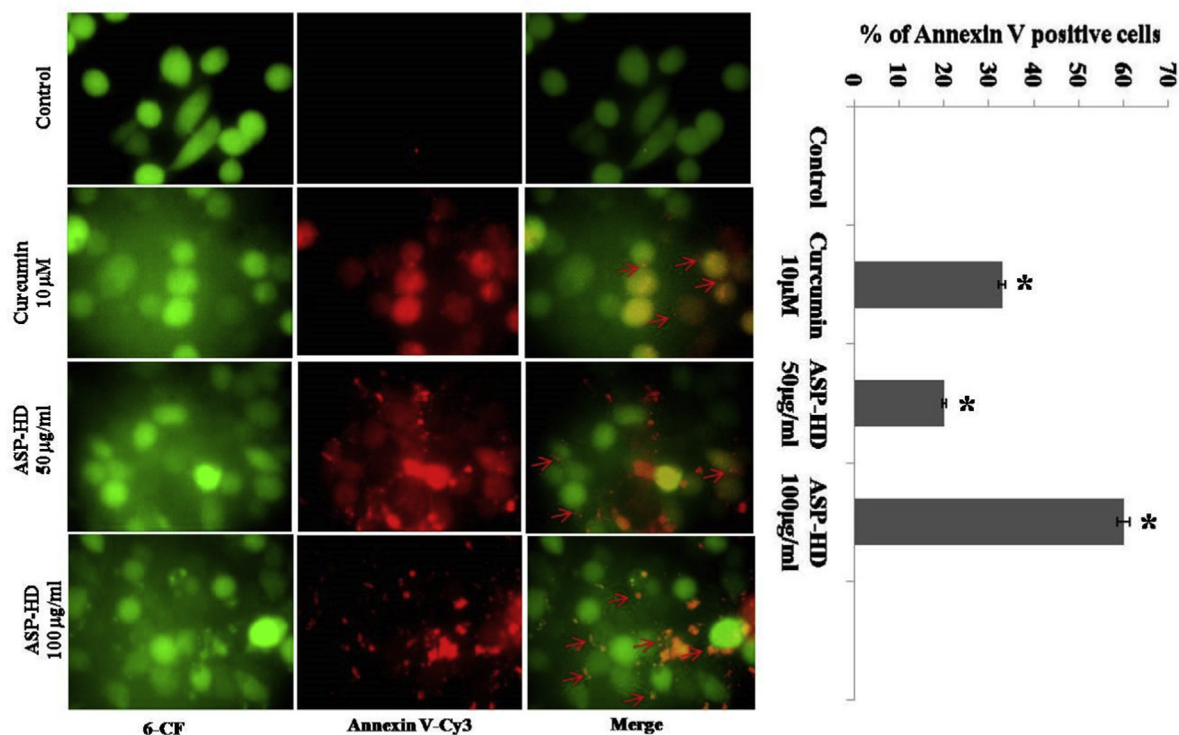


Fig. 6. Annexin V staining - Translocated phosphatidyl serine was stained with annexin V labelled with Cy3 (indicated by red arrows) in the treated cells. The percentage of annexin V cells are shown in the bar diagram. Values are the average of three independent experiments \pm SD and * $p < 0.05$ when compared with control. (For interpretation of the references to color in this figure legend, the reader is referred to the Web version of this article.)

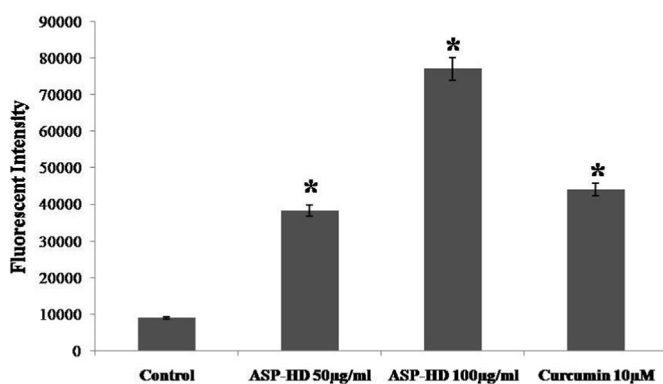


Fig. 7. Caspase 3 activity assay - Increased caspase activity was observed in the treated cells compared with control. Values are the average of three independent experiments \pm SD and * $p < 0.05$ when compared with control.

Bouhallab, 2017). The current study found that amaranth seeds upon heat denaturation followed by simulated gastrointestinal digestion release EAA and peptides with good antioxidant activity. These hydrolysates were checked for *in vitro* anticancer activity in breast cancer cells. Different concentrations of ASP-HD were used for the cytotoxicity effects for 24 h. The results (Fig. 4A) indicated that there was a concentration-dependent inhibition of the growth of cells when treated with ASP-HD with a GI_{50} value of $48.3 \pm 0.2 \mu\text{g/ml}$. The morphology of cells treated with ASP-HD was also observed and the results shown in Fig. 4B indicated that ASP-HD treatment lead to significant changes like membrane breakage, decrease in cell number and blebbing similar to that of curcumin (positive control) treated cells. Bioactive peptides from natural sources are being identified developing as anticancer agents because of their specificity for cancer cells. These peptides are non-toxic to normal cells (Wang, Dong, Li, Han, & Su, 2017). Like amaranth, maize bioactive peptides were also reported to have

anticancer property along with many other health-promoting effects (Díaz-Gómez, Castorena-Torres, Preciado-Ortiz, & García-Lara, 2017).

Since the initial studies with ASP-HD showed cytotoxicity and morphological changes similar to that of curcumin, further analysis was carried out to test whether the cytotoxic effects are due to apoptosis. Nuclear fragmentation is an important event in apoptosis and the effects of ASP-HD on nuclear fragmentation was studied using DAPI staining. The results shown in Fig. 5A indicated significant changes in nuclear morphology such as fragmentation and condensation which are indicated by red arrows. The graph indicated the percentage of cells with a fragmented nucleus. Apoptotic cells undergo membrane damage and the intensity of this was studied using acridine orange/ethidium bromide co-staining. The results shown in Fig. 5B showed significant loss in membrane integrity which was observed as an orange color (indicated by red arrows) with the co-staining of ethidium bromide (red) along with acridine orange (green) in the treated cells. The control cells were green in color because they had intact membrane structure. The graph in Fig. 5B shows the percentage of cells with a distorted membrane as a result of treatment. PS translocation results are shown in Fig. 6 which indicated a significant increase in the number of cells with annexin V on their outer membrane (indicated by red arrows) in the treated cells compared to control. The percentage of annexin V positive cells in a colony of 100 cells was calculated and the results are shown as a graph in Fig. 6. Caspase 3 activity was also increased in the treated compared to control cells and the results are shown in Fig. 7. These results indicated that ASP-HD could induce apoptosis in breast cancer cells similar to that of the standard drug curcumin. The soy peptide lunasin has been studied for its apoptosis-inducing potential in different cancer cells. In colon cancer cells it exerted G2M cell cycle arrest, mitochondrial apoptosis, and expression of p21 protein. It stopped the integrin signaling and PI3K/AKT signaling in skin cancer cells through its antimetastatic effects. Lunasin is the first natural peptide found with an established epigenetic mechanism of action preventing cancer growth (Hsieh, Martinez-Villaluenga, de Lumen, &

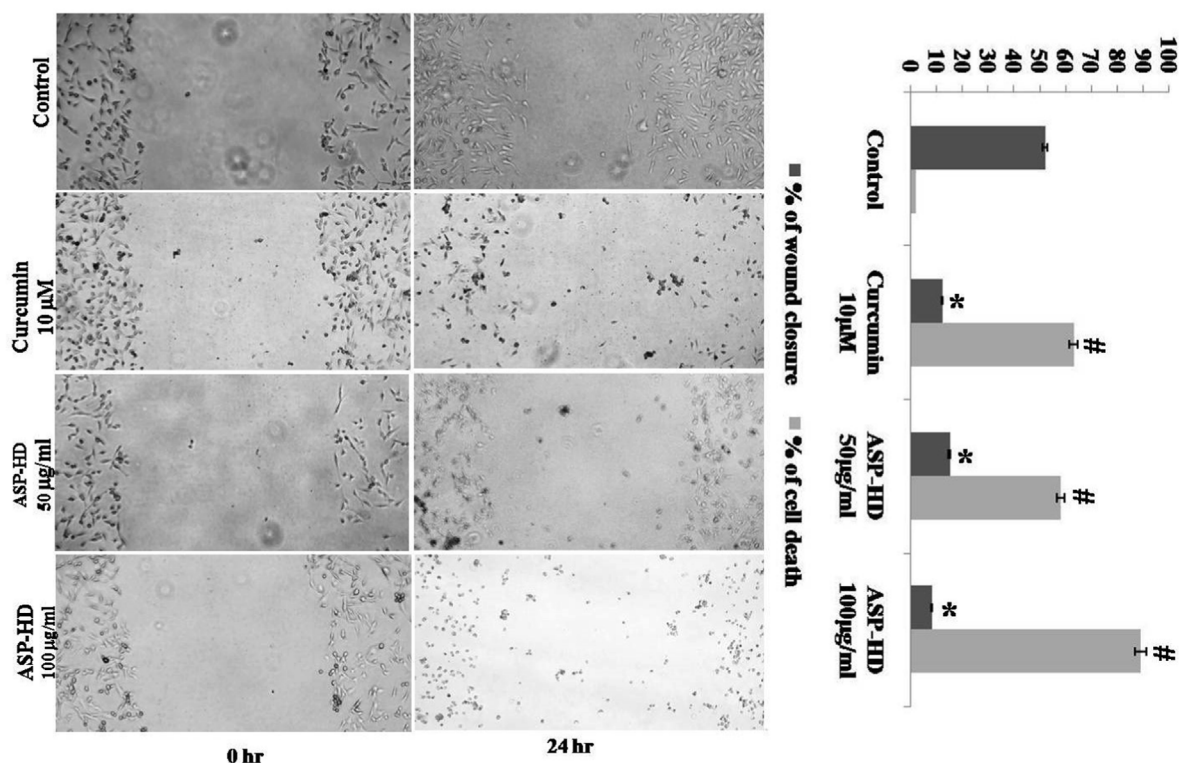


Fig. 8. Scratch wound assay - The antimigratory effects of ASP-HD and curcumin were evaluated using the percentage of wound closure in a period of 24 h. The bar diagram indicated the percentages of wound closures and cell deaths that occurred with treatment. Values expressed are the average of three independent experiments \pm SD and * $p < 0.05$ when compared with control.

Hernandez-Ledesma, 2018). *Amaranthus caudatus* protein hydrolysate contains multifunctional peptides with antioxidant and α -amylase inhibitory action along with cytotoxic effects (Vilcacundo, Martinez-Villaluenga, Miralles, & Hernandez-Ledesma, 2018).

Cellular migration is an important prerequisite for cancer cells to undergo invasion and metastasis, inhibition of cellular migration is important in cancer drug discovery (Bravo-Cordero, Hodgson, & Condeelis, 2012). Experiments were done to study the ability of ASP-HD to inhibit the cellular migration of breast cancer cells across an artificial wound. The results are shown in Fig. 8. In the control cells within 24 h, > 50% of cell migration and wound closure was observed when compared to the treated cells where it was < 10%. The percentage of dead cells was zero in the control at 24 h but it was > 50% in the treated cells. These results indicated that ASP-HD also have anti-metastatic potential similar to that of curcumin. It was observed that the heat denaturation amaranth proteins before gastrointestinal digestion released more peptides with significant anticancer activity.

4. Conclusions

Amaranth is the most widely used pseudocereal. The peptides and EAA released during digestion were responsible for various biological effects of protein. Heat denaturation followed by simulated digestion released more EAA and bioactive peptides from amaranth seed protein. The protein hydrolysate has antioxidant activity and anticancer potential with breast cancer cells. Further work is needed to characterize these anticancer peptides.

Author contributions

Taniya MS had isolated the protein and did all the experimental works and wrote the first draft of the publication. Reshma MV contributed to the digestion studies and analysis of amino acid data. Shanamol PS and Gayatri Krishnan were involved in the standardization

of the protocol for protein isolation and a few biochemical assays. Priya S conceived the idea, planned the experiments, raised money for the work and corrected the manuscript.

Declaration of competing interest

The authors declare that they have no conflicts of interest.

Acknowledgements

The authors thank the Kerala State Council for Science, Technology & Environment (KSCSTE), Kerala, India (Grant no. 02/YIPB/KBC/2014/KSCSTE) for the financial support. Sincere thanks to Dr. Binod P, Senior Scientist, Microbial Process and Technology Division of CSIR-NIIST for the amino acid analysis.

Appendix A. Supplementary data

Supplementary data to this article can be found online at <https://doi.org/10.1016/j.fbio.2020.100588>.

References

- Al-Mamun, M. A., Husna, J., Khatun, M., & Ferdousi, Z. (2016). Assessment of antioxidant, anticancer and antimicrobial activity of two vegetable species of *Amaranthus* in Bangladesh. *BMC Complementary and Alternative Medicine*, 16, 157.
- Alvarez-Jubete, L., Arend, E. K., & Gallagher, E. (2010). Nutritive value of pseudocereals and their increasing use as functional gluten free ingredients. *Trends in Food Science & Technology*, 21, 106–113.
- Alvarez-Jubete, L., Arendt, E. K., & Gallagher, E. (2009). Nutritive value and chemical composition of pseudocereals as gluten free ingredients. *International Journal of Food Sciences & Nutrition*, 4, 240–257.
- Bouglé, D., & Bouhallab, S. (2017). Dietary bioactive peptides: Human studies. *Critical Reviews in Food Science and Nutrition*, 57, 335–343.
- Bravo-Cordero, J. J., Hodgson, L., & Condeelis, J. (2012). Directed cell invasion and migration during metastasis. *Current Opinion in Cell Biology*, 24, 277–283.

- Chakrabarti, S., Guha, S., & Majumdar, K. (2018). Food derived bioactive peptides in human health: Challenges and opportunities. *Nutrients*, *10*, 1738.
- Chiu, C. Y., Li, C. Y., Chiu, C. C., Niwa, M., Kitanaka, S., Damu, A. G., et al. (2005). Constituents of leaves of *Phellodendron japonicum* Maxim. and their antioxidant activity. *Chemical and Pharmaceutical Bulletin*, *53*, 1118–1121.
- Díaz-Gómez, J. L., Castorena-Torres, F., Preciado-Ortiz, R. E., & García-Lara, S. (2017). Anti-cancer activity of maize bioactive peptides. *Frontiers in Chemistry*, *5*, 44.
- Hsieh, C. C., Martínez-Villalunga, C., de Lumen, B. O., & Hernandez-Ledesma, B. (2018). Updating the research on the chemopreventive and therapeutic role of the peptide Lunasin. *Journal of the Science of Food and Agriculture*, *98*, 2070–2079.
- Huby, R. D. J., Dearman, J. R., & Kimber, I. (2000). Why are some proteins allergens? *Toxicological Sciences*, *55*, 235–246.
- Janssen, F., Pauly, A., Rombouts, I., Jansens, K. J. A., Deleu, L. J., & Delcour, J. A. (2017). Proteins of amaranth (*Amaranthus* spp.), buckwheat (*Fagopyrum* spp.), and quinoa (*Chenopodium* spp.): A food science and technology perspective. *Comprehensive Reviews in Food Science and Food Safety*, *16*, 39–58.
- Jin, Y., Xuan, Y., Chen, M., Chen, J., Jin, Y., Jin, Y., et al. (2013). Antioxidant, anti-inflammatory and anticancer activities of *Amaranthus viridis* extracts. *Asian Journal of Chemistry*, *25*, 8901–8904.
- Lado, M. B., Burini, J., Rinaldi, G., Anon, M. C., & Tironi, V. A. (2015). Effects of the dietary addition of amaranth (*Amaranthus mantegazzianus*) protein isolate on antioxidant status, lipid profiles and blood pressure of rats. *Plant Foods for Human Nutrition*, *70*, 371–379.
- Laemmli, U. K. (1970). Cleavage of structural proteins during the assembly of the head of bacteriophage T4. *Nature*, *227*, 680–685.
- Liang, Y., Lin, Q., Huang, P., Wang, Y., Li, J., Zhang, L., et al. (2018). Rice bioactive peptide binding with TLR4 to overcome H2O2 induced injury in human umbilical vein endothelial cells through NFκB signaling. *Journal of Agricultural and Food Chemistry*, *66*, 440–448.
- Lowry, O. H., Rosenbrough, N. J., Farr, A. L., & Randall, R. J. (1951). Protein measurement with the folin phenol reagent. *Journal of Biological Chemistry*, *193*, 265–275.
- Luna-Vital, D. A., Gonzalez de Mejia, E., & Loarca-Pina, G. (2017). Dietary peptides from *Phaseolus vulgaris* L. reduced AOM/DSS-induced colitis-associated colon carcinogenesis in Balb/c Mice. *Plant Foods for Human Nutrition*, *72*, 445–447.
- Moore, S., & Stein, W. H. (1948). Photometric ninhydrin method for use in the chromatography of amino acids. *Journal of Biological Chemistry*, *176*, 367–388.
- Mota, C., Santos, M., Mauro, R., Samman, N., Matos, A. S., Torres, D., et al. (2016). Protein content and amino acids profile of pseudocereals. *Food Chemistry*, *193*, 55–61.
- Orona-Tamayo, D., Valverde, M. E., & Paredes-Lopez, O. (2018). Bioactive peptides from selected Latin American food crops - a nutraceutical and molecular approach. *Critical Reviews in Food Science and Nutrition*, *1*, 1–27.
- Pesta, D. H., & Samuel, V. T. (2014). A high-protein diet for reducing body fat: Mechanisms and possible caveats. *Nutrition & Metabolism*, *11*, 53.
- Prieto, P., Pineda, M., & Aguilar, M. (1999). Spectrophotometric quantitation of antioxidant capacity through the formation of a phosphomolybdenum complex: Specific application to the determination of vitamin E. *Annals of Clinical Biochemistry*, *269*, 337–341.
- Sabbione, A. C., Ibañez, S. M., Martínez, E. N., Añón, M. C., & Scilingo, A. A. (2016). Antithrombotic and antioxidant activity of amaranth hydrolysate obtained by activation of an endogenous protease. *Plant Foods for Human Nutrition*, *71*, 174–182.
- Salvamani, S., Gunasekaran, B., Shukor, M. Y., Shaharuddin, N. A., Sabullah, M. K., & Ahmad, S. A. (2016). Anti HMG-CoA reductase, antioxidant and anti-inflammatory activities of *Amaranthus viridis* leaf extracts as potential treatment for hypercholesterolemia. *Evidence-based Complementary and Alternative Medicine*, 8090841.
- Sen, S., Chakraborty, R., Maramba, N., Basak, M., Deka, S., & Dey, B. K. (2015). *In vitro* anti-inflammatory activity of *Amaranthus caudatus* L. leaves. *Indian Journal of Natural Products and Resources*, *6*, 326–329.
- Theethira, T. G., & Dennis, M. (2015). Celiac disease and the gluten-free diet: Consequences and recommendations for improvement. *Digestive Diseases*, *33*, 175–182.
- Uraipong, C., & Zhao, J. (2017). *In vitro* digestion of rice bran proteins produces peptides with potent inhibitory effects on α-glucosidase and angiotensin I converting. *Journal of the Science of Food and Agriculture*, *98*, 758–766.
- Vilcacundo, R., Martínez-Villalunga, C., Miralles, B., & Hernandez-Ledesma, B. (2018). Release of multifunctional peptides from kiwicha (*Amaranthus caudatus*) protein under *in vitro* gastrointestinal digestion. *Journal of the Science of Food and Agriculture*. <https://doi.org/10.1002/jsfa.9294> [Epub ahead of print].
- Wada, Y., & Lonnerda, B. (2014). Proactive peptides released from *in vitro* digestion of human milk with or without pasteurization. *Pediatric Research*, *77*, I546–I553.
- Wang, L., Dong, C., Li, X., Han, W., & Su, X. (2017). Anticancer potential of bioactive peptides from animal sources (Review). *Oncology Reports*, *38*, 637–651.



Natural Product Research

Formerly Natural Product Letters

ISSN: 1478-6419 (Print) 1478-6427 (Online) Journal homepage: <https://www.tandfonline.com/loi/gnpl20>


Semi-synthetic diversification of coronarin D, a labdane diterpene, under Ugi reaction conditions

Kollery S. Veena, Murikkinthara S. Taniya, Jaice Ravindran, Arun Kumar Thangarasu, Sulochana Priya & Ravi Shankar Lankalapalli

To cite this article: Kollery S. Veena, Murikkinthara S. Taniya, Jaice Ravindran, Arun Kumar Thangarasu, Sulochana Priya & Ravi Shankar Lankalapalli (2020): Semi-synthetic diversification of coronarin D, a labdane diterpene, under Ugi reaction conditions, Natural Product Research

To link to this article: <https://doi.org/10.1080/14786419.2020.1782406>

 View supplementary material 

 Published online: 25 Jun 2020.

 Submit your article to this journal 

 View related articles 

 View Crossmark data 



Semi-synthetic diversification of coronarin D, a labdane diterpene, under Ugi reaction conditions

Kollery S. Veena^{a,b}, Murikkinthara S. Taniya^{b,c}, Jaice Ravindran^{a,b}, Arun Kumar Thangarasu^{a,b}, Sulochana Priya^{b,c} and Ravi Shankar Lankalapalli^{a,b}

^aChemical Sciences and Technology Division, CSIR-National Institute for Interdisciplinary Science and Technology (CSIR-NIIST), Thiruvananthapuram, Kerala, India; ^bAcademy of Scientific and Innovative Research (AcSIR), Ghaziabad, Uttar Pradesh, India; ^cAgro-Processing and Technology Division, CSIR-National Institute for Interdisciplinary Science and Technology (CSIR-NIIST), Thiruvananthapuram, Kerala, India

ABSTRACT

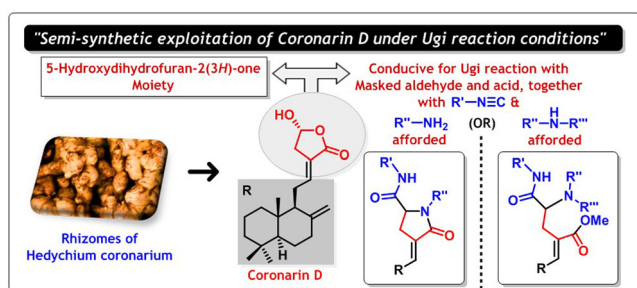
The prevalence of 5-hydroxydihydrofuran-2(3H)-one moiety in natural products is exploited for the first time using coronarin D, a labdane diterpene, to afford Ugi reaction product **1a** and interrupted Ugi product **2a**. The potential of the Ugi reaction was further extended to L-phenylalanine, 2-aminopyridine, and D-glucosamine, which afforded Ugi reaction products **3a–f**, **4**, and **5a–d**, respectively. Cytotoxicity studies in RAW cells reveal that compounds **3e** and **5b** were non-toxic up to 50 μ M, and these compounds were able to reduce the LPS stimulated NO production in RAW cells in par with the standard anti-inflammatory drug dexamethasone.

ARTICLE HISTORY

Received 14 April 2020
Accepted 4 June 2020


KEYWORDS


Semi-synthesis; multicomponent reaction; Ugi reaction; labdane diterpene; 5-hydroxydihydrofuran-2(3H)-one; coronarin D



1. Introduction

Labdane diterpene (LD) core is a bicyclic framework present in a wide variety of bio-active natural products that possess a broad range of biological properties such as antimicrobial, antileishmanial, antimutagenic, antiproliferative, anti-inflammatory, analgesic, cardiotoxic and immunomodulatory activities (Singh et al. 1999; Demetzos and

CONTACT Ravi S. Lankalapalli  ravishankar@niist.res.in

 Supplemental data for this article can be accessed at <https://doi.org/10.1080/14786419.2020.1782406>.

© 2020 Informa UK Limited, trading as Taylor & Francis Group

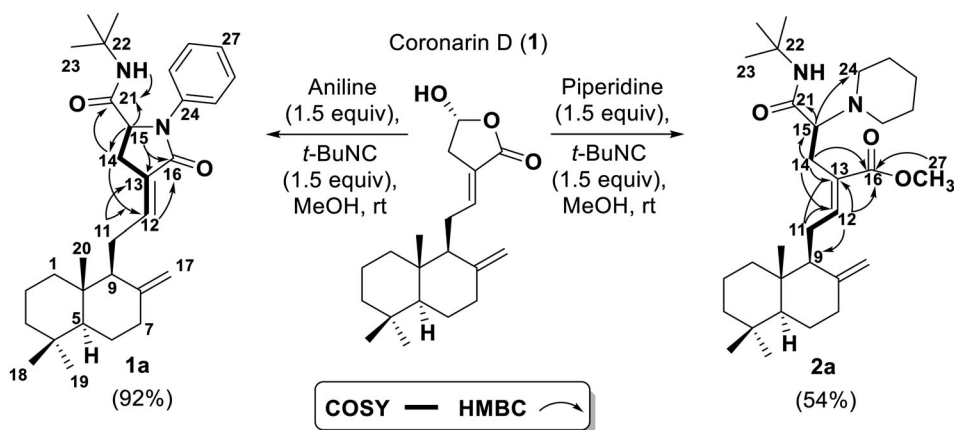


Figure 1. Semi-synthetic derivatization of coronarin D (**1**) under Ugi reaction conditions and key 2D NMR correlations of compounds **1a** and **2a**.

Dimas 2001; Frija et al. 2011). LDs are susceptible to bio- and chemical-modifications owing to the presence of reactive functionalities appended to the B ring, which produces medicinally relevant molecules (Frija et al. 2011; Marcos et al. 2012). Semi-synthetic modifications that are carried out to enhance potency, improve physico-chemical, biochemical, and pharmacokinetic properties of natural products enable the discovery of novel drugs (Newman and Cragg 2016; Guo 2017; Yao et al. 2017). Rhizomes of *Hedychium coronarium* Koen., a Zingiberaceae plant, is well-known in both Indian Ayurvedic and Chinese traditional medicine as an excellent source for LDs. LDs isolated from *H. coronarium* were reported primarily for their cytotoxic and anti-inflammatory properties. Herein, we report unprecedented semi-synthetic modifications of 5-hydroxydihydrofuran-2(3*H*)-one moiety of coronarin D (**1**), an LD isolated from *H. coronarium*, under Ugi reaction conditions (Figure 1). The essence of Ugi reaction lies in building complex molecular architectures with ample diversity and high relevance for medicinal chemistry research (Bienaymé et al. 2000; Dömling and Ugi 2000; Ugi et al. 2003; Dömling 2006).

The embedded aldehyde and carboxylic acid functionalities present in 5-hydroxydihydrofuran-2(3*H*)-one moiety of coronarin D qualifies it as a suitable precursor for Ugi reaction. There are few reports on Ugi reaction, employing 3-hydroxyisobenzofuran-1(3*H*)-one synthetic substrate, which exhibits an embedded benzaldehyde and benzoic acid functionalities (Bjoere et al. 2008; Macsari et al. 2012). Riguet reported the application of a Ugi reaction on a 5-hydroxyfuran-2(5*H*)-one synthetic substrate in a post-Friedel-Crafts alkylation sequence (Riguet 2011). In coronarin D, the intrinsic aldehyde functionality is C(sp³)-CHO, and the carboxylic acid is acrylic acid. To the best of our knowledge, semi-synthetic modifications of coronarin D are unexplored except for a report which includes a simple conjugation of coronarin D with chlorambucil through an ester linkage (Khunnawutmanotham et al. 2012). More importantly, even though many natural products offer diverse functionalities amenable for Ugi based semi-synthetic transformation, only a few reports of such an attempt have been made (Avilés and Rodríguez 2010; Avilés et al. 2015; Lesma et al. 2016). The presence of 5-hydroxydihydrofuran-2(3*H*)-one moiety in natural products hyphodontal, lamellodysidine A,

dendocarin A, marasmal B, findlayine C, ophiobolin P, and ememogin indicate the prospects for their semi-synthetic modifications by Ugi reaction. Also, there are several terpenoids which contain 5-hydroxyfuran-2(5*H*)-one moiety conducive for Ugi reaction such as acemeremophilane E, eremophilane, stictic acid, 18-hydroxy-4-acetoxycrenulide, linderagalactones, bishomoscalaranes, teuvislactones, atractylenolide III, plebeiolide B, glomeremophilanes D, nepetaefolins J, chloranthalactone E, etc. Reports of chemical transformations of 5-hydroxydihydrofuran-2(3*H*)-one moiety are scarce, but related 3-hydroxyisobenzofuran-1(3*H*)-one synthetic intermediates are known where the reactions are mostly confined to simple substitutions on its anomeric carbon (Freskos et al. 1985; Magnus and Cairns 1986; Niedek et al. 2016).

2. Results and discussion

2.1. Chemistry

Coronarin D (**1**) was isolated from the acetone extract of the rhizomes of *H. coronarium*. In our initial attempt, coronarin D was subjected to standard Ugi reaction conditions by using 1.5 equivalents each of *tert*-butylisocyanide and aniline in methanol at room temperature. An overnight reaction afforded a clean transformation of coronarin D to a non-polar product **1a** in 92% yield (Figure 1), confirmed by detailed 2D NMR analysis as Ugi reaction product.

The molecular formula of compound **1a**, determined from HR-ESI-MS ion at m/z 477.3490 $[M + H]^+$, was $C_{31}H_{44}N_2O_2$ indicating 11 degrees of unsaturation. The 1H and ^{13}C NMR data (Table S1, Supplementary Material) along with DEPT NMR data revealed the presence of 8 quaternary carbons which include 2 amide carbonyls (δ_C 167.9, 170.5 ppm), 5 aromatic protons, 3 sp^3 methines, 1 exomethylene, 1 sp^2 methine, 7 sp^3 methylenes, and 6 methyls. The duplicated resonances which are more prominent in ^{13}C than 1H NMR suggest the presence of an epimeric mixture due to $C\alpha$ of Ugi reaction product as well as the existence of a combination of amide rotamers. The presence of *tert*-butyl group, two amide carbonyls, phenyl ring in compound **1a** are supportive of the Ugi reaction pathway, further confirmed by COSY and HMBC correlations (Figure 1). The presence of HMBC correlations from NH to C-21 (C=O), C-22, and C-23 reveal one of the amide moieties that arise from the isocyanide component. Characteristic $C\alpha$ was identified from the proton NMR as H-15 (δ 4.52 ppm) which exhibits HMBC correlation with C-21, C-16 (C=O), C-14 (CH_2), C-13 (4°), and correlations from H-14 to C-15, C-21, C-13 and C-12 (sp^2 methine) indicate the presence of *N*-phenyl-*exo*-ethylidene- γ -lactam akin to *exo*-ethylidene-dihydrofuran-2(3*H*)-one moiety of coronarin D. Additionally, HMBC correlations from H-12 to C-14, C-16; H-11 to C-9, C-13, C12, and presence of allylic 4J COSY correlations between H-12 and H-14, and 3J COSY correlations between H-15 and H-14 unambiguously confirms the linkage between bicyclic core moiety with the newly formed diamide Ugi moiety. The chemical shifts were assigned for the rest of the bicyclic framework from literature (Chenda et al. 2014), along with consideration of other HMBC correlations.

We envisaged an interrupted Ugi pathway while treating coronarin D with a secondary amine in the presence of isocyanide and methanol, and indeed a four-component product **2a** is obtained in 54% yield (Figure 1). The structure of compound

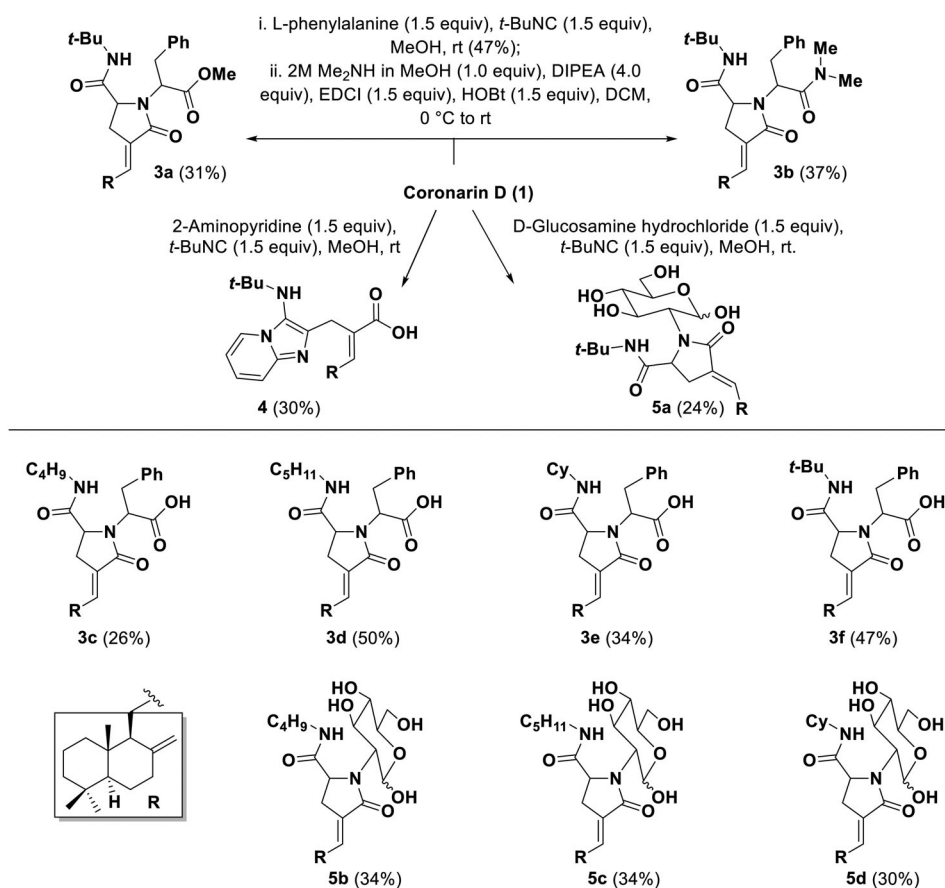


Figure 2. Diversification of coronarin D (**1**) under Ugi reaction conditions.

2a was confirmed by detailed 2D NMR analysis (Figure 1). The molecular formula of compound **2a**, determined by HR-ESI-MS ion at m/z 501.4049 $[M+H]^+$, was C₃₁H₅₂N₂O₃ indicating 7 degrees of unsaturation. The ¹H and ¹³C NMR data (Table S1, Supplementary Material) along with DEPT NMR data revealed the presence of 7 quaternary carbons, which include 2 carbonyls (δ_C 171.5, 168.4 ppm), 3 sp³ methines, 1 exomethylene, 1 sp² methine, and 7 methyls. Similar to compound **1a**, ¹³C and ¹H NMR of compound **2a** also exhibited duplicated resonances. The interrupted Ugi reaction is the reason for the presence of an additional methyl group (δ_H 3.6 ppm), which exhibits HMBC correlation with C-16 (ester carbonyl). C α -hydrogen (H-15, δ 3.16 ppm) exhibits ³J COSY correlation with H-14, and HMBC correlations with C-21 (amide carbonyl), C-24 (N-CH₂), C-14. In addition, HMBC correlations from H-14 to C-16, C-12, C-13, C-15; H-12 to C-16, C-13, C-9, C-14; and H-11 to C-9, C-13, C12, ³J COSY correlation with H-12 confirm the structure of interrupted Ugi product **2a**.

To explore the compatibility of 5-hydroxydihydrofuran-2(3*H*)-one moiety of coronarin D for Ugi reaction, we attempted variations with few amines *viz.* L-phenylalanine, 2-aminopyridine, and D-glucosamine (Figure 2). In an initial attempt with L-phenylalanine, an expected Ugi reaction product was obtained, which was isolated and confirmed by HRMS; subsequently, the product was treated with dimethylamine in

methanol in the presence of EDCl as the coupling agent. As an outcome, both methyl-ester **3a** and *N,N*-dimethylamide **3b** products were obtained. In the presence of 2-aminopyridine, a imidazo[1,2-*a*]pyridine derivative **4** was obtained via the Groebke–Blackburn–Bienayme reaction (Vidyacharan et al. 2014). Finally, Ugi reaction in the presence of *D*-glucosamine hydrochloride afforded the respective Ugi reaction product **5a**. Attempts with purines, however, did not afford the particular Ugi reaction products.

2.2. Biological activity

We intended to explore the *in vitro* anti-inflammatory activity of Ugi derivatives of coronarin D (**1**), however, compounds **1a**, **2a**, **3a–b** were insoluble in DMSO. Hence, a small library of compounds **3c–f** and **5b–d** from *L*-phenylalanine and *D*-glucosamine by variation of isocyanides were synthesised, respectively, which were soluble in DMSO. In order to obtain the suitable concentration of compounds for the study in RAW cells, we have carried out a cell viability test using MTT assay. From the results (Figure S1, Supplementary Material), we have observed that the compounds **3e** and **5b** were not toxic up to 50 μ M. Hence, the effect of **3e** and **5b** on LPS induced NO production in RAW cells was investigated. RAW cells were pre-treated for 2 hours with 10 and 20 μ M concentrations of **3e** and **5b**, and then stimulated with LPS for 18 hours. After the time period, the medium were collected and NO was estimated as described in methods. Dexamethasone was used as the standard drug. LPS increased NO production was down-regulated on pre-treatment with **3e** and **5b** in a concentration dependent manner similar to that of the standard drug dexamethasone (Figure S2, Supplementary Material).

3. Experimental section

The Supplementary Material contains experimental procedures, biological data, ^1H , ^{13}C and 2D NMR data.

4. Conclusions

In conclusion, the potential of 5-hydroxydihydrofuran-2(3*H*)-one moiety in natural products for semi-synthetic modification under Ugi reaction conditions has been demonstrated with coronarin D. The Ugi reaction products were obtained by variation of primary amines, including *L*-phenylalanine, 2-aminopyridine, *D*-glucosamine, and isocyanides. Coronarin D afforded the interrupted Ugi products with secondary amines in a four-component condensation. Preliminary cytotoxicity studies in RAW cell reveals Ugi derivatives **3e** and **5b** are non-toxic upto 50 μ M. Interestingly, these compounds were able to reduce the LPS stimulated NO production in RAW cells similar to that of the standard anti-inflammatory drug dexamethasone. The present study warrants exploitation of 5-hydroxydihydrofuran-2(3*H*)-one moiety and the related 5-hydroxyfuran-2(5*H*)-one moiety of natural products for semi-synthetic modifications by Ugi reaction. Semi-synthetic Ugi transformations of coronarin D by using a diverse range

of amines and isocyanides is underway in our laboratory for medicinal chemistry studies.

Disclosure statement

There are no conflicts of interest to declare.

Funding

Financial support from Department of Science and Technology (DST), India, grant no. CRD/2018/000064 is gratefully acknowledged.

References

- Avilés E, Prudhomme J, Le Roch KG, Franzblau SG, Chandrasena K, Mayer AMS, Rodríguez AD. 2015. Synthesis and preliminary biological evaluation of a small library of hybrid compounds based on Ugi isocyanide multicomponent reactions with a marine natural product scaffold. *Bioorganic Med Chem Lett.* 25(22):5339–5343.
- Avilés E, Rodríguez AD. 2010. Monamphilectine A, a potent antimalarial β -lactam from marine sponge hymeniacidon sp: isolation, structure, semisynthesis, and bioactivity. *Org Lett.* 12(22): 5290–5293.
- Bienaymé H, Hulme C, Oddon G, Schmitt P. 2000. Maximizing synthetic efficiency: multi-component transformations lead the way. *Chem Eur J.* 6(18):3321–3329.
- Bjoere A, Bostroem J, Davidsson O, Emtenaes H, Gran U, Iliefski T, Kajanus J, Olsson R, Sandberg L, Strandlund G, et al. 2008. Isoindoline derivatives for the treatment of arrhythmias. WO2008008022A1.
- Chenda LBN, Kouam SF, Lamshöft M, Kusari S, Talontsi FM, Ngadjui BT, Spiteller M. 2014. Isolation and characterization of six labdane diterpenes and one pregnane steroid of *Turraeanthus africanus*. *Phytochemistry.* 103:137–144.
- Demetzos C, Dimas KS. 2001. Labdane -type diterpenes: chemistry and biological activity. *Stud Nat Prod Chem.* 25:235–292.
- Dömling A. 2006. Recent developments in isocyanide based multicomponent reactions in applied chemistry. *Chem Rev.* 106(1):17–89.
- Dömling A, Ugi I. 2000. Multicomponent reactions with isocyanides. *Angew Chem Int Ed.* 39(18): 3168–3210.
- Freskos JN, Morrow GW, Swenton JS. 1985. Synthesis of functionalized hydroxyphthalides and their conversion to 3-cyano-1(3H)-isobenzofuranones. The diels-alder reaction of methyl 4,4-diethoxybutynoate and cyclohexadienes. *J Org Chem.* 50(6):805–810.
- Frija LMT, Frade RFM, Afonso C. 2011. Isolation, chemical, and biotransformation routes of labdane-type diterpenes. *Chem Rev.* 111(8):4418–4452.
- Guo Z. 2017. The modification of natural products for medical use. *Acta Pharm Sin B.* 7(2): 119–136.
- Khunnawutmanotham N, Chimnoi N, Champathong W, Lerdsirisuk P, Khotmor T, Techasakul S. 2012. Coronarin D conjugated to methylene homologues of chlorambucil: synthesis and evaluation of their cytotoxicity. *J Chem Res.* 36(6):374–378.
- Lesma G, Luraghi A, Rainoldi G, Mattiuzzo E, Bortolozzi R, Viola G, Silvani A. 2016. Multicomponent approach to bioactive peptide-ecdysteroid conjugates: creating diversity at C6 by means of the Ugi reaction. *Synthesis.* 48(22):3907–3916.
- Macdari I, Besidski Y, Csajernyik G, Nilsson LI, Sandberg L, Yngve U, Ahlin K, Bueters T, Eriksson AB, Lund P-E, et al. 2012. 3-oxoisindoline-1-carboxamides: potent, state-dependent blockers

- of voltage-gated sodium channel Na V 1.7 with efficacy in rat pain models. *J Med Chem.* 55(15):6866–6880.
- Magnus P, Cairns PM. 1986. Methods for indole alkaloid synthesis. enantiospecific synthesis of pentacyclic desethylaspidosperma-type alkaloids using an exceptionally mild retro-diels-alder reaction. *J Am Chem Soc.* 108(2):217–221.
- Marcos IS, Castaneda L, Basabe P, Diez D, Urones JG. 2012. Labdane diterpenes with highly functionalized B rings. *MROC.* 9(1):54–86.
- Newman DJ, Cragg GM. 2016. Natural products as sources of new drugs from 1981 to 2014. *J Nat Prod.* 79(3):629–661.
- Niedek D, Schuler SMM, Eschmann C, Wende RC, Seitz A, Keul F, Schreiner PR. 2016. Synthesis of enantioenriched phthalide and isoindolinone derivatives from 2-formylbenzoic acid. *Synthesis.* 49(2):371–382.
- Riguet E. 2011. Enantioselective organocatalytic friedel–crafts alkylation reaction of indoles with 5-hydroxyfuran-2(5H)-one: access to chiral γ -lactones and γ -lactams via a Ugi 4-center 3-component reaction. *J Org Chem.* 76(20):8143–8150.
- Singh M, Pal M, Sharma RP. 1999. Biological activity of the labdane diterpenes. *Planta Med.* 65(1):2–8.
- Ugi I, Werner B, Dömling A. 2003. The chemistry of isocyanides, their multicomponent reactions and their libraries. *Molecules.* 8(1):53–66.
- Vidyacharan S, Shinde AH, Satpathi B, Sharada DS. 2014. A facile protocol for the synthesis of 3-aminoimidazo-fused heterocycles via the Groebke-Blackburn-Bienayme reaction under catalyst-free and solvent-free conditions. *Green Chem.* 16(3):1168–1175.
- Yao H, Liu J, Xu S, Zhu Z, Xu J. 2017. The structural modification of natural products for novel drug discovery. *Expert Opin Drug Discov.* 12(2):121–140.